

The Pennsylvania State University

The Graduate School

Eberly College of Science

**DESIGN OF REAGENTS FOR TRACE-LEVEL CHEMICAL DETECTION
AND SIGNAL AMPLIFICATION**

A Dissertation in

Chemistry

by

Hemakesh Mohapatra

© 2014 Hemakesh Mohapatra

Submitted in Partial Fulfillment

of the Requirements

for the Degree of

Doctor of Philosophy

December 2014

This dissertation of Hemakesh Mohapatra was reviewed and approved* by the following:

Scott T. Phillips

Associate Professor of Chemistry

Dissertation Advisor

Chair of Committee

Kenneth S. Feldman

Professor of Chemistry

Chair of the Graduate Program of the Department of Chemistry

Ayusman Sen

Distinguished Professor of Chemistry

Robert M Rioux

Associate Professor of Chemical Engineering

*Signatures are on file in the Graduate School

ABSTRACT

Current state-of-the-art diagnostic tests are designed to perform well in laboratory settings, where clean water, continuous electric supply, chemical reagents, highly engineered equipment, and trained personnel are available. However, these tests cannot be performed in resource-limited settings, such as in remote areas of the developing world, in hospital emergency rooms, and at home. Consequently, there is a need for developing new diagnostic tests that can be performed quickly in these analytically challenging environments. One possible solution to this problem is to develop thermally stable small molecule reagents that can be used in a variety of diagnostic tests.

This thesis describes the design and synthesis of several classes of small molecule reagents that enable selective and sensitive detection of various analytes. We use these reagents to develop simple diagnostic tests that: (i) enable quantification of enzyme biomarkers using a commercially available, hand-held electrochemical reader (a glucose meter), and (ii) triage assays for enzyme biomarkers using the odor generated during the assay. We also describe the design and synthesis of small molecule reagents that enable signal amplification to enhance the sensitivity of diagnostic tests. We have developed two classes of amplification reagents that operate through self-propagating reaction sequences mediated by (i) thiols and (ii) amines.

TABLE OF CONTENTS

List of Figures	ix
List of Schemes	xiii
List of Tables	xiv
Acknowledgments	xv
Chapter 1: Reagents for point-of-care diagnostic assays	1
1.1 Introduction to diagnostic assays	1
1.2 State-of-the-art methods for disease diagnosis	3
1.2.1 Cell cultures	3
1.2.2 Enzyme assays	3
1.2.3 Enzyme-linked immunosorbent assay (ELISA)	5
1.2.4 Polymerase chain reaction (PCR)	5
1.2.5 Bio-barcode assay	7
1.3 Challenges for performing state of the art diagnostic tests in resource limited environment.	8
1.4 Point-of-care tests for disease diagnosis	10
1.5 Use of small molecule reagents in point-of-care disease diagnostics	11
1.6 Conclusions	15
1.7 References	16

Chapter 2: Development of reagents for quantifying active enzymes using a personal glucose meter	24
2.1 Introduction	24
2.2 Experimental design	26
2.2.1 A single step assay to quantify enzyme biomarkers using a glucose meter	26
2.2.2 Design of reagents that release glucose in the presence of enzyme analytes	27
2.3 Results and discussion	28
2.3.1 Synthesis of detection reagents	28
2.3.2 First generation enzyme assay	30
2.3.3 Second generation assay strategy	33
2.3.4 Quantification of alkaline phosphatase in blood serum	35
2.3.5 Evaluation of the stability of the detection reagent 2-4	37
2.4 Conclusions	40
2.5 References	41
 Chapter 3: Reagents that enable rapid triaging of enzyme assays using smell as an output	 46
3.1 Introduction	46
3.2 Experimental design	48
3.2.1 Design of a reagent that generates two distinct readouts	48
3.2.2 Design of a single-step enzyme assay strategy for triaging of samples by odor	49

3.3 Results and discussion	50
3.3.1 Synthesis of controlled release reagent 3-1	50
3.3.2 The response of reagent 3-1 to H ₂ O ₂	50
3.3.3 Single-step enzyme assay strategy for triaging of samples (by odor) and quantifying enzyme concentrations (by fluorescence)	52
3.4 Conclusions	55
3.5 References	56
 Chapter 4: Signal amplification via a self-propagating, thiol-mediated reaction sequence	 58
4.1 Introduction	58
4.2 Experimental design	63
4.3 Results and discussions	64
4.3.1 Synthesis of amplification reagent 4-9	64
4.3.2 Preliminary assay to demonstrate signal amplification using reagent 4-9	65
4.3.3 Design of amplification reagents 4-10 and 4-11 to reduce background hydrolysis	66
4.3.4 Time-dependent LC-MS study of the signal amplification reaction using reagent 4-11	68
4.3.5 Dose-dependent signal amplification using reagent 4-11	70
4.3.6 Analysis of the kinetics of signal amplification using reagent 4-11	71
4.3.7 Generality of the response of amplification reagent 4-11 to thiols	75
4.4 Conclusions	76

4.5 References	77
Chapter 5: Signal amplification via an autocatalytic, base-mediated elimination reaction	82
5.1 Introduction	82
5.2 Experimental design	83
5.2.1 Design of amplification reagent	83
5.2.2 Design of an assay strategy to detect trace levels of an analyte	84
5.3 Results and discussions	85
5.3.1 Synthesis of amplification reagent 5-1 , 5-2 , and 5-3	85
5.3.2 Time-dependent LC-MS study of the signal amplification reaction using reagent 5-1	87
5.3.3 Dose-dependent signal amplification using reagent 5-1	88
5.3.4 Evaluation of the effect of methyl ether on the rate of signal amplification using 5-1	91
5.3.5 Evaluation of the effect of releasing multiple equivalents of piperidine on the rate of signal amplification	91
5.3.6 A palladium detection assay using reagent 5-1 for signal amplification	92
5.4 Conclusions	94
5.5 References	95

Chapter 6: Material, Methods, Experimental Procedures, and Characterizations	98
6.1 Material, methods, and general experimental procedures	98
6.2 Chapter 2: Experimental procedures and characterizations	99
6.3 Chapter 3: Experimental procedures and characterizations	107
6.4 Chapter 4: Experimental procedures and characterizations	112
6.5 Chapter 5: Experimental procedures and characterizations	121
6.6 References	133
 Appendix A: NMR Spectra	135
 Appendix B: Data tables	185
 Appendix C: Permissions to Reuse Copyrighted Material	205

LIST OF FIGURES

Figure 1-1. General scheme for a diagnostic assay.	2
Figure 1-2. General scheme for a colorimetric ELISA.	5
Figure 1-3. General scheme showing the steps of (a) PCR and (b) Immuno-PCR.	6
Figure 1-4. General scheme showing the steps of the bio-barcode assay for detection of proteins.	7
Figure 2-1. A one-step assay strategy to quantify active enzymes using small molecule activity-based detection reagents and a glucose meter.	26
Figure 2-2. Activity-based detection reagents designed to release glucose for use in assays to quantify four different active enzymes using a glucose meter.	27
Figure 2-3. Calibration curve for the detection of β -galactosidase using 2-1 .	31
Figure 2-4. Calibration curve for the detection of esterase using 2-2 .	31
Figure 2-5. Calibration curve for the detection of alkaline phosphatase using 2-3 .	32
Figure 2-6. Calibration curve for the detection of penicillin-G-amidase (PGA) using 2-4 .	32
Figure 2-7. Calibration curve for the detection of β -galactosidase using 2-1 .	34
Figure 2-8. Calibration curve for the detection of alkaline phosphatase using 2-3 .	34
Figure 2-9. Calibration curve for the detection of penicillin-G-amidase (PGA) using 2-4 .	35
Figure 2-10. Calibration curve for the detection of alkaline phosphatase in blood serum using 2-3 .	36
Figure 2-11. Time-dependent LC-MS analysis of the reaction of 2-4 with penicillin-G-amidase (PGA)	37
Figure 2-12. Time-dependent LC-MS analysis of the stability of 2-4 .	38

Figure 2-13. Study of the thermal stability of detection reagent 2-4 .	39
Figure 3-1. Assay strategy for triaging samples (a) using odor generated from activity-based detection reagents present in the assay (b).	46
Figure 3-2. Reaction of the controlled release reagent 3-1 with H ₂ O ₂ (a signal-transduction molecule) to generate the dual readouts of fluorescence (3-2) and odor (ethanethiol).	48
Figure 3-3. A single-step assay strategy using controlled release reagent 3-1 and a general detection reagent (3-3).	49
Figure 3-4. Overlaid LC-MS spectra for three sequential injections of aliquots of the reaction mixture containing 0.5 mM 3-1 and 5 equivalents of H ₂ O ₂ .	51
Figure 3-5. Time dependent fluorescence emission spectra for a reaction containing 20 μM 3-1 and 1.1 equivalents of H ₂ O ₂ .	51
Figure 3-6. Dose-response curve obtained when 3-1 was treated with varying concentrations of H ₂ O ₂ .	52
Figure 3-7. The structures of specific detection reagents used in combination with 3-1 in the single-step enzyme detection assay depicted in Figure 3-3.	53
Figure 3-8. Calibration curves for the quantitative detection of the enzymes β-galactosidase and ALP using the reagents 3-1 and 3-3 .	54
Figure 4-1. Signal amplification in the context of diagnostic tests.	58
Figure 4-2. A palladium detection assay using palladium catalyzed Tsuji-Trost deallylation reaction.	59
Figure 4-3. Reaction sequence describing a F ⁻ mediated autoinductive signal amplification strategy.	60
Figure 4-4. Reaction sequence that depicts signal amplification using a reaction network.	61

Figure 4-5. Signal generated by amplification reactions that follow catalytic kinetics and autocatalytic kinetics.	62
Figure 4-6. Reaction scheme depicting a signal amplification strategy using reagents 4-9 , 4-10 , or 4-11 .	63
Figure 4-7. Normalized fluorescence signal obtained when signal amplification reagents 4-9 , 4-10 , or 4-11 were exposed to L-cysteine (0.1 or 0 equiv).	65
Figure 4-8. Presumed formation of a ketene intermediate that is responsible for background hydrolysis of 4-9 .	66
Figure 4-9. Structures of fluorescent products 4-20 , 4-21 , and 4-22 generated in amplification reactions containing reagents 4-9 , 4-10 , and 4-11 , respectively.	67
Figure 4-10. Analysis of the reaction products obtained when 4-11 was exposed to 0.1 equiv of L-cysteine.	69
Figure 4-11. Normalized fluorescence data obtained when amplification reagent 4-11 was treated with different initial quantities of ethanethiol.	70
Figure 4-12. Effect of additive 4-22 on the kinetics of signal amplification reaction using 4-11 and ethanethiol.	73
Figure 4-13. Effect of additive 4-25 on the kinetics of the signal amplification reaction using 4-11 and ethanethiol.	74
Figure 4-14. Effect of the structure of added thiol on the time required for amplification reactions using 4-11 to reach half of the maximum fluorescent signal (T_{50}).	75
Figure 5-1. General scheme depicting an autocatalytic reaction.	82
Figure 5-2. Reaction scheme depicting a base-mediated, signal amplification strategy using reagents 5-1–5-3 .	83
Figure 5-3. Reaction scheme depicting a palladium detection assay with detection reagent 5-4 and signal amplification reagents 5-1–5-3 .	84

Figure 5-4. Analysis of the reaction products obtained when 5-1 was exposed to 0.02 equiv of piperidine.	87
Figure 5-5. Normalized absorbance data obtained when amplification reagent 5-1 was treated with various initial quantities of piperidine.	88
Figure 5-6. Demonstration of autocatalytic base amplification using reagent 5-1 .	90
Figure 5-7. Effect of methyl ether (R = OMe) on the rate of release of piperidine via aza-quinone methide elimination.	91
Figure 5-8. Effect of the inclusion of methyl ether in the 4-aminobenzyl linker (5-1), and the release of two equivalents of piperidine (5-3) on the rate of signal amplification	92
Figure 5-9. Palladium detection assay using the reaction of Pd (analyte), 5-4 (detection reagent), and 5-1 (amplification reagent).	93
Figure 6-1. UV-Vis spectra of bromocresol green after addition of a solution of selected amines.	132

LIST OF SCHEMES

Scheme 1-1. Reaction scheme describing the ZstatFlu test for influenza diagnosis.	12
Scheme 1-2. Reaction scheme describing a β -lactamase fluorescence assay for tuberculosis diagnosis.	13
Scheme 1-3. Reaction scheme depicting the chemistry used in a colorimetric ALP assay for liver function testing.	14
Scheme 2-1. Synthesis of esterase detection reagent 2-2 .	29
Scheme 2-2. Synthesis of protease detection reagent 2-4 .	29
Scheme 3-1. Synthetic route to controlled release reagent 3-1 .	50
Scheme 4-1. Synthetic route to amplification reagent 4-9 .	64
Scheme 4-2. Synthetic route to amplification reagent 4-10 .	66
Scheme 4-3. Synthetic route to amplification reagent 4-11 .	67
Scheme 5-1. Synthesis of amplification reagent 5-1 .	85
Scheme 5-2. Synthesis of amplification reagent 5-2 .	86
Scheme 5-3. Synthesis of amplification reagent 5-3 .	86

LIST OF TABLES

Table 1-1. Summary of select biomarkers that are quantified in various biological samples for diagnosis of some major diseases worldwide.	1
Table 1-2. Examples of common enzyme assays used in diagnostics	4
Table 1-3. Summary of key requirements for performing select diagnostic tests for several major communicable diseases.	9
Table 1-4. The ASSURED criteria.	10
Table 1-5. Examples of POCT that are commercially available.	11
Table 2-1. Determination of the concentration of alkaline phosphatase in various serum samples.	36
Table 2-2. The effect of the decomposition of 2-4 on the results of the assay for PGA.	39

ACKNOWLEDGEMENTS

I would like to thank my dissertation advisor, Professor Scott Phillips, for his support and guidance. I appreciate his continuous efforts in making me a better researcher, writer, and speaker. His incredible creativity and capacity for hard work will continue to inspire me when I pursue my own independent career. I would also like to thank the members of my doctoral committee, Professor Kenneth Feldman, Professor Ayusman Sen, and Professor Robert Rioux, for their valuable feedback for my oral comprehensive examination and thesis defense.

I would like to express my gratitude to all the current and former members of the Phillips research group for the welcoming work environment and for all the great scientific discussions we had. I would also like to thank Anthony DiLauro and Dr. Kyle Schmid for all the help with writing my dissertation and research reports.

Lastly, I would like to thank my family for their unconditional love and support.

CHAPTER 1

Reagents for point-of-care diagnostic assays

1.1 Introduction to diagnostic assays

Diagnostic assays for the detection (and quantification) of trace analytes play a critical role in healthcare, such as in timely identification of diseases, choosing appropriate treatment, preventing worsening of symptoms, preventing transmission of diseases, and ensuring the quality of food, drinking water, and drugs.¹⁻³ For example, diagnosis and management of diabetes mellitus relies heavily on the quantification of glucose in urine and blood. Similarly, quantifying various biomarkers in biological samples is crucial for reducing the burden of various diseases on human health (Table 1-1). These biomarkers can be ions (e.g., nitrite⁴), small molecules (e.g., glucose⁵), proteins (e.g., prostate-specific antigen⁶), nucleic acids (e.g., HIV-1 RNA⁷), and whole cells (e.g., malaria parasite⁸).

Table 1-1. Summary of select biomarkers that are quantified in various biological samples for diagnosis of some major diseases worldwide.

Diseases	Estimated worldwide deaths in 2008 ⁹	Biomarkers for diagnosis (biological fluid)
Ischaemic heart disease	7,254,444	Myeloperoxidase (blood), cardiac troponin T (blood) ¹⁰
Lower respiratory infections (Pneumonia, Bronchitis, Influenza, etc.)	3,463,294	Influenza neuraminidase (nasal aspirate, sputum) ¹¹ , microorganism specific antigen (blood, nasal aspirate, sputum) ¹²
Diarrheal diseases	2,464,425	Microorganism specific antigen (stool) ¹³ , β -D-glucuronidase (drinking water) ¹⁴
HIV/AIDS	1,776,270	HIV DNA (blood), HIV p24 antigen (blood), HIV-1 RNA (blood) ⁷
Tuberculosis	1,341,771	INF- γ (blood) ¹⁵ , TB β -lactamase (sputum) ¹⁶ , TB protease (blood) ¹⁷
Malaria	826,908	<i>P. falciparum</i> histidine-rich protein-2 (blood) ¹⁸ , plasmodium aldolase (blood) ¹⁸ , plasmodium lactate dehydrogenase (blood). ¹⁹

Concentrations of diagnostic biomarkers in biological fluids are usually small. Detection and quantification of these biomarkers requires diagnostic assays that are extremely sensitive (i.e., ideally only a few copies of the biomarker should be able to generate a measurable signal) and selective (i.e., the biomarker can be detected in a complex mixture without interference from other species with similar structure or reactivity).

Selectivity in diagnostic assays is achieved by using a detection reagent (Figure 1-1). The detection reagent responds selectively to the target biomarker and generates a signaling molecule. Detection reagents can be natural receptors (e.g., antibodies specific to HIV-1 RNA⁷), synthetic receptors (e.g., aptamers that selectively bind cocaine²⁰), enzymes (e.g., glucose oxidase²¹ for glucose quantification), or reaction-based detection reagents (e.g., 5-bromo-4-chloro-3-indolyl- β -D-galactopyranoside, which selectively reacts with β -galactosidase²²).

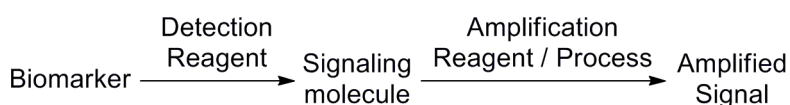


Figure 1-1. General scheme for a diagnostic assay.

The response of a signaling molecule in a diagnostic assay can sometimes be directly quantified. However, most sensitive assays require an amplification step to achieve detection of the target biomarkers. The amplification step can be reaction-based (e.g., enzyme catalysis) or a downstream physical change that is a direct consequence of the detection event (e.g., aggregation of nanoparticles leading to a color enhancement due to surface plasmon resonance).²³ The most sensitive techniques currently used for disease diagnosis typically utilize a combination of amplification processes to achieve the highest sensitivity. This chapter highlights the state of the art techniques for quantitative detection of disease biomarkers, the challenges in employing these methods in resource limited settings (such as in a remote village), and some recent attempts to address these challenges using small molecule reagents.

1.2 State-of-the-art methods for disease diagnosis

1.2.1 Cell cultures

For decades, cell culture has been the standard method for diagnosing bacterial diseases. For example, bacterial culture remains the primary method to confirm the presence of *V. cholera* in stool samples when a cholera epidemic is suspected.¹³ The high sensitivity of this method arises from rapid multiplication of bacterial colonies (the amplification process) in a nutrient rich medium. Selective identification of bacteria is usually achieved by observing the response of the cultured medium to anti-serum (detection reagent) that is selective towards a particular bacterial species.

1.2.2 Enzyme assays

Enzyme assays are perhaps the most widely used methods to quantify critical metabolites and protein biomarkers in biological samples.²⁴ These diagnostic tests utilize enzyme-catalyzed chemical transformations of small molecule substrates accompanied by a measurable physical change. Although a majority of enzyme assays generate a colorimetric signal, they can be adapted to include a variety of measurement techniques, including fluorescence²⁵, chemiluminiscence²⁶, phosphorescence^{27–28}, amperometry²⁹, calorimetry³⁰, radiometry³¹, and magnetic resonance^{32–34}. The selectivity of enzymatic assays depends on the substrate-specificity of the enzyme, while the signal amplification is innate to enzyme-catalyzed transformations due to enzymatic turnover. Enzyme assays in the context of diagnostic assays can be classified into two categories: (i) enzyme as the biomarker, and (ii) enzyme as the detection reagent (Table 1-2)

Table 1-2. Examples of common enzyme assays used in diagnostics

Type	Biomarkers	Detection reagents	Conditions being tested
Enzymes as reagents	D-Glucose ⁵	Glucose oxidase + horseradish peroxidase (HRP) + chromogenic mediator	Diabetes mellitus, hyperthyroidism, Cushing's syndrome, liver diseases, shock
	Urea ²⁴	Urease + glutamate dehydrogenase + 2-oxoglutarate + NADH	Kidney health
	Creatinine ²⁴	Creatininase + creatinase sarcosine oxidase + HRP + chromogenic mediator	Kidney health
	Cholesterol ²⁴	Cholesterol oxidase + HRP + chromogenic mediator	Coronary health
Enzymes as biomarkers	Alkaline phosphatase ³⁵	p-Nitrophenylphosphate or 5-bromo-4-chloro-3-indolyl phosphate	Liver health, bile duct obstruction
	Aspartate aminotransferase ³⁶	α -oxoglutarate + NADH	Liver health, cardiac health
	Alanine transaminase ³⁷	L-alanine + pyruvate oxidase + horseradish peroxidase + chromogenic mediator	Liver health
	β -glucuronidase ¹⁴	Phenolphthalein glucuronide	<i>E. coli</i> contamination of water
	β -galactosidase ²²	5-bromo-4-chloro-3-indolyl- β -D-galactopyranoside	Fecal contamination of water
	Viral neuraminidase ³⁸	2'-(4-Methylumbelliferyl)- α -D-N-acetylneuraminic acid	Influenza (Type A & B)

1.2.3 Enzyme-linked immunosorbent assay (ELISA)

Enzyme assays require substrates that are selectively processed by the enzyme. However, it is not always possible to find an enzyme-substrate pair to achieve selective detection of a biomarker in a complex mixture. This limitation is avoided in enzyme-linked immunosorbent assays (ELISA).³⁹ Unlike enzyme assays, ELISA (Figure 1-2) uses three different reagents: a solid-supported antibody (the detection reagent), a labeled antibody (the linker), and a labeled enzyme (the amplification reagent). The selective binding of the target by the solid-supported antibody is followed by the co-immobilization of the labeled enzyme through the linker antibody. Signal amplification is achieved through an enzyme-catalyzed transformation. A similar immunoassay that does not use the enzyme based amplification, but directly translates the antibody-based detection into a colorimetric read-out also is used widely.

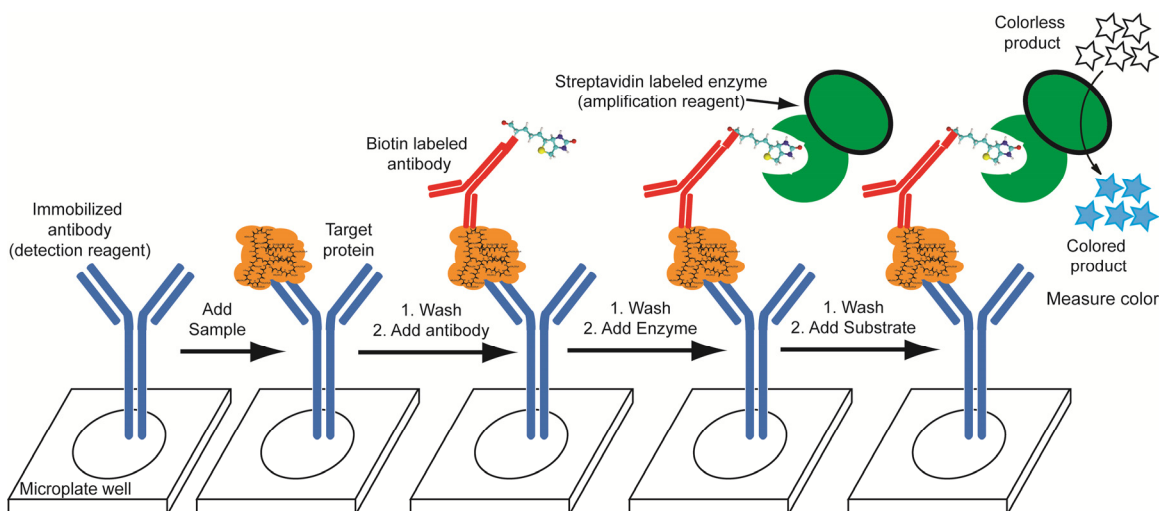


Figure 1-2. General scheme for a colorimetric ELISA.

1.2.4 Polymerase chain reaction (PCR)

The polymerase chain reaction (PCR) is the gold standard method for quantification of nucleic acid targets.⁴⁰ Compared to enzyme-based assays (including ELISA), PCR achieves higher sensitivities through target amplification (rather than signal amplification as seen in enzyme assays). Using a sequence of temperature controlled reactions (Figure 1-3a), PCR achieves doubling of the DNA target for every

reaction cycle. Multiple cycles of the reaction sequence results in exponential rise in the concentration of the target in the reaction mixture. The concentration of the target is usually followed in real time (quantitative PCR) using fluorescently labeled DNA probes that selectively hybridize with the target.

Real-time quantitative PCR can only quantify nucleic acid targets. This limitation can be solved using a variant of PCR called immuno-PCR.⁴¹ In immuno-PCR the detection of non-nucleic acid targets (like proteins) is achieved using antibodies (Figure 1-3b). The detection event is followed by the co-immobilization of a DNA-labeled antibody. The immobilized DNA is then amplified using PCR and quantified using fluorescent probes.

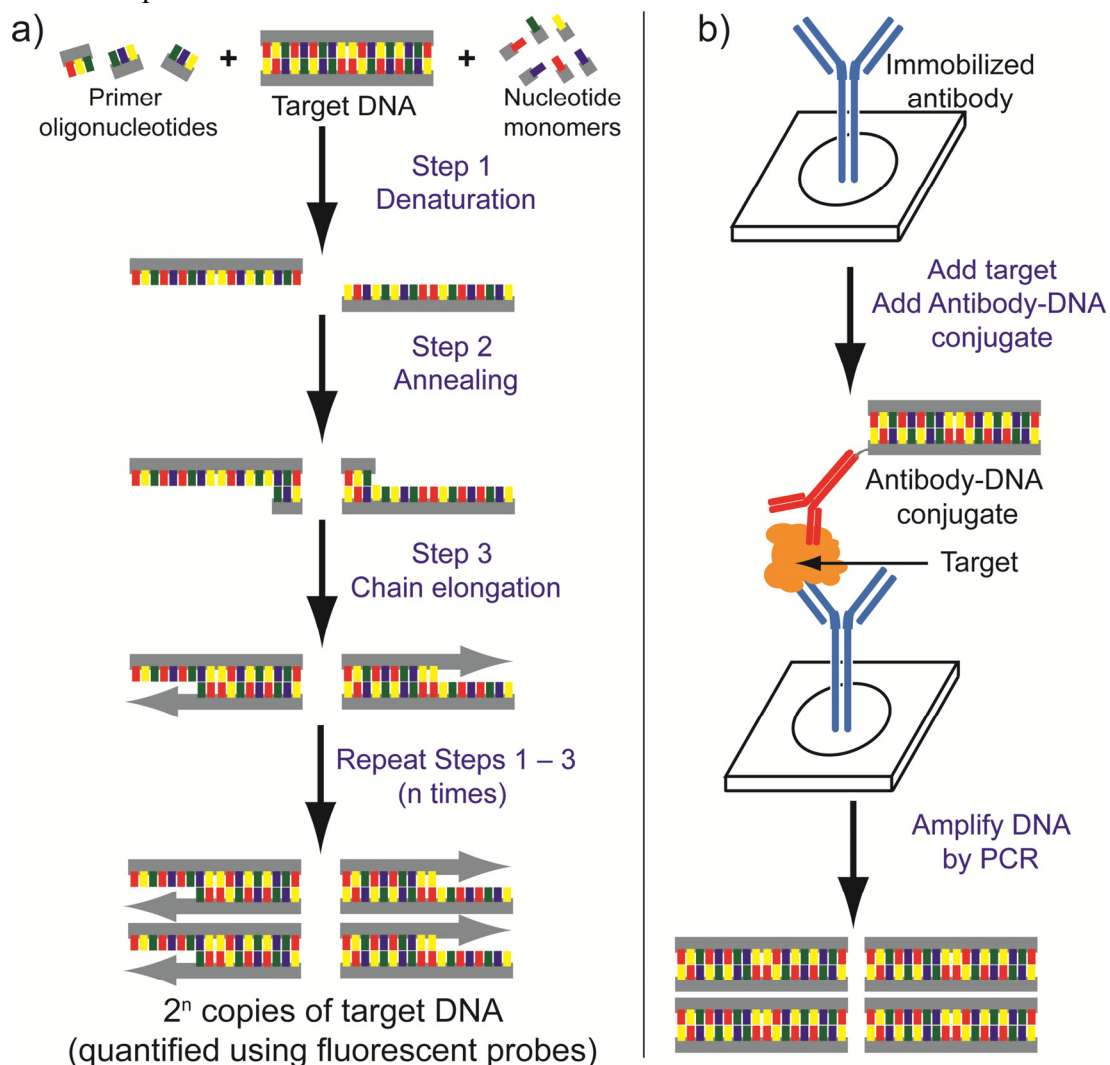


Figure 1-3. General scheme showing the steps of (a) PCR and (b) Immuno-PCR

1.2.5 Bio-barcode assay

The bio-barcode assay is an alternative to immuno-PCR.⁴²⁻⁴³ It uses DNA functionalized gold nanoparticles (AuNP) to achieve both target and signal amplification. Similar to immuno-PCR, the bio-barcode assay uses antibodies to capture and concentrate the target (Figure 1-4). Using DNA functionalized AuNPs, a single captured target undergoes signal transduction to produce multiple copies of the barcode DNA (target amplification). The released barcode DNA and a second DNA functionalized AuNP are then co-immobilized on a solid substrate. The immobilized AuNP is used as a catalyst for reduction of Ag(I) salt to precipitate Ag(0). The precipitated Ag(0) can be quantified by measuring the reflectance of the reaction spot on the substrate. The multiple amplification steps of the bio-barcode technique allows for detection of atto molar levels of the target.⁴²

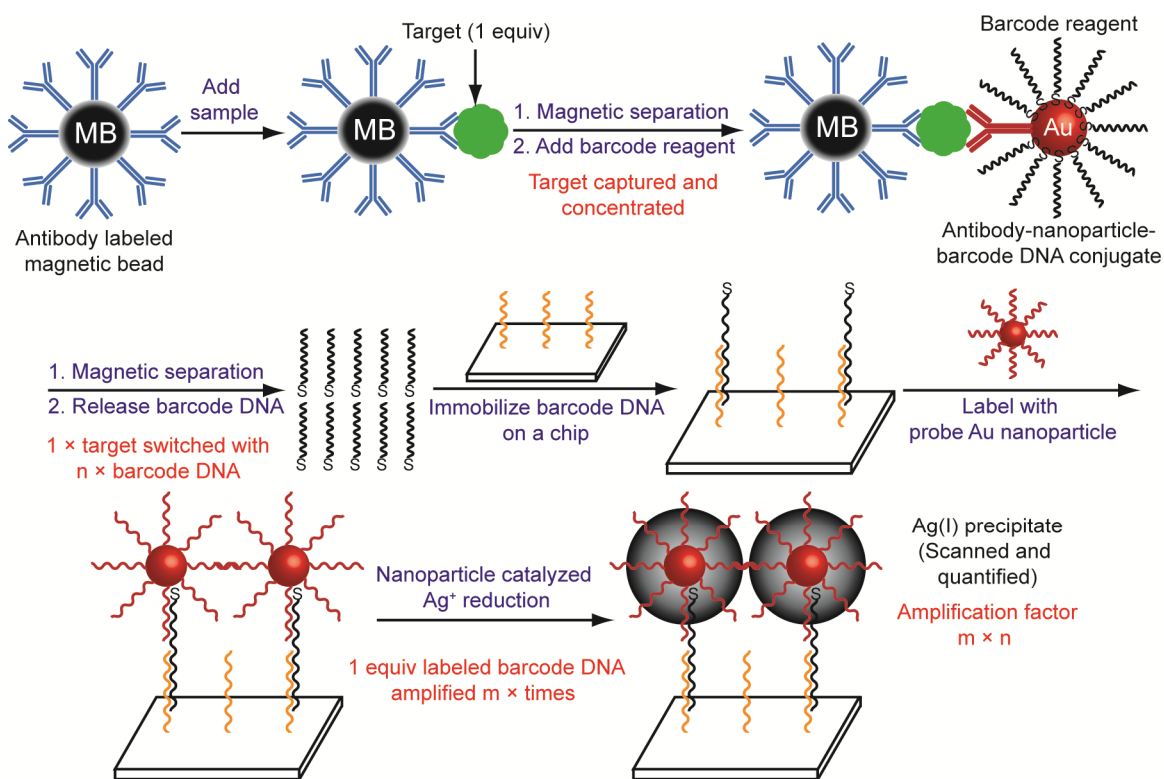


Figure 1-4. General scheme showing the steps of the bio-barcode assay for detection of proteins.⁴³

1.3 Challenges for performing state of the art diagnostic tests in resource limited environment.

The state of the art methods for diagnostic tests have been implemented in hospitals throughout the developed world. In fact, modern hospitals now have automated systems that can run several tests on a sample of blood and store the test results in electronic format.^{1,44} However, these tests cannot routinely be done in resource limited environments (such as rural areas of the developing world).^{1,3} The limitations of these diagnostic tests that prevent their widespread use are:

1. *Require well-equipped laboratory:* These tests usually require expensive equipment for running the test and analyzing the test results. For example, PCR assays require a thermal cycler and a spectrophotometer to follow the reaction in real-time. Moreover, these assays routinely require access to clean water, reliable electricity, and efficient waste disposal systems. This limits their use to well funded health-care facilities with well-equipped laboratories, such as large hospitals.
2. *Require trained technicians to run the tests:* These diagnostic tests usually involve several steps that need to be carried out in a controlled environment by trained technicians. For example, the immuno-PCR and the bio-barcode assays require several time-sensitive steps to be performed sequentially to achieve the highest levels of sensitivity.
3. *Require refrigeration for reagent storage:* The majority of reagents used in these tests require refrigeration for long term storage stability. The performance of some detection reagents can drop significantly if they experience large temperature fluctuations during transportation and storage. For example, the recommended storage temperature for labeled antibody specific to INF- γ for TB diagnostic test is 2–8 °C.⁴⁵ The performance of improperly stored antibodies can sometimes be too variable to run accurate quantitative diagnostic assays.

Table 1-3 summarizes the key requirements of running diagnostic tests for several major communicable diseases.

Table 1-3. Summary of key requirements for performing select diagnostic tests for several major communicable diseases.

Diseases	Molecular diagnostic tests	Reagents required	Equipment required
Influenza ¹¹	PCR and reverse transcriptase PCR	Oligonucleotide primers, probe nucleotide, enzymes (polymerase, reverse transcriptase)	Refrigerator, thermocycler, spectrometer, centrifuge
	Immunoassay	Capture antibody, labeled antibody	Refrigerator, spectrometer
	Neuraminidase assay	NA-Star [®] substrate ^a	Refrigerator ^a , chemiluminiscent reader
Malaria ⁴⁶	Immunoassay ^b	Capture antibody, labeled antibody	Refrigerator, UV-Vis spectrophotometer or fluorometer
Tuberculosis ¹⁵	Tuberculin skin test (TST) ^c	Purified protein from <i>M. tuberculosis</i>	Refrigerator
	ELISA (QuantiFERON [®] Gold-TB test and T-SPOT [®] -TB test)	Purified protein from <i>M. tuberculosis</i> , capture antibody, enzyme labeled antibody	Refrigerator, UV-Vis spectrophotometer or fluorometer
HIV/AIDS ⁷	PCR	Oligonucleotide primers, probe nucleotide, enzymes (polymerase)	Refrigerator, thermocycler, UV-Vis spectrometer
	Immunoassay ^d	Capture antibody, labeled antibody	Refrigerator, UV-Vis spectrophotometer or fluorometer
Diarrheal diseases ¹³ (Cholera, <i>E. coli</i> , Botulism, etc.)	Bacterial culture	Culture medium, proteins	Infectious waste disposal
	Immunoassay	Capture antibody, labeled antibody	Refrigerator

- NA-Star[®] Substrate is a small molecule neuraminidase substrate that generates a chemiluminiscent product in presence of viral neuraminidase; this reagent can be stored at room temperatures (20 °C) for a short period of time.³⁸
- Microscopic detection of the parasite is the most reliable method for diagnosing malaria.
- The commonly used tuberculin skin testing (TST) can give false positive or false negative results in some individuals.
- Simple diagnostic tests for HIV specific antigen exist. These tests are robust but are not sufficiently sensitive for early detection of infection.

1.4 Point-of-care tests for disease diagnosis

Point-of-care tests (POCT) refer to diagnostic tests that can be performed near the patient, such as at home, patient's bedside, a physician's clinic, or by first-responders at an accident site. The importance of POCT becomes more apparent in remote areas of the world where diagnostic tests must be performed in areas far away from a hospital setting. The World Health Organization (WHO) has outlined the ASSURED criteria that should be met by an ideal POCT (Table 1-4).³ These recommendations aim to make diagnostic test more accessible for use in the most resource limited areas of the world.

Healthcare centers in remote areas of the world usually do not have the resources or the trained laboratory technicians to run molecular diagnostics tests. Disease diagnosis in such areas is usually based upon symptoms and local prevalence of the disease. This situation can sometimes lead to over-diagnosis and unnecessary treatment.^{1,3}

Therefore, an ideal POCT should be inexpensive, user-friendly, and require minimal user input, so as to allow for improved accuracy in disease diagnosis. Ideally, these tests should be very sensitive and selective, so that there are minimal false negative or false positive test results. These tests also should be robust and avoid using thermally sensitive reagents. This criterion is particularly important for these tests to be deliverable to patients in remote areas of tropical countries, where temperatures frequently exceed 40 °C.¹

Table 1-4. The ASSURED criteria.

WHO criteria for ideal POCT	
A	Affordable by those at risk
S	Sensitive
S	Selective
U	User-friendly
R	Rapid and Robust
E	Equipment free
D	Deliverable to those at risk

The most commonly performed POCT is urinalysis using urine test strips.⁴⁷ These test strips provide semi-quantitative measurements of several metabolites and proteins in urine that can assist a physician in diagnosing diabetes, renal and urinary tract diseases, and liver diseases. Apart from urine test strips, electrochemical assays for blood glucose (using a glucose meter) and lateral-flow immunoassays are also available (Table 1-5). Most of the lateral-flow immunoassays are qualitative tests and are usually not sensitive enough for early detection of disease biomarkers; hence, there is a need for developing new assay strategies that meet the ASSURED criteria.

Table 1-5. Examples of POCT that are commercially available

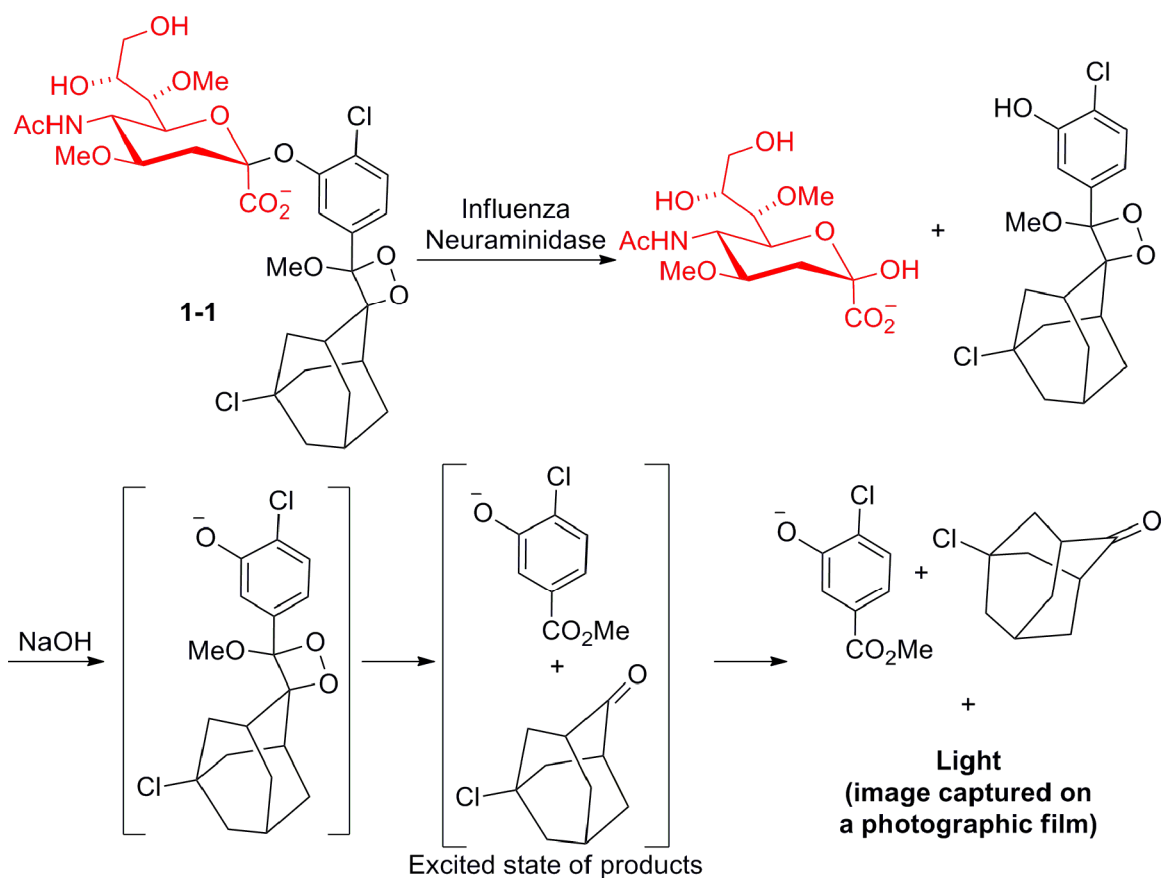
Test	Detection reagents used	Notes
Blood glucose test ²⁹	Glucose oxidase, $\text{Fe}(\text{CN})_6^{3-}$ (coupled redox reaction)	Widely used
Home pregnancy test ⁴⁸	hCG capture antibody, control antibody, AuNP-antibody conjugate (lateral flow immunoassay)	Widely used
HIV home test ⁷	anti-HIV antibody capture antibody, control antibody, AuNP-antibody conjugate (lateral flow immunoassay)	Not sensitive enough for early detection
Malaria rapid diagnostic tests ⁴⁶	<i>P. falciparum</i> lactate dehydrogenase capture antibody, control antibody, AuNP-antibody conjugate (lateral flow immunoassay)	Qualitative test, variability in test performance
Influenza (A and B subtypes) test ¹¹	Influenza antigen capture antibody, control antibody, AuNP-antibody conjugate (lateral flow immunoassay)	Poor sensitivity, requires confirmation by other methods
Drug abuse test ⁴⁹	Drug metabolite capture antibody, enzyme-metabolite conjugate, control antibody, Au NP-antibody conjugate (enzyme multiplied lateral flow immunoassay)	Poor sensitivity and selectivity, requires confirmation by other methods

1.5 Use of small molecule reagents in point-of-care disease diagnostics

Many of the currently used POCT require thermally sensitive reagents like antibodies and enzymes. These biomolecular detection reagents can irreversibly denature and lose their function if they experience elevated temperatures during transportation and storage. Consequently, these test frequently do not meet the standards of the ASSURED criteria. A possible solution is to develop small molecule, stimuli-responsive reagents for use in POCT. Small molecule reagents are more stable than antibodies and enzymes and can potentially address several other limitations of the currently used assay strategies. Thus, there is a need for developing thermally stable reagents that: (a) selectively detect biomarkers for disease, and (b) amplify signal to enhance the sensitivity of the detection assay. Only a few small molecule reagents have been used in the context of POCT; select examples are described below.

The ZstatFlu test for influenza diagnosis^{50,51}: Influenza A and B viruses require the enzyme neuraminidase to detach from the host cell and infect new cells.⁵² As the infection progresses, viral particles (along with the neuraminidase enzyme) are shed in the upper respiratory tract of the infected host. The neuraminidase enzyme activity in respiratory mucus is a useful biomarker for influenza. The ZstatFlu is a chemiluminescence based enzyme assay that uses a small molecule substrate to measure viral neuraminidase activity in mucus collected by a nasal swab.

Scheme 1-1. Reaction scheme describing the ZstatFlu test for influenza diagnosis



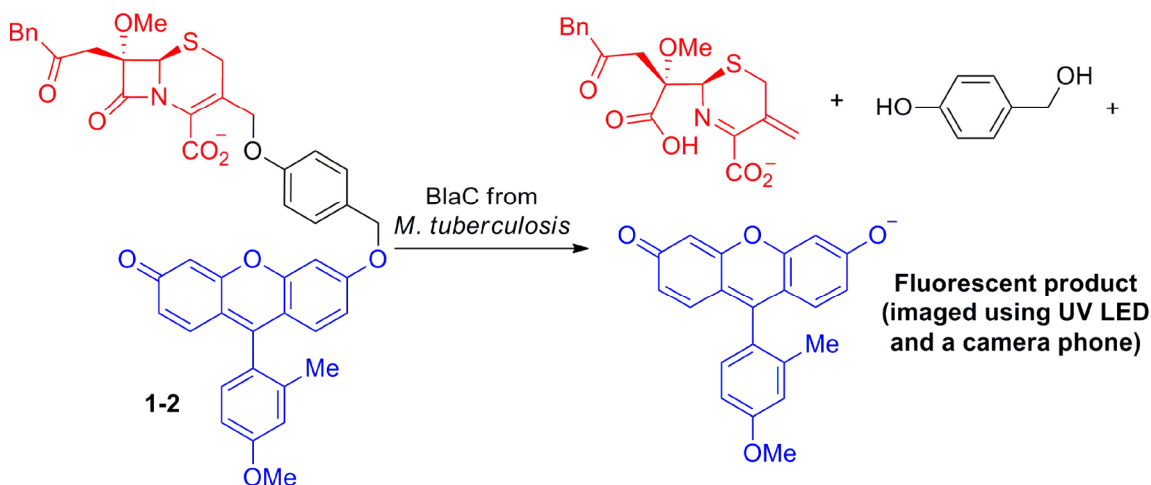
The detection reagent (**1-1**) used in the ZstatFlu test is a derivative of N-acetyl neuraminic acid with a pendant 1,2-dioxetane moiety. In the presence of viral neuraminidase, the glycosidic bond of the N-acetyl neuraminic acid derivative is cleaved. The pH of the resulting solution is then raised to a value (~ 9.0) that is optimal for chemiluminescence measurements. The intermediate phenoxide undergoes thermolysis to form carbonyl compounds in their excited state. The excited species then relax to their respective ground states, resulting in the release of photons.^{53,54} In the ZstatFlu test, the chemiluminescent light produced is captured on a Polaroid

photographic film. A semi-quantitative measure of viral neuraminidase activity can then be obtained by reading the photographic plate using a portable imaging device. A quantitative measure of enzyme activity can also be obtained using a luminometer in a laboratory setting.

The ZstatFlu test is extremely sensitive (it can detect pM levels of viral neuraminidase), selective (it is not affected by other upper respiratory infectious agents like adenoviruses, streptococcus, staphylococcus, etc.), and rapid (a 15-minute assay time is sufficient to confirm the presence of viral neuraminidase in nasal aspirate of influenza patients).

β -Lactamase assay for tuberculosis diagnosis: *Mycobacterium tuberculosis* (MycTB), the causative agent of TB, releases a β -lactamase enzyme to protect itself from β -lactam antibiotics. Consequently, there are many colorimetric and fluorescence probes to image MycTB and other β -lactamase releasing bacteria.^{55–57} Until recently, there were no probes specific for β -lactamase from MycTB (BlaC). Rao and coworkers screened several synthetic cephalosporin substrates and found compound **1-2** to be selective towards BlaC (over similar β -lactamases).⁵⁸ In the presence of BlaC, **1-2** undergoes a series of hydrolytic elimination reactions to release a fluorescent reporter (Scheme 1-2). The fluorescent product was quantified using a portable device containing a UV-LED and a camera phone. The assay for MycTB using **1-2** was sensitive (about 100 bacilli of MycTB in human sputum could be detected) and selective (the assay could quantify MycTB over other species like *P. aeruginosa*, *S. Aureus*, *M. smegmatis*, MRSA, and *E. Coli*).

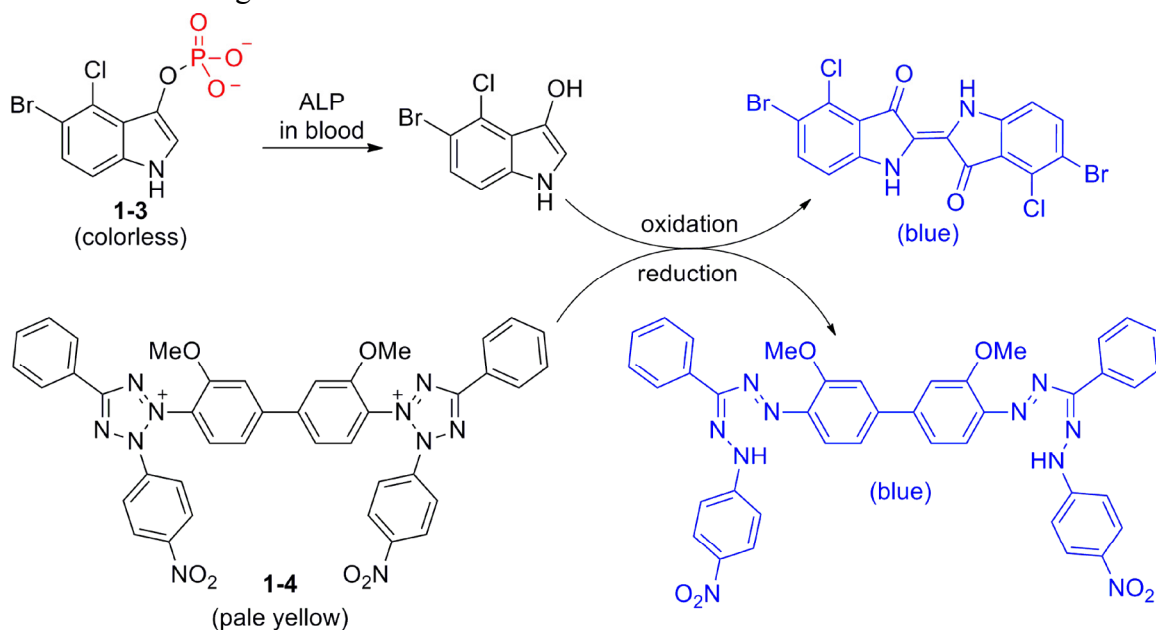
Scheme 1-2. Reaction scheme describing a β -lactamase fluorescence assay for tuberculosis diagnosis.



Liver function tests using a paper based microfluidic device: Liver function tests (assays for alkaline phosphatase (ALP), aspartate aminotransferase (AST), alanine transaminase (ALT), total protein, etc.) are a class of enzyme assays that are crucial to evaluate liver function in at-risk individuals, such as patients with hepatitis B and C, alcohol liver diseases, bile-duct obstruction, and patients being treated for HIV-AIDS and TB.⁵⁹ Currently, the liver function tests are limited to laboratory settings in hospitals, which make them unsuitable for use at the POC.

Whitesides and coworkers have developed a paper-based microfluidic device that can run multiplexed enzyme assays to quantify ALP, AST, ALT, and other proteins in blood.⁶⁰ These assays use thermally-stable small molecule reagents stored within the device. Scheme 1-3 depicts one of the chemical transformations used to assay ALP in blood obtained from a finger prick. Briefly, ALP catalyzes the hydrolysis of the phosphate group on a 3-indolyl phosphate substrate (**1-3**). The hydroxy indole reaction product is oxidized in presence of tetrazolium blue T dye (**1-4**) to produce bright blue products. These reactions take place in hydrophilic channels of the microfluidic device. The blue color generated from the reaction can then be compared with a color chart to obtain a semi-quantitative measurement of the levels of enzyme present in the blood sample. The assay time for the quantification of clinically relevant levels of ALP in blood (30 – 120 UL⁻¹) was 20 minutes.

Scheme 1-3. Reaction scheme depicting the chemistry used in a colorimetric ALP assay for liver function testing.



1.6 Conclusions

This chapter has outlined several diagnostic tests that achieve impressive levels of sensitivity under ideal conditions. These tests, however, have not been used widely in point-of-care (POC) settings. Limitations that need to be addressed include the dependence on thermally sensitive reagents and complexity of running these tests. The use of small molecule reagents provides a useful alternative to the current state-of-the art diagnostic tests. There are a few simple diagnostic tests that use small molecule reagents, but there remains a need for new reagents that can achieve sensitive and selective detection of disease biomarkers through tests that are simple to perform.

This thesis describes the design and synthesis of several classes of small molecule reagents that enable quantitative detection of enzyme biomarkers. We have used these reagents to develop assay strategies that will allow us to run diagnostic tests both at POC and in laboratory settings. We also describe the design and synthesis of reagents that enable signal amplification in diagnostic assays. Signal amplification strategies will allow us to enhance the sensitivity of diagnostic assays.

1.7 References

1. Yager, P.; Domingo, G. J.; Gerdes, J. Point-of-Care Diagnostics for Global Health. *Annu. Rev. Biomed. Eng.* **2008**, *10*, 107–144.
2. Giljohann, D. A.; Mirkin, C. A. Drivers of Biodiagnostic Development. *Nature* **2009**, *462*, 461–464.
3. Urdea, M.; Penny, L. A.; Olmsted, S. S.; Giovanni, M. Y.; Kaspar, P.; Shepherd, A.; Wilson, P.; Dahl, C. A.; Buchsbaum, S.; Moeller, G.; Burgess, D. C. H. Requirements for High Impact Diagnostics in the Developing World. *Nature* **2006**, *444*, 73–79.
4. Tsikas, D.; Gutzki, F.-M.; Stichtenoth, D. O. Circulating and Excretory Nitrite and Nitrate as Indicators of Nitric Oxide Synthesis in Humans: Methods of Analysis. *Eur. J. Clin. Pharmacol.* **2006**, *62*, 51–59.
5. Kondepati, V. R.; Heise, H. M. Recent Progress in Analytical Instrumentation for Glycemic Control in Diabetic and Critically Ill Patients. *Anal. Bioanal. Chem.* **2007**, *388*, 545–563.
6. Bock, J. L.; Klee, G. G. How Sensitive Is a Prostate-Specific Antigen Measurement? How Sensitive Does It Need to Be? *Arch. Pathol. Lab. Med.* **2004**, *128*, 341–343.
7. WHO recommendations. Diagnosis of HIV infection in infants and children, 2010. <http://www.who.int/hiv/pub/paediatric/diagnosis/en/> (accessed 06/24/2014).
8. WHO publications. Parasitological confirmation of malaria diagnosis, 2009. <http://www.who.int/malaria/publications/atoz/9789241599412/en/> (accessed 06/24/2014).

9. Global Health Observatory Data Repository, WHO. Mortality and global health estimates: Cause-specific mortality, 2008. <http://apps.who.int/gho/data/node.main.886?lang=en> (accessed 06/24/2014).
10. Baldus, S.; Heeschen, C.; Meinertz, T.; Zeiher, A. M.; Eiserich, J. P.; Münzel, T.; Simoons, M. L.; Hamm, C. W. Myeloperoxidase Serum Levels Predict Risk in Patients with Acute Coronary Syndromes. *Circulation* **2003**, *108*, 1440–1445.
11. WHO Global Influenza Surveillance Network. WHO Recommendations. Manual for the laboratory diagnosis and virological surveillance of influenza, 2011 http://www.who.int/influenza/gisrs_laboratory/manual_diagnosis_surveillance_influenza/en/ (accessed 06/24/2014).
12. Lim, W. S.; Baudouin, S. V.; George, R. C.; Hill, A. T.; Jamieson, C.; Le Jeune, I.; Macfarlane, J. T.; Read, R. C.; Roberts, H. J.; Levy, M. L.; Wani, M.; Woodhead, M. A. British Thoracic Society Guidelines for the Management of Community Acquired Pneumonia in Adults: Update 2009. *Thorax* **2009**, *64*, 1–55.
13. Global Disease Detection (GDD) Manual: Rapid Diagnostic Test for Cholera, CDC. Laboratory Testing for Cholera, 2011. <http://www.cdc.gov/cholera/laboratory.html> (accessed 06/24/2014).
14. Frampton, E. W.; Restaino, L. Methods for *Escherichia coli* Identification in Food, Water and Clinical Samples Based on β -glucuronidase Detection. *J. Appl. Bacteriol.* **1993**, *74*, 223–233.
15. Morbidity and Mortality Weekly Report, CDC. Updated Guidelines for Using Interferon Gamma Release Assays to Detect *Mycobacterium tuberculosis* Infection, U. S. A., 2010. <http://www.cdc.gov/mmwr/preview/mmwrhtml/rr5905a1.html> (accessed 06/24/2014).

16. Flores, A. R.; Parsons, L. M.; Pavelka, M. S. Genetic Analysis of the β -Lactamases of *Mycobacterium Tuberculosis* and *Mycobacterium Smegmatis* and Susceptibility to β -Lactam Antibiotics. *Microbiology* **2005**, *151*, 521–532.
17. Shende, N.; Gupta, S.; Bhatia, A. S.; Kumar, S.; Harinath, B. C. Detection of Free and Immune-Complexed Serine Protease and its Antibody in TB Patients with and without HIV Co-Infection. *Int. J. Tuberc. Lung Dis.* **2005**, *9*, 915–919.
18. Richter, J.; Göbels, K.; Müller-Stöver, I.; Hoppenheit, B.; Häussinger, D. Co-Reactivity of Plasmodial Histidine-Rich Protein 2 and Aldolase on a Combined Immuno-Chromographic-Malaria Dipstick (ICT) as a Potential Semi-Quantitative Marker of High *Plasmodium falciparum* Parasitaemia. *Parasitol. Res.* **2004**, *94*, 384–385.
19. Grigg, M. J.; William, T.; Barber, B. E.; Parameswaran, U.; Bird, E.; Piera, K.; Aziz, A.; Dhanaraj, P.; Yeo, T. W.; Anstey, N. M. Combining Parasite Lactate Dehydrogenase-Based and Histidine-Rich Protein 2-Based Rapid Tests To Improve Specificity for Diagnosis of Malaria Due to *Plasmodium knowlesi* and Other Plasmodium Species in Sabah, Malaysia. *J. Clin. Microbiol.* **2014**, *52*, 2053–2060.
20. Tombelli, S.; Minunni, M.; Mascini, M. Aptamers-Based Assays for Diagnostics, Environmental and Food Analysis. *Biomol. Eng.* **2007**, *24*, 191–200.
21. Wilson, R Turner, A. P. F. Glucose Oxidase : An Ideal Enzyme. *Biosens. Bioelectron.* **1992**, *7*, 165–185.
22. Kiernan, J. A. Indigogenic Substrates for Detection and Localization of Enzymes. *Biotech. Histochem.* **2007**, *82*, 73–103.
23. Tokel, O.; Inci, F.; Demirci, U. Advances in Plasmonic Technologies for Point of Care Applications. *Chem. Rev.* **2014**, *114*, 5728–5752.

24. Burtis, C. A.; Ashwood, E. R.; Border, B.; Tietz, N. W. *Tietz Fundamentals of Clinical Chemistry*, 5th ed.; W. B. Saunders Company: U. S. A., 2001.
25. Goddard, J.-P.; Reymond, J.-L. Recent Advances in Enzyme Assays. *Trends Biotechnol.* **2004**, 22, 363–370.
26. Kricka, L. J.; Voyta, J. C.; Bronstein, I. Chemiluminescent Methods for Detecting and Quantitating Enzyme Activity. *Methods Enzymol.* **2000**, 305, 370–390.
27. Wu, P.; He, Y.; Wang, H.-F.; Yan, X.-P. Conjugation of Glucose Oxidase onto Mn-Doped ZnS Quantum Dots for Phosphorescent Sensing of Glucose in Biological Fluids. *Anal. Chem.* **2010**, 82, 1427–1433.
28. Yan, H.; Wang, H.-F. Turn-on Room Temperature Phosphorescence Assay of Heparin with Tunable Sensitivity and Detection Window Based on Target-Induced Self-Assembly of Polyethyleneimine Capped Mn-Doped ZnS Quantum Dots. *Anal. Chem.* **2011**, 83, 8589–8595.
29. Heller, A.; Feldman, B. Electrochemical Glucose Sensors and Their Applications in Diabetes Management. *Chem. Rev.* **2008**, 108, 2482–2505.
30. Todd, M. J.; Gomez, J. Enzyme Kinetics Determined Using Calorimetry: A General Assay for Enzyme Activity? *Anal. Biochem.* **2001**, 296, 179–187.
31. Glick, D.; Oldham, K. G. Radiometric Methods of Enzyme Assay. In *Methods of Biochemical Analysis, Volume 21*; 2006; John Wiley & Sons, Inc., Hoboken, NJ, U. S. A.
32. Stockman, B. J.; Lodovice, I. J.; Fisher, D. A.; McColl, A. S.; Xie, Z. A Nuclear Magnetic Resonance-Based Functional Assay for Nicotinamide Adenine Dinucleotide Synthetase. *J. Biomol. Screen.* **2007**, 12, 457–463.

33. Stockman, B. J.; Dalvit, C. NMR Screening Techniques in Drug Discovery and Drug Design. *Prog. Nucl. Magn. Reson. Spectrosc.* **2002**, *41*, 187–231.
34. Eicher, J. J.; Snoep, J. L.; Rohwer, J. M. Determining Enzyme Kinetics for Systems Biology with Nuclear Magnetic Resonance Spectroscopy. *Metabolites* **2012**, *2*, 818–843.
35. Keiding, R.; Hörder, M.; Denmark, G. W.; Pitkänen, E.; Tenhunen, R.; Strömme, J. H.; Theodorsen, L.; Waldenström, J.; Tryding, N.; Westlund, L. Recommended Methods for the Determination of Four Enzymes in Blood. *Scand. J. Clin. Lab. Investig.* **1974**, *33*, 291–306.
36. Huang, X.-J.; Choi, Y.-K.; Im, H.-S.; Yarimaga, O.; Yoon, E.; Kim, H.-S. Aspartate Aminotransferase (AST/GOT) and Alanine Aminotransferase (ALT/GPT) Detection Techniques. *Sensors* **2006**, *6*, 756–782.
37. Karmen, A.; Wroblewski, F.; Ladue, J. S. Transaminase Activity in Human Blood. *J. Clin. Invest.* **1955**, *34*, 126–133.
38. Buxton, R. C.; Edwards, B.; Juo, R. R.; Voyta, J. C.; Tisdale, M.; Bethell, R. C. Development of a Sensitive Chemiluminescent Neuraminidase Assay for the Determination of Influenza Virus Susceptibility to Zanamivir. *Anal. Biochem.* **2000**, *280*, 291–300.
39. Lequin, R. M. Enzyme Immunoassay (EIA)/Enzyme-Linked Immunosorbent Assay (ELISA). *Clin. Chem.* **2005**, *51*, 2415–2418.
40. Heid, C. A.; Stevens, J.; Livak, K. J.; Williams, P. M. Real Time Quantitative PCR. *Genome Res.* **1996**, *6*, 986–994.
41. Sano, T.; Smith, C. L.; Cantor, C. R. Immuno-PCR: Very Sensitive Antigen Detection by Means of Specific Antibody-DNA Conjugates. *Science* **1992**, *258*, 120–122.

42. Nam, J.-M.; Thaxton, C. S.; Mirkin, C. A. Nanoparticle-Based Bio-Bar Codes for the Ultrasensitive Detection of Proteins. *Science* **2003**, *301*, 1884–1886.
43. Hill, H. D.; Mirkin, C. A. The Bio-Barcode Assay for the Detection of Protein and Nucleic Acid Targets Using DTT-Induced Ligand Exchange. *Nat. Protoc.* **2006**, *1*, 324–336.
44. Thompson, M.; Sheikh, S.; Blaszykowski, C.; Romaschin, A. Biosensor Technology and the Clinical Biochemistry Laboratory – Issue of Signal Interference from the Biological Matrix. In *RSC Detection Science Series No. 2, Detection Challenges in Clinical Diagnostics*; Vadgama, P.; Peteu, S., Ed. The Royal Society of Chemistry: London, U. K., 2013; pp. 1–34.
45. IFN-gamma Mouse Antibody Pair. Invitrogen, Life technologies: Camarillo, CA, U.S.A. <http://www.lifetechnologies.com/order/catalog/product/CMC4033?ICID=search-cmc4033> (accessed 06/24/2014).
46. Malaria rapid diagnostic test performance. Results of WHO product testing of malaria RDTs: Round 4, 2012. http://www.who.int/malaria/publications/rapid_diagnostic/en/ (accessed 06/24/2014).
47. Strasinger, S. K.; Lorenzo, M. S. Di. *Urinalysis in Clinical Laboratory Practice*; F.A. Davis: Philadelphia, PA, U.S.A., 2008.
48. Butler, S. A.; Khanlian, S. A.; Cole, L. A. Detection of Early Pregnancy Forms of Human Chorionic Gonadotropin by Home Pregnancy Test Devices. *Clin. Chem.* **2001**, *47*, 2131–2136.

49. Drugs of Abuse Home Use Test, FDA, United States, 2014.
<http://www.fda.gov/MedicalDevices/ProductsandMedicalProcedures/InVitroDiagnostics/DrugsofAbuseTests/default.htm> (accessed 06/24/2014).
50. Achyuthan, K. E.; Pence, L. M.; Appleman, J. R.; Shimasaki, C. D. ZstatFlu[®]-II Test: A Chemiluminescent Neuraminidase Assay for Influenza Viral Diagnostics. *Luminescence* **2003**, *18*, 131–139.
51. Achyuthan, K. E.; Pence, L. M.; Mantell, D. R.; Nangeroni, P. E.; Mauchan, D. M.; Aitken, W. M.; Appleman, J. R.; Shimasaki, C. D. Engineering a Chemical Implementation Device and an Imaging Device for Detecting Chemiluminescence with a Polaroid[™] High-Speed Detector Film: Application to Influenza Diagnostics with the ZstatFlu[®]-II Test. *Luminescence* **2003**, *18*, 79–89.
52. Seto, J. T.; Rott, R. Functional Significance of Sialidase during Influenza Virus Multiplication. *Virology* **1966**, *30*, 731–737.
53. Turro, N. J.; Lechtken, P. Thermal Generation of Organic Molecules in Electronically Excited States. Evidence for a Spin Forbidden, Diabatic Pericyclic Reaction. *J. Am. Chem. Soc.* **1973**, *95*, 264–266.
54. Murphy, S.; Adam, W. The Elusive 1,4-Dioxy Biradical: Revised Mechanism for the Formation of Diol from 3,3-Dimethyldioxetane in Cyclohexadiene. *J. Am. Chem. Soc.* **1996**, *118*, 12916–12921.
55. Yao, H.; So, M.-K.; Rao, J. A Bioluminogenic Substrate for in Vivo Imaging of β -Lactamase Activity. *Angew. Chem. Int. Ed.* **2007**, *46*, 7031–7034.
56. Gao, W.; Xing, B.; Tsien, R. Y.; Rao, J. Novel Fluorogenic Substrates for Imaging β -Lactamase Gene Expression. *J. Am. Chem. Soc.* **2003**, *125*, 11146–11147.

57. Xing, B.; Khanamiryan, A.; Rao, J. Cell-Permeable near-Infrared Fluorogenic Substrates for Imaging β -Lactamase Activity. *J. Am. Chem. Soc.* **2005**, *127*, 4158–4159.
58. Xie, H.; Mire, J.; Kong, Y.; Chang, M.; Hassounah, H. A.; Thornton, C. N.; Sacchettini, J. C.; Cirillo, J. D.; Rao, J. Rapid Point-of-Care Detection of the Tuberculosis Pathogen Using a BlaC-Specific Fluorogenic Probe. *Nat. Chem.* **2012**, *4*, 802–809.
59. Pollock, N. R.; Rolland, J. P.; Kumar, S.; Beattie, P. D.; Jain, S.; Noubary, F.; Wong, V. L.; Pohlmann, R. A.; Ryan, U. S.; Whitesides, G. M. A Paper-Based Multiplexed Transaminase Test for Low-Cost, Point-of-Care Liver Function Testing. *Sci. Transl. Med.* **2012**, *4*, 152ra129
60. Vella, S. J.; Beattie, P.; Cademartiri, R.; Laromaine, A.; Martinez, A. W.; Phillips, S. T.; Mirica, K. A.; Whitesides, G. M. Measuring Markers of Liver Function Using a Micropatterned Paper Device Designed for Blood from a Fingertick. *Anal. Chem.* **2012**, *84*, 2883–2891.

CHAPTER 2

Development of reagents for quantifying active enzymes using a personal glucose meter

2.1 Introduction

Diagnostic assays for the quantification of active enzyme biomarkers permit early disease diagnosis and facilitate the choice of therapeutic intervention.¹⁻² Diagnostic assays that can be performed at the point-of-care are of great importance, particularly in a variety of resource limited environments that lack laboratory infrastructure (such as remote villages in the developing world). Many point-of-care (POC) diagnostic assays use colorimetric output to signal the presence of the target biomarkers. The colorimetric output in an assay can be quantified using specialized readers that measure the changes in absorbance³, transmittance⁴, or reflectance⁵ of the assay solution. Recently, camera phones have become a popular alternative to specialized readers for measuring the colorimetric signal due to their ubiquity.⁶⁻⁸ Despite the simplicity of analyzing these assays, colorimetric diagnostic assays suffer from interference from background color of the sample and particulate matter present in complex samples (such as blood). Additionally, the performance of colorimetric assays that use camera phones are affected by variations in lighting conditions, focus, and differences in the brand of camera phone used.

Electrochemical detection of biomarkers is an alternative to colorimetric diagnostic assays.⁹ Enzyme coupled electrochemical transformations¹⁰ and biomarker triggered changes in electrochemical donor-acceptor distance¹¹ have been exploited for detection of various biomarkers in laboratory settings. The most successful electrochemical assay used in the context of POC testing is the quantification of blood glucose using a hand-held glucose meter. The low cost and ease of use makes the glucose meter an ideal platform to develop POC assays. Although commercially available glucose meters are designed to measure blood glucose levels, recent work has shown that they can be used to quantify other analytes using carefully designed detection reagents.¹²⁻²³

In one example, Lu and coworkers have developed DNA aptamer-based detection reagents were used to quantify a few different analytes using a glucose meter.¹⁴ The detection reagent consisted of invertase enzyme immobilized on a solid support using a DNA-based

aptamer as a linker. If the target is present in the sample, it binds to the aptamer, leading to the release of invertase into the solution. The free invertase enzyme catalyzes the hydrolysis of sucrose present in the assay mixture to generate glucose, which is then quantified using a glucose meter. Using this strategy, the authors detected μM levels of targets like cocaine, adenosine, uranium ions and nM levels of interferon- γ . Several variations of this strategy have also been developed using other biomolecular linkers, such as DNA¹⁵⁻¹⁶, antibodies¹⁷⁻¹⁹, and DNA-functionalized nanoparticles²⁰⁻²².

An interesting alternative to using solid supported aptamer-based detection reagents was developed by Yang and coworkers.²³ They used a DNA-based aptamer as a crosslinker in a hydrogel material. The binding of the target to the aptamer resulted in the dissolution of the hydrogel and simultaneous release of the enzyme amylase, which was trapped in the hydrogel. Amylase then catalyzed the hydrolysis of amylose (a polymer of glucose) present in the assay mixture to generate several equivalents of glucose into the solution, which could be measured using the glucose meter.

Detection reagents using aptamers and antibodies can sensitively detect several targets under laboratory conditions. However, these assays are not suitable for use in resource-limited POC environments because of the complexity of the assay procedures and the dependence on thermally unstable reagents. An alternative to using aptamers and antibodies in diagnostic assays is to develop activity-based small molecule reagents that release glucose in the presence of enzyme biomarkers.¹² Compared to protein and nucleic acid-based detection reagents, small molecule reagents have superior thermal stability and are easier to modify to target several classes of analytes. We describe here the design and synthesis of small molecule reagents that release glucose in the presence of several classes of enzyme biomarkers. We also describe a single step assay for quantifying the enzyme biomarkers using a hand-held glucose meter.

2.2 Experimental design

2.2.1 A single step assay to quantify enzyme biomarkers using a glucose meter

Our goal was to design a simple, single-step assay to quantify several enzyme biomarkers using a glucose meter (Figure 1). To achieve this goal, we developed several small molecule reagents that released glucose when the target enzyme analyte was present in the assay mixture. We designed the assay to have as few steps as possible. The user only has to deposit the test sample (e.g., a sample of blood) in a disposable reaction tube pre-loaded with the detection reagent, wait for a fixed amount of time, and then measure the released glucose using a glucose meter. The simplicity of the assay procedure and the use of thermally-stable reagents are particularly important when the assay needs to be conducted in environments that lack trained personnel, access to laboratory infrastructure, and refrigeration.

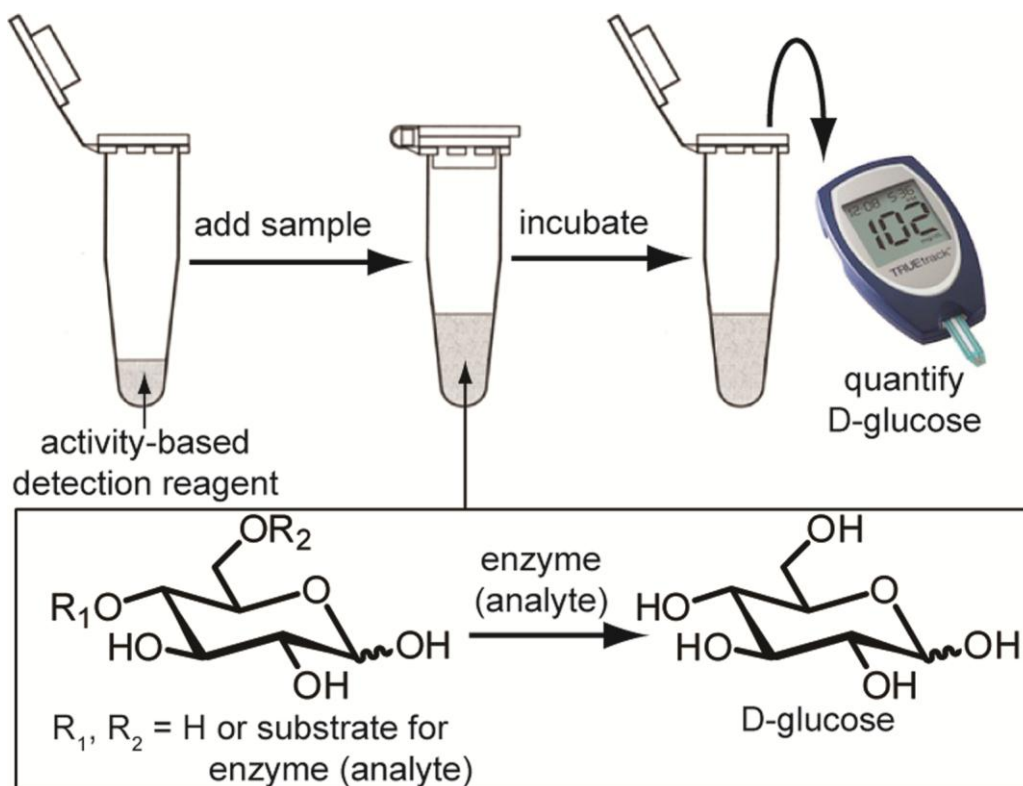


Figure 2-1. A one-step assay strategy to quantify active enzymes using small molecule activity-based detection reagents and a glucose meter.¹²

2.2.2 Design of reagents that release glucose in the presence of enzyme analytes

The selectivity of the single-step assay in Figure 1 originates from specific functionalities on the detection reagents that trigger the release of glucose in the presence of the specific target enzyme (Figure 2). The detection reagents are designed in such a way that the triggering functionality (blue in Figure 2) can be switched to target several enzymes. The four controlled released reagents depicted in Figure 2 respond to four enzymes that belong to four general classes of enzymes: glycosidases, esterases, phosphatases and proteases.

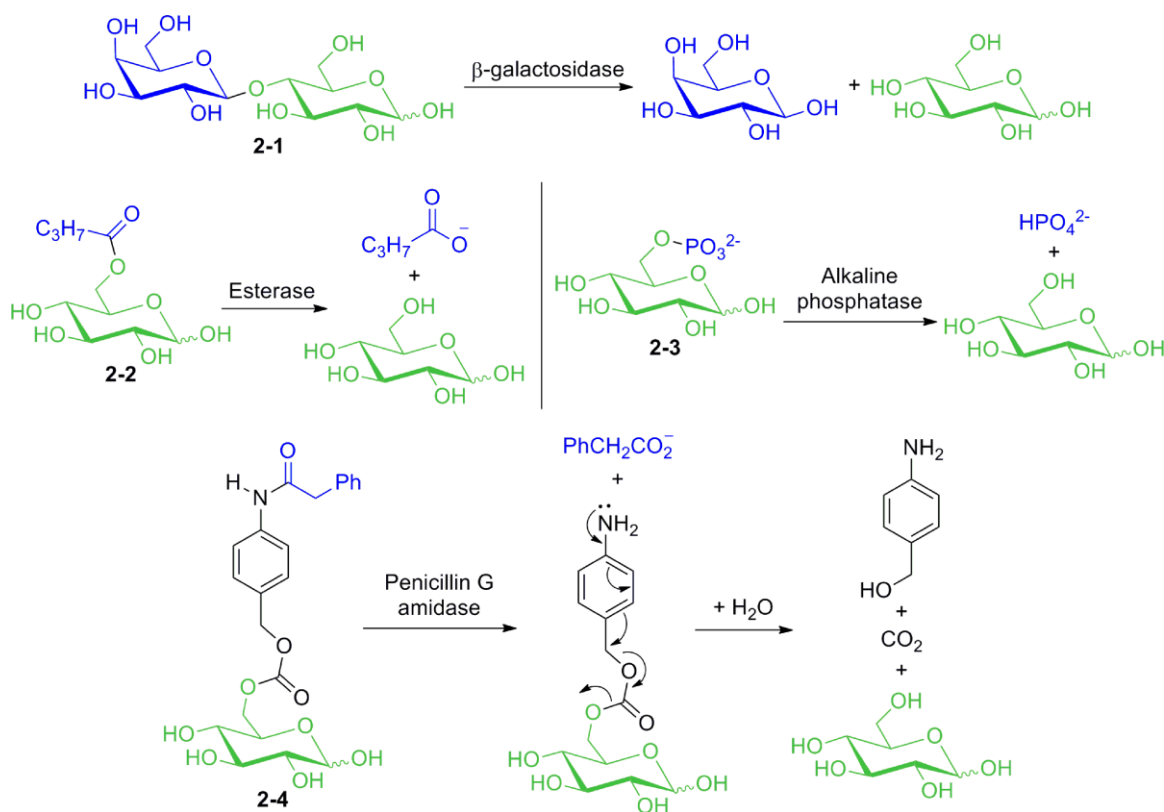


Figure 2-2. Activity-based detection reagents designed to release glucose for use in assays to quantify four different active enzymes using a glucose meter. The four enzyme targets belong to four classes of enzymes: glycosidases (2-1), esterases (2-2), phosphatases (2-3), and proteases (2-4).

Since different classes of enzymes require different strategies to release glucose, we have demonstrated three general strategies of controlled release of glucose. The glucose may be generated through:

(i) *Cleavage of glycosidic bonds.* Detection reagent **2-1** responds to β -galactosidase (a general biomarker of fecal contamination in drinking water²⁴). β -galactosidase catalyzes the hydrolysis of the glycosidic bond in **2-1** to generate an equivalent of glucose. Other enzyme biomarkers that can be targeted using glycosidic substrates include β -glucuronidase (a general biomarker for *E. coli* contamination in food²⁵), viral neuraminidase (a biomarker for influenza viral infection in respiratory tract mucus²⁶), and α -N-acetylgalactosaminidase (a biomarker for skin cancer in blood serum²⁷⁻²⁸).

(ii) *Hydrolysis of esters of glucose.* Detection reagent **2-2** (a butyric acid ester of glucose) and **2-3** (a phosphoric acid ester of glucose) target the enzymes esterase (a biomarker for *Salmonella* contamination in food²⁹) and alkaline phosphatase (a biomarker for liver health and bile duct obstruction³⁰ and a general indicator for the effectiveness of pasteurization in the dairy industry³¹), respectively. These enzymes catalyze ester hydrolysis reactions of their respective detection reagents.

(iii) *Controlled release of glucose through a 1,4-elimination-based linker.* Detection reagent **2-4** is designed to respond to penicillin-G-amidase (a model protease that catalyzes the hydrolysis of phenacetyl amides³²) to release glucose through a 1,4-azaquinone methide elimination. A linker is necessary for targeting proteases to ensure that the cleavage of an amide bond is translated into the rapid release of glucose. The phenacetyl functionality in **2-4** can be replaced with short peptides to target several other biomarkers (e.g., cysteine proteases from *P. falciparum*³³, serine proteases from cancerous cells³⁴, and other proteases³⁵⁻³⁶ specific to several species of bacteria.)

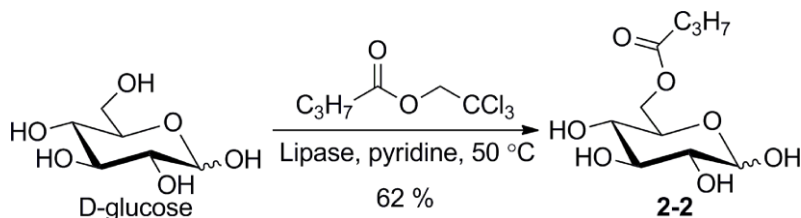
2.3 Results and discussion

2.3.1 Synthesis of detection reagents

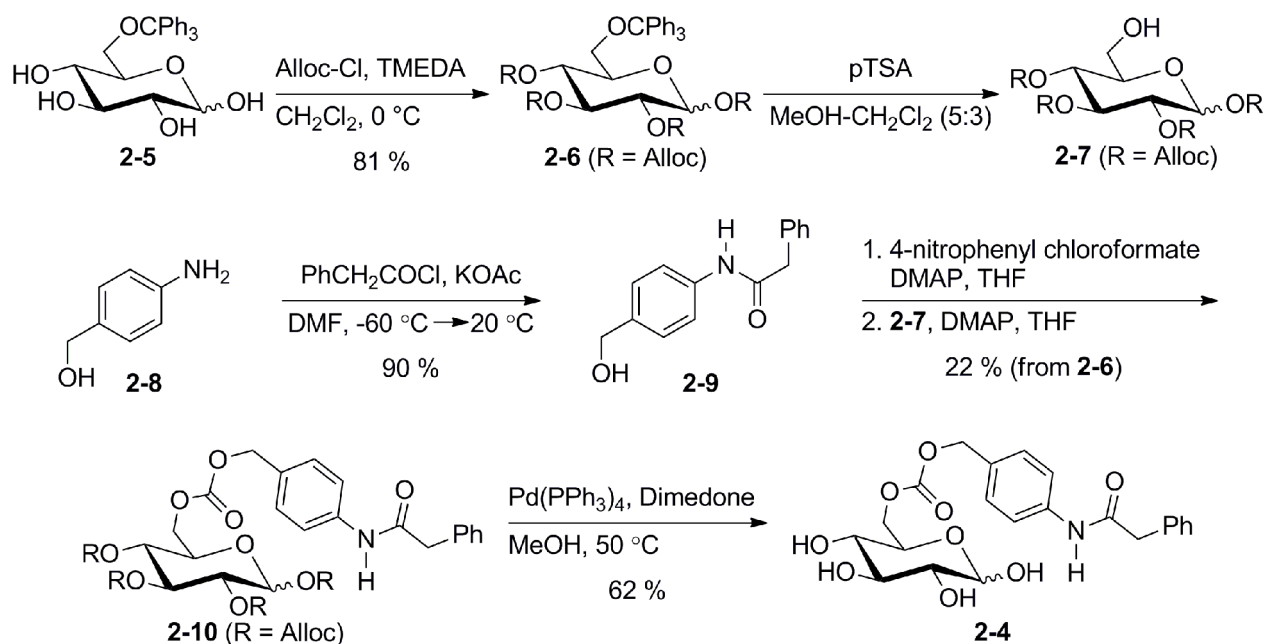
Detection reagent **2-2** was obtained through an enzyme catalyzed transesterification reaction in organic solvent (Scheme 2-1). Detection reagents **2-1** and **2-3** are commercially available and were used as obtained. The detection reagent for penicillin-G-amidase (**2-4**) was synthesized using a convergent synthesis from commercially available starting materials (Scheme 2-2). Briefly, the partially protected glucose intermediate **2-7** was prepared in two steps

from 6-O-trityl-D-glucose (**2-5**). The amide half of the detection reagent (**2-9**) was prepared in a single step from 4-aminobenzyl alcohol (**2-8**) and phenacetyl chloride. Phenacetyl chloride can be replaced with a C-terminus activated peptide to target other proteases. Amide intermediate **2-9** and the protected glucose intermediate **2-7** were coupled using a carbonate linkage. We chose a carbonate linker because of the ease of synthesis. Other linkers like amins³⁷ and acetals³⁸ can also be used.

Scheme 2-1. Synthesis of esterase detection reagent **2-2**.



Scheme 2-2. Synthesis of protease detection reagent **2-4**.



2.3.2 First generation enzyme assay

With the enzyme detection reagents in hand, we evaluated the performance of these reagents in the single-step assay described in Figure 1. Exposure of **2-1** to various quantities of β -galactosidase in buffered water gave us a reproducible dose-response curve (Figure 2-3), which can be used as a calibration curve for quantifying β -galactosidase (a biomarker for bacterial contamination in water). Similar calibration curves were obtained for esterase (Figure 2-4), alkaline phosphatase (Figure 2-5), and penicillin-G-amidase (Figure 2-6) using their respective detection reagents.

The sensitivity of the first generation assay procedure is similar to that of colorimetric assays.³⁹ The current assay strategy is advantageous over quantitative colorimetric assays as the color of the sample does not affect the quantitative signal obtained using a glucose meter. For example, alkaline phosphatase is present in blood at concentrations between 30–120 U L⁻¹, whereas a concentration above 120 U L⁻¹ indicates impaired liver function.³⁰ The current assay is sufficiently sensitive to differentiate normal (30–120 U L⁻¹) and elevated levels of alkaline phosphatase in blood using a glucose meter. Moreover, quantification of alkaline phosphatase is expected to be unaffected by the color of the sample as a glucose meter is engineered to work well with blood.

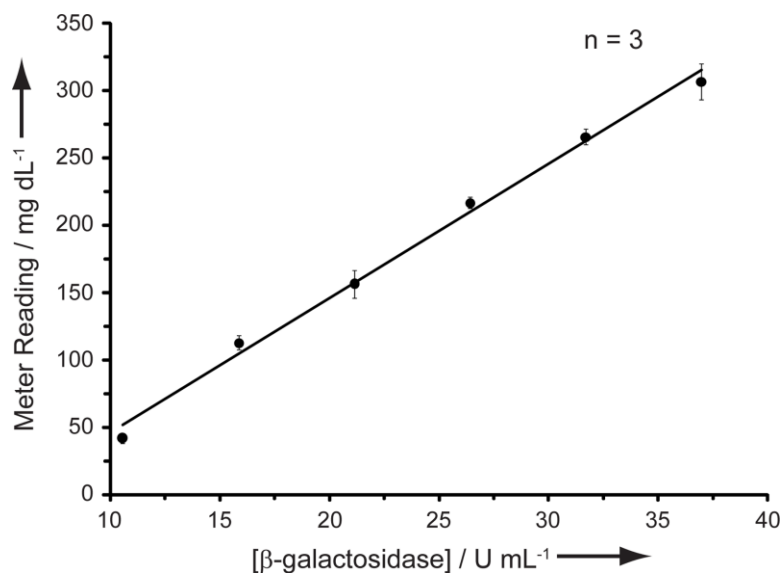


Figure 2-3. Calibration curve for the detection of β -galactosidase using 2-1. The assay solution was in 10 mM phosphate buffer (pH 7.4) and the assay time was 2 h. The data points are the average of three measurements and the error bars reflect the standard deviations from these averages.¹²

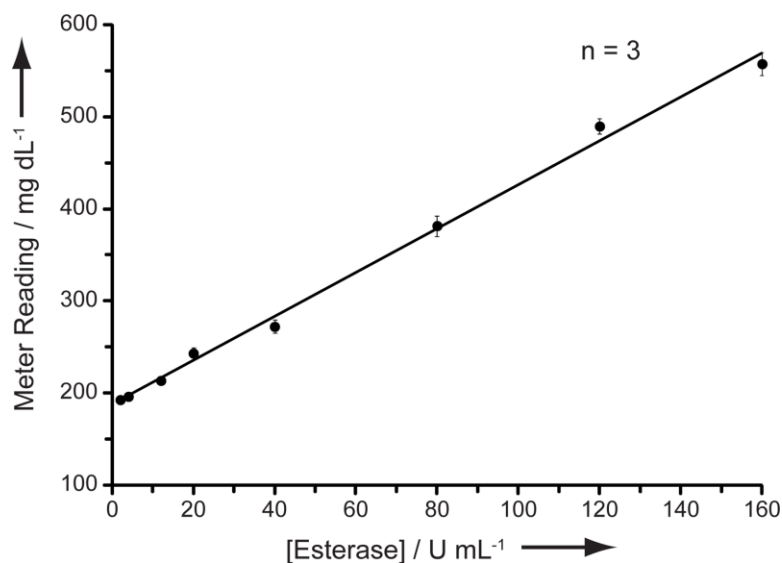


Figure 2-4. Calibration curve for the detection of esterase using 2-2. The assay solution was in 75 mM phosphate buffer (pH 8.0 with 0.42% (v/v) Triton X-100). The assay time was 1 h at 40 °C. The data points are the average of three measurements and the error bars reflect the standard deviations from these averages.¹²

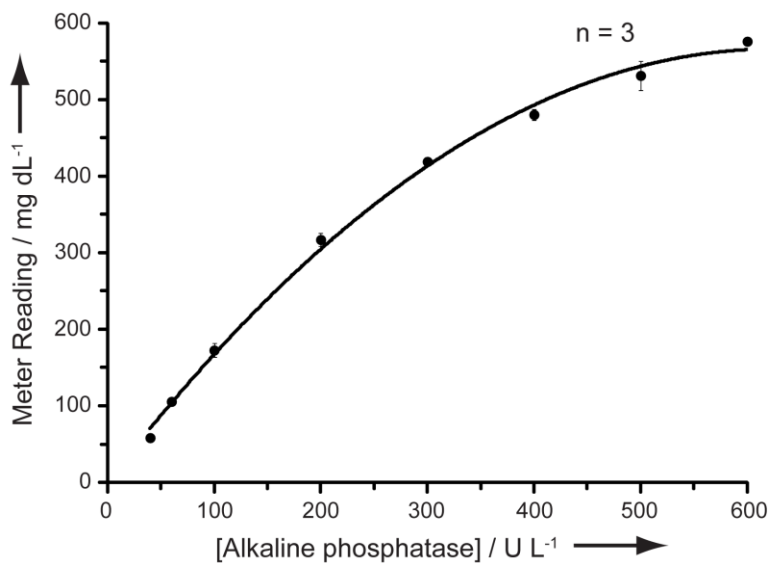


Figure 2-5. Calibration curve for the detection of alkaline phosphatase using **2-3**. The assay solution was in 0.1 M diethanolamine buffer (pH 7.4 with 0.5 mM MgCl₂). The assay time was 1 h at 37 °C. The data points are the average of three measurements and the error bars reflect the standard deviations from these averages.¹²

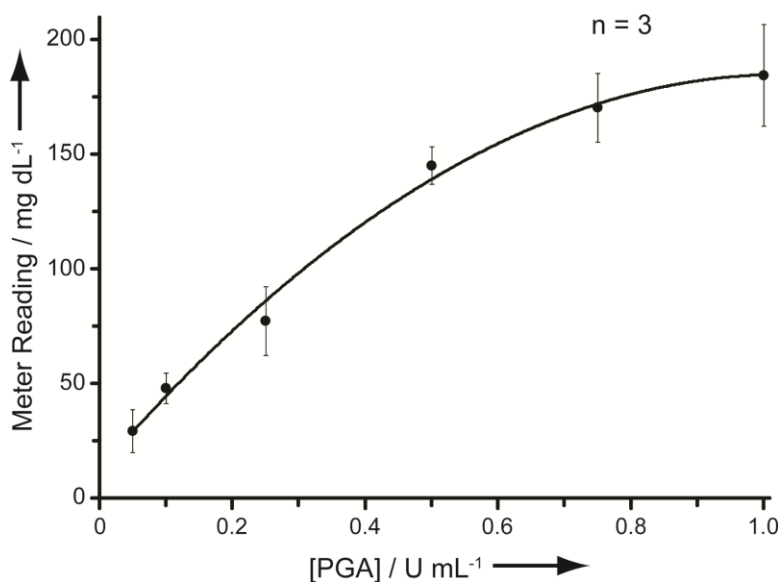


Figure 2-6. Calibration curve for the detection of penicillin-G-amidase (PGA) using **2-4**. The assay solution was in 0.1 M phosphate buffer (pH 7.5) and the assay time was 1 h at 20 °C. The data points are the average of three measurements and the error bars reflect the standard deviations from these averages.¹²

2.3.3 Second generation assay strategy

The first generation assay allowed us to quantify several enzymes in simple, one-step assays within an hour. We reasoned that a shorter assay time would be more useful in the context of enzyme quantification at point-of-care. Assays using nucleic acids and antibodies can potentially enhance the amount of glucose generated, and thereby reduce assay time.¹⁴⁻²² However, these types of assays usually require multiple sample handling steps and use thermally sensitive reagents. We sought a simpler solution to reduce the assay time without introducing multiple assay steps. Since the commercially available glucose meter is designed to measure blood glucose concentrations above 20 mg dL⁻¹ (~ 1 mM), we included a small amount of D-glucose along with the detection reagent in the pre-loaded assay tube. The amount of glucose included was sufficient to provide a low-level reading on the glucose meter. The enzyme target in the sample would then elevate the level of glucose (as it processes the detection reagents) within the quantification window of the glucose meter. Consequently, the lag time during which the enzyme generates enough glucose to obtain a glucose meter reading is eliminated.

The inclusion of glucose resulted in assay times that were 2–12 times shorter than the first generation assays. Figures 2-7, 2-8, and 2-9 show the calibration curves for the quantification of three of the enzyme targets. The second generation assays were more sensitive than the first generation assays with considerably shorter assay durations. The limits-of-detection (LOD) for the quantification of β -galactosidase, alkaline phosphatase, and penicillin-G-amidase were 4 U mL⁻¹ (~ 38 nM) (15 min assay time), 1.5 U L⁻¹ (~ 1.3 nM) (5 min assay time), and 0.01 U mL⁻¹ (30 min assay) respectively. The dynamic range of the second generation assay was noteworthy. For example, we could quantify alkaline phosphatase levels between 1.5 U L⁻¹ to 160 U L⁻¹ (1.3 nM to 140 nM), which is within the clinically-relevant window for the enzyme analyte. The sensitivity of these assays can be further improved with longer assay times.

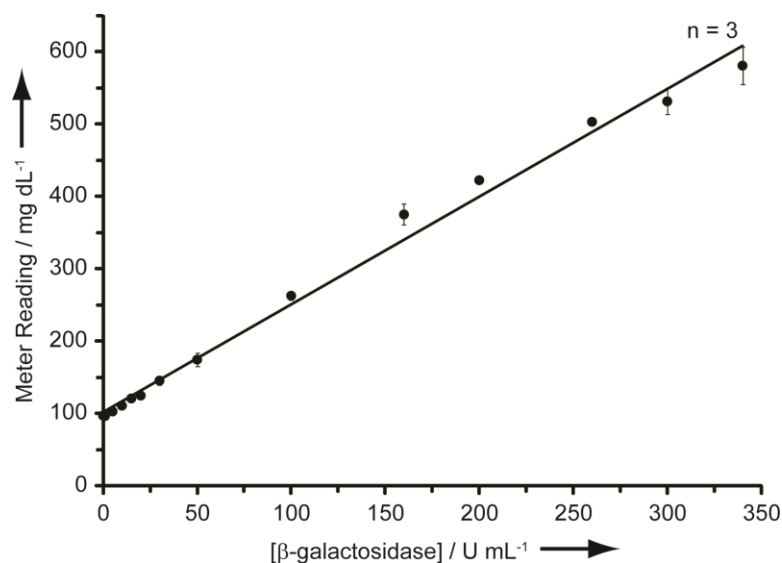


Figure 2-7. Calibration curve for the detection of β -galactosidase using 2-1. The assay included 0.3 mg/mL glucose prior to the start of the assay. The assay solution was in 10 mM phosphate buffer (pH 7.4) and the assay time was 15 min at 20 °C. The data points are the average of three measurements and the error bars reflect the standard deviations from these averages.¹²

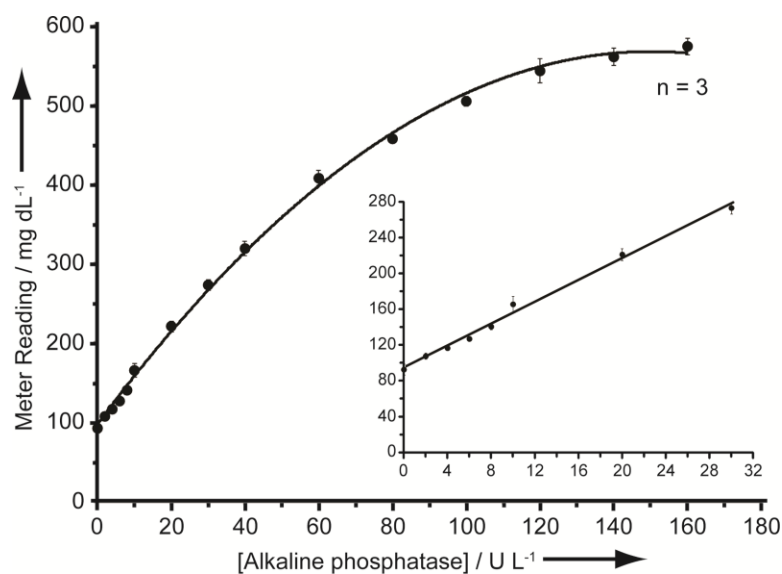


Figure 2-8. Calibration curve for the detection of alkaline phosphatase using 2-3. The assay included 0.3 mg/mL glucose prior to the start of the assay. The assay solution was in 0.1 M HEPES buffer (pH 8.0) and the assay time was 5 min at 37 °C. The data points are the average of three measurements and the error bars reflect the standard deviations from these averages.¹²

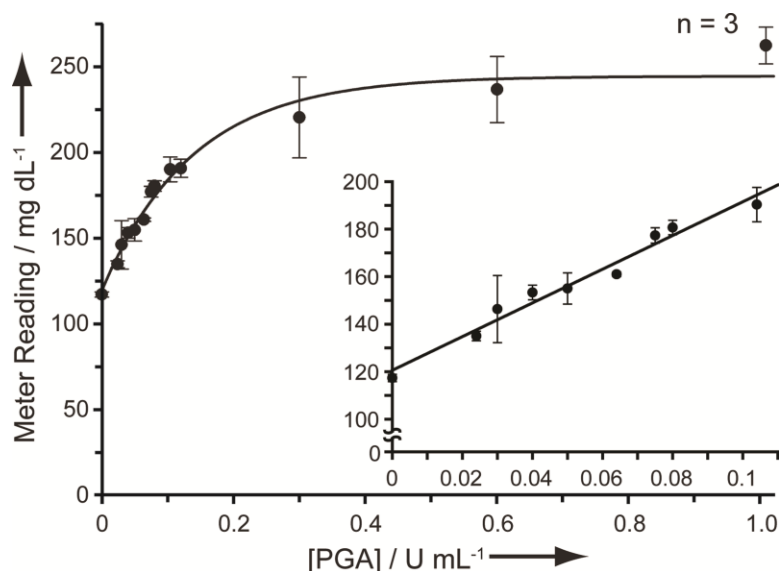


Figure 2-9. Calibration curve for the detection of penicillin-G-amidase (PGA) using **2-4**. The assay included 0.3 mg/mL glucose prior to the start of the assay. The assay solution was in 0.1 M phosphate buffer (pH 7.5 with 0.5% (v/v) Tween 20). The assay time was 30 min at 20 °C. The data points are the average of three measurements and the error bars reflect the standard deviations from these averages.¹²

2.3.4 Quantification of alkaline phosphatase in blood serum

The single-step assay for quantifying active enzymes described here is designed to perform effectively in complex fluids (such as blood). Since a glucose meter is commonly used to quantify glucose in blood, we reasoned that an assay for the quantification of alkaline phosphatase in blood using a glucose meter will remain unaffected by the color of the sample or the presence of other proteins present in the blood. To evaluate the performance of an assay for alkaline phosphatase in a complex fluid, we performed a 5 min assay for various concentrations of alkaline phosphatase in blood serum. We could quantify alkaline phosphatase in blood serum with a dynamic range of 2 U L⁻¹ to 160 U L⁻¹ (2 nM to 140 nM), with a limit of detection of 2 U L⁻¹ (2 nM) (Figure 2-10). The range and sensitivity of the assay in blood serum was nearly identical to those obtained using buffered water as the solvent.

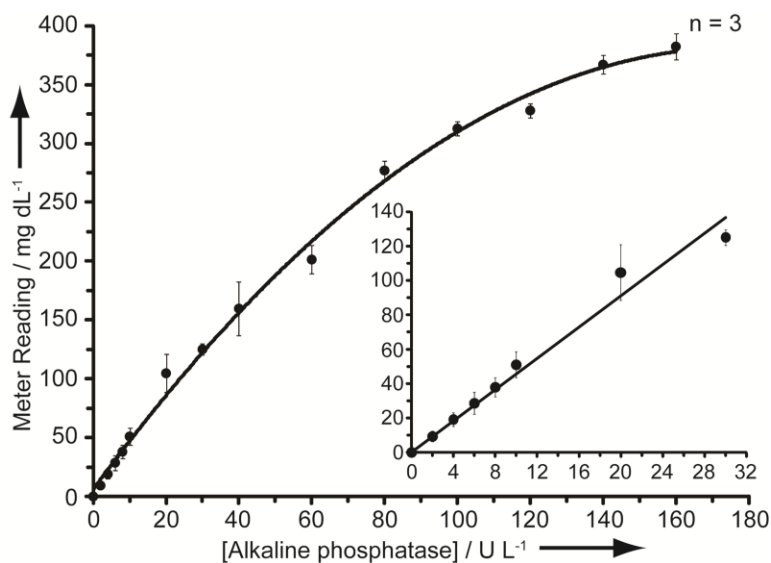


Figure 2-10. Calibration curve for the detection of alkaline phosphatase in blood serum using **2-3**. The meter reading values on the y-axis here refer to the difference between the glucose concentration in the assay mixture and the glucose concentration in a negative control. The assay solution was in 0.1 M HEPES buffer (pH 8.0) and the assay time was 5 min at 37 °C. The data points are the average of three measurements and the error bars reflect the standard deviations from these averages.¹²

We then spiked the serum samples with varying quantities of glucose (in addition to the glucose already present in the serum) to simulate real world blood serum samples that usually contain varying levels of glucose. The quantity of alkaline phosphatase (20 U L^{-1}) was quantified in these serum samples by conducting two assays, one without the presence of the detection reagent (**2-3**) and one with the presence of the detection reagent. The difference in glucose measurements obtained from these two assays was used to determine the concentration of the enzyme in the sample (Table 2-1). The results of these experiments demonstrate that the assay can be used for the quantification of alkaline phosphatase in blood serum samples.

Table 2-1. Determination of the concentration of alkaline phosphatase in various serum samples.

Serum sample ^a	Meter reading / (mg dL^{-1})		Calculated ^b [Alkaline phosphatase] / (U L^{-1})
	Control	Test sample	
1	142 ± 2	242 ± 12	22 ± 3
2	351 ± 2	439 ± 5	19 ± 1
3	270 ± 8	351 ± 3	18 ± 1

a. The serum samples contained various quantities of glucose and 20 U L^{-1} of alkaline phosphatase.

b. The concentration of the enzyme was obtained using the calibration curve in Figure 2-10 (inset).

2.3.5 Evaluation of the stability of the detection reagent 2-4

Since the single step assays for quantification of enzymes using a glucose meter must perform under real world conditions, we wanted to demonstrate the stability of one of the detection reagents. We chose to demonstrate the stability of **2-4**, which we expected to be the least stable of the detection reagents used in these studies because of the carbonate linkage (carbonates can be susceptible to hydrolysis under basic conditions³⁸).

Reagent **2-4** responds rapidly to the enzyme PGA. To establish a reaction timeline for this enzymatic reaction, we treated **2-4** (20 mM in 0.1 M phosphate buffer, pH 7.5, 1% (v/v) Tween 20) with catalytic amount of PGA (0.5 U mL⁻¹) and followed the enzymatic transformation using LC-MS. We observed rapid consumption of **2-4** (Figure 2-11) and the generation of glucose (as measured using a glucose meter). In the absence of the enzyme, we observed about 2% decomposition of the substrate after 1 hour (Figure 2-12) and only 7.5% decomposition after 5 hours, the latter being 10 times longer than the duration of the second generation of assay.

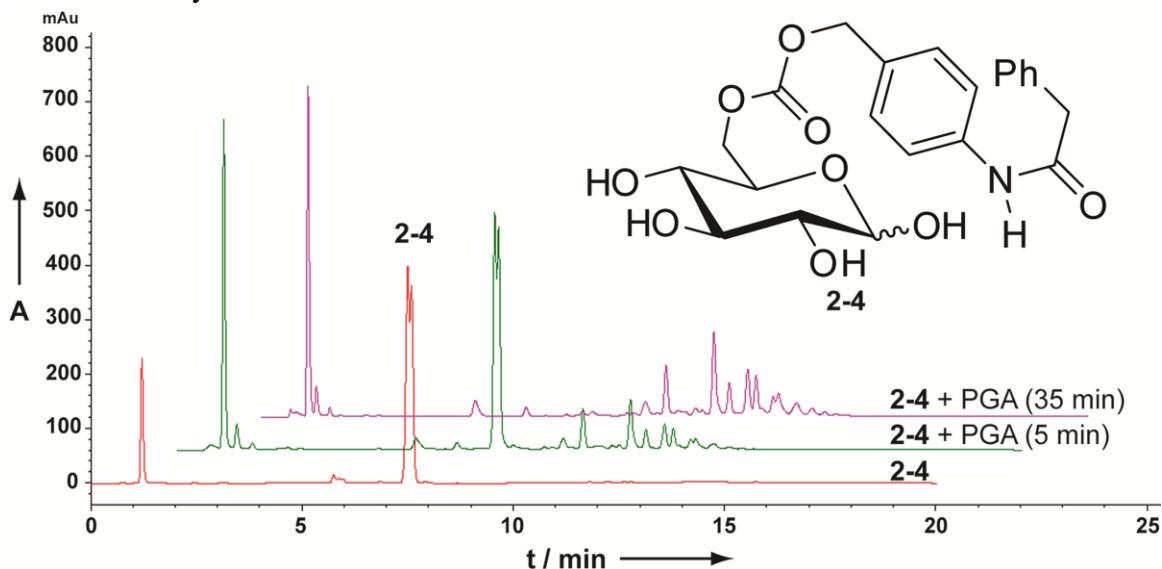


Figure 2-11. Time-dependent LC-MS analysis of the reaction of **2-4** with penicillin-G-amidase (PGA) (0.5 U mL⁻¹) in 0.1 M phosphate buffer (pH 7.5, 0.5% (v/v) Tween 20, 20 °C). The absorbance value (A) was recorded at 254 nm. The peaks appearing between 10 and 15 min (t) after exposure to PGA most likely are byproducts of quinone methide that is generated during the elimination reaction.¹²

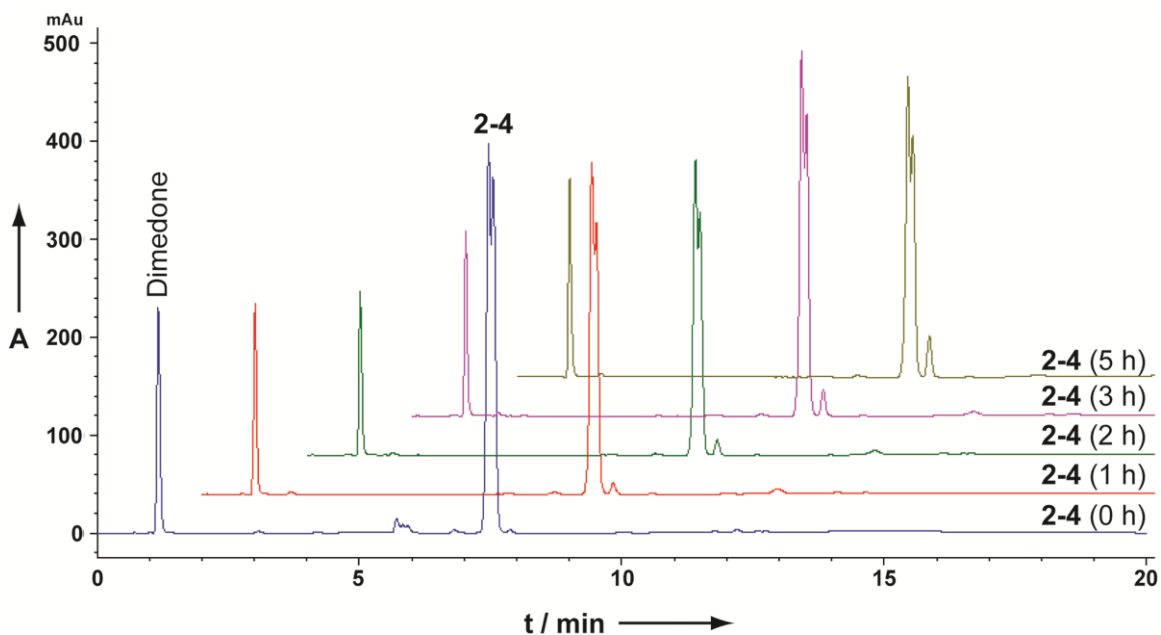


Figure 2-12. Time-dependent LC-MS analysis of the stability of **2-4** in 0.1 M phosphate buffer (pH 7.5, 0.5% (v/v) Tween 20, 20 °C). The absorbance value (A) was recorded at 254 nm. The peak for dimezone (internal standard) at 1.1 min (t) was used to determine the % decomposition.¹²

Since the detection reagents will be stored and transported as a dry powder before its use in an assay, we subjected **2-4** to extreme conditions (stored at 40 °C open to air). We observed no detectable decomposition in 24 hours and only 6% decomposition after a period of 7 days at 40 °C open to air (Figure 2-13). We also evaluated the effect of the small amount of decomposition on the performance of the enzyme quantification assay. We assayed a sample containing PGA (0.06 U mL⁻¹) using freshly prepared **2-4** and the sample of **2-4** that was held at 40 °C open to air for 7 days. We did not observe a measurable change in the assay result (Table 2-2). Since the accuracy of the glucose meter is about $\pm 20\%$, a decomposition of about 6% in **2-4** does not significantly affect the outcome of the assay.

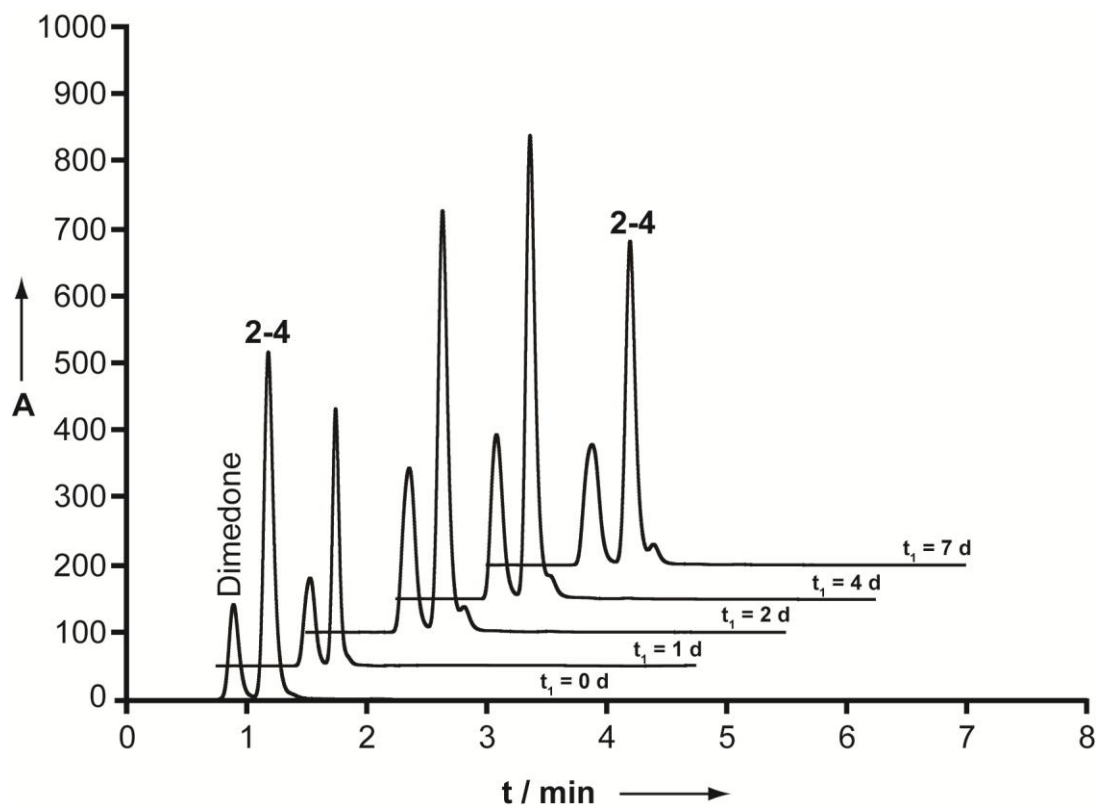


Figure 2-13. Study of the thermal stability of detection reagent **2-4**. Samples of **2-4** were held at 40 °C open to air for 7 days. At intervals, the samples were dissolved in 10 mM phosphate buffer (pH 7.5, 0.5% (v/v) Tween 20, 20 °C) and analyzed by LC-MS. The absorbance value (A) was recorded at 254 nm and dimedone ($t = 0.8$ min) was used as an internal standard to calculate peak areas.¹²

Table 2-2. The effect of the decomposition of **2-4** on the results of the assay for PGA

Sample of 2-4 used	[PGA] / (U mL ⁻¹)	Meter reading / (mg dL ⁻¹)	Calculated ^a [PGA] / (U mL ⁻¹)
Freshly prepared	0.06	171±5	0.07±0.01
Sample held at 40 °C for 7 days	0.06	153±2	0.05±0.00

- a. The second generation assay was used to determine the concentration of PGA.
The linear region of the calibration curve in Figure 2-9 (inset) was used for calculations.

2.3 Conclusions

In conclusion, we describe here a simple, rapid, one-step assay strategy to quantify active enzymes using a glucose meter. The assays use small molecule, activity-based detection reagents that generate glucose in the presence of the target enzymes. The assays only measure the concentration of the active enzymes in the samples rather than the total amount of enzyme antigen present in the sample. This ability to distinguish active enzymes from inactive (denatured) enzymes can prove to be useful in the context of liver function tests and quantifying enzymes associated with presence of live pathogens. Since the assay strategy only uses a hand-held glucose meter and thermally stable, small molecule reagents, it is amenable for use in point-of-care settings that lack laboratory infrastructure or refrigeration. The availability of cell phone based personal glucose meter makes the assay strategy a powerful alternative to colorimetric assays.⁴⁰

2.4 References

1. Burtis, C. A.; Ashwood, E. R.; Border, B.; Tietz, N. W. *Tietz Fundamentals of Clinical Chemistry*, 5th ed.; W. B. Saunders Company: U. S. A., 2001.
2. Vadgama, P.; Peteu, S., Ed. *RSC Detection Science Series No. 2, Detection Challenges in Clinical Diagnostics*; The Royal Society of Chemistry: London, U. K., 2013.
3. For an example of a portable commercial UV/Vis spectrophotometer for absorbance measurements see: PhotoLab UV/Vis portable spectrophotometers, Xylem Inc.: White Plains, NY USA <http://www.globalw.com/products/photolab.html> (accessed 07/07/2014).
4. Ellerbee, A. K.; Phillips, S. T.; Siegel, A. C.; Mirica, K. A.; Martinez, A. W.; Striehl, P.; Jain, N.; Prentiss, M.; Whitesides, G. M. Quantifying Colorimetric Assays in Paper-Based Microfluidic Devices by Measuring the Transmission of Light through Paper. *Anal. Chem.* **2009**, *81*, 8447–8452.
5. For an example of a commercial reflectance reader see: ESEQuant Lateral Flow System, QIAGEN N. V. Hilden, Germany <http://www.qiagen.com/about-us/contact/oem-services/ese-instruments/esequant-lateral-flow-system/> (accessed 07/07/2014).
6. Martinez, A. W.; Phillips, S. T.; Carrilho, E.; Thomas, S. W.; Sindi, H.; Whitesides, G. M. Simple Telemedicine for Developing Regions: Camera Phones and Paper-Based Microfluidic Devices for Real-Time, off-site Diagnosis. *Anal. Chem.* **2008**, *80*, 3699–3707.
7. Schwaebel, T.; Trapp, O.; Bunz, U. H. F. Digital Photography for the Analysis of Fluorescence Responses. *Chem. Sci.* **2013**, *4*, 273–281.
8. Shen, L.; Hagen, J. A.; Papautsky, I. Point-of-Care Colorimetric Detection with a Smartphone. *Lab Chip* **2012**, *12*, 4240–4243.

9. Vasilescu, A.; Wolfgang, S.; Gaspar, S. Recent Progress in the Electrochemical Detection of Disease-Related Diagnostic Biomarkers. In *RSC Detection Science Series No. 2, Detection Challenges in Clinical Diagnostics*; Vadgama, P.; Petcu, S., Ed. The Royal Society of Chemistry: London, U. K., 2013; pp. 89–128.
10. Ikeda, T.; Kano, K. An Electrochemical Approach to the Studies of Biological Redox Reactions and Their Applications to Biosensors, Bioreactors, and Biofuel Cells. *J. Biosci. Bioeng.* **2001**, *92*, 9–18.
11. Lubin, A. A.; Plaxco, K. W. Folding-Based Electrochemical Biosensors: The Case for Responsive Nucleic Acid Architectures. *Acc. Chem. Res.* **2010**, *43*, 496–505.
12. Mohapatra, H.; Phillips, S. T. Reagents and Assay Strategies for Quantifying Active Enzyme Analytes Using a Personal Glucose Meter. *Chem. Commun.* **2013**, *49*, 6134–6136.
13. Nie, Z.; Deiss, F.; Liu, X.; Akbulut, O.; Whitesides, G. M. Integration of Paper-Based Microfluidic Devices with Commercial Electrochemical Readers. *Lab Chip* **2010**, *10*, 3163–3169.
14. Xiang, Y.; Lu, Y. Using Personal Glucose Meters and Functional DNA Sensors to Quantify a Variety of Analytical Targets. *Nat. Chem.* **2011**, *3*, 697–703.
15. Xiang, Y.; Lu, Y. Using Commercially Available Personal Glucose Meters for Portable Quantification of DNA. *Anal. Chem.* **2012**, *84*, 1975–1980.
16. Xiang, Y.; Lu, Y. An Invasive DNA Approach toward a General Method for Portable Quantification of Metal Ions Using a Personal Glucose Meter. *Chem. Commun.* **2013**, *49*, 585–587.

17. Xiang, Y.; Lu, Y. Portable and Quantitative Detection of Protein Biomarkers and Small Molecular Toxins Using Antibodies and Ubiquitous Personal Glucose Meters. *Anal. Chem.* **2012**, *84*, 4174–4178.
18. Su, J.; Xu, J.; Chen, Y.; Xiang, Y.; Yuan, R.; Chai, Y. Personal Glucose Sensor for Point-of-Care Early Cancer Diagnosis. *Chem. Commun.* **2012**, *48*, 6909–6911.
19. Zhu, X.; Zheng, H.; Xu, H.; Lin, R.; Han, Y.; Yang, G.; Lin, Z.; Guo, L.; Qiu, B.; Chen, G. A Reusable and Portable Immunosensor Using Personal Glucose Meter as Transducer. *Anal. Methods* **2014**, *6*, 5264.
20. Xu, J.; Jiang, B.; Xie, J.; Xiang, Y.; Yuan, R.; Chai, Y. Sensitive Point-of-Care Monitoring of HIV Related DNA Sequences with a Personal Glucometer. *Chem. Commun.* **2012**, *48*, 10733–10735.
21. Zhou, J.; Xu, K.; Zhou, P.; Zheng, O.; Lin, Z.; Guo, L.; Qiu, B.; Chen, G. A Portable Chemical Sensor for Histidine Based on the Strategy of Click Chemistry. *Biosens. Bioelectron.* **2014**, *51*, 386–390.
22. Su, J.; Xu, J.; Chen, Y.; Xiang, Y.; Yuan, R.; Chai, Y. Sensitive Detection of copper(II) by a Commercial Glucometer Using Click Chemistry. *Biosens. Bioelectron.* **2013**, *45*, 219–222.
23. Yan, L.; Zhu, Z.; Zou, Y.; Huang, Y.; Liu, D.; Jia, S.; Xu, D.; Wu, M.; Zhou, Y.; Zhou, S.; Yang, C. G. Target-Responsive “Sweet” Hydrogel with Glucometer Readout for Portable and Quantitative Detection of Non-Glucose Targets. *J. Am. Chem. Soc.* **2013**, *135*, 3748–3751.
24. Davies, C.; Apte, S. Field Evaluation of a Rapid Portable Test for Monitoring Fecal Coliforms in Coastal Waters. *Environ. Toxicol.* **1999**, *14*, 355–359.

25. Frampton, E. W.; Restaino, L. Methods for *Escherichia coli* Identification in Food, Water and Clinical Samples Based on Beta-Glucuronidase Detection. *J. Appl. Bacteriol.* **1993**, *74*, 223–233.
26. Liav, A.; Hansjergen, J. A.; Achyuthan, K. E.; Shimasaki, C. D. Synthesis of Bromoindolyl 4,7-Di-O-Methyl-Neu5Ac: Specificity toward Influenza A and B Viruses. *Carbohydr. Res.* **1999**, *317*, 198–203.
27. Reddi, A. L.; Sankaranarayanan, K.; Arulraj, H. S.; Devaraj, N.; Devaraj, H. Serum α -N-Acetylgalactosaminidase is Associated with Diagnosis/prognosis of Patients with Squamous Cell Carcinoma of the Uterine Cervix. *Cancer Lett.* **2000**, *158*, 61–64.
28. Greco, M.; Mitri, M. De; Chiriaco, F.; Leo, G.; Brienza, E.; Maffia, M. Serum Proteomic Profile of Cutaneous Malignant Melanoma and Relation to Cancer Progression: Association to Tumor Derived Alpha-N-Acetylgalactosaminidase Activity. *Cancer Lett.* **2009**, *283*, 222–229.
29. Jokerst, J. C.; Adkins, J. A.; Bisha, B.; Mentele, M. M.; Goodridge, L. D.; Henry, C. S. Development of a Paper-Based Analytical Device for Colorimetric Detection of Select Foodborne Pathogens. *Anal. Chem.* **2012**, *84*, 2900–2907.
30. Vella, S. J.; Beattie, P.; Cademartiri, R.; Laromaine, A.; Martinez, A. W.; Phillips, S. T.; Mirica, K. A.; Whitesides, G. M. Measuring Markers of Liver Function Using a Micropatterned Paper Device Designed for Blood from a Fingerstick. *Anal. Chem.* **2012**, *84*, 2883–2891.
31. Aschaffenburg, R.; Mullen, J. E. C. *J. Dairy Res.* **1949**, *16*, 58–67.
32. Arroyo, M.; de la Mata, I.; Acebal, C.; Castellón, M. P. Biotechnological Applications of Penicillin Acylases: State-of-the-Art. *Appl. Microbiol. Biotechnol.* **2003**, *60*, 507–514.

33. Pandey, K. C.; Sijwali, P. S.; Singh, A.; Na, B.-K.; Rosenthal, P. J. Independent Intramolecular Mediators of Folding, Activity, and Inhibition for the *Plasmodium falciparum* Cysteine Protease Falcipain-2. *J. Biol. Chem.* **2004**, *279*, 3484–3491.
34. Madu, C. O.; Lu, Y. Novel Diagnostic Biomarkers for Prostate Cancer. *J. cancer* **2010**, *1*, 150–177.
35. Shende, N.; Gupta, S.; Bhatia, A. S.; Kumar, S.; Harinath, B. C. Detection of Free and Immune-Complexed Serine Protease and Its Antibody in TB Patients with and without HIV Co-Infection. *Int. J. Tuberc. Lung Dis.* **2005**, *9*, 915–919.
36. Dutta, P. R.; Cappello, R.; Navarro-garcía, F.; Nataro, J. P.; Phylogenetic, S. Functional Comparison of Serine Protease Autotransporters of Enterobacteriaceae. *Infect. Immun.* **2002**, *70*, 7105–7113.
37. Karton-Lifshin, N.; Vogel, U.; Sella, E.; Seeberger, P. H.; Shabat, D.; Lepenies, B. Enzyme-Mediated Nutrient Release: Glucose-Precursor Activation by β -Galactosidase to Induce Bacterial Growth. *Org. Biomol. Chem.* **2013**, *11*, 2903–2910.
38. Nuñez, S. A.; Yeung, K.; Fox, N. S.; Phillips, S. T. A Structurally Simple Self-Immolative Reagent That Provides Three Distinct, Simultaneous Responses per Detection Event. *J. Org. Chem.* **2011**, *76*, 10099–10113.
39. Bowers, N.; McComb, B. A Continuous Spectrophotometric Method for Measuring the Activity of Serum Alkaline Phosphatase. *Clin. Chem.* **1965**, *12*, 70–89.
40. For an example of a cell phone-based glucose meter see: iBGStar blood glucometer, Sanofi-Aventis U.S. LLC: Bridgewater, NJ USA <http://www.ibgstar.us/> (07/08/2014).

Chapter 3

Reagents that enable rapid triaging of enzyme assays using smell as an output

3.1 Introduction

Rapid and sensitive assays for the detection of disease biomarkers and environmental pollutants are necessary to reduce the burden of disease and pollution on human health. Although currently available diagnostic assays can achieve remarkable sensitivities, these assays usually require laboratory infrastructure and are time-consuming to perform.¹⁻² Quantitative assays for disease biomarkers are usually more time intensive and expensive to perform compared to qualitative assays that provide a simple yes or no answer if the analyte being assayed is present or absent in the sample. For example, a quantitative ELISA to determine PSA (a protein biomarker for prostate cancer³) concentrations in blood serum involves several assay steps and usually takes a few hours to perform. In contrast, it takes only a few minutes to perform a qualitative, lateral-flow assay to detect the presence of the hormone biomarker hCG in urine (home-pregnancy test).⁴ The difficulty in performing quantitative assays in resource-limited settings can be even more significant if a large number of samples must be tested quickly for disease biomarkers to determine the appropriate treatment. The time constraint for performing quantitative assays can be minimized by triaging the large number of samples by qualitative yes/no assays and then performing quantitative assays only on the samples that have provided a positive indication for the presence of the biomarker. Figure 3-1 illustrates such a general strategy to triage samples (using odor as an assay output), while simultaneously including the option of quantitative measurements (using fluorescence as an assay output).

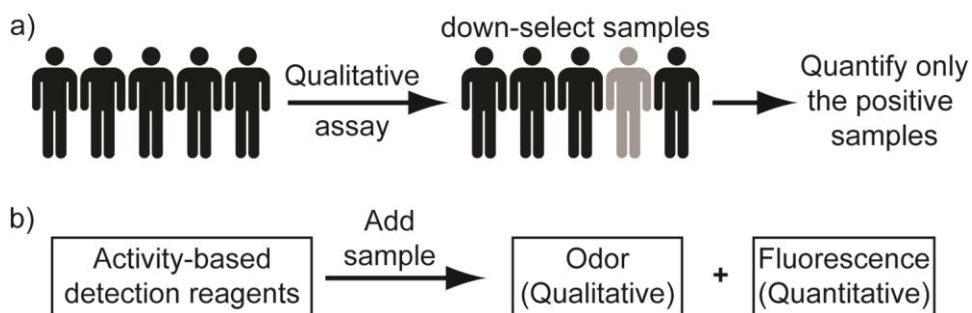


Figure 3-1. Assay strategy for triaging samples (a) using odor generated from activity-based detection reagents present in the assay (b).⁵

The use of odor as an assay output for triaging samples has certain advantages. First, it does not require any special equipment for detecting the qualitative readout (the human nose is ubiquitous). Second, the sensitivity of the assay using odor can be modified by using particularly odorous reporters. For example, the use of thiol as an assay reporter should make the assay very sensitive as the human nose is particularly receptive to thiols.⁶ Human nose can detect thiols at concentrations as low as 2 ppb in air. Third, unlike a colorimetric assay, odor-based assays remain unaffected by the color of the assay mixture. Consequently, we wanted to develop a single-step assay for detection of enzyme biomarkers using odor as an output, with the additional ability to obtain quantitative measurement of the biomarker concentration in the sample, if needed.

Odor has been used in diagnosis of skin infections, tuberculosis, diabetic ketoacidosis, liver diseases, and cancer.⁷ However, these diagnostic tests are usually anecdotal and are unlikely to replace molecular diagnostic tests. In contrast, synthetic reagents capable of controlled release of odorous compounds can be useful for certain applications, such as diagnostics. For example, Phillips and coworkers developed controlled release reagents that released fragrant molecules for potential deodorization applications.⁸ These reagents simultaneously released two fragrant alcohols (e.g., citronellol and 2-phenylethanol) and a colored reporter as a response to β -glucuronidase (an enzyme biomarker for *E. coli* infection). In the context of diagnostic assays, Filipe and coworkers developed a variant of ELISA that released odorous compounds (instead of the commonly used colorimetric ELISA).⁹ They used tryptophanase enzyme conjugated to an antibody as a detection reagent. The co-immobilization of the labeled antibody onto a solid support in the presence of the target antigen was followed by enzymatic transformations to generate odorous methanethiol or indole. However, like most diagnostic assays based on ELISA, this odor based ELISA remains difficult to implement in resource-limited settings because of the complexity of the assay procedure and the use of thermally-sensitive reagents.

We describe here the design of an activity-based detection reagent that simultaneously releases highly odorous ethanethiol and a fluorescent reporter as a response to hydrogen peroxide (a signaling molecule). We use this small-molecule reagent in a single-step enzyme detection assay to triage samples by odor and then to quantify enzyme concentrations using the fluorescent signal.

3.2 Experimental design

3.2.1 Design of a reagent that generates two distinct readouts

To develop a single step enzyme detection assay that simultaneously allows triaging of samples by odor and quantitative measurement of enzyme levels (Figure 3-1), we designed controlled release reagent **3-1**. Reagent **3-1** contains an aryl boronate that reacts with hydrogen peroxide (H_2O_2) to reveal a short-lived intermediate phenol (Figure 3-2). The phenol intermediate undergoes a rapid 6-*exo*-trig cyclization to generate a coumarin-based fluorophore (**3-2**) and an equivalent of ethanethiol.

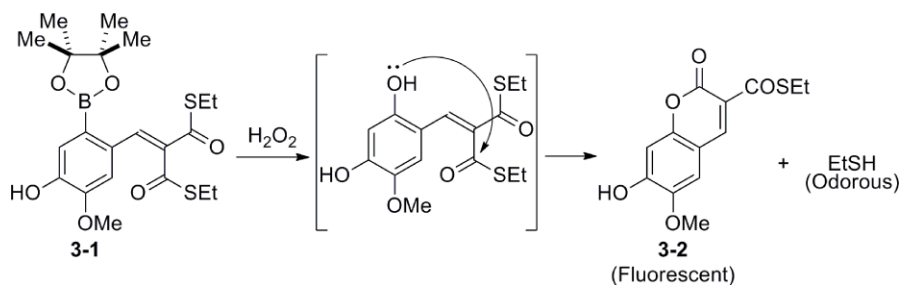


Figure 3-2. Reaction of the controlled release reagent **3-1** with H_2O_2 (a signal-transduction molecule) to generate the dual readouts of fluorescence (**3-2**) and odor (ethanethiol).

The development of the reagent **3-1** involved certain design criteria that had to be met for the odor-based assay strategy to work effectively. Firstly, the odor-generating reagent must be compatible with the conditions used for enzyme detection assays in biological samples. We included an aryl boronate functional group that reacts selectively with H_2O_2 and undergoes a rapid oxidative cleavage reaction in aqueous environment to reveal a phenol functionality. The use of aryl boronate functionalities for fluorescence imaging of H_2O_2 in biological samples has been demonstrated previously.¹⁰ Moreover, H_2O_2 can also be used as a signal transduction molecule in coupled enzyme assays.¹¹ Secondly, to achieve the highest level of sensitivity, **3-1** should be designed to induce the highest levels of odor response. We included a thiol releasing unit (a thioester) in the design of reagent **3-1**. A volatile thiol (ethanethiol) was specifically chosen as the reporter molecule since the human nose is especially sensitive to low molecular weight thiols and can detect concentrations as low as 2 ppb of thiols in air.⁶ Finally, there should

be matching in sensitivity between the qualitative (i.e., odor) and the quantitative (i.e., fluorescence) signals in the single-step assay depicted in Figure 3-1. To achieve this goal, reagent **3-2** was designed to generate a coumarin-based fluorescence reporter (along with a thiol). Compared to colorimetric assays, fluorescence assays are more sensitive and are expected to have a better sensitivity matching with assays that generate thiols with very low odor threshold concentrations.

3.2.1 Design of a single-step enzyme assay strategy for triaging of samples by odor

Once we had designed a reagent that gave two distinct readouts, our goal was to develop a single-step assay to detect enzymes both qualitatively (i.e., using odor) and quantitatively (i.e., using fluorescence). To achieve this goal, we used the combination of controlled release reagent **3-1** and a general detection reagent **3-3** to develop a single-step assay (Figure 3-3). Detection reagent **3-3** generates glucose in the presence of a specific enzyme analyte. Glucose oxidase present in the assay solution catalyzes the oxidation of the released glucose to generate gluconic acid and H_2O_2 (the signal transduction molecule). Controlled release reagent **3-1** then reacts with H_2O_2 to generate the fluorescent and the odorous products. Since reagents **3-1** and **3-3** are designed to work in tandem in a single assay solution, several enzyme analytes can be detected by simply switching the detection reagent **3-3**.

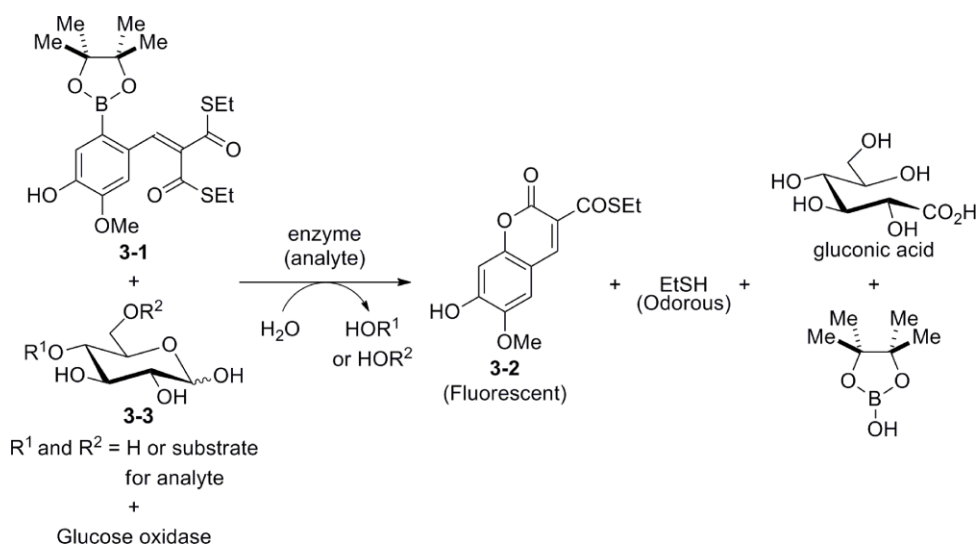


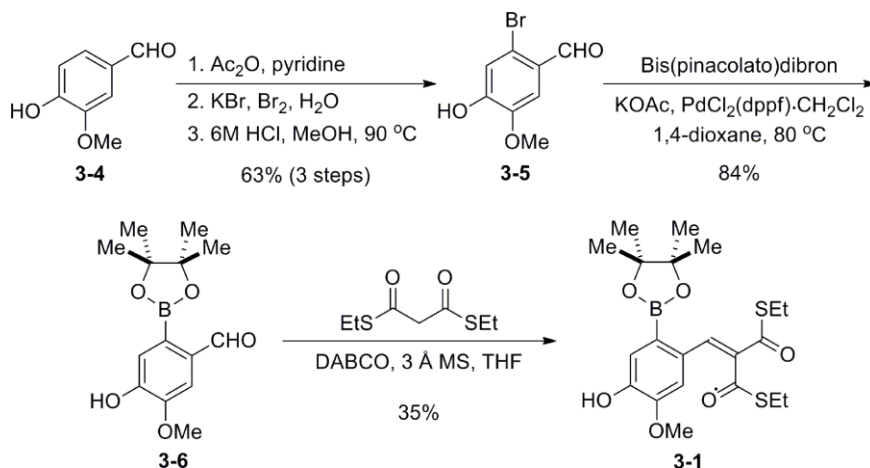
Figure 3-3. A single-step assay strategy using controlled release reagent **3-1** and a general detection reagent (**3-3**).

3.3 Results and discussion

3.3.1 Synthesis of controlled release reagent 3-1.

Controlled release reagent **3-1** was synthesized from commercially available starting material vanillin (**3-4**). Briefly, 6-bromovanillin (**3-5**) was synthesized from vanillin in three steps with a yield of 63%. The aryl boronate (**3-6**) was synthesized using a Miyaura borylation of **3-5**. A base-catalyzed Knoevenagel condensation was used to transform intermediate **3-6** to controlled release reagent **3-1**. Although the condensation reaction had a modest yield (35%), the remainder of the material from the reaction was recovered starting material **3-6**, which could be recovered and used again.

Scheme 1. Synthetic route to controlled release reagent **3-1**.



3.3.2 The response of reagent 3-1 to H₂O₂.

Controlled release reagent **3-1** is designed to react rapidly with H₂O₂ in aqueous solutions to generate the coumarin derivative **3-2**. To demonstrate the reactivity of **3-1**, we treated a 0.5 mM solution of **3-1** in 1:1 MeOH/10 mM phosphate buffer (pH 7.4) with 5 equivalents of H₂O₂ and monitored the reaction using LC-MS. Reagent **3-1** was consumed within minutes and a LC-MS peak corresponding to **3-2** was observed (Figure 3-4). The cyclization reaction to generate **3-2** (Figure 3-2) is very rapid and none of the oxidative cleavage product (i.e., the phenol intermediate) was observed by LC-MS. The characteristic odor of ethanethiol was also detected during the reaction.

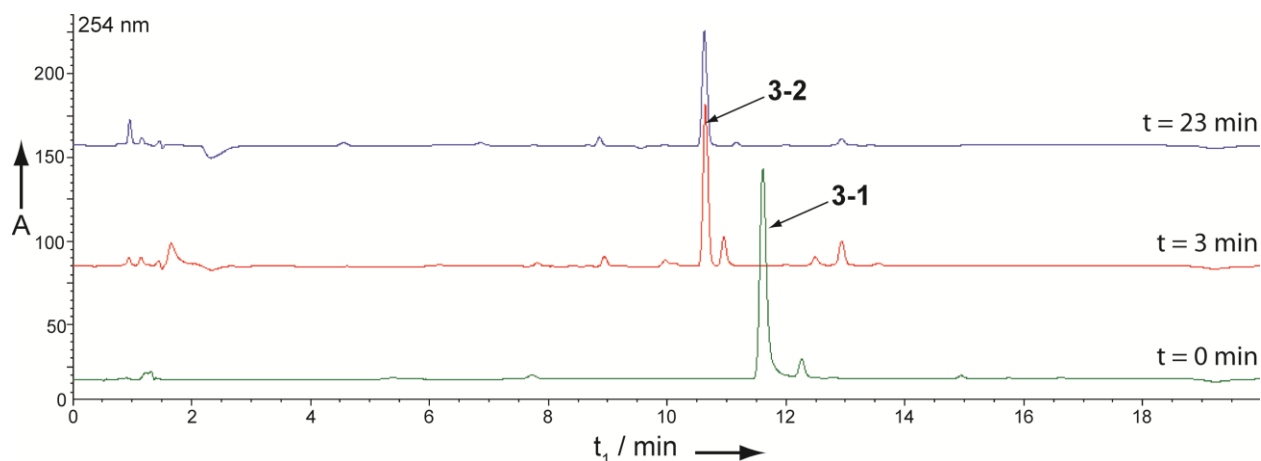


Figure 3-4. Overlaid LC-MS spectra for three sequential injections of aliquots of the reaction mixture containing 0.5 mM **3-1** and 5 equivalents of H_2O_2 . The reaction solvent was 1:1 MeOH/ 10 mM phosphate buffer (pH 7.4) at 20 °C.⁵

We also followed the progress of the reaction by fluorescence spectroscopy. Specifically, when **3-1** (20 μM in 10 mM phosphate buffer containing 1% (v/v) MeOH) was treated with H_2O_2 (1.1 equiv) the fluorescence emission intensity around 500 nm increased rapidly over 12 minutes (Figure 3-5), providing further evidence that **3-1** is converted to the fluorescent product **3-2** in the presence of H_2O_2 .

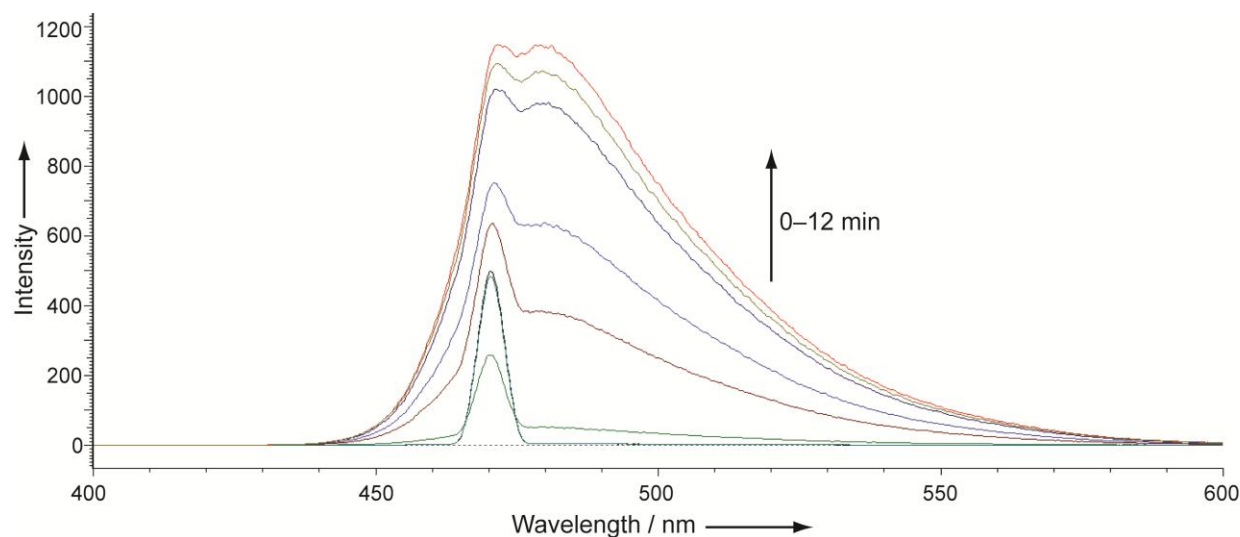


Figure 3-5. Time dependent fluorescence emission spectra for a reaction containing 20 μM **3-1** and 1.1 equivalents of H_2O_2 . The reaction solvent was 10 mM phosphate buffer (pH 7.4) with 1% (v/v) MeOH. The excitation wavelength (λ_{ex}) was 470 nm and the experiment was conducted at 20°C. Fluorescence spectra were acquired every 2 minutes.⁵

When controlled release reagent **3-1** was exposed to varying concentrations of H_2O_2 in a fixed-time assay, a reproducible dose-response curve was obtained (Figure 3-6). Correlation between the fluorescence emission intensity and the concentrations of H_2O_2 provided further evidence for the generation of the fluorescent product **3-2**. The predictable response of **3-1** to H_2O_2 also suggested that H_2O_2 can operate effectively as a signal-transduction molecule in a single-step, two-component enzyme detection assay as depicted in Figure 3-3.

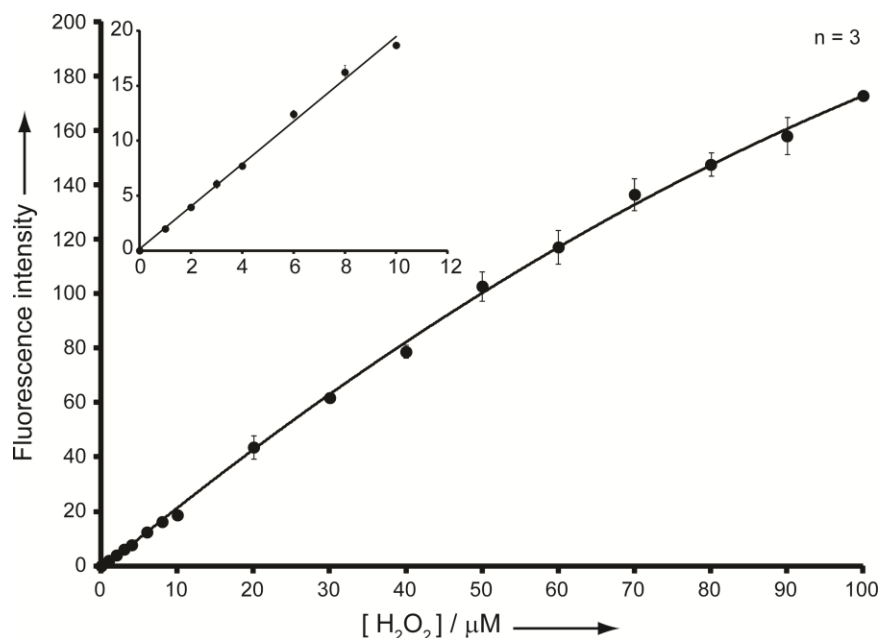


Figure 3-6. Dose-response curve obtained when **3-1** was treated with varying concentrations of H_2O_2 . The final concentration of **3-1** in the assay was 20 μM in 10 mM phosphate buffer (pH 7.4) containing 1% (v/v) MeOH. The fluorescence emission intensity was measured at 510 nm with $\lambda_{\text{ex}} = 470$ nm. All data points represent the average of three independent measurements and the error bars reflect the standard deviation from these averages.⁵

3.3.3 Single-step enzyme assay strategy for triaging of samples (by odor) and quantifying enzyme concentrations (by fluorescence).

To test the idea that H_2O_2 can be used as a signal-transduction molecule in a fluorescence-based enzyme assay (Figure 3-3), we set up two separate assays for the detection of β -galactosidase and alkaline phosphatase (ALP). Briefly, a mixture of controlled release reagent **3-1**, the general detection reagent **3-3** (**2-1** or **2-3**) (Figure 3-7), and glucose oxidase was treated

with aqueous samples containing varying concentrations of the enzyme (β -galactosidase or ALP). The fluorescence emission intensity of the assay solution was measured after an interval of 1 hour. Two calibration curves were prepared using the fluorescence measurement data.

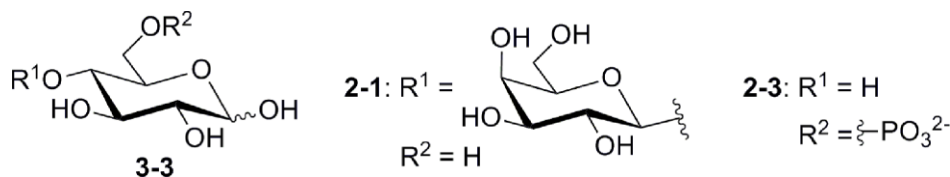


Figure 3-7. The structures of specific detection reagents used in combination with **3-1** in the single-step enzyme detection assay depicted in Figure 3-3. The enzymes β -galactosidase and alkaline phosphatase catalyze the hydrolysis of the reagents **3-3a** and **3-3b** to generate glucose.⁵

These single-step, fluorescence assays using the reagents **3-1** and **3-3** are sensitive enough to detect low nM levels of enzymes (Figure 3-8). For example, the limit-of-detection (LOD) for the assay for β -galactosidase was 21 nM (enzyme activity of 2.2 U L^{-1}) with a linear dynamic range extending up to 500 nM. Similarly, the calibration curve for the detection of ALP provided a LOD of 10 U L^{-1} with a dynamic range of 10 U L^{-1} – 1000 U L^{-1} .

To demonstrate the effectiveness of the assay strategy (Figure 3-3) to triage samples by the odor of the assay, we conducted a double blind odor panel test. Briefly, ten individuals (member of the Phillips group) each were given four different samples, two of which were control assays. The other two assays were chosen randomly from a selection that contained either 0 nM or 200 nM β -galactosidase. Using only the odor of the assays, 80% of the samples were identified correctly as containing either 0 nM or 200 nM of β -galactosidase. Since 200 nM of β -galactosidase lies approximately at the center of the linear dynamic range of the fluorescence-based assay, the sensitivity of the qualitative odor panel test matches perfectly with the quantitative assay. Similar sensitivity matching was also observed for the assay for ALP. The odor panel test for ALP showed that 70% of the samples were identified correctly as containing either 0 U L^{-1} or 100 U L^{-1} . The matching in sensitivities between the odor-based qualitative assays and the fluorescence-based quantitative assays suggests that the former can be used to triage samples without using expensive equipment.

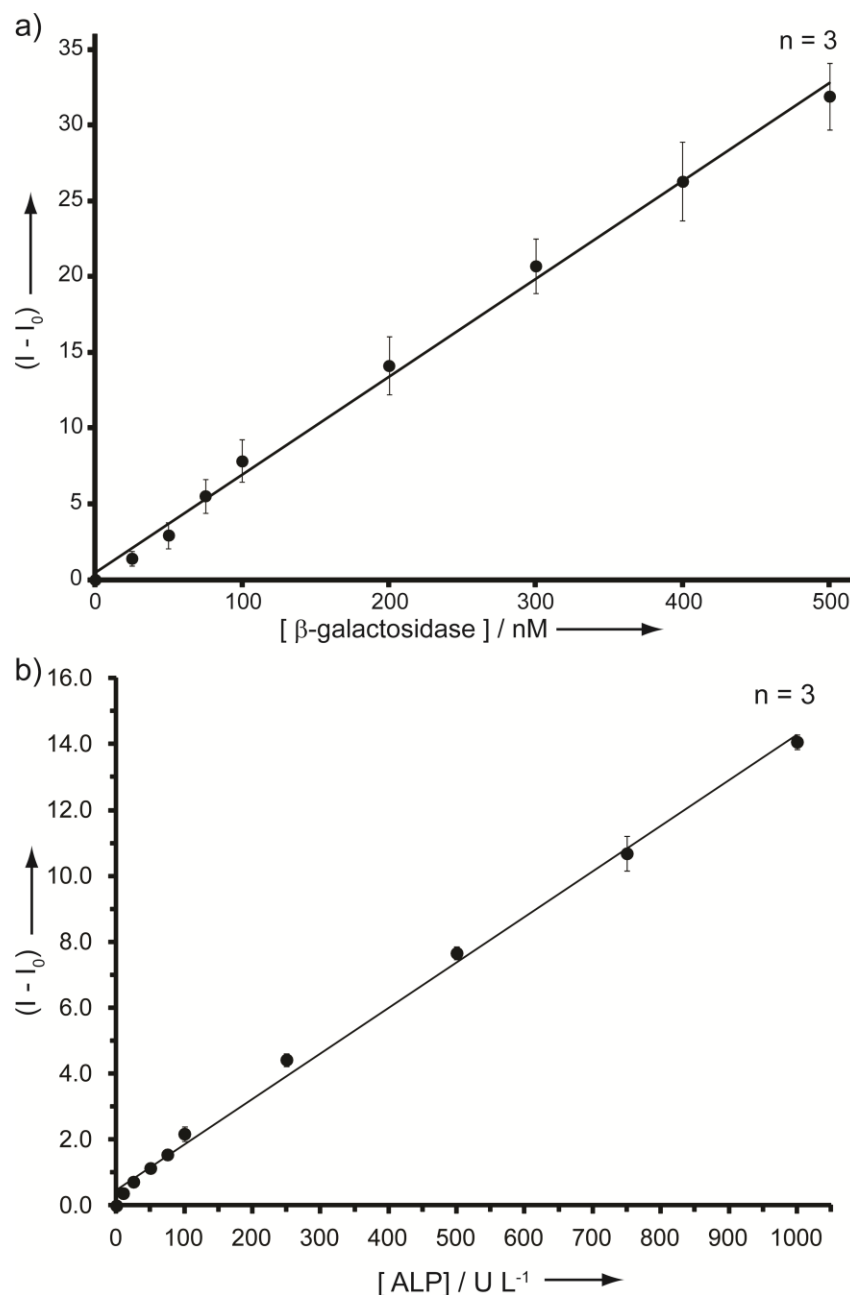


Figure 3-8. Calibration curves for the quantitative detection of the enzymes (a) β -galactosidase, and (b) ALP using the reagents **3-1** and **3-3**. The final concentrations of **3-1**, **3-3a** (or **3-3b**), and glucose oxidase were 20 μM , 10 mM, and 1000 U L^{-1} respectively. The assay solutions were in 10 mM phosphate buffer, pH 7.4, containing 1% (v/v) MeOH (for a) and 50 mM Tris buffer, pH 7.4 containing 1% (v/v) MeOH (for b). The fluorescence emission intensities (I) were measured at 510 nm using $\lambda_{\text{ex}} = 470 \text{ nm}$, and the assay times were 1 h. I_0 denotes the fluorescence intensities obtained in the absence of the enzyme analyte. All data points represent the average of three independent measurements and the error bars reflect the standard deviation from these averages.⁵

3.4 Conclusions

In conclusion, we have developed a single-step enzyme assay strategy with dual-output (odor and fluorescence) that allows triaging of samples using odor. The odor output is generated using a controlled release reagent that releases ethanethiol in the presence of H_2O_2 . The odor can be used to obtain a qualitative indication of the presence of enzyme biomarkers through a sequence of chemical transformations in a single assay vessel. The odor-based qualitative assay is amenable for use in resource limited environments, since it removes the need for specialized equipment. The assay also generates a fluorescent product that can be used to quantify the enzyme target. The quantitative fluorescence assay can be accomplished by using inexpensive hand-held fluorescence readers or an even less expensive paper-based device with internal microfluidic batteries to power a miniature fluorimeter.¹² This assay strategy with dual-outputs should reduce the time burden associated with running many quantitative assays in point-of-care settings.

3.5 References

1. Yager, P.; Domingo, G. J.; Gerdes, J. Point-of-Care Diagnostics for Global Health. *Annu. Rev. Biomed. Eng.* **2008**, *10*, 107–144.
2. Giljohann, D. A.; Mirkin, C. A. Drivers of Biodiagnostic Development. *Nature* **2009**, *462*, 461–464.
3. Madu, C. O.; Lu, Y. Novel Diagnostic Biomarkers for Prostate Cancer. *J. Cancer* **2010**, *1*, 150–177.
4. Butler, S. A.; Khanlian, S. A.; Cole, L. A. Detection of Early Pregnancy Forms of Human Chorionic Gonadotropin by Home Pregnancy Test Devices. *Clin. Chem.* **2001**, *47*, 2131–2136.
5. Mohapatra, H.; Phillips, S. T. Using Smell to Triage Samples in Point-of-Care Assays. *Angew. Chem. Int. Ed.* **2012**, *51*, 11145–11148.
6. Greenman, J.; El-Maaytah, M.; Duffield, J.; Spencer, P.; Rosenberg, M.; Corry, D.; Saad, S.; Lenton, P.; Majerus, G.; Nachnani, S. Assessing the Relationship between Concentrations of Malodor Compounds and Odor Scores from Judges. *JADA* **2005**, *136*, 749–757.
7. Bijland, L. R.; Bomers, M. K.; Smulders, Y. M. Smelling the Diagnosis: A Review on the Use of Scent in Diagnosing Disease. *Neth. J. Med.* **2000**, *71*, 300–307.
8. Nuñez, S. A.; Yeung, K.; Fox, N. S.; Phillips, S. T. A Structurally Simple Self-Immolative Reagent That Provides Three Distinct, Simultaneous Responses per Detection Event. *J. Org. Chem.* **2011**, *76*, 10099–10113.

9. Xu, Y.; Zhang, Z.; Ali, M. M.; Sauder, J.; Deng, X.; Giang, K.; Aguirre, S. D.; Pelton, R.; Li, Y.; Filipe, C. D. M. Turning Tryptophanase into Odor-Generating Biosensors. *Angew. Chem. Int. Ed. Engl.* **2014**, *53*, 2620–2622.
10. Miller, E. W.; Albers, A. E.; Pralle, A.; Isacoff, E. Y.; Chang, C. J. Boronate-Based Fluorescent Probes for Imaging Cellular Hydrogen Peroxide. *J. Am. Chem. Soc.* **2005**, *127*, 16652–16659.
11. Zhou, M.; Diwu, Z.; Panchuk-Voloshina, N.; Haugland, R. P. A Stable Nonfluorescent Derivative of Resorufin for the Fluorometric Determination of Trace Hydrogen Peroxide: Applications in Detecting the Activity of Phagocyte NADPH Oxidase and Other Oxidases. *Anal. Biochem.* **1997**, *253*, 162–168.
12. Thom, N. K.; Lewis, G. G.; Yeung, K.; Phillips, S. T. Quantitative Fluorescence Assays Using a Self-Powered Paper-Based Microfluidic Device and a Camera-Equipped Cellular Phone. *RSC Adv.* **2014**, *4*, 1334–1340.

Chapter 4

Signal amplification via a self-propagating, thiol-mediated reaction sequence

4.1 Introduction

Diagnostic tests for disease biomarkers usually employ signal amplification reactions to achieve the levels of sensitivity required for rapid disease diagnosis. Current state-of-the-art diagnostic tests (such as ELISA, PCR, and bio-barcode assays) require multistep procedures to achieve signal amplification.¹⁻³ Recently, several single step amplification strategies have been developed using synthetic polymers,⁴⁻⁵ supramolecular catalysts,⁶⁻⁷ certain biomolecules,^{1,8} or small molecule amplification reagents.⁹ Signal amplification strategies using small molecule reagents are particularly attractive as they have the added advantage of high reagent stability (as compared to biomolecules), and the ease with which these reagents can be modified (as compared to synthetic polymers) to meet desired diagnostic requirements. Small molecule-based signal amplification strategies in the context of diagnostic tests can be described by the general reaction sequence depicted in Figure 4-1. Briefly, an activity-based detection reagent responds selectively to the target analyte to generate a signaling molecule. The signaling molecule is then converted to multiple copies of an output using an amplification reagent. Ideally, the detection and the signal amplification steps occur concurrently in a single assay solution.

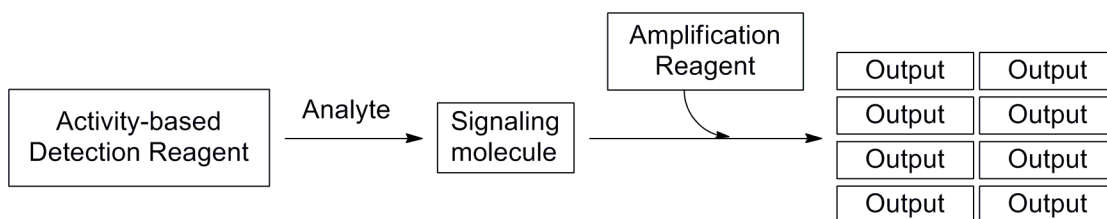


Figure 4-1. Signal amplification in the context of diagnostic tests.

Depending on the mechanism by which they function, small molecule signal amplification reagents can be classified as:

(i) *Reagents that amplify signal through catalysis.* In catalytic signal amplification strategies, the target analyte accelerates the conversion of multiple copies of a small molecule substrate to an easily quantifiable product. Enzyme assays are the most common examples of diagnostic assays

that use catalysis for signal amplification.¹⁰ Chapter 1 (Table 1-2) describes several examples of common enzyme assays used in clinical settings. Catalytic signal amplification is also widely used for the detection of heavy metals (as a pollutant). For example, Koide and coworkers developed an activity-based probe for the detection of palladium (Figure 4-2).¹¹ Probe **4-1** undergoes a palladium catalyzed Tsuji-Trost deallylation reaction to generate a fluorescent product (**4-2**), which can be quantified using a fluorimeter and correlated with the concentration of palladium in the original sample.

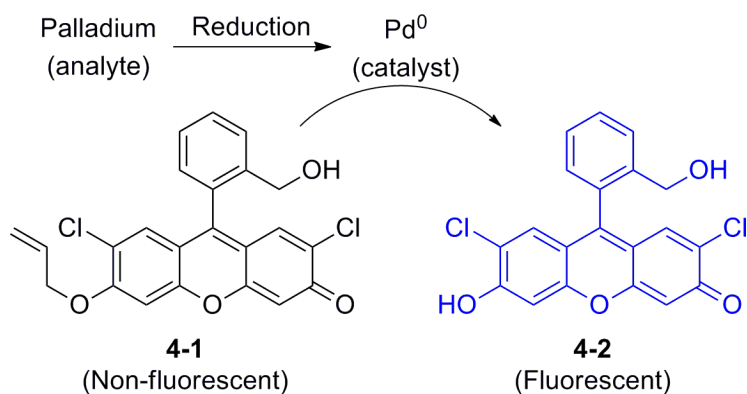


Figure 4-2. A palladium detection assay using palladium catalyzed Tsuji-Trost deallylation reaction.¹¹

(ii) *Reagents that amplify signal through autocatalysis.* In autocatalytic signal amplification reactions, the target analyte reacts with an amplification reagent and generates an active signaling species that catalyzes its own formation. An example of autocatalysis in the context of diagnostics is the silver reduction reaction.¹² In the silver reduction reaction (i.e., $\text{Ag(I)} \rightarrow \text{Ag(0)}$), trace levels of the product (i.e., Ag(0)) catalyze the reaction, leading to rapid deposition of insoluble metallic silver. Silver reduction is commonly used in microscopy, immunoassays, and biobarcode assays.^{3,12} Autocatalytic amplification reactions usually follow sigmoidal reaction kinetics. In Chapter 5, we describe an autocatalytic signal amplification reaction that amplifies signal using a base-mediated reaction sequence.

(iii) *Reagents that amplify signal using autoinductive reagents.* Autoinductive reagents belong to a new class of amplification reagents. These reagents generate two or more copies of an active signaling species in response to the target analyte.¹³⁻¹⁶ The signaling species are subsequently

consumed by additional copies of the autoinductive reagents to produce more copies of the signaling species. The amplification reaction continues to generate the signaling species until all of the autoinductive reagent is consumed. Phillips and coworkers developed a fluoride-mediated autoinductive amplification strategy (Figure 4-3).¹⁴ Briefly, autoinductive reagent **4-3** reacts with trace levels of fluoride (F^-), and through a sequence of chemical transformations generates two copies of F^- and a colored reporter (**4-4**). The generation of two equivalents of F^- ensures that the cyclic reaction sequence continues to generate the colorimetric readout until all of **4-3** is consumed. The autoinductive reaction sequence can be used to measure F^- in drinking water, or can be used to detect a variety of targets using suitable detection reagents that release F^- into an assay solution containing **4-3**. A conceptually similar autoinductive reagent that uses H_2O_2 as the signaling species also has been developed.¹⁶

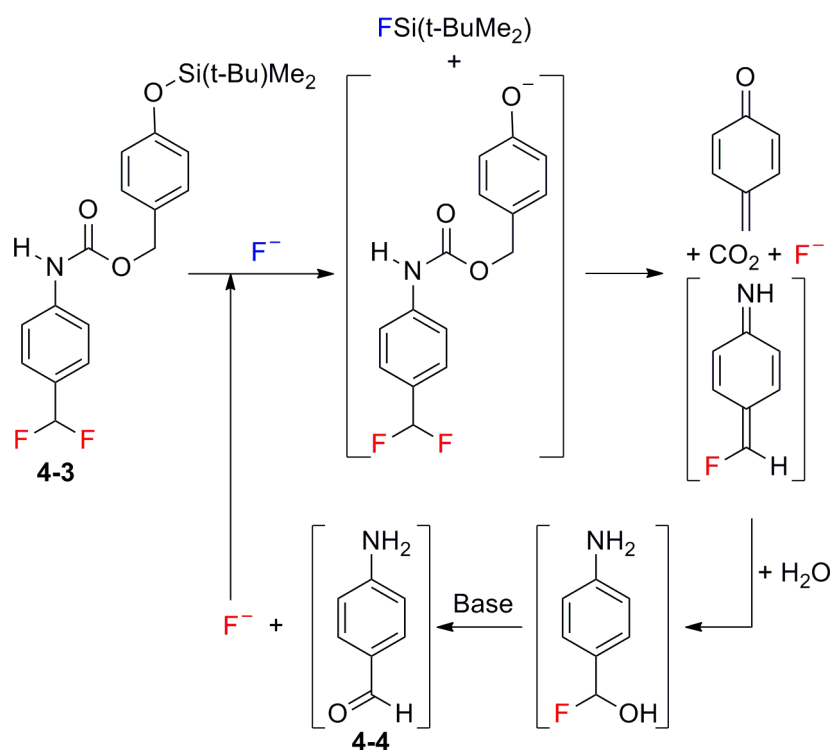


Figure 4-3. Reaction sequence describing a F^- mediated autoinductive signal amplification strategy. The reaction can be used to detect F^- or other targets using a separate detection reagent.¹⁴

(iv) *Reagents that amplify signal using reaction networks.* Amplification strategies using reaction networks employ multiple reagents to detect an analyte and generate an amplified response. At

least one of the reagents used in such a reaction network amplifies signal through catalysis,^{6,7,17} autocatalysis,¹⁸ or as an autoinductive reagent.¹⁹⁻²³ For example, Shabat and coworkers developed a reaction network-based signal amplification strategy using H_2O_2 as the signaling molecule (Figure 4-4).¹⁹ The various components of this reaction network are detection reagent **4-5**, choline (**4-6**), the enzyme choline oxidase, H_2O_2 , and amplification reagent **4-7**. In the presence of the enzyme analyte (penicillin-G-amidase), the reaction network generates the colorimetric product **4-8**. Signal amplification is achieved over time because of catalytic turnover (for the enzymatic transformation of choline to betaine aldehyde) and the ability of the autoinductive signal amplification reagent **4-7** to generate multiple copies of the signaling molecule. Unlike autocatalytic and autoinductive reagents, signal amplification using a reaction networks require multiple reagents to work in tandem.

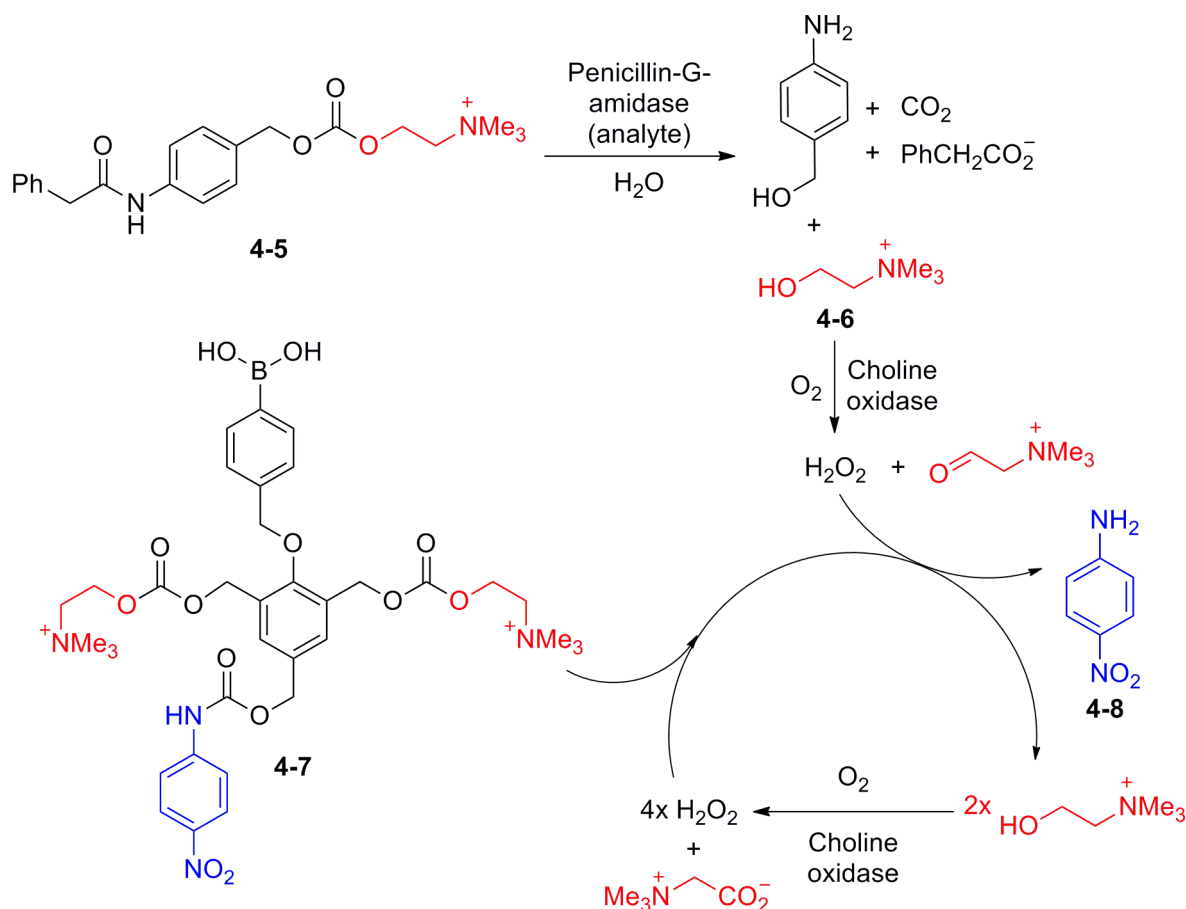


Figure 4-4. Reaction sequence that depicts signal amplification using a reaction network.¹⁹

Signal amplification strategies that use autocatalytic and autoinductive reagents usually follow sigmoidal kinetics with an initial lag phase (Figure 4-5).²⁴ In diagnostic assays, this lag phase can introduce a wait time before the effect of signal amplification is observed. Catalysts, in contrast, amplify signal without a lag phase. We describe here a new class of signal amplification reagents (4-9–4-11) that amplify signal using a self-propagating, thiol-mediated reaction sequence (Figure 4-6). The amplification reaction follows reaction kinetics that is neither catalytic, nor autocatalytic, but is still self-propagating as depicted in Figure 4-6. In the context of diagnostic assays, these amplification reagents can be used in combination with detection reagents to achieve sensitive and selective detection of disease biomarkers.

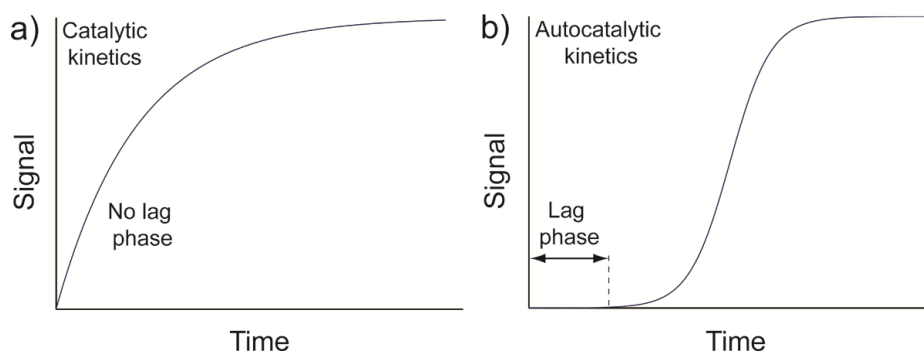


Figure 4-5. Signal generated by amplification reactions that follow (a) catalytic kinetics, and (b) autocatalytic kinetics.

4.2 Experimental design

The amplification reagents (**4-9–4-11**) are designed to respond to thiols and generate an equivalent each of a fluorescent coumarin derivative and ethanethiol (Figure 4-6). The released copy of ethanethiol sets up a self-propagating reaction sequence that amplifies fluorescent signal. We used a 2,4-dinitrobenzene sulfonyl (DNBS) group (green in Figure 4-6) as the thiol responsive unit. The DNBS group reacts selectively with thiols over other nucleophiles.²⁵ In the presence of thiols, the DNBS group is cleaved, revealing a short-lived 2-hydroxy-Z-cinnamate (phenol) intermediate. The intermediate undergoes a rapid 6-*exo*-trig cyclization to simultaneously generate an equivalent of ethanethiol and a coumarin fluorophore. The structure of amplification reagents **4-9–4-11** includes design elements similar to those of the controlled release reagent **3-1**. Consequently, a detection reagent structurally similar to **3-1** can be used to generate the thiol needed to initiate the amplification reaction.

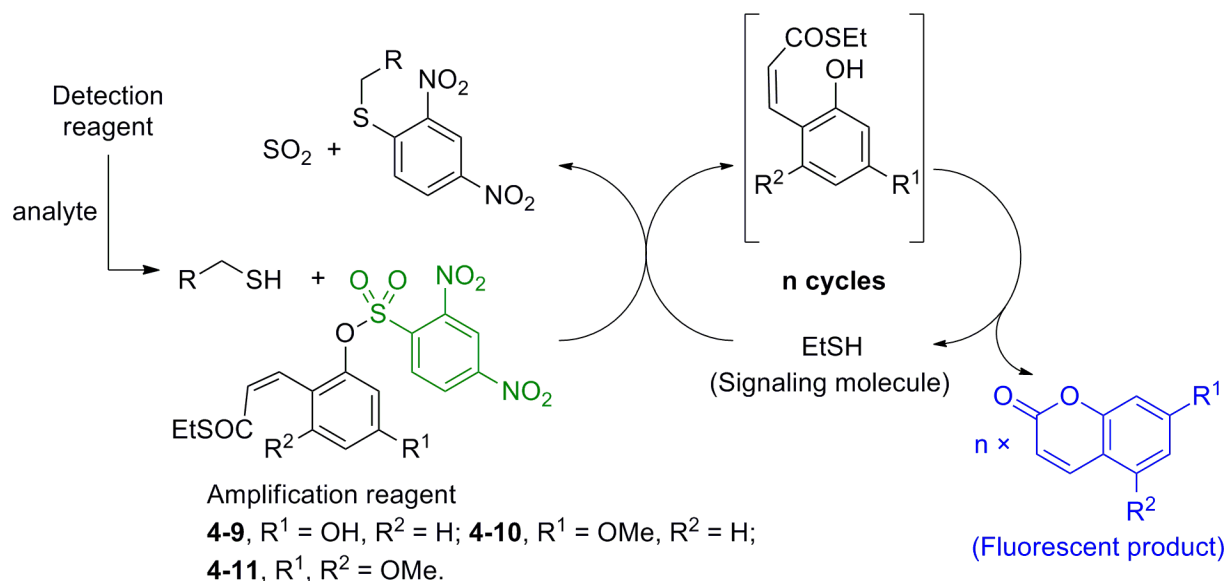


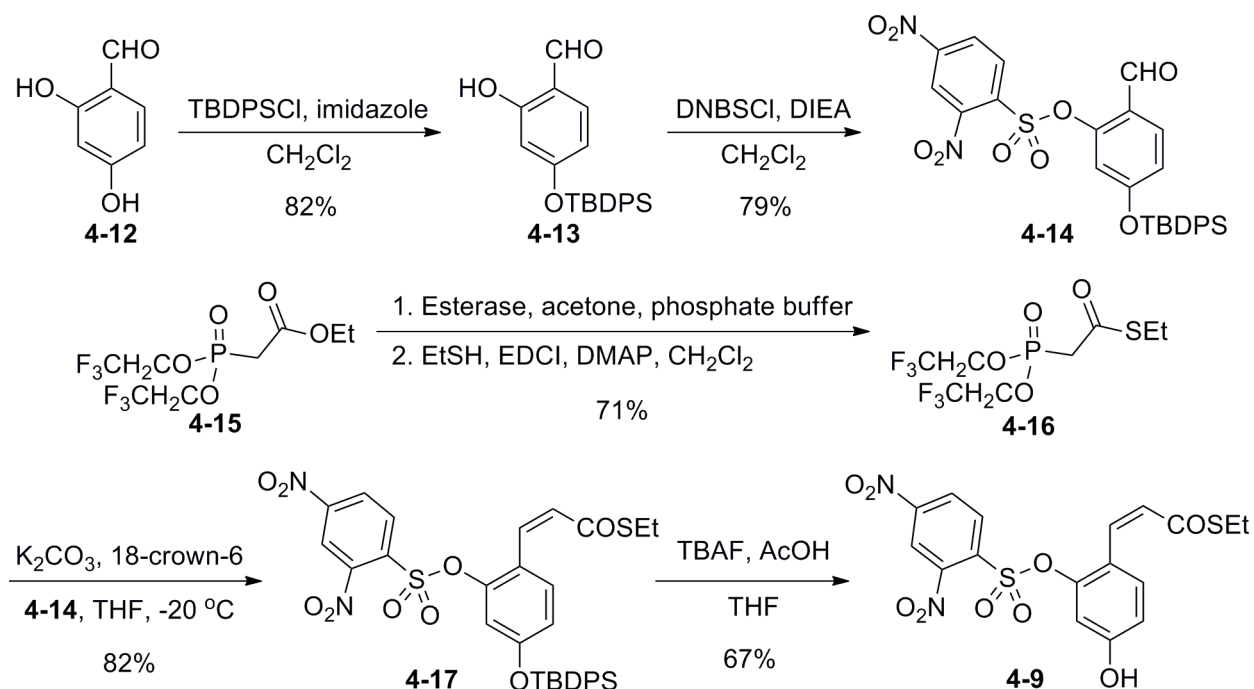
Figure 4-6. Reaction scheme depicting a signal amplification strategy using reagents **4-9**, **4-10**, or **4-11**. The amplification reagents react with trace levels of thiol to generate an equivalent of thiol and a fluorescent product. The reaction sequence continues to generate the fluorescent product until the signal amplification reagent is consumed.

4.3 Results and discussions

4.3.1 Synthesis of amplification reagent 4-9

Amplification reagent **4-9** was prepared using a convergent synthetic route from known starting material **4-12** (Scheme 4-1). Briefly, the phenols on **4-12** were sequentially protected with TBDPS and DNBS groups to obtain the intermediate **4-14**. The phosphoryl thioester intermediate **4-16** was synthesized concurrently using a two-step route. The Z-cinnamate intermediate **4-17** was then prepared from **4-14** and **4-15** using a Horner-Wadsworth-Emmons reaction. Deprotection of the TBDPS group on **4-17** provided amplification reagent **4-9** with an overall yield of 25% (6 steps).

Scheme 4-1. Synthetic route to amplification reagent **4-9**.



4.3.2 Preliminary assay to demonstrate signal amplification using reagent 4-9

To demonstrate the ability of reagent **4-9** to sustain a self-propagating reaction, we treated **4-9** with 0.1 equivalent of L-cysteine and followed the progress of the reaction by measuring the fluorescent output (Figure 4-7). The plot in Figure 4-7 reveals that **4-9** generates a fluorescent signal with increasing intensity, even when the amplification reagent is initiated by only 0.1 equivalent of L-cysteine. The result of the fluorescence-based experiment also suggests that the signal amplification reaction follow kinetics that are similar to that of a catalytic reaction (Figure 4-5). The graph in Figure 4-7 also shows that the amplification reaction has a small amount of background signal (i.e., when no L-cysteine was used in the reaction). This background signal can limit the sensitivity of a detection assay that uses **4-9** for signal amplification. We designed amplification reagents **4-10** and **4-11** to minimize the background reactions, while still retaining the ability to amplify fluorescent signal without a lag phase.

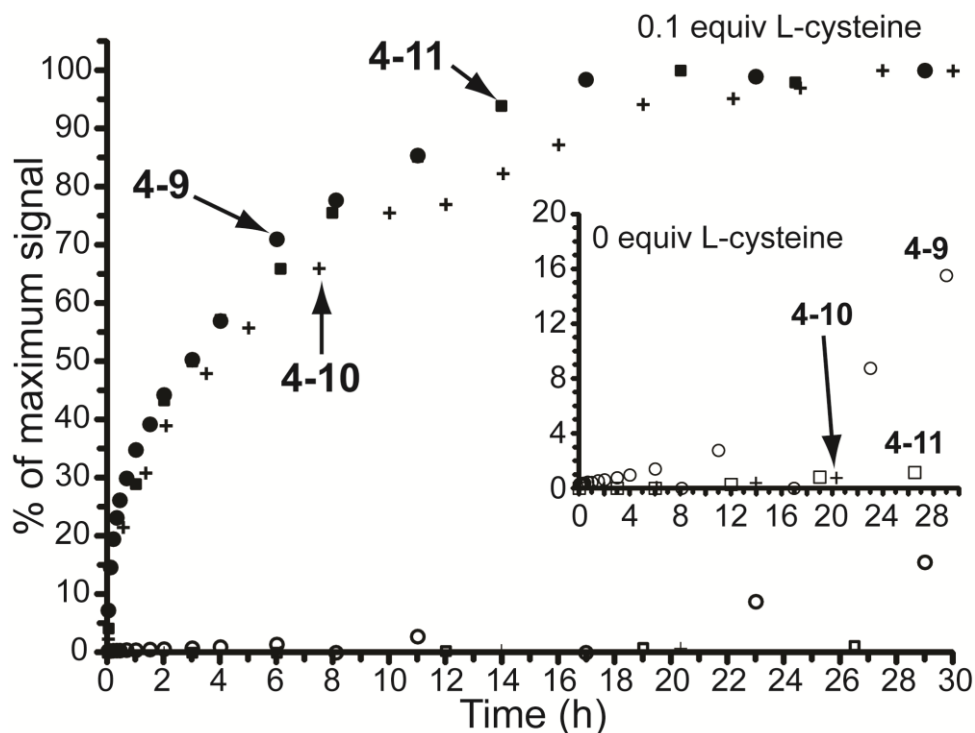


Figure 4-7. Normalized fluorescence signal obtained when signal amplification reagents **4-9**, **4-10**, or **4-11** were exposed to L-cysteine (0.1 or 0 equiv). The concentration of the amplification reagent in each reaction was 2 mM in 1:1 CH₃CN/0.1 HEPES buffer, pH 7.4, 1 mM EDTA. Fluorescence data were obtained after dilution of a 20 μ L aliquot of the reaction mixture in 2 mL of 1:1 CH₃CN/0.1 HEPES buffer, pH 7.4, 1 mM EDTA.

4.3.3 Design of amplification reagents **4-10** and **4-11** to reduce background hydrolysis

We hypothesized that the small amount of background fluorescence signal observed for **4-9** is presumably due to hydrolysis of the thioester via assistance of the phenol resonating through the benzene ring to form a ketene intermediate (Figure 4-8). To test this hypothesis, we prepared amplification reagent **4-10**, in which the phenol is protected as a methyl ether and the presumed resonance effect is reduced.

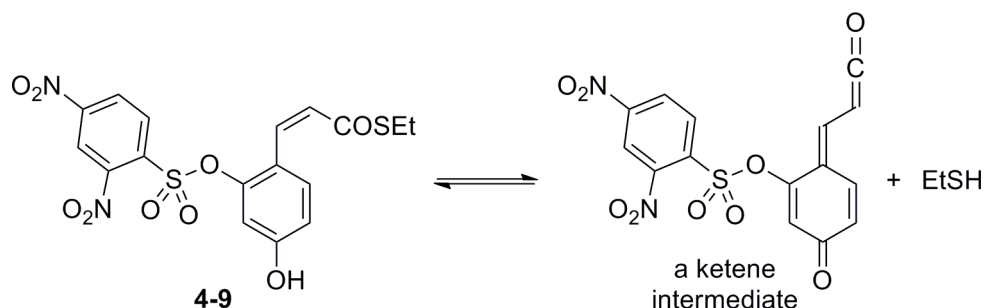
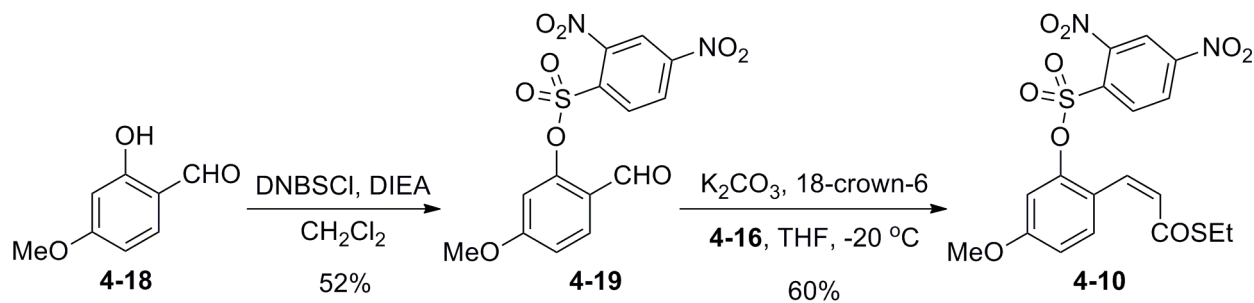


Figure 4-8. Presumed formation of a ketene intermediate that is responsible for background hydrolysis of **4-9**.

Amplification reagent **4-10** was prepared in two steps from commercially available reagents (Scheme 4-2) with an overall yield of 31%. Treatment of amplification reagent **4-10** with 0.1 equivalent of L-cysteine provided a reaction kinetic profile that was similar to that of **4-9**, albeit with a slightly slower reaction rate (Figure 4-7). The background hydrolysis for **4-10** was negligible within the observation window, which suggests that the resonance effect may indeed contribute to the background hydrolysis for **4-9**.

Scheme 4-2. Synthetic route to amplification reagent **4-10**.



The methyl ether group in amplification reagent **4-10** reduces the fluorescence quantum yield of the fluorescent product. The fluorescent product **4-21** (generated from the signal amplification reaction containing **4-10**) is approximately 1.8 times less fluorescent than **4-20** (generated from signal amplification reaction containing **4-9**).²⁶ To offset this reduction in the fluorescent signal, we synthesized a third-generation signal amplification reagent **4-11** (Scheme 4-3). Signal amplification using **4-11** generates the fluorescent product **4-22** (Figure 4-9), which has a fluorescent quantum yield 1.5 times higher than **4-21**.²⁷ Consequently, using **4-11** as a signal amplification reagent results in the recovery of the fluorescent signal that was lost when the methyl ether was included in the amplification reagent, while retaining the lower levels of background hydrolysis.

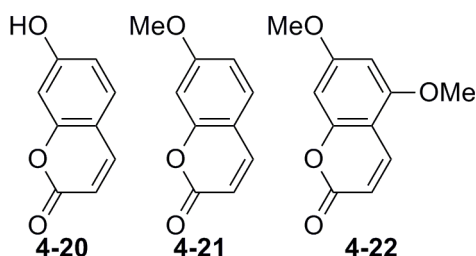
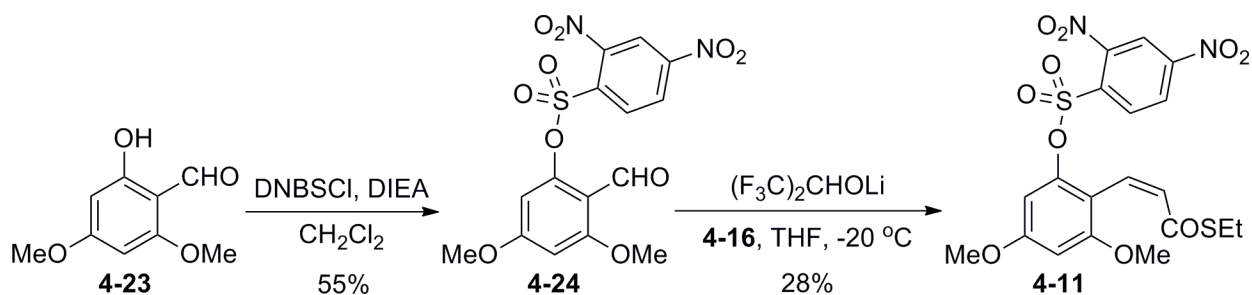


Figure 4-9. Structures of fluorescent products **4-20**, **4-21**, and **4-22** generated in amplification reactions containing reagents **4-9**, **4-10**, and **4-11**, respectively.

Scheme 4-3. Synthetic route to amplification reagent **4-11**.



4.3.4 Time-dependent LC-MS study of the signal amplification reaction using reagent **4-11**

To verify the reactivity of amplification reagent **4-11** as depicted in Figure 4-6, we exposed a solution of **4-11** to 0.1 equivalents of L-cysteine and followed the progress of the reaction using LC-MS (Figure 4-10). We observed the formation of the expected products (**4-22**, **4-25**, and **4-26**). The presence of these products in the reaction mixture was confirmed either by mass spectra, or by co-injection of products prepared by independent syntheses. The reaction mixture was bright yellow, a color consistent with **4-26**, which is formed by a known Smiles rearrangement reaction of the L-cysteine adduct with dinitrobenzene.²⁸ The absence of a peak corresponding to the phenolic intermediate (Figure 4-6) suggests that the 6-*exo*-trig cyclization reaction is fast and that the thiol-mediated cleavage of the DNBS group is the rate-limiting step in the amplification reaction.

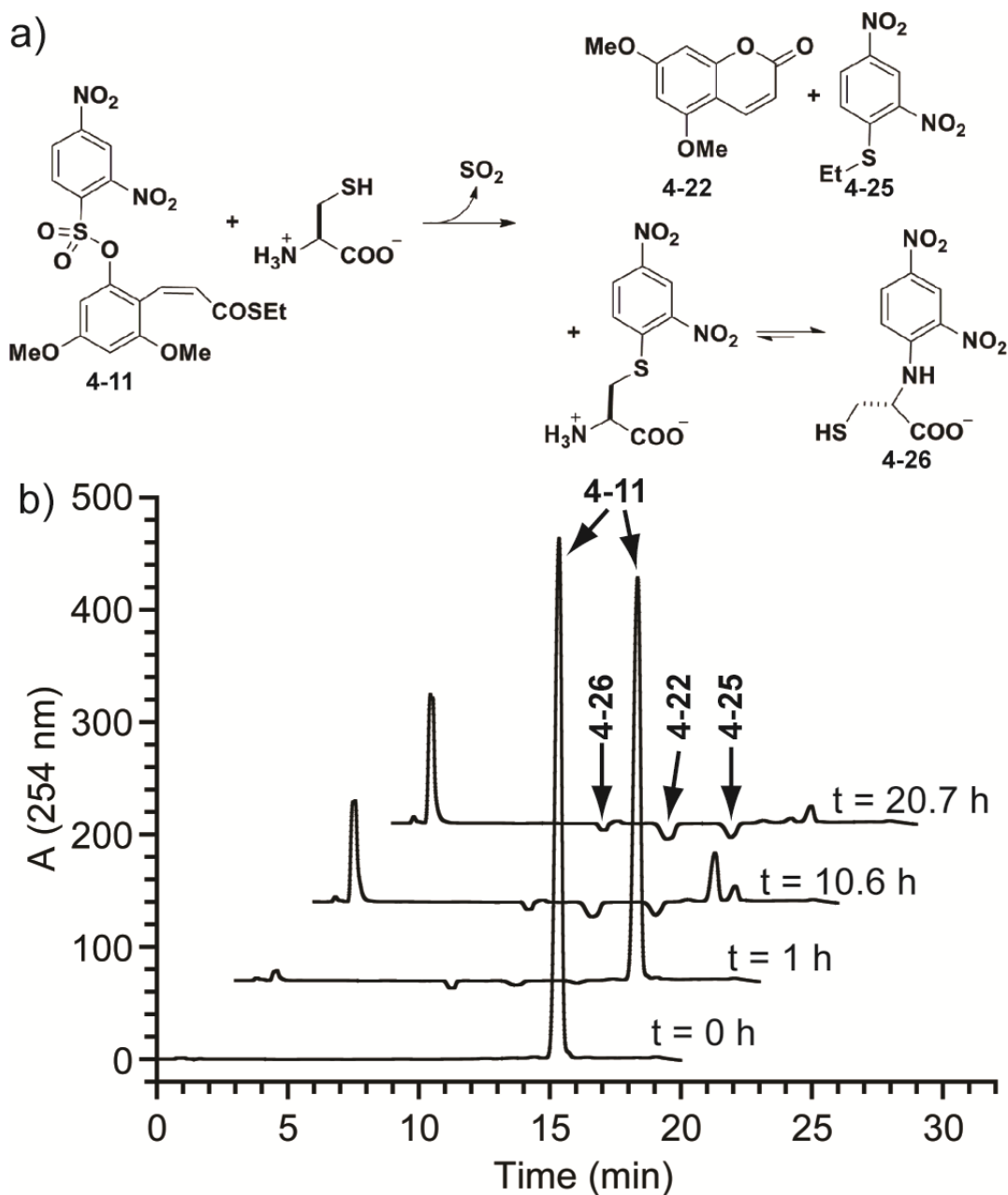


Figure 4-10. Analysis of the reaction products obtained when **4-11** was exposed to 0.1 equiv of L-cysteine. L-cysteine was used to initiate the amplification reaction to facilitate ionization and identification of products. (a) Reaction scheme depicting the reaction, and (b) overlaid LC-MS spectra for four sequential injections of aliquots of the reaction containing **4-11** (2 mM) and L-cysteine (0.2 mM) in 1:1 CH₃CN/ 0.1 M HEPES buffer, pH 7.4, 1 mM EDTA.

4.3.5 Dose-dependent signal amplification using reagent **4-11**

When amplification reagent **4-11** was treated with varying initial quantities of ethanethiol (a signaling molecule that could be generated from a detection event), we observed a dose-dependent generation of fluorescent signal (Figure 4-11). The kinetics profile depicted in Figure 4-11 reveals that regardless of the initial quantity of ethanethiol, the amplification reactions using **4-11** provide the same maximum level of signal. Additionally, the time required to obtain a signal with a defined fluorescent intensity is dependent on the quantity of ethanethiol used to initiate the reactions. These observations suggest that **4-11** can perform effectively as a signal amplification reagent as depicted in Figure 4-6.

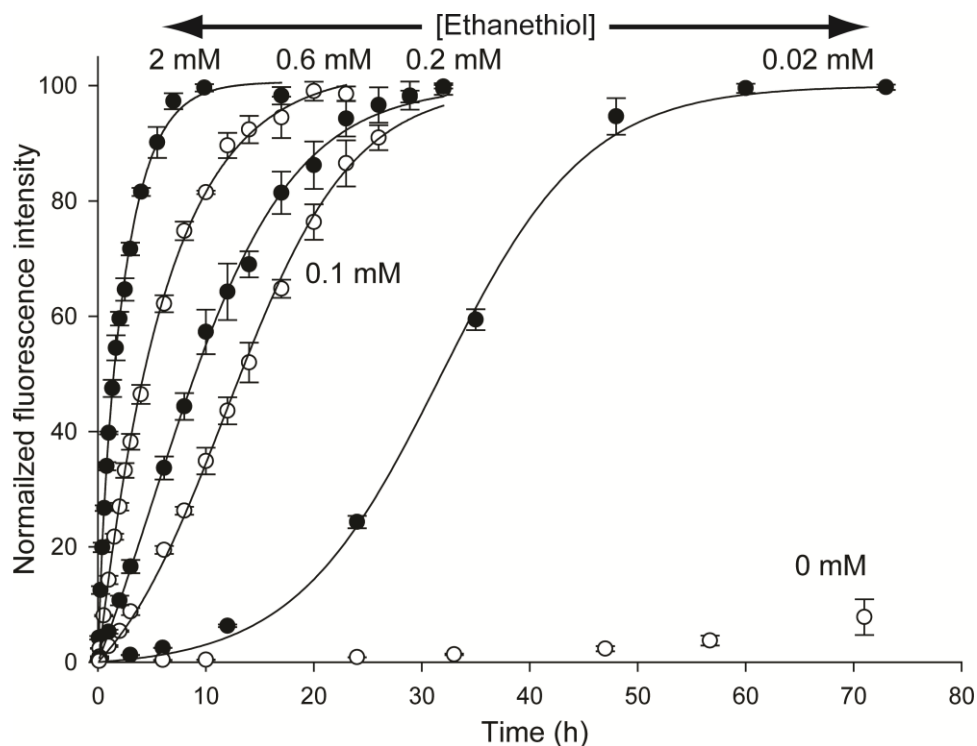


Figure 4-11. Normalized fluorescence data obtained when amplification reagent **4-11** was treated with different initial quantities of ethanethiol. The concentration of **4-11** in each reaction mixture was 2 mM in 1:1 CH₃CN/0.1 M HEPES buffer, pH 7.4, containing 1 mM EDTA. Fluorescence measurements ($\lambda_{\text{excitation}} = 325$ nm; $\lambda_{\text{emission}} = 430$ nm) were obtained after the dilution of 20 μ L aliquots of the reaction mixture in 2 mL of 1:1 CH₃CN/0.1 M HEPES buffer, pH 7.4, containing 1 mM EDTA. The data points represent the average of three independent measurements and the error bars represent the standard deviations from these averages. The normalized fluorescence data were fit using equation 4.6, which is described in the next section.

4.3.6 Analysis of the kinetics of signal amplification using reagent **4-11**

Amplification reagent **4-11** was designed to provide amplification kinetics similar to catalytic signal amplification reactions, i.e., without a lag-phase (Figure 4-5). The fluorescent signal profiles obtained using **4-11** (2 mM) and initial ethanethiol concentrations greater than 0.05 equiv (100 μ M) follow the expected second-order kinetics without a lag phase. However, at lower levels of ethanethiol (i.e., ≤ 0.05 equiv), we observed a deviation from the expected kinetics (i.e., kinetic profiles appear sigmoidal). A possible reason for such a deviation could be the manifestation of autocatalysis in the amplification reaction depicted in Figure 4-6 (i.e., one of the reaction products catalyses the amplification reaction). To further evaluate if autocatalysis is observed in the amplification reaction, we constructed a kinetics model that included product catalysis in the rate equation. Briefly, for the overall reaction:



where P is a reaction product (Figure 4-6) that promotes the reaction.

The rate equation for the reaction takes the form:

$$\begin{aligned} d[\mathbf{4-22}]/dt &= k_a[\mathbf{4-11}][\text{EtSH}] + k_b[\mathbf{4-11}][\text{EtSH}][\text{P}] \\ &= [\mathbf{4-11}][\text{EtSH}]\{ k_a + k_b[\text{P}] \} \end{aligned} \quad (4.1)$$

where, $[\mathbf{4-22}]$, $[\mathbf{4-11}]$, $[\text{EtSH}]$, and $[\text{P}]$ are the time-dependent concentrations of **4-22**, **4-11**, EtSH, and P respectively. k_a and k_b are rate constants. Rate equations similar to 4.1 have previously been used to explain the effect of product catalysis in nucleophilic substitution reactions.²⁹⁻³⁰

At steady state:

$$[\mathbf{4-11}] + [\mathbf{4-22}] = [\mathbf{4-11}]_0 \quad (4.2)$$

$$[\mathbf{4-22}] = [\text{P}] \quad (4.3)$$

$$[\mathbf{4-11}]_0 + [\text{EtSH}]_0 = [\mathbf{4-11}] + [\text{EtSH}] + [\text{P}] \quad (4.4)$$

where, $[\mathbf{4-11}]_0$, $[\text{EtSH}]_0$ are initial concentrations of **4-11** and ethanethiol respectively. The $[\mathbf{4-11}]$, $[\text{EtSH}]$, $[\mathbf{4-22}]$, and $[\text{P}]$ are the time-dependent concentrations of **4-11**, EtSH, **4-22**, and P respectively. Equations 4.2–4.4 were derived by balancing the stoichiometry in reactions depicted in Figure 4-6.

Substituting equations 4.2–4.4 in equation 4.1, we obtain:

$$\begin{aligned} d[\mathbf{4-22}]/dt &= [\mathbf{4-11}][\text{EtSH}]\{k_a + k_b[\text{P}]\} \\ &= \{[\mathbf{4-11}]_0 - [\mathbf{4-22}]\}\{[\text{EtSH}]_0\}\{k_a + k_b[\text{P}]\} \end{aligned} \quad (4.5)$$

Equation 4.5 is a first order differential equation with the solution:

$$y = \frac{a(e^{mt} - 1)}{ak + mt} \quad (4.6)$$

where, $a = [\mathbf{4-11}]_0$, $k = k_b / k_a$, $m = (1 + a k) k_a [\text{EtSH}]_0$, and t = reaction time.

The normalized fluorescence data in Figure 4-11 were fit with equation 4.6 and we observed good correlation between the experimental data and the predicted data generated using the kinetic model described by equation 4.1.

To obtain further insight into the nature of catalysis observed in the amplification reactions using **4-11**, we performed control experiments in which we added 0.5 equivalents of reaction products **4-22** (5,7-dimethoxycoumarin) and **4-25** (2,4-dinitrophenylethyl thioether) to separate amplification reactions containing **4-11** (2 mM) and ethanethiol (0.02 mM), and compared the kinetics of these reactions with a similar reaction that contained no additives. Figures 4-12 and 4-13 show that the reaction products (**4-22** and **4-25**) do not affect the rate of the amplification reactions, thus we needed to consider other alternative explanation for the sigmoidal kinetics. Cleavage of the DNBS group is known to follow an $\text{S}_{\text{N}}\text{Ar}$ reaction mechanism.³¹⁻³³ However, the exact nature of the unusual kinetic behavior demonstrated by **4-11** is difficult to ascertain since $\text{S}_{\text{N}}\text{Ar}$ reactions can be catalyzed by a variety of species including base,³⁴ nucleophilic amines,²⁹ and micelles.³⁵⁻³⁶ Alternatively, non-covalent interactions could also be responsible for the apparent autocatalytic behavior.³⁷ Ultimately, the autocatalytic

behavior at low concentrations of thiol appear to originate from the unusual kinetics associated with the cleavage of the DNBS group.

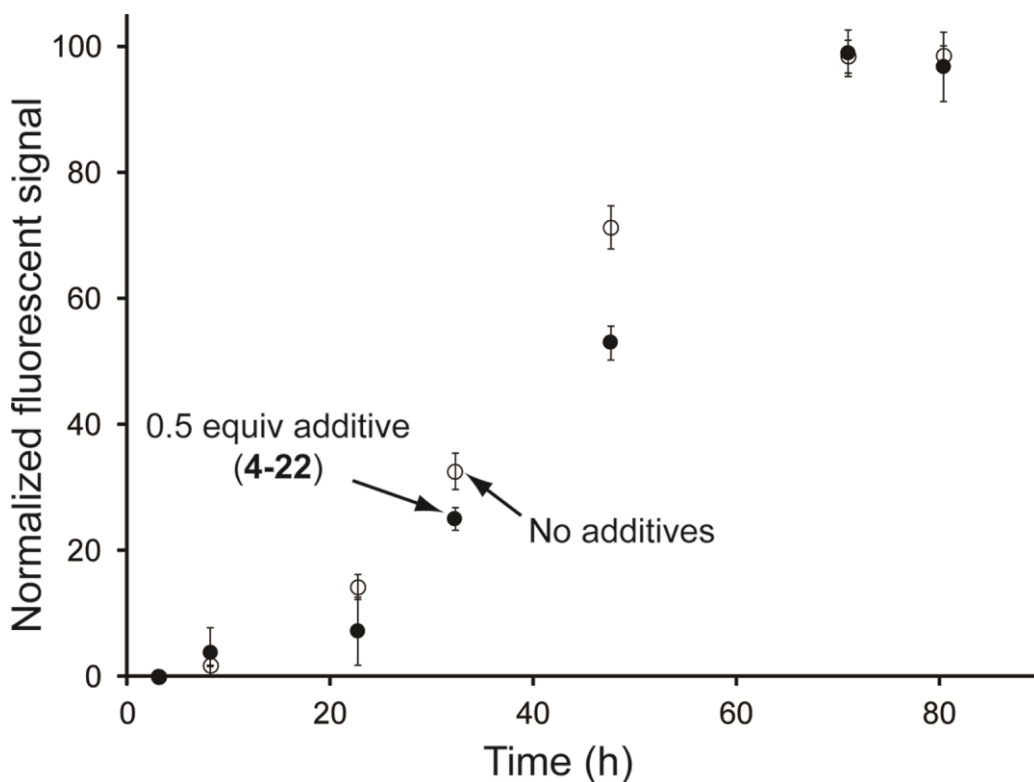


Figure 4-12. Effect of additive **4-22** (1 mM) on the kinetics of signal amplification reaction using **4-11** (2 mM) and ethanethiol (0.02 mM). The reaction solvent was 1:1 CH₃CN/0.1 M HEPES buffer, pH 7.4, containing 1 mM EDTA. Fluorescence data ($\lambda_{\text{excitation}} = 325$ nm; $\lambda_{\text{emission}} = 430$ nm) was obtained after dilution of 20 μL aliquots of the reaction mixture in 2 mL of 1:1 CH₃CN/0.1 M HEPES buffer, pH 7.4, containing 1 mM EDTA. The data points represent the average of three independent measurements and the error bars represent the standard deviations from these averages.

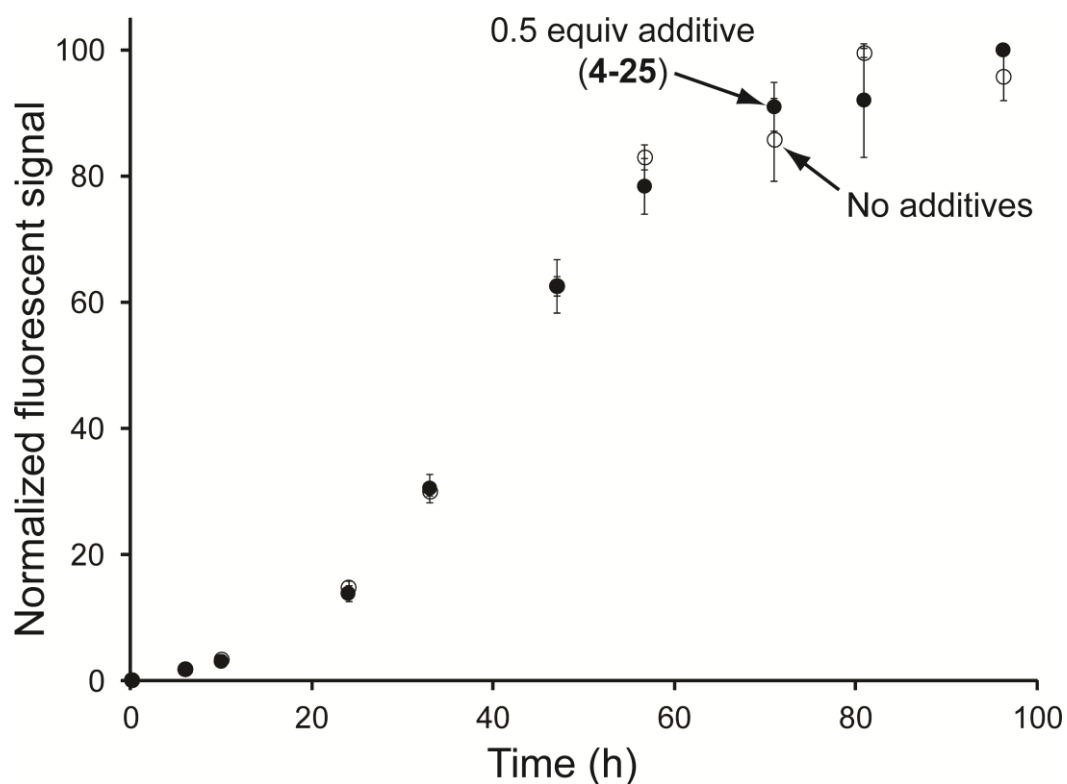


Figure 4-13. Effect of additive **4-25** (1 mM) on the kinetics of the signal amplification reaction using **4-11** (2 mM) and ethanethiol (0.02 mM). The reaction solvent was 1:1 CH₃CN/0.1 M HEPES buffer, pH 7.4, containing 1 mM EDTA. Fluorescence data ($\lambda_{\text{excitation}} = 325$ nm; $\lambda_{\text{emission}} = 430$ nm) was obtained after dilution of 20 μL aliquots of the reaction mixture in 2 mL of 1:1 CH₃CN/0.1 M HEPES buffer, pH 7.4, containing 1 mM EDTA. The data points represent the average of three independent measurements and the error bars represent the standard deviations from these averages.

4.3.7 Generality of the response of amplification reagent **4-11** to thiols

A useful feature of the thiol-mediated signal amplification strategy we describe here is its ability to respond to various types of added thiols (the signaling molecule that would originate from a detection event). In separate experiments, we exposed **4-11** to 0.3 equivalents of various thiols and followed the progress of the reactions using fluorimetry (Figure 4-14). Primary and secondary thiols, including thiophenols provided similar reaction kinetics, but tertiary thiols yielded substantially lower rates of signal amplification. These results further confirm that the cleavage of the DNBS is the rate-limiting step in the amplification reaction. More importantly, these results demonstrate that signal amplification using **4-11** can be initiated using a variety of thiols with approximately similar rates.

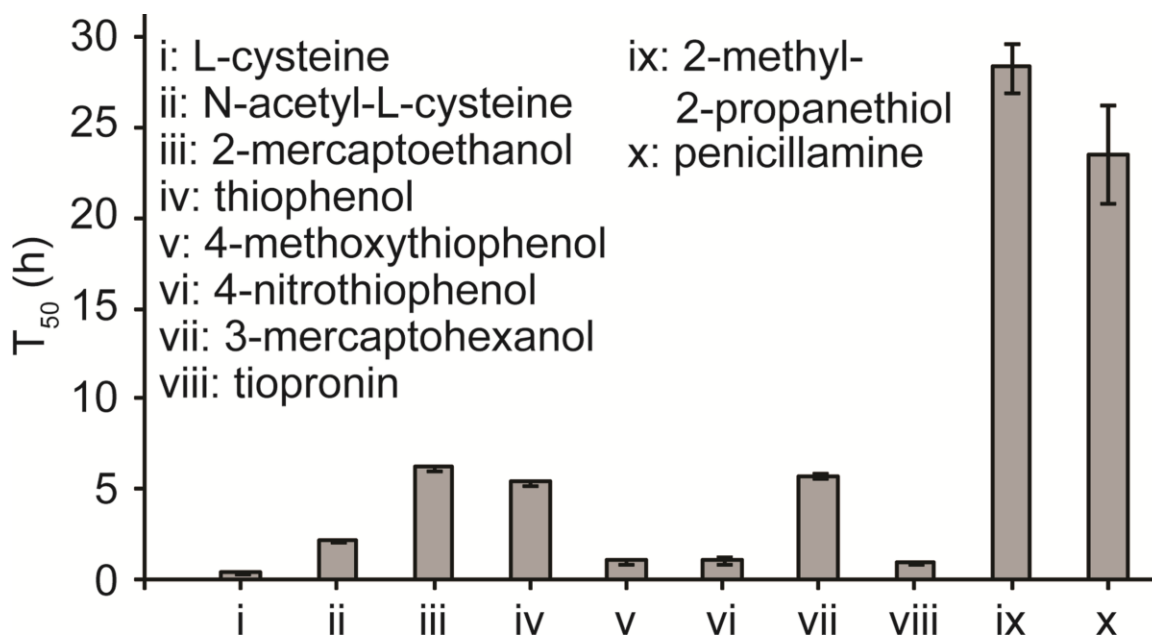


Figure 4-14. Effect of the structure of added thiol on the time required for amplification reactions using **4-11** to reach half of the maximum fluorescent signal (T_{50}). The amplification reactions contained **4-11** (2 mM) and thiol (0.6 mM) in 1:1 $\text{CH}_3\text{CN}/0.1$ M HEPES buffer, pH 7.4, containing 1 mM EDTA. The data presented here are the average of three independent measurements and the error bars represent the standard deviations from the averages.

4.4 Conclusions

In conclusion, we have developed signal amplification reagents **4-9-4-11** that provide an amplified fluorescent output through a thiol-mediated self-propagating reaction. The rate of signal amplification depends on the initial concentration of thiol used to start the signal amplification reaction. Signal amplification using reagents **4-10** and **4-11** operates with minimal competition from background reaction and is compatible with aqueous samples. Unlike networks of reactions, the thiol-mediated amplification reaction described here does not require multiple reagents to achieve signal amplification. The simplicity of design and the broad temporal control observed for signal amplification using these reagents may be particularly useful in the context of stimuli-responsive materials, where the presence of an analyte induces macroscopic changes in materials.³⁸⁻⁴⁰

4.5 References

1. Giljohann, D. A.; Mirkin, C. A. Drivers of Biodiagnostic Development. *Nature* **2009**, *462*, 461–464.
2. Price, C. P. The Evolution of Immunoassay as Seen Through the Journal Clinical Chemistry. *Clin. Chem.* **1998**, *44*, 2071–2074.
3. Hill, H. D.; Mirkin, C. A. The Bio-Barcode Assay for the Detection of Protein and Nucleic Acid Targets Using DTT-Induced Ligand Exchange. *Nat. Protoc.* **2006**, *1*, 324–336.
4. Thomas, S. W.; Joly, G. D.; Swager, T. M. Chemical Sensors Based on Amplifying Fluorescent Conjugated Polymers. *Chem. Rev.* **2007**, *107*, 1339–1386.
5. Phillips, S. T.; Dilauro, A. M. Continuous Head-to-Tail Depolymerization: An Emerging Concept for Imparting Amplified Responses to Stimuli-Responsive Materials. *ACS Macro Lett.* **2014**, *3*, 298–304.
6. Wiester, M. J.; Ulmann, P. A.; Mirkin, C. A. Enzyme Mimics Based upon Supramolecular Coordination Chemistry. *Angew. Chem. Int. Ed.* **2011**, *50*, 114–137.
7. Zhu, L.; Anslyn, E. V. Signal Amplification by Allosteric Catalysis. *Angew. Chem. Int. Ed.* **2006**, *45*, 1190–1196.
8. Zhang, H.; Li, F.; Dever, B.; Li, X.-F.; Le, X. C. DNA-Mediated Homogeneous Binding Assays for Nucleic Acids and Proteins. *Chem. Rev.* **2013**, *113*, 2812–2841.
9. Scrimin, P.; Prins, L. Sensing through Signal Amplification. *Chem. Soc. Rev.* **2011**, *40*, 4488–4505.

10. Goddard, J.-P.; Reymond, J.-L. Recent Advances in Enzyme Assays. *Trends Biotechnol.* **2004**, *22*, 363–370.
11. Bu, X.; Koide, K.; Carder, E. J.; Welch, C. J. Rapid Analysis of Residual Palladium in Pharmaceutical Development Using a Catalysis-Based Fluorometric Method. *Org. Process Res. Dev.* **2013**, *17*, 108–113.
12. Newman, G. R.; Jasani, B. Silver Development in Microscopy and Bioanalysis: A New Versatile Formulation for Modern Needs. *Histochem. J.* **1998**, *30*, 635–645.
13. Baker, M. S.; Phillips, S. T. A Two-Component Small Molecule System for Activity-Based Detection of Threshold Levels of Pd(II). *J. Am. Chem. Soc.* **2011**, *133*, 5170–5173.
14. Baker, M. S.; Phillips, S. T. A Small Molecule Sensor for Fluoride Based on an Autoinductive, Colorimetric Signal Amplification Reaction. *Org. Biomol. Chem.* **2012**, *10*, 3595–3599.
15. Perry-Feigenbaum, R.; Sella, E.; Shabat, D. Autoinductive Exponential Signal Amplification: A Diagnostic Probe for Direct Detection of Fluoride. *Chem.–A Eur. J.* **2011**, *17*, 12123–12128.
16. Yeung, K.; Schmid, K. M.; Phillips, S. T. A Thermally-Stable Enzyme Detection Assay That Amplifies Signal Autonomously in Water without Assistance from Biological Reagents. *Chem. Commun.* **2013**, *49*, 394–396.
17. Yoon, H. J.; Mirkin, C. A. PCR-like Cascade Reactions in the Context of an Allosteric Enzyme Mimic. *J. Am. Chem. Soc.* **2008**, *130*, 11590–11591.
18. Mohapatra, H.; Schmid, K. M.; Phillips, S. T. Design of Small Molecule Reagents That Enable Signal Amplification via an Autocatalytic, Base-Mediated Cascade Elimination Reaction. *Chem. Commun.* **2012**, *48*, 3018–3020.

19. Sella, E.; Shabat, D. Dendritic Chain Reaction. *J. Am. Chem. Soc.* **2009**, *131*, 9934–9936.
20. Sella, E.; Lubelski, A.; Klafter, J.; Shabat, D. Two-Component Dendritic Chain Reactions: Experiment and Theory. *J. Am. Chem. Soc.* **2010**, *132*, 3945–3952.
21. Sella, E.; Weinstein, R.; Erez, R.; Burns, N. Z.; Baran, P. S.; Shabat, D. Sulfhydryl-Based Dendritic Chain Reaction. *Chem. Commun.* **2010**, *46*, 6575–6577.
22. Sella, E.; Shabat, D. Hydroquinone-Quinone Oxidation by Molecular Oxygen: A Simple Tool for Signal Amplification through Auto-Generation of Hydrogen Peroxide. *Org. Biomol. Chem.* **2013**, *11*, 5074–5078.
23. Karton-Lifshin, N.; Shabat, D. Exponential Diagnostic Signal Amplification via Dendritic Chain Reaction: The Dendritic Effect of a Self-Immolative Amplifier Component. *New J. Chem.* **2012**, *36*, 386–393.
24. Blackmond, D. G. An Examination of the Role of Autocatalytic Cycles in the Chemistry of Proposed Primordial Reactions. *Angew. Chem. Int. Ed.* **2009**, *48*, 386–390.
25. Maeda, H.; Matsuno, H.; Ushida, M.; Katayama, K.; Saeki, K.; Itoh, N. 2,4-Dinitrobenzenesulfonyl Fluoresceins as Fluorescent Alternatives to Ellman's Reagent in Thiol-Quantification Enzyme Assays. *Angew. Chem. Int. Ed.* **2005**, *44*, 2922–2925.
26. Setsukinai, K.; Urano, Y.; Kikuchi, K.; Higuchi, T.; Nagano, T. Fluorescence Switching by O-Dearylation of 7-Aryloxycoumarins. Development of Novel Fluorescence Probes to Detect Reactive Oxygen Species with High Selectivity. *J. Chem. Soc. Perkin Trans. 2* **2000**, 2453–2457.
27. Wood, P. D.; Johnston, L. J. Photoionization and Photosensitized Electron-Transfer Reactions of Psoralens and Coumarins. *J. Phys. Chem. A* **1998**, *102*, 5585–5591.

28. Kondo, H.; Moriuchi, F.; Sunamoto, J. S \rightarrow N and N \rightarrow S Reverse Rearrangement of S- and N-(2,4-dinitrophenyl)cysteines. *J. Org. Chem.* **1981**, *46*, 1333–1336.
29. Forlani, L.; Bosi, M. Catalysis in Nucleophilic Aromatic Substitution. A Reinvestigation of the Reaction between 1-Fluoro-2,4-Dinitrobenzene and *n*-Butylamine. *J. Phys. Org. Chem.* **1992**, *5*, 429–434.
30. Forlani, L.; Boga, C.; Forconi, M. Kinetics and Mechanism of Reactions between 2,4,6-Trinitro Fluorobenzene and Alcohols. *J. Chem. Soc. Perkin Trans. 2* **1999**, *2*, 1455–1458.
31. Fukuyama, T.; Cheung, M.; Chung-Kuang, J.; Hidai, Y.; Kan, T. 2,4-Dinitrobenzenesulfonamides: A Simple and Practical Method for the Preparation of a Variety of Secondary Amines and Diamines. *Tetrahedron Lett.* **1997**, *38*, 5831–5834.
32. Malwal, S. R.; Sriram, D.; Yogeewari, P.; Konkimalla, V. B.; Chakrapani, H. Design, Synthesis, and Evaluation of Thiol-Activated Sources of Sulfur Dioxide (SO₂) as Antimycobacterial Agents. *J. Med. Chem.* **2012**, *55*, 553–557.
33. Jiang, W.; Cao, Y.; Liu, Y.; Wang, W. Rational Design of a Highly Selective and Sensitive Fluorescent PET Probe for Discrimination of Thiophenols and Aliphatic Thiols. *Chem. Commun.* **2010**, *46*, 1944–1946.
34. Sidney, D. R.; Petersen, R. C. Base Catalysis in Nucleophilic Aromatic Substitution. *Tetrahedron Lett.* **1968**, *45*, 4699–4702.
35. Zingaretti, L.; Boscatto, L.; Chiacchiera, S. M.; Silber, J. J. Kinetics and Mechanism for the Reaction of 1-Chloro-2,4-Dinitrobenzene with *n*-Butylamine and Piperidine in AOT/*n*-Hexane/water Reverse Micelles. *ARKIVOC* **2003**, *2003*, 189–200.

36. Correa, N. M.; Durantini, E. N.; Silber, J. J. Catalysis in Micellar Media. Kinetics and Mechanism for the Reaction of 1-Fluoro-2,4-Dinitrobenzene with *n*-Butylamine and Piperidine in N -Hexane and AOT/*n* -Hexane/ Water Reverse Micelles. *J. Org. Chem.* **1999**, *64*, 5757–5763.
37. Forlani, L. Are Weak Interactions Responsible for Kinetic Catalytic Behaviour in S_NAr Reactions? *J. Phys. Org. Chem.* **1999**, *12*, 417–424.
38. Baker, M. S.; Yadav, V.; Sen, A.; Phillips, S. T. A Self-Powered Polymeric Material That Responds Autonomously and Continuously to Fleeting Stimuli. *Angew. Chem. Int. Ed. Engl.* **2013**, *52*, 10295–10299.
39. Zhang, H.; Yeung, K.; Robbins, J. S.; Pavlick, R. A.; Wu, M.; Liu, R.; Sen, A.; Phillips, S. T. Self-Powered Microscale Pumps Based on Analyte-Initiated Depolymerization Reactions. *Angew. Chem. Int. Ed.* **2012**, *51*, 2400–2404.
40. DiLauro, A. M.; Zhang, H.; Baker, M. S.; Wong, F.; Sen, A.; Phillips, S. T. Accessibility of Responsive End-Caps in Films Composed of Stimuli-Responsive, Depolymerizable Poly(phthalaldehydes). *Macromolecules* **2013**, *46*, 7257–7265.

Chapter 5

Signal amplification via an autocatalytic, base-mediated elimination reaction

5.1 Introduction

Signal amplification reactions are useful in the context of clinical diagnostics,¹ and stimuli-responsive materials.^{2,3} However, amplification reactions often use reagents that are thermally unstable (such as enzymes and antibodies), or are difficult to modify in order to alter the properties of the amplified response (like degradable polymers and macromolecular catalysts). In contrast, small molecule signal amplification reagents are thermally-stable, easier to modify, and can be synthesized in large quantities. Amplification reagents that operate through autocatalysis (Figure 5-1) are one of the simplest kinds of amplification reagents, since they do not require multiple components to generate an amplified response.⁴ In an autocatalytic reaction, one of the reaction products promotes the overall reaction, leading to enhancement of reaction rates (i.e., the quantifiable output is generated faster).

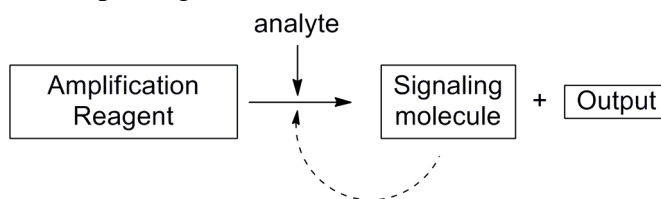


Figure 5-1. General scheme depicting an autocatalytic reaction.

Autocatalysis is observed in a variety of reactions, such as vinegar syndrome (the autocatalytic degradation of cellulose acetate films),⁵ tin pest (the autocatalytic, allotropic transformation of β -tin into α -tin),⁶ the Soai reaction (the autocatalytic enhancement of enantiomeric excess during the alkylation of pyrimidine-5-carbaldehydes by diisopropylzinc),⁷ and silver reduction (the reduction of Ag(I) to Ag(0), which is catalyzed by the product).⁸ Certain product template-mediated reactions^{4,9} and multi-component reaction networks^{10,11} also show autocatalytic behavior. These autocatalytic reactions (with the exception of silver reduction) are difficult to implement in a diagnostic tests. We describe here a class of reagents (**5-1–5-3**) that amplify signal using a base-mediated, autocatalytic reaction sequence.¹² We also demonstrate that these reagents can be used in diagnostic assays for signal amplification.

5.2 Experimental design

5.2.1 Design of the amplification reagent

To develop an autocatalytic signal amplification strategy using small molecules, we designed three amplification reagents: **5-1**, **5-2**, and **5-3**. Reagents **5-1–5-3** were designed to respond to trace levels of amine base (e.g., piperidine), and release one or more equivalents of piperidine (Figure 5-2). Since we wanted the amplification reagents to operate via an autocatalytic reaction sequence, we employed acid-base chemistry that allows rapid recycling of the signaling molecule (i.e., piperidine). The autocatalytic behavior of the reaction sequence arises from the regeneration of the signaling molecule during the course of the reaction.

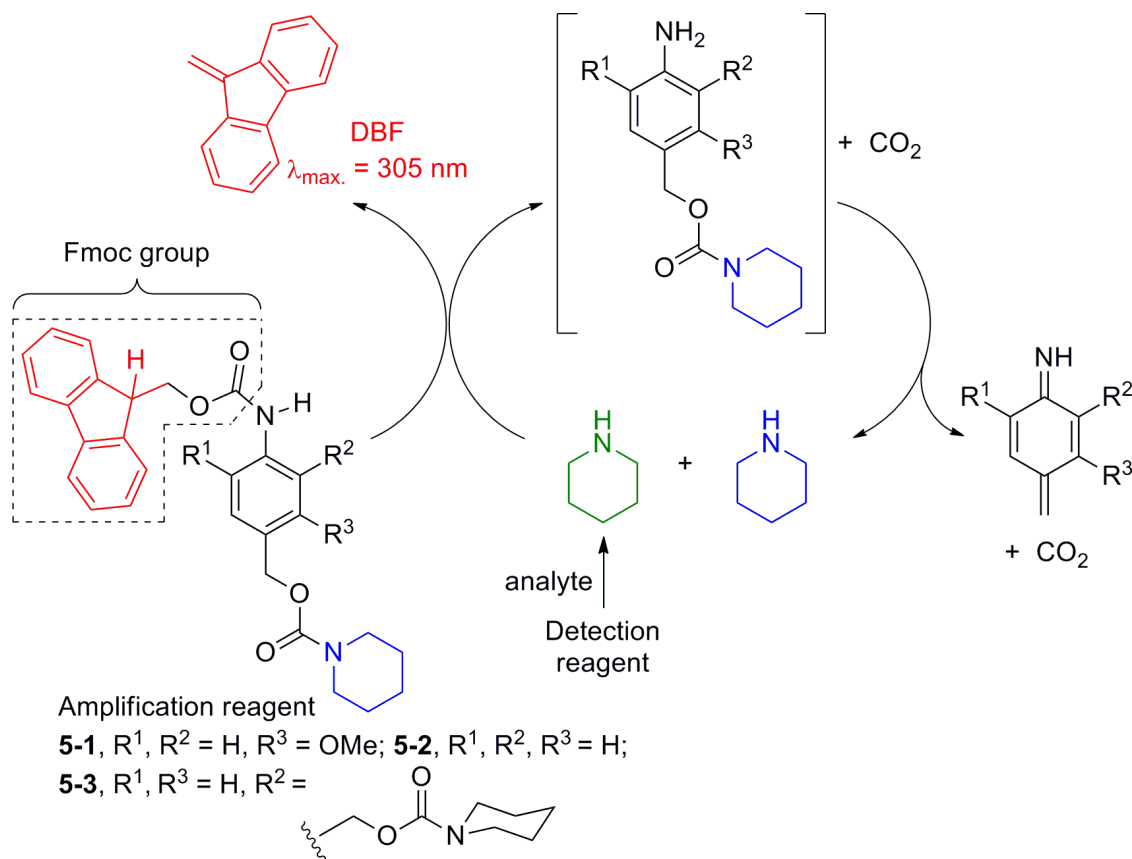


Figure 5-2. Reaction scheme depicting a base-mediated, signal amplification strategy using reagents **5-1–5-3**. The amplification reagents react with trace levels of piperidine to generate an equivalent each of dibenzofulvene (DBF) and piperidine. The equivalent of piperidine that initiates the reaction cycle is regenerated during the reaction.¹²

The development of amplification reagents **5-1–5-3** included certain design elements that enable base-mediated signal amplification. First, the Fmoc group in reagents **5-1–5-3** was chosen as the base responsive functionality because it reacts rapidly with piperidine to generate an easily quantifiable chromophore (dibenzofulvene (DBF)). Second, we included a 4-aminobenzyl alcohol linker to connect the Fmoc group to piperidine. The linker allows greater control over the degree of amplification by accommodating the release of one (for **5-1** and **5-2**), or two (**5-3**) equivalents of piperidine. Finally, we included a methyl ether in the 3 position of the linker (i.e., *meta* to the amino group) to enable faster release of piperidine (i.e., **5-1** releases piperidine faster than **5-2**).

5.2.2 Design of an assay strategy to detect trace levels of an analyte

Once we had designed amplification reagents **5-1–5-3**, our goal was to develop an activity-based detection reagent that generated piperidine in response to an analyte. To achieve this goal, we developed detection reagent **5-4** (Figure 5-3). Reagent **5-4** contains an Alloc group linked to piperidine through a 4-aminobenzyl alcohol linker. In the presence of ligand-stabilized Pd(0) (PdL₂, generated *in-situ* under reducing conditions from the environmental pollutant Pd²⁺/Pd(0)), **5-4** releases piperidine, which can be converted into an amplified signal using reagents **5-1–5-3**.

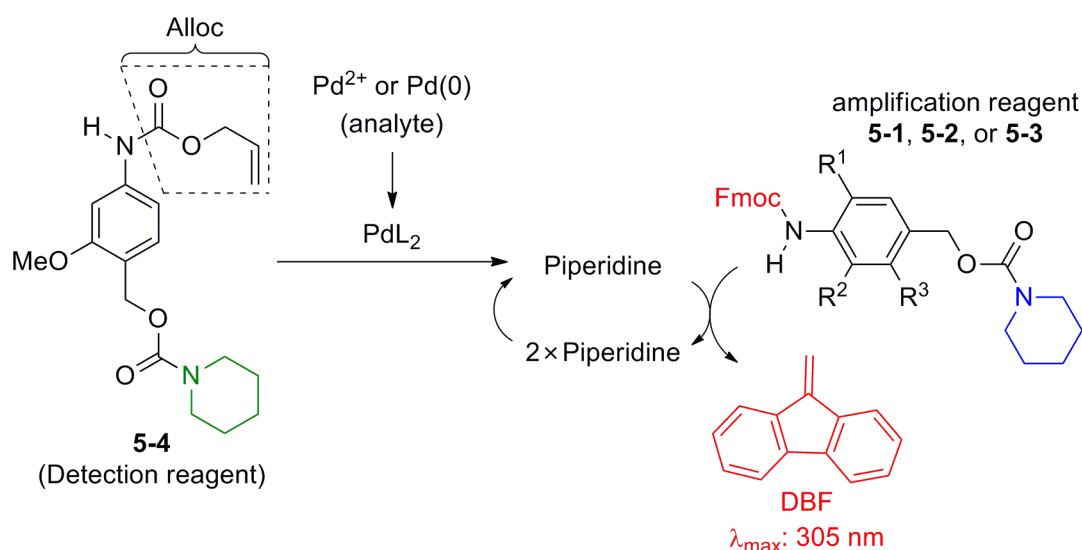


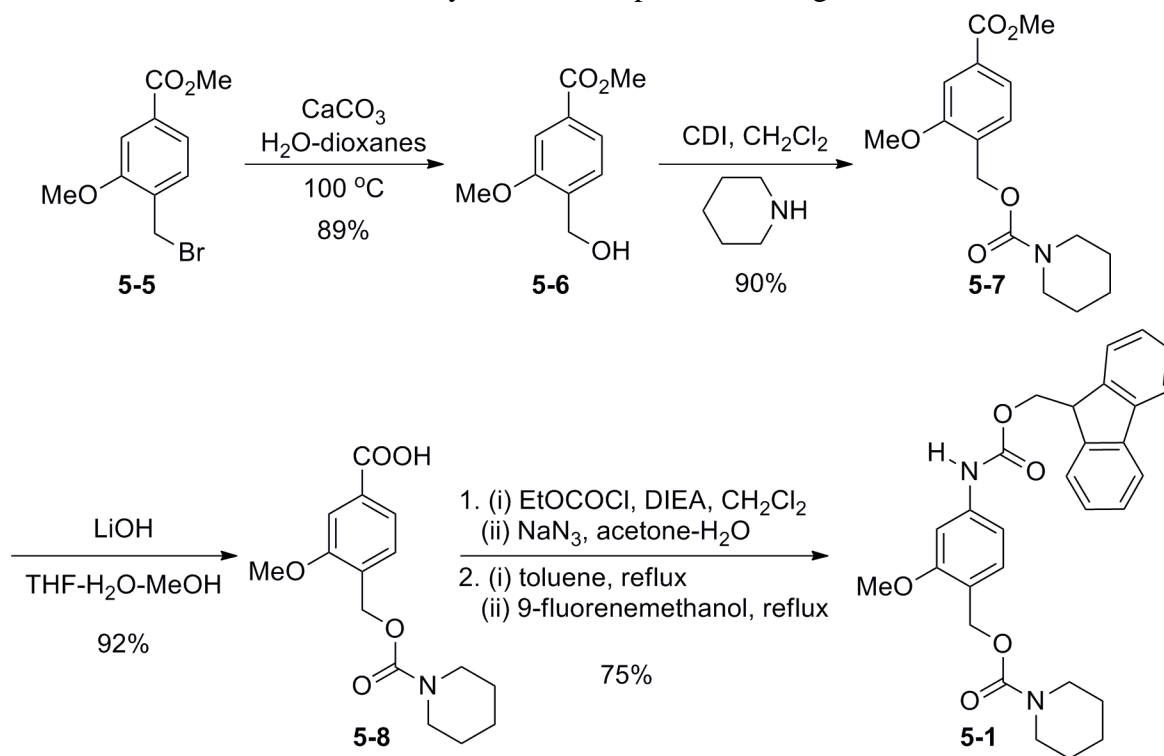
Figure 5-3. Reaction scheme depicting a palladium detection assay with detection reagent **5-4** and signal amplification reagents **5-1–5-3**.¹²

5.3 Results and discussions

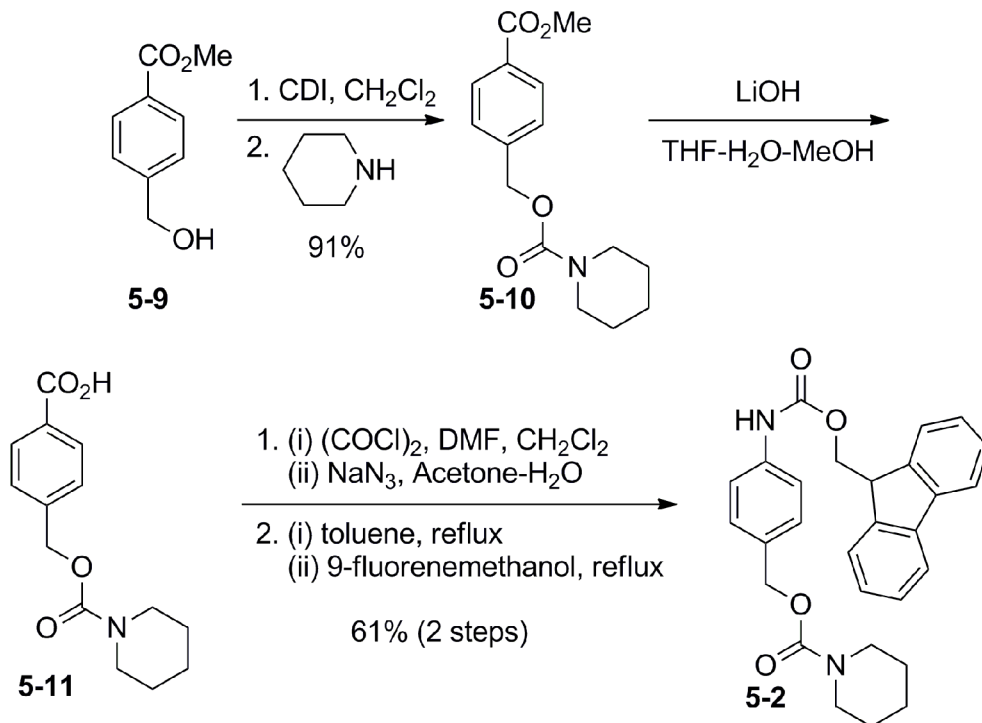
5.3.1 Synthesis of amplification reagent 5-1, 5-2, and 5-3

Amplification reagent **5-1** was prepared using a four-step synthetic route from commercially available starting material **5-5** (Scheme 5-1). Briefly, alcohol intermediate **5-6** was prepared by the hydrolysis of the benzyl bromide on the starting material (**5-5**). Carbamate intermediate **5-7** was then prepared by linking piperidine with alcohol intermediate **5-6** using CDI. The base-mediated hydrolysis of the methyl ester in the intermediate **5-6** yielded carboxylic acid **5-7**. The Fmoc group was then installed using a one-pot sequence of reactions that involved the synthesis of an acyl azide intermediate, a subsequent Curtius rearrangement, and the condensation of 9-fluorenemethanol with the resulting isocyanate intermediate. This synthetic route afforded **5-1** with an overall yield of 55% over four steps. Since amplification reagent **5-1** is designed to respond to trace levels of piperidine, the order of the synthetic steps was carefully chosen to avoid the exposure of synthetic intermediates containing the Fmoc group to basic conditions. Amplification reagents **5-2** and **5-3** were prepared using similar synthetic routes (Scheme 5-2 and 5-3).

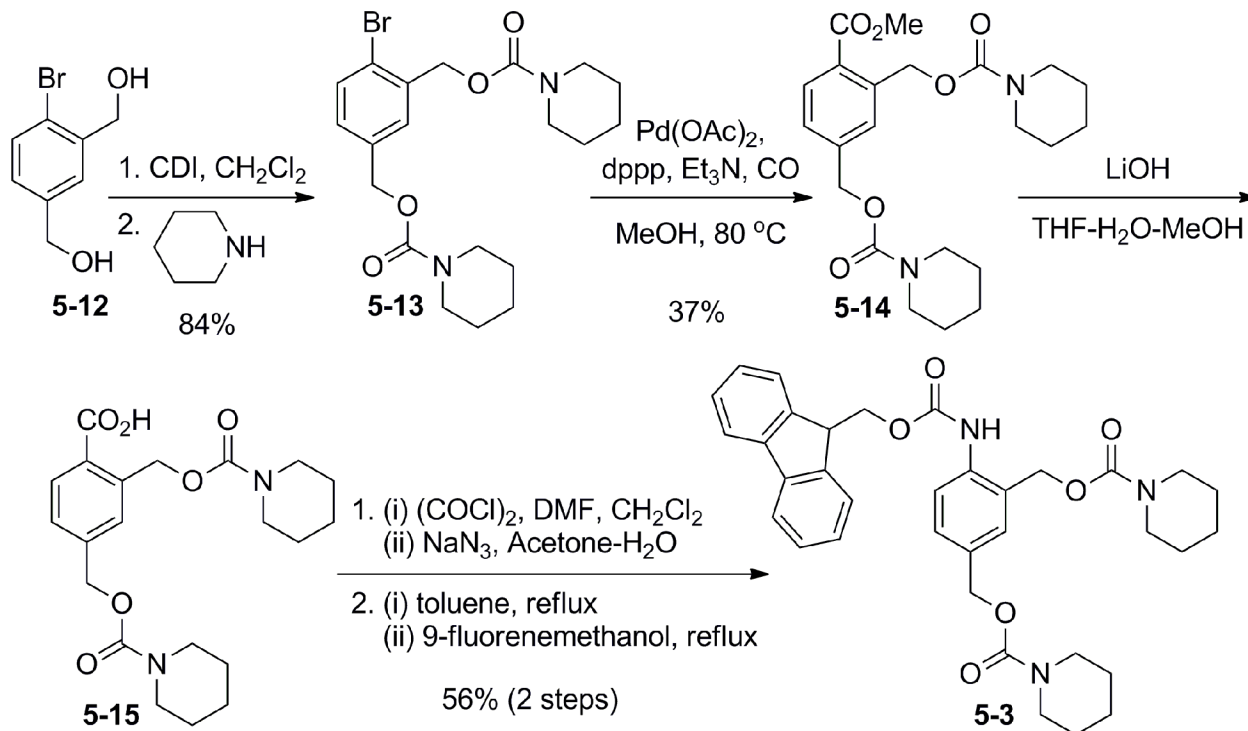
Scheme 5-1. Synthesis of amplification reagent **5-1**.



Scheme 5-2. Synthesis of amplification reagent **5-2** (performed by Kyle Schmid).



Scheme 5-3. Synthesis of amplification reagent **5-3**.



5.3.2 Time-dependent LC-MS study of the signal amplification reaction using reagent **5-1**

To verify that reagent **5-1** proceeded through the base-mediated reaction as depicted in Figure 5-2, we exposed a solution of **5-1** to 0.02 equivalents of piperidine. The reaction solvent was 50:1 DMSO-H₂O. Time-dependent LC-MS analysis of the reaction mixture (Figure 5-4) revealed a clean and quantitative conversion of **5-1** to DBF. The aniline intermediate resulting from the base-mediated cleavage of the Fmoc group was not observed by LC-MS. This observation suggests that the elimination of piperidine (along with release of CO₂ and the aza-quinone methide intermediate) is rapid. We did not observe a peak corresponding to the aza-quinone methide intermediate. Instead, we observed mass spectra consistent with the formation of short oligomers of aza-quinone methide under the reaction conditions. Similar oligomerization of aza-quinone methides have been observed previously.¹³

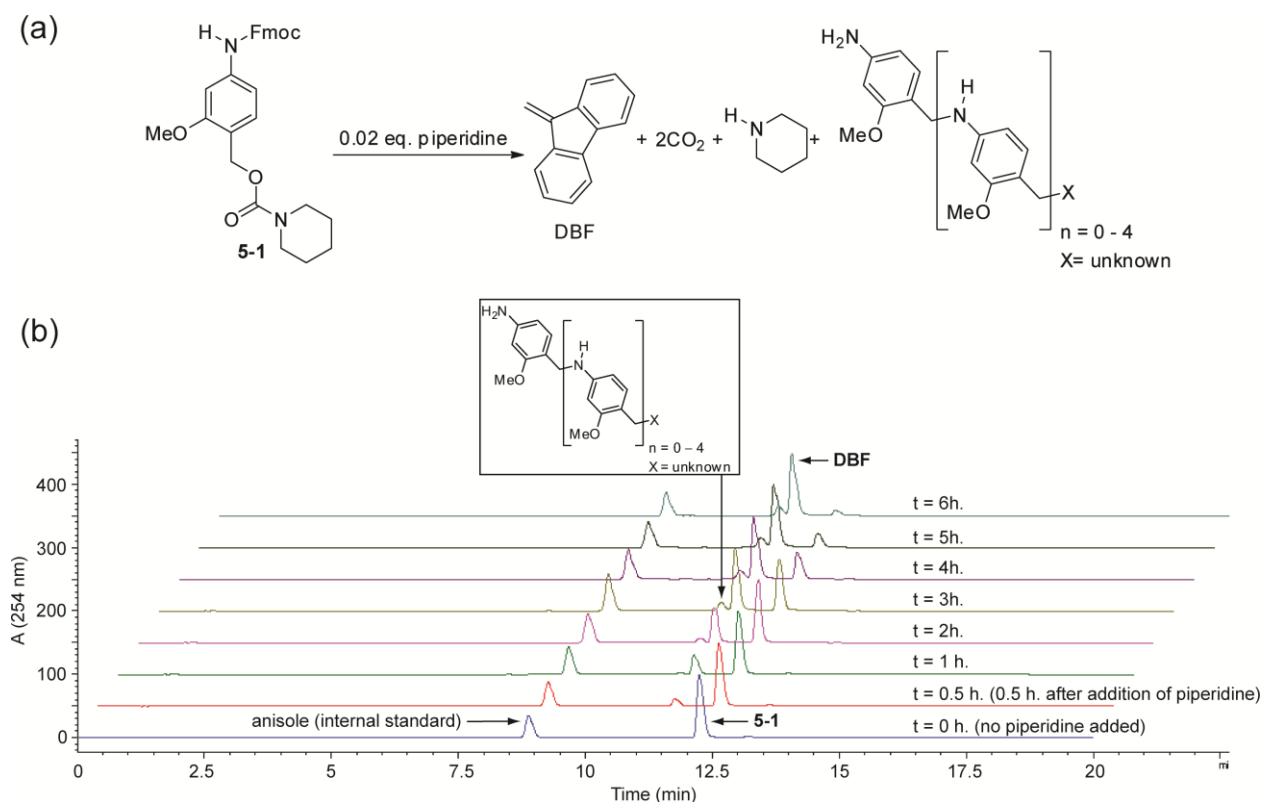


Figure 5-4. Analysis of the reaction products obtained when **5-1** was exposed to 0.02 equiv of piperidine. (a) Reaction scheme depicting the products of the reaction between **5-1** and piperidine; (b) overlaid LC-MS spectra for successive injections of aliquots of reaction containing **5-1** (40 mM) and piperidine (0.8 mM) in 50:1 DMSO-H₂O.¹²

5.3.3 Dose-dependent signal amplification using reagent **5-1**

To demonstrate the ability of reagent **5-1** to amplify signal, we exposed **5-1** to various substoichiometric quantities of piperidine (a signaling molecule that could be generated from a separate detection event). The progress of the amplification reaction was followed by measuring the absorbance at 305 nm (i.e., the λ_{max} for DBF). The normalized absorbance data (Figure 5-5) reveals several features of the amplification reaction using **5-1**. First, reagent **5-1** is completely consumed to generate the same maximum level of signal, even when exposed to only 0.001 equivalents of piperidine. This observation demonstrates that reagent **5-1** is capable of over 1000 \times signal amplification. Second, the background signal from non-specific hydrolysis of **5-1** is negligible over the course of the experiment. The lack of background signal is particularly important in the context of detection assays, where non-specific hydrolysis would limit the sensitivity of the assay. Finally, the kinetics profile of the reaction of **5-1** with piperidine is sigmoidal, which is characteristic of an autocatalytic reaction. Similar sigmoidal kinetics profiles are also observed in other autocatalytic reactions.⁴

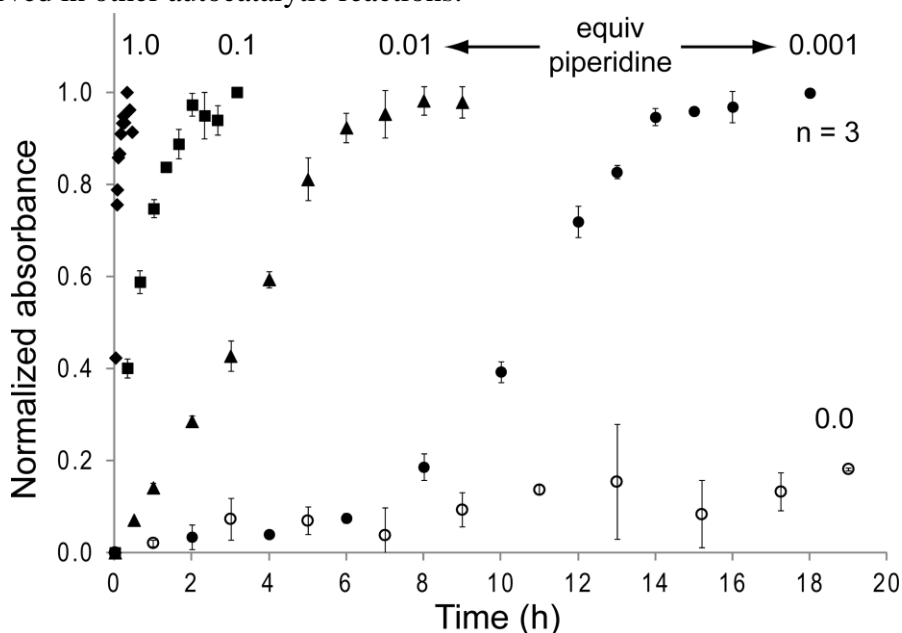


Figure 5-5. Normalized absorbance data obtained when amplification reagent **5-1** was treated with various initial quantities of piperidine. The concentration of amplification reagent **5-1** was 40 mM in 45:5:1 DMSO-THF-H₂O. Absorbance measurements (at 305 nm) were obtained after the dilution of 1 μ L aliquots of the reaction mixture in 600 μ L THF. The experiments were performed in triplicate, and the error bars represent the standard deviations from the average values.¹²

To show that piperidine (and not just DBF) is amplified during the signal amplification reaction using **5-1**, we measured the amount of free base that is produced during the course of the reaction (Figure 5-6). Briefly, we exposed aliquots of an amplification reaction (containing **5-1** and 0.01 equivalents of initial piperidine) to a solution of the pH indicator bromocresol green and measured the change in color of the resulting solution. A sigmoidal increase in the absorbance signal at 625 nm (which corresponds to the deprotonated form of the pH indicator) was observed. The normalized absorbance at 625 nm increased at a rate that was identical to the rate of generation of DBF (measured at 305 nm), thus demonstrating that the two reaction products (piperidine and DBF) are generated simultaneously in the amplification reaction. Control experiments using either 3-methoxyaniline or 4-aminobenzylalcohol (instead of **5-1**) revealed that the aniline reaction intermediate is not sufficiently basic to deprotonate the pH indicator to generate a signal at 625 nm. These observations provide further evidence that additional equivalents of base are generated during the course of the amplification reaction as depicted in Figure 5-2.

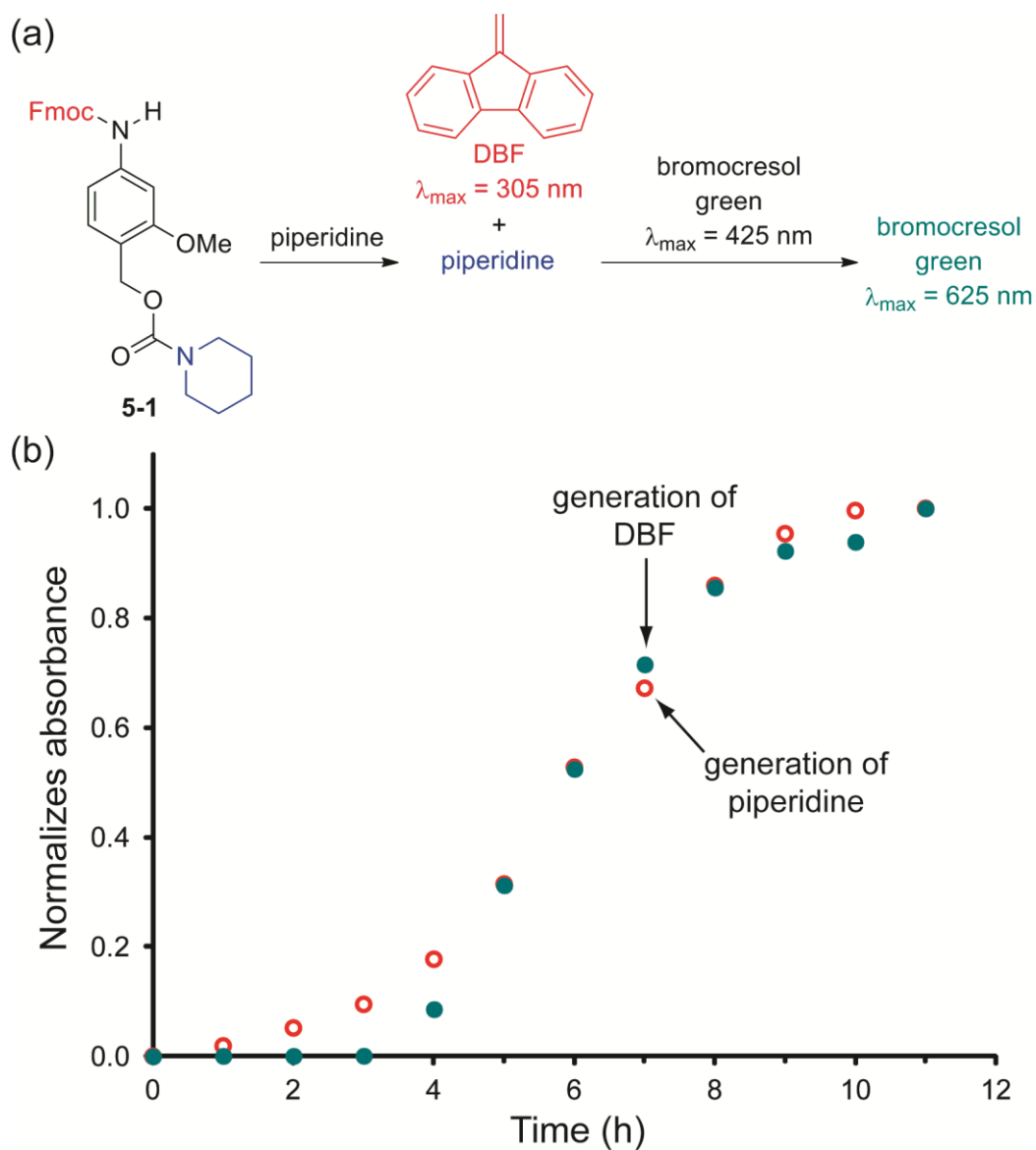


Figure 5-6. Demonstration of autocatalytic base amplification using reagent **5-1**. (a) Reaction scheme, and (b) Normalized absorbance of bromocresol green (green circular data points) at 625 nm and DBF (red circular data points) at 305 nm.¹²

5.3.4 Evaluation of the effect of methyl ether on the rate of signal amplification using **5-1**

Amplification reagent **5-1** was designed to include a methyl ether at the 3-position (i.e., *meta* to the amino group) of the 4-aminobenzyl linker. The presence of the electron donating substituent was expected to accelerate the rate of release of piperidine via aza-quinone methide elimination (Figure 5-7). Similar rate enhancement of rate of quinone methide-based elimination reactions has been observed previously.¹⁴ As predicted, the reaction kinetics profiles in Figure 5-8 reveal that **5-1** (contains a methyl ether in the linker) amplifies signal at a faster rate than **5-2** (which lacks the methyl ether).

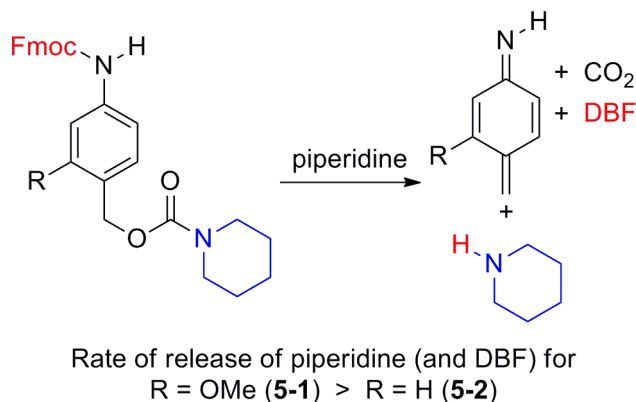


Figure 5-7. Effect of methyl ether (R = OMe) on the rate of release of piperidine via aza-quinone methide elimination.

5.3.5 Evaluation of the effect of releasing multiple equivalents of piperidine on the rate of signal amplification

Another method to increase the rate of signal amplification of the base-mediated signal amplification reaction (in addition to the inclusion of the methyl ether substituent) is to release multiple equivalents of piperidine from the 4-aminobenzyl linker. Reagent **5-3** releases two equivalents of piperidine for each cleavage of the Fmoc group. Consequently, an amplification reaction using **5-3** generated signal (i.e., the reaction product DBF) at a faster rate than a reaction using **5-2** (Figure 5-8).

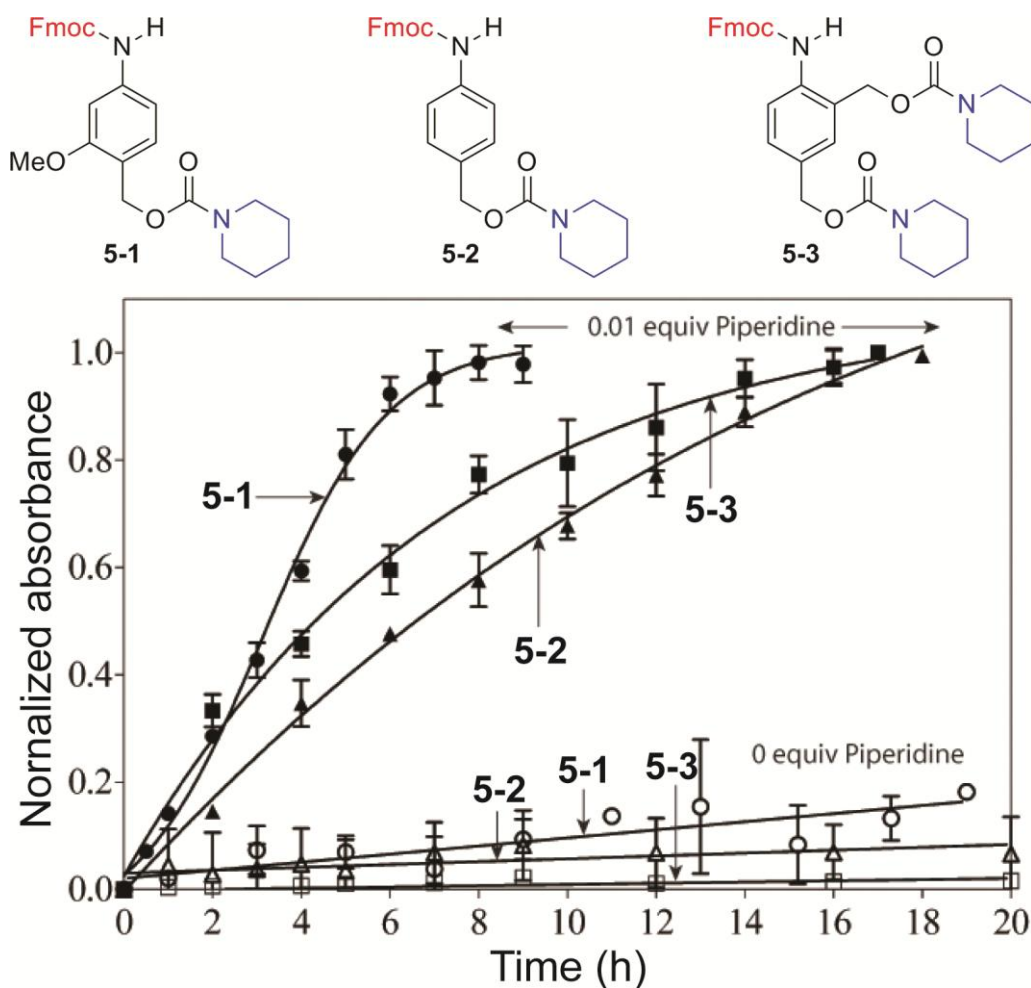


Figure 5-8. Effect of the inclusion of methyl ether in the 4-aminobenzyl linker (**5-1**), and the release of two equivalents of piperidine (**5-3**) on the rate of signal amplification (and the background hydrolysis) using the reaction depicted in Figure 5-2. The concentration of amplification reagent (**5-1**, **5-2**, or **5-3**) was 40 mM in 45:5:1 DMSO-THF-H₂O. Absorbance measurements (at 305 nm) were obtained after the dilution of 1 μ L aliquots of the reaction mixture in 600 μ L THF. The experiments were performed in triplicate, and the error bars represent the standard deviations from the average values.¹²

5.3.6 A palladium detection assay using reagent **5-1** for signal amplification

Once we had demonstrated that reagent **5-1** amplified signal through a base-mediated reaction sequence, we evaluated whether a combination of amplification reagent **5-1** and activity-based detection reagent **5-4** could be used in diagnostic assays. We used a two-step assay (Figure 5-9a) to translate the detection of palladium (using **5-4**) into the release of a

signaling molecule (i.e., piperidine), and then amplify the small amount of piperidine using amplification reagent **5-1**. The dose-response curve obtained from the assay (Figure 5-9b) shows that we can detect 12 ppm Pd (which is approximately the threshold level of Pd permitted in drugs.^{15,16}). Most importantly, the result in Figure 5-9b reveal that the amplification reagent **5-1** can be paired with activity-based detection reagents (like **5-4**) to achieve detection of trace-levels of an analyte.

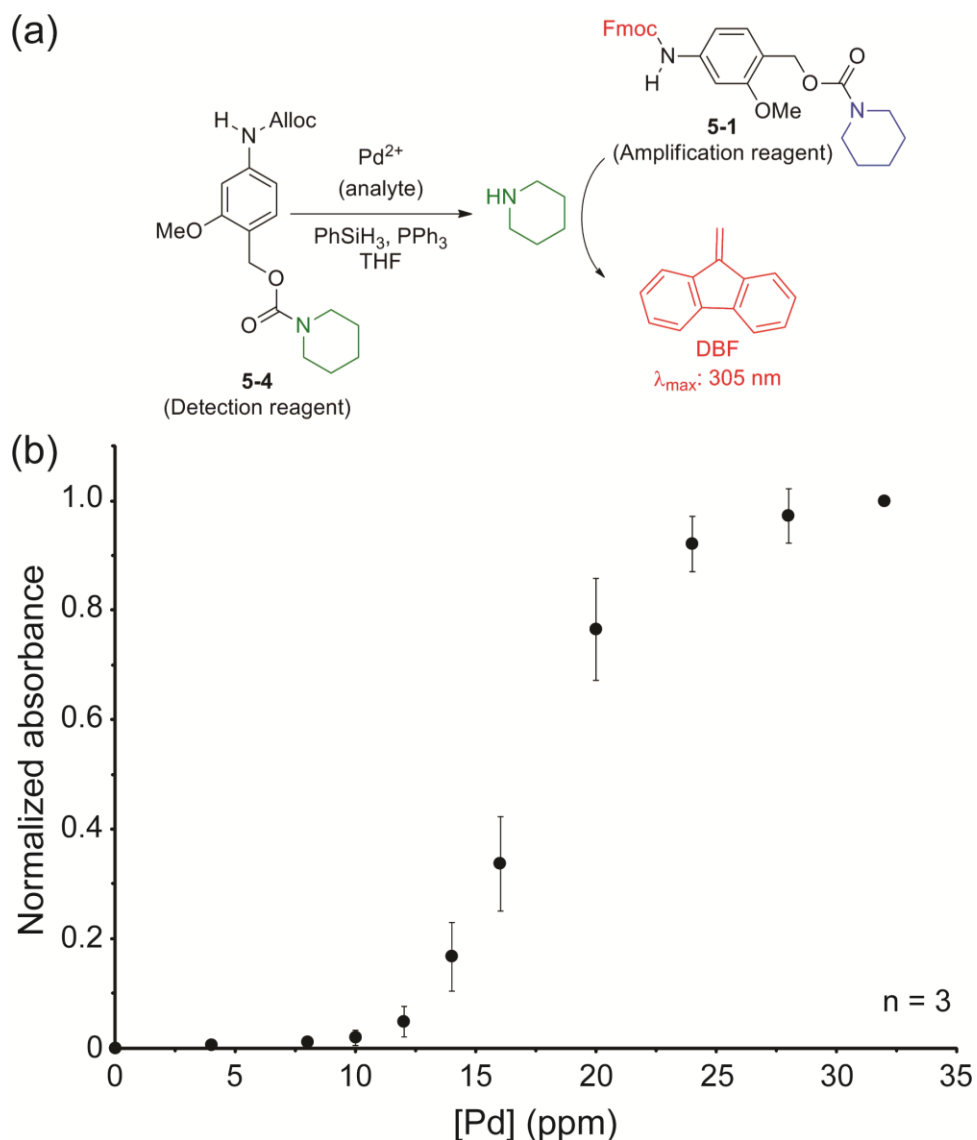


Figure 5-9. Palladium detection assay using (a) an assay involving the reaction of Pd (analyte), **5-4** (detection reagent), and **5-1** (amplification reagent). (b) Dose-response curve using normalized absorbance data (305 nm). The assays were performed in triplicate, and the error bars represent the standard deviations from average values.¹²

5.4. Conclusions

In conclusion, we demonstrated a signal amplification strategy using reagents **5-1**, **5-2**, and **5-3**. The base-mediated amplification reaction simultaneously amplifies base and an easily quantifiable colorimetric signal. The pairing of amplification reagent **5-1** with detection reagent **5-4** allows sensitive and selective detection of a model analyte. The reactive functionality on **5-4** can be modified to target a variety of analytes. Amplification reagents, like **5-1**, do not yet provide rapid signal amplification, and are therefore not ideal for some diagnostic assays. However, these types of reagents serve as a starting point for the design of autocatalytic reaction systems. Additionally, these reagents can be useful in the context of stimuli-responsive materials that respond autonomously to a variety of chemical signals.¹⁷⁻¹⁹

5.5 References

1. Scrimin, P.; Prins, L. Sensing through Signal Amplification. *Chem. Soc. Rev.* **2011**, *40*, 4488–4505.
2. Ito, H. Chemical Amplification Resists for Microlithography. *Adv. Polym. Sci.* **2005**, 37–245.
3. Phillips, S. T.; DiLauro, A. M. Continuous Head-to-Tail Depolymerization: An Emerging Concept for Imparting Amplified Responses to Stimuli-Responsive Materials. *ACS Macro Lett.* **2014**, *3*, 298–304.
4. Bissette, A. J.; Fletcher, S. P. Mechanisms of Autocatalysis. *Angew. Chem. Int. Ed.* **2013**, *52*, 12800–12826.
5. Allen, N. S.; Edge, M.; Appleyard, J. H.; Jewitt, T. S.; Horie, C. V.; Francis, D. Degradation of Historic Cellulose Triacetate Cinematographic Film: The Vinegar Syndrome. *Polym. Degrad. Stab.* **1987**, *19*, 379–387.
6. Plumbridge, W. J. Tin Pest Issues in Lead-Free Electronic Solders. *J. Mater. Sci. Mater. Electron.* **2006**, *18*, 307–318.
7. Sato, I.; Urabe, H.; Ishiguro, S.; Shibata, T.; Soai, K. Amplification of Chirality from Extremely Low to Greater than 99.5% *ee* by Asymmetric Autocatalysis. *Angew. Chem. Int. Ed.* **2003**, *42*, 315–317.
8. Newman, G. R.; Jasani, B. Silver Development in Microscopy and Bioanalysis: A New Versatile Formulation for Modern Needs. *Histochem. J.* **1998**, *30*, 635–645.

9. Rotello, V.; Jong-In, H.; Rebek Jr., J. Sigmoidal Growth in a Self-Replicating System. *J. Am. Chem. Soc.* **1996**, *113*, 9422–9423.
10. Sirimungkala, A.; Forsterling, H.-D.; Dlask, V.; Field, R. J. Bromination Reactions Important in the Mechanism of the Belousov - Zhabotinsky System. *J. Phys. Chem. A* **1999**, *1-3*, 1038–1043.
11. Yoon, H. J.; Mirkin, C. A. PCR-like Cascade Reactions in the Context of an Allosteric Enzyme Mimic. *J. Am. Chem. Soc.* **2008**, *130*, 11590–11591.
12. Mohapatra, H.; Schmid, K. M.; Phillips, S. T. Design of Small Molecule Reagents That Enable Signal Amplification via an Autocatalytic, Base-Mediated Cascade Elimination Reaction. *Chem. Commun.* **2012**, *48*, 3018–3020.
13. Iwatsuki, S.; Itoh, T.; Itoh, H. Preparation of Novel Electron-Accepting Quinone Methide Imines and Their Polymerizations. *Chem. Lett.* **1988**, *7*, 1187–1190.
14. Schmid, K. M.; Jensen, L.; Phillips, S. T. A Self-Immolative Spacer That Enables Tunable Controlled Release of Phenols under Neutral Conditions. *J. Org. Chem.* **2012**, *77*, 4363–4374.
15. Garner, A. L.; Song, F.; Koide, K. Enhancement of a Catalysis-Based Fluorometric Detection Method for Palladium through Rational Fine-Tuning of the Palladium Species. *J. Am. Chem. Soc.* **2009**, *131*, 5163–5171.

16. Garrett, C. E.; Prasad, K. The Art of Meeting Palladium Specifications in Active Pharmaceutical Ingredients Produced by Pd-Catalyzed Reactions. *Adv. Synth. Catal.* **2004**, *346*, 889–900.
17. Baker, M. S.; Yadav, V.; Sen, A.; Phillips, S. T. A Self-Powered Polymeric Material That Responds Autonomously and Continuously to Fleeting Stimuli. *Angew. Chem. Int. Ed.* **2013**, *52*, 10295–10299.
18. Esser-Kahn, A. P.; Odom, S. a.; Sottos, N. R.; White, S. R.; Moore, J. S. Triggered Release from Polymer Capsules. *Macromolecules* **2011**, *44*, 5539–5553.
19. Phillips, S. T.; Dilauro, A. M. Continuous Head-to-Tail Depolymerization: An Emerging Concept for Imparting Amplified Responses to Stimuli-Responsive Materials. *ACS Macro Lett.* **2014**, *3*, 298–304.

Chapter 6

Material, Methods, Experimental Procedures, and Characterizations

Parts of the text in this chapter were reproduced from references 3, 6, and 8 by permission of The Royal Society of Chemistry and WILEY-VCH Verlag GmbH & Co.

6.1 Material, methods, and general experimental procedures

All reactions requiring inert atmosphere were performed in flame-dried glassware under a positive pressure of argon. Air- and moisture-sensitive liquids were transferred by syringe or stainless steel cannula. Organic solutions were concentrated by rotary evaporation (25–40 mmHg) at ambient temperature, unless otherwise noted. All reagents and buffer salts were purchased commercially and were used as received. Tetrahydrofuran, diethyl ether, methylene chloride, acetonitrile, toluene, benzene, DMF, DMSO, methanol were purified by the method developed by Pangborn et al.¹ Flash-column chromatography was performed as described by Still et al.,² employing silica gel (60-Å pore size, 32–63 µm, standard grade, Dynamic Adsorbents). Thin layer chromatography was carried out on Dynamic Adsorbents silica gel TLC (20 × 20 cm w/h, F-254, 250 µm). Deionized water was purified with a Millipore-purification system (Barnstead EASYpure[®] II UV/UF).

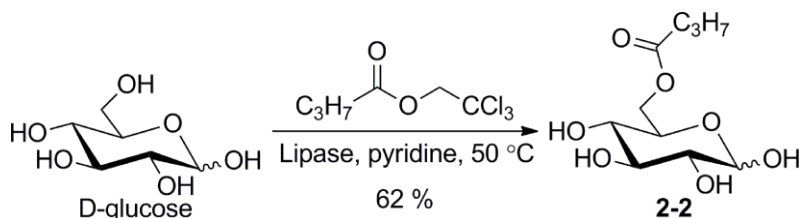
Proton nuclear magnetic resonance (¹H NMR) spectra were recorded using a Bruker AV-360 (360 MHz), DRX-400 (400 MHz), or DPX-300 (300 MHz) at 20 °C. Proton chemical shifts are expressed in parts per million (ppm, δ scale) and are referenced to tetramethylsilane ((CH₃)₄Si, 0.00 ppm) or residual protium in the nmr solvent. Data are represented as follows: Chemical shift, integration, multiplicity (s = singlet, d = doublet, t = triplet, q = quartet, m = multiplet and/or multiple resonances, br s = broad singlet, dd = doublet of doublet, hex = sextet), and coupling constant (*J*) in hertz. Carbon nuclear magnetic resonance spectra (¹³C NMR) were recorded using Bruker AV-360 (360 MHz), DRX-400 (400 MHz), or DPX-300 (300 MHz) at 20 °C. Carbon chemical shifts are expressed in parts per million (ppm, δ scale) and are referenced to the carbon resonance of the NMR solvent (CDCl₃, δ 77.16 ppm; CD₃OD, 49.00). LC-MS data were obtained on an Agilent Technologies 1200 series analytical reverse-phase HPLC coupled to an Agilent Technologies 6120 quadrupole mass spectrometer. The columns used were BETASIL

Phenyl-Hexyl column (150 mm × 2.1 mm, 5 μm particle size). A True Track™ personal glucometer was used for all measurements of glucose levels. All UV-Vis data were obtained using a Beckman-Coulter DU®-800 spectrophotometer. All fluorescence data were obtained using a HITACHI F-7000 spectrofluorometer.

6.2 Chapter 2: Experimental procedures and characterizations³

Synthetic procedures

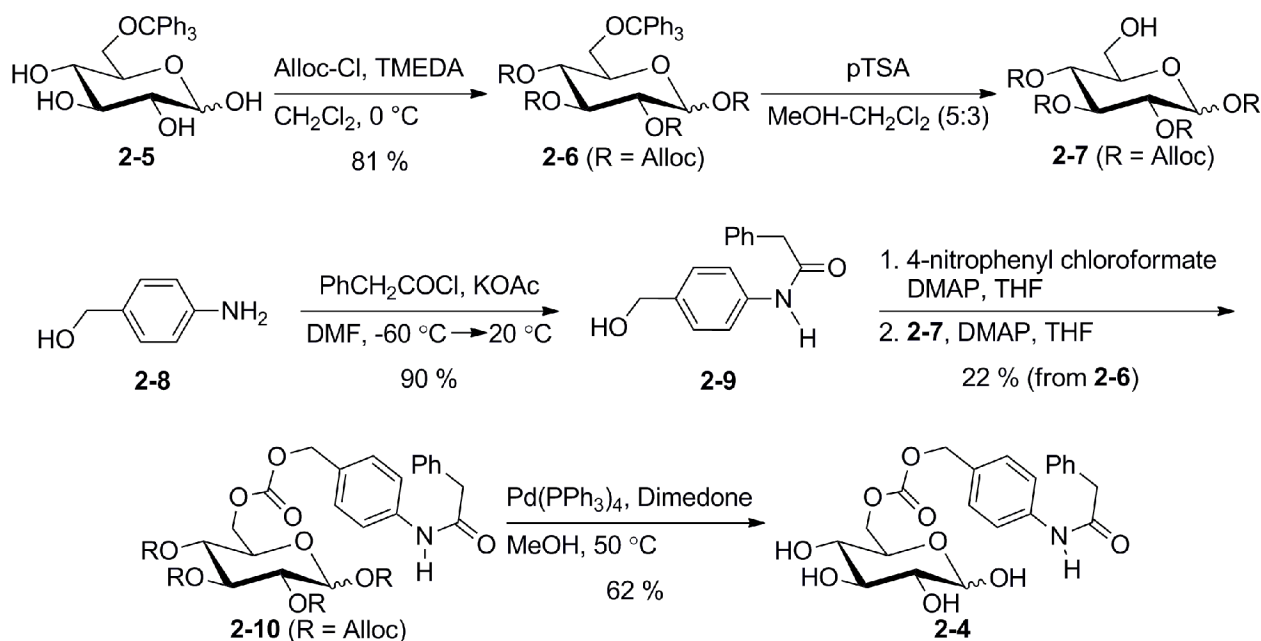
Synthesis of detection reagent 2-2.



6-O-Butyrylglucose (2-2).

Porcine liver lipase (0.38 g) was added to a stirred solution of β-D-glucose (1.0 g, 5.8 mmol, 1 equiv) and 2,2,2-trichloroethyl butyrate (1.5 g, 7.0 mmol, 1.2 equiv) in dry pyridine (25 mL) at 45 °C. The resulting suspension was stirred at 45 °C for 48 h. The reaction mixture was filtered and the filtrate was concentrated. The resulting oil was purified using column chromatography (elution with 2% methanol/EtOAc) to obtain 6-O-butyrylglucose **2-2** as a white solid (800 mg, 3.2 mmol, 55%) ¹H-NMR (400 MHz, CDCl₃, anomeric pair): δ 5.26 (0.5H, m), 4.69 (0.5 H, d, *J* = 8.0), 4.49–4.29 (1.6H, m), 4.08–4.05 (0.5H, m), 3.80–3.60 (1H, m), 3.58–3.48 (2H, m), 3.30 (0.4 H, t, *J* = 8.0), 2.45 (2H, t, *J* = 7.2), 2.45 (2H, hex, *J* = 7.2), 2.45 (2H, t, *J* = 7.2); ¹³C-NMR (90 MHz, CDCl₃): δ 176.8, 96.5, 92.6, 90.0, 77.5, 76.1, 74.5, 73.9, 73.1, 71.9, 70.2, 70.1, 69.6, 63.7, 63.7, 36.3, 36.1, 18.5, 18.4, 13.8, 13.3; The NMR data matches previously published data for 6-O-butyrylglucose.⁴

Synthesis of detection reagent 2-4.



Tetraallyl ((3R,4S,5R,6R)-6-((trityloxy)methyl)tetrahydro-2H-pyran-2,3,4,5-tetrayl) tetracarboxylate (2-6).

Allyl chloroformate (1.4 mL, 13 mmol, 4.5 equiv) was added to a solution of 6-*O*-(triphenylmethyl)-D-glucopyranose **2-5** (1.3 g, 3.0 mmol, 1 equiv) and TMEDA (1.4 mL, 6.7 mmol, 2.3 equiv) in dry CH_2Cl_2 (25 mL) at 0 °C. The resulting solution was stirred at 0 °C for 1 h. The reaction mixture was diluted with CH_2Cl_2 (50 mL). The resulting solution was washed with saturated aqueous NaHCO_3 (20 mL). The aqueous layer was collected and was extracted using CH_2Cl_2 (1 \times 100 mL). The combined organic layers were washed with brine (1 \times 20 mL), and dried over anhydrous Na_2SO_4 . The Na_2SO_4 was removed by filtration and the resulting solution was concentrated under reduced pressure. The resulting oil was purified using column chromatography (elution with 30% EtOAc/hexanes) to obtain tetraallyl ((3R,4S,5R,6R)-6-((trityloxy)methyl)tetrahydro-2H-pyran-2,3,4,5-tetrayl) tetracarboxylate **6** (1.8 g, 2.4 mmol, 81%). IR (cm^{-1}) 2948, 2360, 1756, 1230; $^1\text{H-NMR}$ (400 MHz, CDCl_3 , anomeric pair): δ 7.43–7.41 (6H, m), 7.30–7.19 (9H, m), 6.39 (0.6 H, d, $J = 3.5$), 5.94–5.85 (4H, m), 5.64 (0.4 H, d, $J = 7.6$), 5.39–5.21 (8H, m), 5.18–5.15 (1H, m), 5.15–5.01 (2H, m), 4.73–4.59 (6H, m), 4.52–4.37 (2H, m), 4.13–4.10 (0.6 H, m), 3.77–3.45 (0.4 H, m), 3.39–3.34 (1H, m), 3.20–3.12 (1H, m); $^{13}\text{C-NMR}$

(90 MHz, CDCl₃): δ 154.1, 153.8, 153.6, 153.5, 153.4, 153.1, 153.1, 143.5, 143.5, 131.6, 131.2, 131.2, 131.2, 131.1, 130.9, 128.7, 128.7, 128.6, 128.0, 127.9, 127.3, 127.1, 119.6, 119.2, 119.2, 119.1, 118.9, 94.9, 92.6, 86.8, 86.7, 74.0, 73.6, 72.9, 72.1, 72.0, 71.1, 69.3, 69.2, 69.0, 68.9, 68.9, 68.8, 68.5, 61.8, 61.4; MS (TOF MS ES⁺, m/z): 781.4 (M + Na⁺); HRMS (TOF MS ES⁺, m/z) Calculated for C₄₁H₄₂O₁₄Na (M + Na⁺): 781.2472; Found: 781.2485.

Tetraallyl ((3R,4S,5R,6R)-6-(hydroxymethyl)tetrahydro-2H-pyran-2,3,4,5-tetraol) tetracarboxylate (2-7).

p-Toluenesulfonic acid monohydrate (110 mg, 0.58 mmol, 0.25 equiv) was added to a solution of **2-6** (1.7 g, 2.3 mmol, 1 equiv) in 5:3 MeOH-CH₂Cl₂ (24 mL). The resulting solution was stirred at 20 °C for 6 h. Triethylamine (0.3 mL) was added to the reaction mixture and the resulting solution was concentrated. The resulting crude product was partially purified by passing it through a plug of silica gel (elution with 40% EtOAc/hexanes) to obtain tetraallyl ((3R,4S,5R,6R)-6-(hydroxymethyl)tetrahydro-2H-pyran-2,3,4,5-tetraol) tetracarboxylate **2-7**, which was used for subsequent reactions without further purification.

N-(4-(Hydroxymethyl)phenyl)-2-phenylacetamide (2-9).

Phenacetyl chloride (0.92 mL, 6.9 mmol, 1.05 equiv) was added dropwise to a stirred suspension of 4-aminobenzyl alcohol (0.81 g, 6.6 mmol, 1 equiv) and potassium acetate (1.5 g, 15 mmol, 2.3 equiv) in DMF (40 mL) at -60 °C. The resulting solution was stirred at -60 °C for 10 min and at 20 °C for 10 min. The reaction mixture was then diluted with aqueous NaOH solution (20 mL, 1.0 M). The resulting solution was then neutralized to a pH of 7 using HCl (1.0 M) and the product was extracted with CH₂Cl₂ (3 × 20 mL). The combined organic layers were sequentially washed with water (2 × 10 mL), brine (10 mL), and dried over anhydrous Na₂SO₄. The Na₂SO₄ was filtered and the filtrate was concentrated to obtain N-(4-(Hydroxymethyl)phenyl)-2-phenylacetamide **2-9** as a yellow solid (1.4 g, 5.9 mmol, 90%). ¹H-NMR (CD₃OD): δ 7.54–7.52 (m, 2H), 7.36–7.22 (m, 8H), 4.55 (s, 2H), 3.66 (s, 2H). The ¹H-NMR data matches with literature values.⁵

Tetraallyl ((3R,4S,5R,6R)-6-((4'-(2''-phenylacetamido)carboxybenzoxymethyl)tetrahydro-2H-pyran-2,3,4,5-tetrayl) tetracarbonate (2-10).

4-Nitrophenyl chloroformate (210 mg, 1.0 mmol, 1.0 equiv) was added to a solution of N-[4-(hydroxymethyl)phenyl]-2-phenylacetamide **2-9** (245 mg, 1.0 mmol, 1 equiv) and DMAP (130 mg, 1.0 mmol, 1.0 equiv) in dry THF (3.5 mL). The resulting solution was stirred at 20 °C for 8 h. The resulting solution of was treated with a dry THF (6 mL) solution of **2-7** (480 mg, 0.93 mmol, 0.93 equiv) containing DMAP (130 mg, 1.0 mmol, 1.0 equiv). The resulting solution was stirred at 20 °C for 24 h. The reaction mixture was diluted with EtOAc (15 mL). The resulting solution was washed with saturated aqueous NH₄Cl (10 mL). The aqueous layer was collected and was extracted using EtOAc (2 × 15 mL). The combined organic layers were successively washed with water (1 × 15 mL) and brine (1 × 15 mL), and dried over anhydrous Na₂SO₄. The Na₂SO₄ was removed by filtration and the resulting solution was concentrated under reduced pressure. The resulting oil was purified using column chromatography (elution with 30% EtOAc/hexanes) to obtain tetraallyl ((3R,4S,5R,6R)-6-((4'-(2''-phenylacetamido)carboxybenzoxymethyl)tetrahydro-2H-pyran-2,3,4,5-tetrayl) tetracarbonate **2-10** (160 mg, 0.20 mmol, 22%). IR (cm⁻¹) 2960, 1752, 1603, 1225; ¹H-NMR (360 MHz, CDCl₃, anomeric pair): δ 7.44–7.29 (9H, m), 7.18 (1H, s), 6.28 (0.8 H, d, *J* = 3.5), 5.98–5.82 (4H, m), 5.62 (0.2 H, d, *J* = 8.3), 5.43–5.26 (8H, m), 5.25–5.23 (1H, m), 5.18–5.05 (2H, m), 5.03–4.98 (1H, m), 4.94–4.90 (1H, m), 4.65–4.57 (8H, m) 4.35–4.27 (2H, m), 4.25–4.19 (2 H, m), 3.74 (1H, s); ¹³C-NMR (90 MHz, CDCl₃): δ 169.1, 154.6, 154.0, 153.7, 153.7, 152.9, 138.0, 134.3, 131.1, 131.0, 130.9, 130.8, 129.5, 129.4, 129.3, 127.8, 119.7, 119.3, 119.2, 119.0, 100.0, 92.2, 73.4, 72.5, 71.6, 69.7, 69.6, 69.3, 69.2, 69.0, 64.8, 44.9; MS (TOF MS ES⁺, *m/z*): 784.2 (M + H⁺); HRMS (TOF MS ES⁺, *m/z*) Calculated for C₃₈H₄₂NO₁₇ (M + H⁺): 784.2453; Found: 784.2469.

Tetraallyl ((3R,4S,5R,6R)-6-(hydroxymethyl)tetrahydro-2H-pyran-2,3,4,5-tetrayl) tetracarbonate (2-4).

A suspension of **2-10** (100 mg, 0.13 mmol, 1 equiv), Pd(PPh₃)₄ (30 mg, 0.025 mmol, 0.20 equiv), and dimedone (140 mg, 1.0 mmol, 8.0 equiv) in dry MeOH (1.2 mL) was stirred at 50 °C for 1 h. The reaction mixture was cooled to room temperature and concentrated. The resulting

crude product was purified using column chromatography (elution with 20% MeOH/ethyl acetate). The product obtained was further purified by preparatory HPLC to obtain tetraallyl ((3R,4S,5R,6R)-6-(hydroxymethyl)tetrahydro-2H-pyran-2,3,4,5-tetraol) tetracarboxylate **2-4** (35 mg, 0.078 mmol, 62%). IR (cm⁻¹) 3297, 2956, 1741, 1660, 1606, 1215; ¹H-NMR (360 MHz, CD₃OD, anomeric pair): δ 7.57 (2H, d, *J* = 8.4), 7.37–7.30 (6H, m), 7.27–7.25 (1H, m), 5.09 (2H, s), 5.07 (0.6H, d, *J* = 3.6), 5.09 (2H, s), 4.48–4.42 (1H, m), 4.39–4.38 (0.4H, m), 4.30–4.22 (1H, m), 3.98–3.94 (1H, m), 3.68 (2H, s), 3.68–3.63 (0.4H, m), 3.50–3.45 (0.6H, m), 3.36–3.27 (1H, m), 3.26–3.25 (0.4H, m), 3.15–3.10 (0.6H, m); ¹³C-NMR (90 MHz, CDCl₃): δ 172.4, 156.7, 140.1, 136.8, 132.7, 130.1, 129.6, 128.0, 121.1, 98.2, 94.0, 77.89, 94.0, 77.9, 76.1, 75.2, 74.7, 73.7, 71.7, 71.5, 70.6, 70.2, 68.4, 68.3, 44.7; MS (TOF MS ES⁺, *m/z*): 448.2 (M + H⁺); HRMS (TOF MS ES⁺, *m/z*) Calculated for C₂₂H₂₆NO₉ (M + H⁺): 448.1608; Found: 448.1602.

Experimental procedure for first generation enzyme assays

Experimental procedure corresponding to Figure 2-3

A solution of β -galactosidase (100 μ L, 10.6–37.0 U mL⁻¹ in 10 mM phosphate buffer, pH 7.4) was added to a solution of lactose **2-1** (100 μ L, 20 mM in 10 mM phosphate buffer, pH 7.4). The mixture was agitated using a vortex mixer for 2 s. The resulting mixture was incubated at 20 °C for 2 h. The glucose concentration in the assay mixture was determined using a personal glucose meter.

Experimental procedure corresponding to Figure 2-4

A solution of esterase (20 μ L, 2–160 U mL⁻¹ in 50 mM phosphate buffer, pH 8.0) was added to a solution of ester **2-2** (20 μ L, 100 mM in 0.1 M phosphate buffer, pH 8.0, 0.85% (v/v) Triton X-100). The mixture was agitated using a vortex mixer for 2 s. The resulting mixture was incubated at 40 °C for 1 h. The glucose concentration in the assay mixture was determined using a personal glucose meter.

Experimental procedure corresponding to Figure 2-5

A solution of alkaline phosphatase (250 μ L, 40–600 U L⁻¹ in 0.1 M diethanolamine buffer, pH 7.4, 0.5 mM MgCl₂) was added to a solution of glucose-6-phosphate **2-3** (25 μ L, 220 mM in 0.1

M diethanolamine buffer, pH 7.4, 0.5 mM MgCl₂). The mixture was agitated using a vortex mixer for 2 s. The resulting mixture was incubated at 37 °C for 1 h. The glucose concentration in the assay mixture was determined using a personal glucose meter.

Experimental procedure corresponding to Figure 2-6

A solution of PGA (10 µL, 0.05–1.0 U mL⁻¹ in 0.1 M phosphate buffer, pH 7.5) was added to a solution of **2-4** (10 µL, 20 mM in 0.1 M phosphate buffer, pH 7.5, 1% (v/v) Tween 20). The mixture was agitated using a vortex mixer for 2 s. The resulting mixture was incubated at 20 °C for 1 h. The glucose concentration in the assay mixture was determined using a personal glucose meter.

Experimental procedure for second generation enzyme assays

Experimental procedure corresponding to Figure 2-7

A solution of β-galactosidase (100 µL, 0–340 U mL⁻¹ in 10 mM phosphate buffer, pH 7.4) was added to a solution of lactose **2-1** (100 µL, 20 mM in 10 mM phosphate buffer, pH 7.4) containing 62 µg D-glucose. The mixture was agitated using a vortex mixer for 2 s. The resulting mixture was incubated at 20 °C for 15 min. The glucose concentration in the assay mixture was determined using a personal glucose meter.

Experimental procedure corresponding to Figure 2-8

A solution of alkaline phosphatase (100 µL, 0–160 U L⁻¹ in 0.1 M HEPES buffer, pH 8.0, 0.5 mM MgCl₂) was added to a solution of glucose-6-phosphate **2-3** (10 µL, 220 mM in 0.1 M HEPES buffer, pH 8.0, 0.5 mM MgCl₂) containing 62 µg D-glucose. The mixture was agitated using a vortex mixer for 2 s. The resulting mixture was incubated at 37 °C for 5 min. The glucose concentration in the assay mixture was determined using a personal glucose meter.

Experimental procedure corresponding to Figure 2-9

A solution of PGA (10 µL, 0–1 U mL⁻¹ in 0.1 M phosphate buffer, pH 7.5) was added to a solution of **2-4** (10 µL, 20 mM in 0.1 M phosphate buffer, pH 7.5, 1% (v/v) Tween 20, 20 °C) containing 7.2 µg D-glucose. The mixture was agitated using a vortex mixer for 2 s. The

resulting mixture was incubated at 20 °C for 30 min. The glucose concentration in the assay mixture was determined using a personal glucose meter.

Experimental procedure for the quantification of alkaline phosphatase in blood serum

Experimental procedure corresponding to Figure 2-10

A 90 µL aliquot of horse blood serum was spiked with a solution of alkaline phosphatase (10 µL, 0–1600 U L⁻¹ in 0.1 M HEPES buffer, pH 8.0, 0.5 mM MgCl₂). The resulting mixture was added to a solution of glucose-6-phosphate **2-3** (10 µL, 220 mM in 0.1 M HEPES buffer, pH 8.0, 0.5 mM MgCl₂). The mixture was agitated using a vortex mixer for 2 s. The resulting mixture was incubated at 37 °C for 5 min. The glucose concentration in the assay mixture was determined using a personal glucose meter.

Experimental procedure corresponding to Table 2-1

A 90 µL aliquot of a serum sample was spiked with a solution of alkaline phosphatase (10 µL, 200 U L⁻¹ in 0.1 M HEPES buffer, pH 8.0, 0.5 mM MgCl₂). The resulting mixture was added to a solution of glucose-6-phosphate **2-3** (10 µL, 220 mM in 0.1 M HEPES buffer, pH 8.0, 0.5 mM MgCl₂). The mixture was agitated using a vortex mixer for 2 s. The resulting mixture was incubated at 37 °C for 5 min. The glucose concentration in the assay mixture was determined using a personal glucose meter. The serum samples used were commercial horse blood serum spiked with various amounts of D-glucose. The negative control was identical to the assay except buffer (10 µL, 220 mM in 0.1 M HEPES buffer, pH 8.0, 0.5 mM MgCl₂) was used instead of the solution of **2-3**.

Experimental procedure for the evaluation of the stability of the detection reagent 2-4

Experimental procedure corresponding to Figure 2-11 and 2-12

A solution of PGA (100 µL, 1 U mL⁻¹ (for Figure 2-11), or 0 U mL⁻¹ (for Figure 2-12) in 0.1 M phosphate buffer, pH 7.5) was added to a solution of **2-4** (100 µL, 20 mM in 0.1 M phosphate buffer, pH 7.5, 1% (v/v) Tween 20). The mixture was agitated using a vortex mixer for 2 s. An aliquot of the resulting mixture (20 µL) was diluted with 0.1 M phosphate buffer (60 µL, pH 7.5)

and the resulting solution was injected into an analytical reversed-phase HPLC. Additional aliquots were diluted and injected at regular intervals.

Experimental procedure corresponding to Figure 2-13

Aliquots of detection reagent **2-4** (~ 1 mg) in micro-centrifuge tubes were held at 40 °C open to air. At intervals, the samples were dissolved in 1 mL of 10 mM phosphate buffer (pH 7.5, 0.5% (v/v) Tween 20, 20 °C) and the resulting solution was injected into an analytical reversed-phase HPLC.

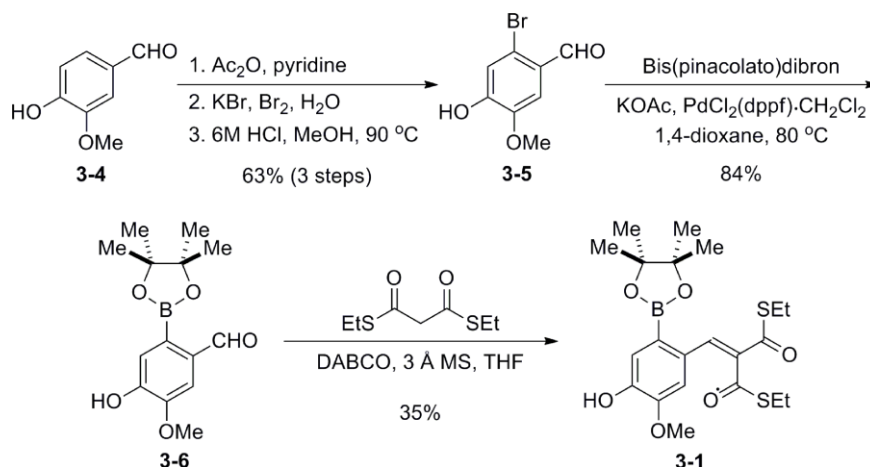
Experimental procedure corresponding to Table 2-2

A freshly prepared sample of **2-4** was used to assay a solution PGA (10 µL, 0.06 U mL⁻¹ in 0.1 M phosphate buffer, pH 7.5) using the standard assay procedure. An aliquot of **2-4** (~ 1 mg) in a microcentrifuge tube was held at 40 °C open to air for 7 days. This old sample of **2-4** was used in an assay for detecting PGA (10 µL, 0.06 U mL⁻¹ in 0.1 M phosphate buffer, pH 7.5) using the standard assay procedure. The concentrations of PGA in these assays were determined using the calibration curve in Figure 2-9. All assays were performed in triplicate.

6.3 Chapter 3: Experimental procedures and characterizations⁶

Synthetic procedures

Synthesis of detection reagent 3-1.



6-Bromovanillin (3-5).

Acetic anhydride (1.0 mL, 10 mmol, 1.5 equiv) was added to a stirred solution of vanillin **3-4** (1.0 g, 6.5 mmol, 1 equiv) in dry pyridine (4 mL) at 0 °C. The resulting solution was stirred at 20 °C for 16 h. The reaction mixture was diluted with water (100 mL). The suspension was collected and was extracted using EtOAc (3 × 20 mL). The combined organic layers were sequentially washed with 1 M HCl (2 × 10 mL), water (10 mL), brine (10 mL), and dried over anhydrous Na₂SO₄. The Na₂SO₄ was filtered and the filtrate was concentrated to obtain vanillin acetate as a white solid. Bromine (0.6 mL, 12 mmol, 1.2 equiv) was added to a vigorously stirred suspension of vanillin acetate and KBr (3.9 g, 33 mmol, 3.3 equiv) in water (20 mL) at 0 °C. The resulting suspension was stirred at 20 °C for 17 h. The reaction mixture was diluted with water (20 mL). The suspension was collected and was extracted using EtOAc (3 × 25 mL). The combined organic layers were sequentially washed with a 10% aqueous solution of Na₂S₂O₃ (2 × 20 mL), brine (10 mL), and dried over anhydrous Na₂SO₄. The Na₂SO₄ was filtered and the filtrate was concentrated. The crude product was partially purified by passing it through a plug of silica gel (elution with 5% ethyl acetate/hexane). The crude 6-bromovanillin acetate was treated with 6 M HCl (30 mL) and the resulting suspension was stirred at 90 °C for 5 h. The reaction mixture was cooled 0 °C, neutralized to a pH of 7 using aqueous NaOH solution (6 M), and the

product was extracted with EtOAc (2 × 100 mL). The combined organic layers were washed with brine (2 × 50 mL), and dried over anhydrous Na₂SO₄. The Na₂SO₄ was filtered and the filtrate was concentrated. The resulting solid was purified using column chromatography (elution with 40% EtOAc/hexanes) to obtain 6-bromovanillin **3-5** (0.92 g, 4.0 mmol, 63%) as a white solid. ¹H-NMR (CDCl₃): δ 10.13 (s, 1H), 7.41 (s, 1H), 7.11 (s, 1H), 3.92 (s, 3H). The ¹H-NMR data matches with literature values.⁷

4-hydroxy-5-methoxy-2-(4,4,5,5-tetramethyl-1,3,2-dioxaborolan-2-yl)benzaldehyde (3-6).

A round-bottom flask equipped with a stir bar was charged with 6-bromovanillin **3-5** (0.59 g, 2.6 mmol, 1 equiv), bis(pinacolato)diboron (0.78 g, 3.0 mmol, 1.2 equiv), PdCl₂(dppf)·CH₂Cl₂ (0.10 mg, 0.13 mmol, 0.05 equiv), potassium acetate (0.75 g, 7.6 mmol, 3.0 equiv), and 1,4-dioxane (10 mL). The resulting brown solution was stirred at 80 °C for 14 h. The reaction mixture was cooled to room temperature and diluted with CH₂Cl₂ (15 mL). The resulting mixture was filtered through a bed of celite and the filtrate was concentrated. The resulting residue was purified using column chromatography (gradient elution with 20–40% EtOAc/hexanes) to obtain 4-hydroxy-5-methoxy-2-(4,4,5,5-tetramethyl-1,3,2-dioxaborolan-2-yl)benzaldehyde **3-6** (0.59 mg, 2.1 mmol, 84%). IR (cm⁻¹) 3199, 2978, 1664, 1596; ¹H NMR (360 MHz, CDCl₃): δ 10.52 (1H, s), 7.55 (1H, s), 7.44 (1H, s), 3.95 (3H, s), 1.37 (12H, s); ¹³C NMR (90 MHz, CDCl₃): δ 193.7, 150.3, 148.8, 135.6, 121.7, 114.6, 84.4, 56.1, 24.9; MS (Q MS ES⁺, m/z): 279.1 (M + H⁺).

S,S-diethyl 2-(4-hydroxy-5-methoxy-2-(4,4,5,5-tetramethyl-1,3,2-dioxaborolan-2-yl)benzylidene)propanebis(thioate) (3-1).

4 Å Molecular sieves (~ 0.50 g) were added to a solution of 4-hydroxy-5-methoxy-2-(4,4,5,5-tetramethyl-1,3,2-dioxaborolan-2-yl)benzaldehyde **3-6** (0.48 g, 1.7 mmol, 1 equiv) and S,S-dithioethoxymalonate (0.37 g, 1.9 mmol, 1.1 equiv) in dry THF (9 mL). The resulting suspension was stirred at 0 °C for 0.5 h. DABCO (0.43 g, 3.8 mmol, 2.2 equiv) was added to the reaction mixture and the resulting suspension was stirred at room temperature for 12 h. The reaction mixture was diluted with CH₂Cl₂ (10 mL). The resulting mixture was filtered through a bed of celite and the filtrate was concentrated. The resulting residue was purified using column chromatography (elution with 25% EtOAc/hexanes). The product obtained was further purified by preparatory HPLC to obtain S,S-diethyl 2-(4-hydroxy-5-methoxy-2-(4,4,5,5-tetramethyl-

1,3,2-dioxaborolan-2-yl)benzylidene)propanebis(thioate) **3-1** (0.28 g, 0.62 mmol, 35 %). IR (cm⁻¹) 3422, 2976, 2932, 2874, 1654, 1564, 1509; ¹H NMR (360 MHz, CDCl₃): δ 8.59 (1H, s), 7.42 (1H, s), 7.07 (1H, s), 5.79 (1H, s), 3.83 (3H, s), 3.01 (2H, q, *J* = 7.4 Hz), 2.95 (2H, q, *J* = 7.4), 1.37 (12H, s), 1.32 (3H, t, *J* = 7.4), 1.26 (3H, t, *J* = 7.4); ¹³C NMR (90 MHz, CDCl₃): δ 195.3, 189.3, 148.2, 147.0, 142.0, 137.3, 131.5, 122.1, 111.8, 84.1, 55.9, 24.9, 24.2, 23.7, 14.8, 14.3; MS (Q MS ES+, *m/z*): 453.2 (*M* + H⁺); HRMS (TOF MS ES+, *m/z*) Calculated for C₂₁H₃₀BO₆S₂ (*M* + H⁺): 453.1577; Found: 453.1566.

Experimental procedures to test the response of **3-4** to H₂O₂

Experimental procedure corresponding to Figure 3-4

An H₂O₂ solution (10 μL, 50 mM in water) was added to a solution of **3-1** (200 μL, 0.48 mM in 1:1 MeOH-10 mM phosphate buffer, pH 7.4). The mixture was agitated using a vortex mixer for 2 s. An aliquot of the resulting mixture was injected into an analytical reversed-phase HPLC coupled to a mass spectrometer and additional aliquots were injected at regular intervals.

Experimental procedure corresponding to Figure 3-5

An H₂O₂ solution (2 mL, 22 μM in 10 mM phosphate buffer, pH 7.4) was added to a solution of **3-1** (20 μL, 2 mM in MeOH). The mixture was agitated using a vortex mixer for 2 s. The fluorescence emission spectrum of the resulting mixture was obtained at regular intervals (λ_{ex} = 470 nm).

Experimental procedure corresponding to Figure 3-6

An H₂O₂ solution (2 mL, 0–100 μM in 10 mM phosphate buffer, pH 7.4) was added to a solution of **3-1** (20 μL, 2 mM in MeOH). The mixture was agitated using a vortex mixer for 2 s. The fluorescence emission (I) of the resulting mixture was obtained after 10 min. (λ_{ex} = 470 nm, λ_{em} = 510 nm). The background subtracted fluorescence emission intensity (I – I₀) was plotted against the H₂O₂ concentration to obtain the dose response curve in Figure 3-6. (I = fluorescence intensity of the assay after 10 min from the start of the assay; I₀ = fluorescence intensity of an assay containing 0 μM of H₂O₂ after 10 min from the start of the assay).

Experimental procedures for the single-step enzyme assay for triaging of samples (by odor) and quantifying enzyme concentrations (by fluorescence)

Experimental procedure corresponding to Figure 3-8a

A solution of β -D-galactosidase (1.8 mL, 0–500 nM in 10 mM phosphate buffer, pH 7.4) was mixed with glucose oxidase (0.1 mL, 200 U mL⁻¹ in 10 mM phosphate buffer, pH 7.4) and **3-1** (20 μ L, 2 mM in MeOH). The resulting solution was treated with a solution of lactose **3-3a** (0.1 mL, 0.2 M in 10 mM phosphate buffer, pH 7.4). The fluorescence emission of the resulting solution was obtained after 1 h ($\lambda_{\text{ex}} = 470$ nm, $\lambda_{\text{em}} = 510$ nm). The background subtracted fluorescence emission intensity ($I - I_0$) was plotted against the β -D-galactosidase concentration to obtain the calibration curve in Figure 3-8a. (I = fluorescence intensity of the assay 1 h from the start of the assay; I_0 = fluorescence intensity of an assay containing 0 nM of β -D-galactosidase 1 h from the start of the assay.)

Experimental procedure corresponding to Figure 3-8b

A solution of ALP (1.8 mL, 0–1000 U L⁻¹ in 50 mM Tris buffer, pH 8.0) was mixed with glucose oxidase (0.1 mL, 200 U mL⁻¹ in 50 mM Tris buffer, pH 8.0) and **3-1** (20 μ L, 2 mM in MeOH). The resulting solution was treated with a solution of D-glucose-6-phosphate **3-3b** (0.1 mL, 0.1 M in 50 mM Tris buffer, pH 8.0). The fluorescence emission of the resulting solution was obtained after 1 h ($\lambda_{\text{ex}} = 470$ nm, $\lambda_{\text{em}} = 510$ nm). The background subtracted fluorescence emission intensity ($I - I_0$) was plotted against the ALP concentration to obtain the calibration curve. (I = fluorescence intensity of the assay 1 h from the start of the assay; I_0 = fluorescence intensity of an assay containing 0 U L⁻¹ of ALP 1 h from the start of the assay.)

General procedure for detection of β -D-galactosidase using a smell-based assay

A solution of β -D-galactosidase (0.9 mL, 0 or 200 nM in phosphate buffer, 10 mM, pH 7.4) was mixed with glucose oxidase (50 μ L, 200 U mL⁻¹ in phosphate buffer, 10 mM, pH 7.4) and **3-1** (20 μ L, 2 mM in MeOH) in a 1.6-ml microcentrifuge tube. A negative control containing no β -D-galactosidase (just phosphate buffer, 10 mM, pH 7.4, 0.9 mL) was mixed with glucose oxidase (50 μ L, 200 U mL⁻¹ in phosphate buffer, 10 mM, pH 7.4) and **3-1** (20 μ L, 2 mM in MeOH) in a separate 1.6-ml microcentrifuge tube. A solution of **3-3a** (50 μ L, 0.2 M in 10 mM phosphate

buffer, pH 7.4) was added to each assay. After an assay time of 1 h, both the sample and the control were given to other researchers (members of the Phillips research group) who were asked if they can distinguish the sample from the control (which was given as a separate sample) by smell alone. A “yes” response implies the sample assay had a stronger thiol smell than the negative control. A “no” response implies the sample assay could not be distinguished from the negative control.

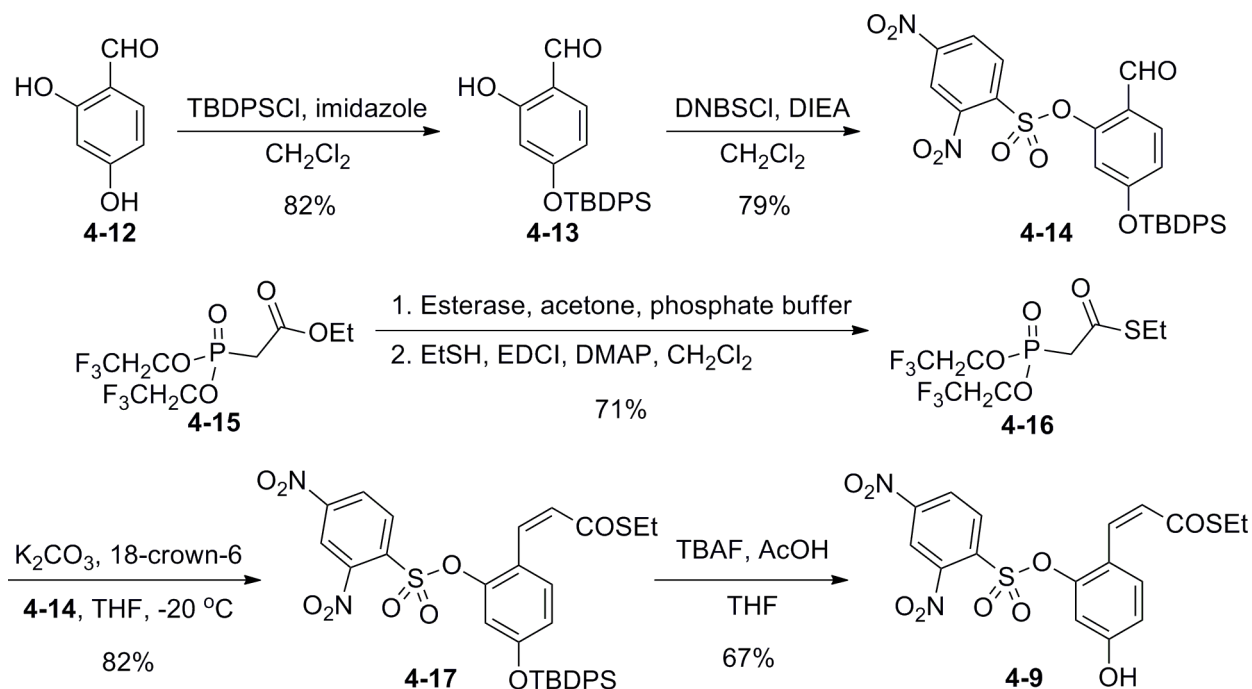
General procedure for detection of ALP using a smell-based assay

A solution of ALP (0.9 mL, 0 or 100 U L⁻¹ in Tris buffer, 50 mM, pH 8.0) was mixed with glucose oxidase (50 µL, 200 U mL⁻¹ in Tris buffer, 50 mM, pH 8.0) and **3-1** (20 µL, 2 mM in MeOH) in a 1.6-ml microcentrifuge tube. A negative control containing no ALP (just Tris buffer, 50 mM, pH 8.0, 0.9 mL) was mixed with glucose oxidase (50 µL, 200 U mL⁻¹ in Tris buffer, 50 mM, pH 8.0) and **3-1** (20 µL, 2 mM in MeOH) in a separate 1.6-ml microcentrifuge tube. A solution of **3-3b** (50 µL, 0.1 M in 10 mM phosphate buffer, pH 7.4) was added to each assay. After an assay time of 1 h, both the sample and the control were given to other researchers (members of the Phillips research group) who were asked if they can distinguish the sample from the control (which was given as a separate sample) by smell alone. A “yes” response implies the sample assay had a stronger thiol smell than the negative control. A “no” response implies the sample assay could not be distinguished from the negative control.

6.4 Chapter 4: Experimental procedures and characterizations

Synthetic procedure

Synthesis of amplification reagent 4-9



4-[[[(1,1-dimethylethyl)diphenylsilyl]oxy]-2-hydroxybenzaldehyde (**4-13**).

TBDPSCl (4.8 mL, 19 mmol, 1.1 equiv) was added to a solution of 2,4-dihydroxybenzaldehyde **4-12** (2.4 g, 18 mmol, 1.0 equiv) and imidazole (1.4 g, 21 mmol, 1.2 equiv) in CH_2Cl_2 (88 mL) at $0\text{ }^\circ\text{C}$. The resulting mixture was stirred at $0\text{ }^\circ\text{C}$ for 10 min and at $20\text{ }^\circ\text{C}$ for 6 h. The reaction mixture was concentrated and the residue was resuspended in EtOAc (50 mL). The resulting mixture was washed with water (50 mL) and brine ($2 \times 50\text{ mL}$). The organic layer was dried over anhydrous Na_2SO_4 . The Na_2SO_4 was filtered and the filtrate was concentrated. The crude product was purified by flash column chromatography (elution with 2% EtOAc/hexanes) to obtain 4-[[[(1,1-dimethylethyl)diphenylsilyl]oxy]-2-hydroxybenzaldehyde **4-13** (5.5 g, 14 mmol, 82%). ^1H -NMR (360 MHz, CDCl_3): δ 11.30 (1H, s), 9.48 (1H, s), 7.73–7.70 (4H, m), 7.38–7.28 (6H, m), 7.09 (1H, d, $J = 7.1$), 6.41 (1H, d, $J = 1.9$), 6.36 (1H, dd, $J = 7.1, 1.9$), 1.11 (9H, s); ^{13}C -NMR (75 MHz, CDCl_3): δ 194.5, 163.9, 163.4, 135.4, 135.3, 131.7, 130.4, 128.1, 115.8, 112.9,

107.8, 26.4, 19.5; MS (TOF MS APCI+, m/z): 377.0 (100, M^+); HRMS (TOF MS ES+, m/z) Calculated for $C_{23}H_{24}O_3Si$ ($M + H^+$): 377.1573; Found: 377.1564.

5-((tert-butyldiphenylsilyl)oxy)-2-formylphenyl 2,4-dinitrobenzenesulfonate (4-14).

DIEA (0.63 mL, 3.6 mmol, 1.2 equiv) was added dropwise to a suspension of 4-(tertbutyldiphenylsilyloxy)-2-hydroxybenzaldehyde **4-13** (1.1 g, 3.0 mmol, 1.0 equiv) and 2,4-dinitrobenzenesulfonyl chloride (0.96 g, 3.6 mmol, 1.2 equiv) in CH_2Cl_2 (19 mL). The resulting mixture was stirred at 20 °C for 4 h. The reaction mixture was diluted with brine (10 mL) and the resulting mixture was extracted with CH_2Cl_2 (2×20 mL). The combined CH_2Cl_2 layers were dried over anhydrous $MgSO_4$. The $MgSO_4$ was filtered and the filtrate was concentrated under reduced pressure. The residue was purified by flash column chromatography (elution with 20% EtOAc/hexanes) to obtain 5-((tertbutyldiphenylsilyl)oxy)-2-formylphenyl 2,4-dinitrobenzenesulfonate **4-14** (1.4 g, 2.4 mmol, 79%). 1H -NMR (300 MHz, $CDCl_3$): δ 10.02 (1H, s), 8.47 (1H, d, $J = 2.0$), 8.09 (1H, dd, $J = 8.7, 2.0$), 7.86 (1H, d, $J = 8.6$), 7.78 (1H, d, $J = 8.6$), 7.60–7.49 (5H, m), 7.49–7.47 (1H, m), 7.47–7.38 (5H, m), 6.95 (1H, dd, $J = 8.7, 2.0$), 6.40 (1H, d, $J = 2.0$), 1.05 (9H, s); ^{13}C -NMR (75 MHz, $CDCl_3$): δ 186.2, 161.9, 151.0, 150.7, 148.5, 135.2, 133.5, 133.3, 131.7, 131.1, 130.7, 128.3, 126.6, 122.9, 120.6, 120.4, 113.7, 26.1, 19.4; MS (TOF MS APCI+, m/z): 607.1 (100, $M + H^+$); HRMS (TOF MS ES+, m/z) Calculated for $C_{29}H_{27}N_2O_9SSi$ ($M + H^+$): 607.1207; Found: 607.1207.

S-ethyl [bis(2,2,2-trifluoroethoxy)phosphoryl]ethanethioate (4-16).

Porcine liver esterase (77 mg, 150 U) was added to a stirred solution of ethyl [bis(2,2,2-trifluoroethoxy)phosphinyl]acetate **4-15** (0.6 mL, 2.5 mmol) in 8:1 potassium phosphate buffer (0.1 M, pH 7.8)-acetone (45 mL). The resulting suspension was stirred at 20 °C for 24 h. The reaction mixture was acidified to pH 1 using concentrated HCl. NaCl (4 g) was then added and the resulting suspension was stirred for 10 minutes. The reaction mixture was then filtered and the filtrate was extracted with EtOAc (3×100 mL). The combined organic layers were dried over anhydrous $MgSO_4$. The $MgSO_4$ was filtered and the filtrate was concentrated to obtain a bis-(2,2,2-trifluoroethyl)phosphonoacetic acid as a brown solid (740 mg, 2.4 mmol, 96%). To a solution of bis-(2,2,2-trifluoroethyl)phosphonoacetic acid (740 mg, 2.4 mmol, 1.0 equiv) and DMAP (29 mg, 0.24 mmol, 0.1 equiv) in CH_2Cl_2 at 0 °C was added ethanethiol (0.90 mL, 12

mmol, 5.0 equiv), followed by EDC hydrochloride (610 mg, 3.2 mmol, 1.3 equiv). The resulting mixture was stirred at 0 °C for 45 min and at 20 °C for 45 min. The reaction mixture was concentrated and the residue was redissolved in Et₂O (20 mL). The resulting solution was washed successively with 1 M aqueous HCl (2 × 15 mL), water (2 × 15 mL) and brine (2 × 15 mL). The organic layer was dried over anhydrous MgSO₄. The MgSO₄ was filtered and the filtrate was concentrated under reduced pressure to obtain S-ethyl [bis(2,2,2-trifluoroethoxy)phosphoryl]ethanethioate **4-16** as a yellow oil (600 mg, 1.7 mmol, 71%). ¹H-NMR (300 MHz, CDCl₃): δ 4.48 (4H, quin, *J* = 8.1), 3.44 (2H, d, *J* = 21), 2.95 (2H, q, *J* = 7.4), 1.28 (3H, t, *J* = 7.4); ¹³C-NMR (75 MHz, CDCl₃): δ 189.4, 128.0 (q), 124.3 (q), 120.6 (q), 116.9 (q), 63.1 (q), 62.6 (q), 62.1 (q), 61.6 (q), 42.8 (d), 41.0 (d), 24.2, 13.9; MS (TOF MS APCI+, *m/z*): 348.9 (56, *M* + *H*⁺); HRMS (TOF MS ES+, *m/z*) Calculated for C₈H₁₂F₆O₄PS (*M* + *H*⁺): 349.0098; Found: 349.0092.

(Z)-S-ethyl 3-(4-((tert-butyldiphenylsilyl)oxy)-2-(((2,4-dinitrophenyl)sulfonyl)oxy)phenyl)prop-2-enethioate (4-17)

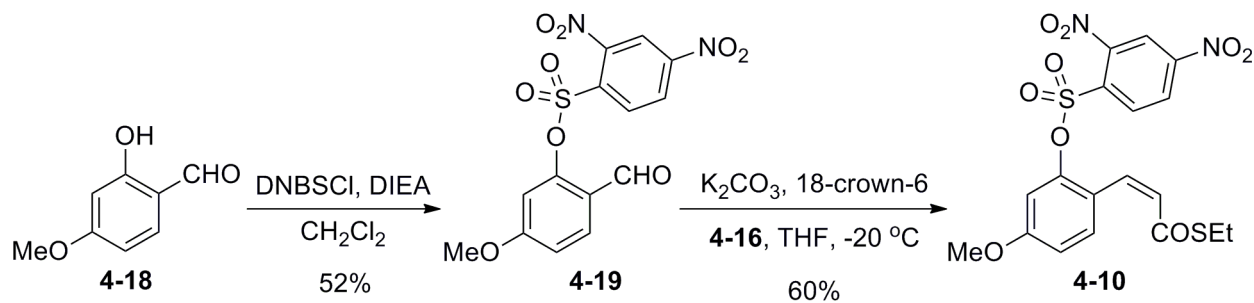
A suspension of K₂CO₃ (96 mg, 0.69 mmol, 2.1 equiv) and 18-crown-6 (110 mg, 0.41 mmol, 1.2 equiv) in THF (6 mL) was stirred at 20 °C for 4 h. The suspension was then cooled to –20 °C. A solution of 5-((tertbutyldiphenylsilyl)oxy)-2-formylphenyl 2,4-dinitrobenzenesulfonate **4-14** (200 mg, 0.33 mmol, 1.0 equiv) in THF (2 mL) was added to the cooled suspension. A solution of S-ethyl [bis(2,2,2-trifluoroethoxy)phosphoryl]ethanethioate **4-16** (130 mg, 0.36 mmol, 1.1 equiv) in THF (1 mL) was added to the reaction mixture and the resulting solution was stirred at –20 °C for 4 h. The reaction mixture was diluted with saturated aqueous NH₄Cl (10 mL) and the resulting mixture was extracted with EtOAc (3 × 20 mL). The combined organic layers were sequentially washed with saturated aqueous NH₄Cl (2 × 20 mL), brine (2 × 20 mL), and dried over anhydrous MgSO₄. The MgSO₄ was filtered and the filtrate was concentrated under reduced pressure. The residue was purified by flash column chromatography (gradient elution with 6%–15% EtOAc-hexanes). The product was further purified by preparatory HPLC to obtain (Z)-S-ethyl 3-(4-((tert-butyldiphenylsilyl)oxy)-2-(((2,4-dinitrophenyl)sulfonyl)oxy)phenyl)prop-2-enethioate **4-17** (74 mg, 0.11 mmol, 32%) as a yellow foam. ¹H-NMR (300 MHz, CDCl₃): δ 8.43 (1H, d, *J* = 2.2), 8.02 (1H, dd, *J* = 8.6, 2.2), 7.66–7.57 (5H, m), 7.52–7.37 (8H, m), 6.69 (1H, d, *J* = 12), 6.54 (1H, d, *J* = 2.4), 5.77 (1H, d, *J* = 12), 2.79 (2H, q, *J* = 7.4), 1.20 (4H, d, *J* = 7.4), 1.07

(9H, s); ^{13}C -NMR (75 MHz, CDCl_3): δ 189.0, 157.9, 150.7, 148.4, 147.7, 135.4, 134.0, 133.4, 133.2, 132.5, 131.8, 130.5, 128.2, 126.3, 121.4, 120.1, 119.4, 114.1, 26.4, 23.8, 19.5, 14.5; MS (TOF MS APCI+, m/z): 693.1 (60, $\text{M} + \text{H}^+$); HRMS (TOF MS ES+, m/z) Calculated for $\text{C}_{33}\text{H}_{33}\text{N}_2\text{O}_9\text{S}_2\text{Si}$ ($\text{M} + \text{H}^+$): 693.1397; Found: 693.1389.

(Z)-S-ethyl 3-(2-(((2,4-dinitrophenyl)sulfonyl)oxy)-4-hydroxyphenyl)prop-2-enethioate (4-9).

Acetic acid (1 M solution in THF, 80 μL , 80 μmol , 3.5 equiv) and TBAF (1 M solution in THF, 25 μL , 25 μmol , 1.1 equiv) were sequentially added to a solution of **4-17** (16 mg, 23 μmol , 1.0 equiv) in THF (150 μL). The resulting solution was stirred at 20 $^\circ\text{C}$ for 10 min. The reaction mixture was diluted with CH_2Cl_2 (5 mL) and the resulting solution was filtered through a bed of silica gel. The silica gel bed was washed with a 1:1 CH_2Cl_2 -Acetone (50 mL) and the combined filtrate was concentrated under reduced pressure. The residue was purified by flash column chromatography (elution with 30% EtOAc/hexanes) to obtain (Z)-S-ethyl 3-(2-(((2,4-dinitrophenyl)sulfonyl)oxy)-4-hydroxyphenyl)prop-2-enethioate **4-9** (7 mg, 15 μmol , 67%) as a yellow solid. ^1H -NMR (300 MHz, 2:1 CDCl_3 - d^6 -acetone): δ 9.13 (1H, br s), 8.70 (1H, d, $J = 2.2$), 8.42 (1H, dd, $J = 8.7, 2.2$), 8.02 (1H, d, $J = 8.6$), 7.58 (1H, d, $J = 8.6$), 6.85–6.83 (2H, m), 6.71 (1H, d, $J = 12$), 5.71 (1H, d, $J = 12$), 2.81 (2H, q, $J = 7.5$), 1.22 (3H, t, $J = 7.5$); ^{13}C -NMR (75 MHz, 2:1 CDCl_3 - d^6 -acetone): δ 188.2, 159.4, 150.8, 148.5, 147.7, 133.9, 133.2, 132.4, 126.4, 125.1, 120.0, 119.9, 119.1, 114.7, 110.0, 23.2, 13.9; MS (TOF MS APCI+, m/z): 455.0 (25, $\text{M} + \text{H}^+$); HRMS (TOF MS ES+, m/z) Calculated for $\text{C}_{17}\text{H}_{15}\text{N}_2\text{O}_9\text{S}_2$ ($\text{M} + \text{H}^+$): 455.0219; Found: 455.0221.

Synthesis of amplification reagent 4-10



2-formyl-5-methoxyphenyl 2,4-dinitrobenzenesulfonate (4-19).

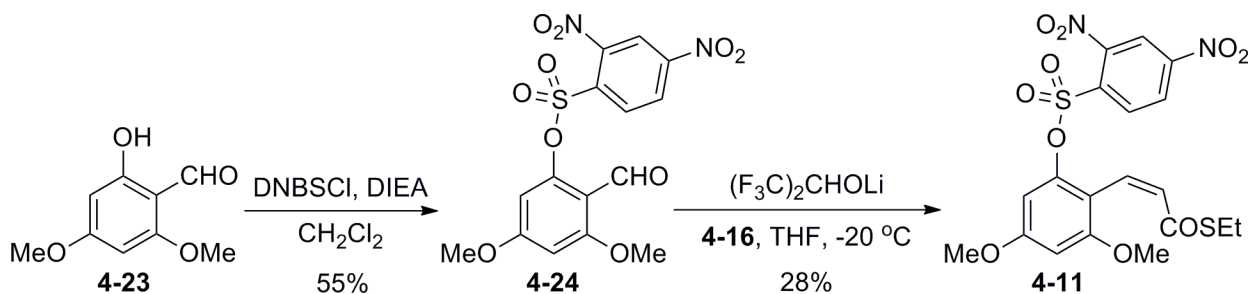
DIEA (0.4 mL, 2.3 mmol, 1.2 equiv) was added dropwise to a suspension of 4-methoxy-2-hydroxybenzaldehyde **4-18** (300 mg, 2.0 mmol, 1.0 equiv) and 2,4-dinitrobenzenesulfonyl chloride (590 mg, 2.2 mmol, 1.1 equiv) in CH₂Cl₂ (10 mL) at 0 °C. The resulting mixture was stirred at 0 °C for 4 h and at 20 °C for 1 h. The reaction mixture was diluted with saturated aqueous NH₄Cl (10 mL) and the resulting mixture was extracted with CH₂Cl₂ (2 × 15 mL). The combined CH₂Cl₂ layers were washed with brine (10 mL) and dried over anhydrous MgSO₄. The MgSO₄ was filtered and the filtrate was concentrated under reduced pressure. The residue was purified by flash column chromatography (elution with 30% EtOAc/hexanes) to obtain 2-formyl-5-methoxyphenyl 2,4-dinitrobenzenesulfonate **4-19** (400 mg, 1.0 mmol, 52%) as a yellow powder. ¹H-NMR (300 MHz, CDCl₃): δ 9.96 (1H, s), 8.70 (1H, d, *J* = 2.1), 8.58 (1H, dd, *J* = 8.6, 2.1), 8.34 (1H, d, *J* = 8.6), 7.87 (1H, d, *J* = 8.7), 7.00 (1H, dd, *J* = 8.7, 2.3), 6.87 (1H, d, *J* = 2.3), 3.91 (3H, s); ¹³C-NMR (75 MHz, CDCl₃): δ 186.4, 165.4, 151.2, 150.9, 149.1, 133.8, 133.6, 133.3, 126.9, 122.2, 120.7, 114.2, 109.4, 56.4; MS (TOF MS APCI+, *m/z*): 383.0 (100, *M* + H⁺); HRMS (TOF MS ES+, *m/z*) Calculated for C₁₄H₁₁N₂O₉S (*M* + H⁺): 383.0185; Found: 383.0181.

(Z)-S-ethyl 3-(2-(((2,4-dinitrophenyl)sulfonyl)oxy)-4-methoxyphenyl)prop-2-enethioate (4-10).

A suspension of K₂CO₃ (100 mg, 0.71 mmol, 2.1 equiv) and 18-crown-6 (110 mg, 0.42 mmol, 1.2 equiv) in THF (6 mL) was stirred at 20 °C for 4 h. The suspension was then cooled to –20 °C. 2-formyl-5-methoxyphenyl 2,4-dinitrobenzenesulfonate **4-19** (130 mg, 0.34 mmol, 1.0 equiv) was added to the cooled suspension. A solution of S-ethyl [bis(2,2,2-trifluoroethoxy)phosphoryl]ethanethioate **4-16** (130 mg, 0.36 mmol, 1.1 equiv) in THF (2.5 mL) was added to the reaction mixture and the resulting solution was stirred at –20 °C for 4 h. The reaction mixture was diluted with saturated aqueous NH₄Cl (10 mL) and the resulting mixture was extracted with EtOAc (3 × 30 mL). The combined organic layers were sequentially washed with saturated aqueous NH₄Cl (2 × 20 mL), brine (2 × 20 mL), and dried over anhydrous MgSO₄. The MgSO₄ was filtered and the filtrate was concentrated under reduced pressure. The residue was purified by flash column chromatography (elution with 10% EtOAc/hexanes). The product was further purified by preparatory HPLC to obtain (Z)-S-ethyl 3-(2-(((2,4-

dinitrophenyl)sulfonyl)oxy)-4-methoxyphenyl)prop-2-enethioate **4-10** (95 mg, 0.20 mmol, 60%) as a yellow solid. $^1\text{H-NMR}$ (300 MHz, CDCl_3): δ 8.58 (1H, d, $J = 2.2$), 8.31 (1H, dd, $J = 8.6$, 2.2), 7.94 (1H, d, $J = 8.6$), 7.55 (1H, d, $J = 8.7$), 6.92 (1H, d, $J = 2.5$), 6.88 (1H, dd, $J = 8.7$, 2.5), 6.73 (1H, d, $J = 12$), 5.67 (1H, d, $J = 12$), 2.79 (2H, q, $J = 7.4$), 1.21 (3H, t, $J = 7.4$); $^{13}\text{C-NMR}$ (75 MHz, CDCl_3): δ 188.8, 161.8, 151.1, 149.0, 148.0, 134.3, 133.8, 133.1, 132.7, 126.6, 126.0, 120.5, 120.1, 113.6, 109.1, 56.0, 23.9, 14.4; MS (TOF MS APCI+, m/z): 469.0 (100, $\text{M} + \text{H}^+$); HRMS (TOF MS ES+, m/z) Calculated for $\text{C}_{18}\text{H}_{17}\text{N}_2\text{O}_9\text{S}_2$ ($\text{M} + \text{H}^+$): 469.0375; Found: 469.0361.

Synthesis of amplification reagent **4-11**



2-formyl-3,5-dimethoxyphenyl 2,4-dinitrobenzenesulfonate (**4-24**)

A solution 2,4-dinitrobenzenesulfonyl chloride (1.0 g, 3.9 mmol, 1.3 equiv) in CH_2Cl_2 (8 mL) was added dropwise to a solution of 4,6-dimethoxy-2-hydroxybenzaldehyde **4-23** (550 mg, 3.0 mmol, 1.0 equiv) and DIEA (0.7 mL, 4.0 mmol, 1.3 equiv) in CH_2Cl_2 (8 mL) at $0\text{ }^\circ\text{C}$. The resulting solution was stirred at $0\text{ }^\circ\text{C}$ for 4 h and at $20\text{ }^\circ\text{C}$ for 2 h. The reaction mixture was diluted with saturated aqueous NH_4Cl (10 mL) and the resulting mixture was extracted with CH_2Cl_2 ($2 \times 15\text{ mL}$). The combined CH_2Cl_2 layers were washed with brine (10 mL) and dried over anhydrous MgSO_4 . The MgSO_4 was filtered and the filtrate was concentrated under reduced pressure. The residue was purified by flash column chromatography (elution with 30% EtOAc/hexanes) to obtain 2-formyl-3,5-dimethoxyphenyl 2,4-dinitrobenzenesulfonate **4-24** (680 mg, 1.6 mmol, 55%) as a yellow powder. $^1\text{H-NMR}$ (300 MHz, CD_2Cl_2): δ 10.11 (1H, s), 8.67 (1H, d, $J = 2.1$), 8.59 (1H, dd, $J = 8.7$, 2.2), 8.35 (1H, d, $J = 8.7$), 6.51 (1H, d, $J = 2.0$), 6.41 (1H, d, $J = 2.0$), 3.91 (3H, s), 3.87 (3H, s); $^{13}\text{C-NMR}$ (75 MHz, CD_2Cl_2): δ 186.0, 165.8, 164.8, 151.1, 149.4, 149.1, 135.2, 134.1, 127.1, 120.6, 112.0, 102.5, 98.0, 56.8, 56.6; MS (TOF MS APCI+,

m/z): 412.9 (100, M + H⁺); HRMS (TOF MS ES⁺, m/z) Calculated for C₁₅H₁₃N₂O₁₀S (M + H⁺): 413.0291; Found: 413.0284.

(Z)-S-ethyl 3-(2-(((2,4-dinitrophenyl)sulfonyl)oxy)-4,6-dimethoxyphenyl)prop-2-enethioate (4-11).

A solution of n-butyllithium in hexanes (2.5 M, 110 μ L, 0.27 mmol, 1.1 equiv) was added to 1,1,1,3,3,3-hexafluoroisopropanol (31 μ L, 0.29 mmol, 1.2 equiv) at -20 °C. A solution of S-ethyl [bis(2,2,2-trifluoroethoxy)phosphoryl]ethanethioate **4-16** (89 mg, 0.25 mmol, 1.0 equiv) in THF (0.5 mL) was added to the reaction mixture and the resulting solution was stirred at -20 °C for 5 min. A suspension of **4-24** (100 mg, 0.24 mmol, 1.0 equiv) in THF (2.0 mL) was added to the reaction mixture in small portions (0.5 mL). The resulting mixture was stirred at -20 °C for 2 h and warmed to 20 °C over 4 h. The reaction mixture was diluted with saturated aqueous NH₄Cl (10 mL) and the resulting mixture was extracted with EtOAc (3 \times 15 mL). The combined organic layers were washed with brine (10 mL) and dried over anhydrous MgSO₄. The MgSO₄ was filtered and the filtrate was concentrated under reduced pressure. The residue was purified by flash column chromatography (elution with 25% EtOAc/hexanes). The product was further purified by preparatory HPLC to obtain (Z)-S-ethyl 3-(2-(((2,4-dinitrophenyl)sulfonyl)oxy)-4,6-dimethoxyphenyl)prop-2-enethioate **4-11** (33 mg, 0.66 mmol, 28%) as a yellow solid. ¹H-NMR (300 MHz, CDCl₃): δ 8.56 (1H, d, *J* = 2.2), 8.36 (1H, dd, *J* = 8.6, 2.2), 8.1 (1H, d, *J* = 8.6), 6.54 (1H, d, *J* = 2.3), 6.48 (1H, d, *J* = 12), 6.40 (1H, d, *J* = 2.3), 5.81 (1H, d, *J* = 12), 3.84 (3H, s), 3.71 (3H, s), 2.75 (2H, q, *J* = 7.4), 1.18 (3H, t, *J* = 7.4); ¹³C-NMR (75 MHz, CDCl₃): δ 188.9, 161.5, 158.4, 150.8, 148.8, 147.8, 134.2, 133.8, 128.8, 128.5, 126.8, 120.0, 112.0, 100.4, 98.2, 55.9, 55.8, 23.5, 14.8; MS (TOF MS APCI⁺, m/z): 498.9 (55, M + H⁺); HRMS (TOF MS ES⁺, m/z) Calculated for C₁₉H₁₉N₂O₁₀S₂ (M + H⁺): 499.0481; Found: 499.0475.

Experimental procedures for the preliminary assay to demonstrate the signal amplification reactions using 4-9–4-11.

Experimental procedure corresponding to Figure 4-7

An L-cysteine solution (300 μ L, 0 or 400 μ M in 0.1 M HEPES buffer, pH 7.4, 1 mM EDTA) was added to a solution of the amplification reagent (**4-9**, **4-10**, or **4-11**) (300 μ L, 4 mM in CH₃CN). The mixture was agitated using a vortex mixer for 2 s. At regular intervals, an aliquot (20 μ L) of the assay mixture was diluted with 1:1 CH₃CN-0.1 M HEPES buffer, pH 7.4, 1 mM EDTA (2 mL). The fluorescence emission intensity of the resulting mixture was obtained (λ_{ex} = 325 nm, λ_{em} = 430 nm). The fluorescent intensity was recorded as % of maximum fluorescence intensity obtained for the assay mixture containing 200 μ M L-cysteine.

Experimental procedure corresponding to Figure 4-10

An L-cysteine solution (150 μ L, 400 μ M in 0.1 M HEPES buffer, pH 7.4, 1 mM EDTA) was added to a solution of the amplification reagent **4-11** (150 μ L, 4 mM in CH₃CN). The mixture was agitated using a vortex mixer for 2 s. At regular intervals, an aliquot (2 μ L) of the reaction mixture was injected into an analytical reversed-phase HPLC coupled to a mass spectrometer.

Experimental procedure to demonstrate dose-dependent signal amplification using 4-11 (Experimental procedure corresponding to Figure 4-11)

An ethanethiol solution (200 μ L, 0–4 mM in 0.1 M HEPES buffer, pH 7.4, 1 mM EDTA) was added to a solution of the amplification reagent **4-11** (200 μ L, 4 mM in CH₃CN). The mixture was agitated using a vortex mixer for 2 s. At regular intervals, an aliquot (20 μ L) of the assay mixture was diluted with 1:1 CH₃CN-0.1 M HEPES buffer, pH 7.4, 1 mM EDTA (2 mL). The fluorescence emission intensity of the resulting mixture was obtained (λ_{ex} = 325 nm, λ_{em} = 430 nm). The fluorescent intensity was recorded as % of maximum fluorescence intensity obtained for the assay.

Experimental procedure to probe the effect of additives on the signal amplification reaction using 4-11 (Experimental procedure corresponding to Figure 4-12 and 4-13)

An ethanethiol solution (200 μ L, 0.04 mM in 0.1 M HEPES buffer, pH 7.4, 1 mM EDTA) was added to a solution (200 μ L) containing **4-11** (4 mM in CH₃CN) and the additives **4-22** (or **4-25**) (0 or 2 mM in CH₃CN). The mixture was agitated using a vortex mixer for 2 s. At regular intervals, an aliquot (20 μ L) of the assay mixture was diluted with 1:1 CH₃CN-0.1 M HEPES buffer, pH 7.4, 1 mM EDTA (2 mL). The background subtracted fluorescence emission intensity ($I - I_0$) of the resulting mixture was obtained ($\lambda_{\text{ex}} = 325$ nm, $\lambda_{\text{em}} = 430$ nm). The fluorescent intensity was recorded as % of maximum background subtracted fluorescence intensity obtained for the assay. (I = fluorescence intensity of the assay; I_0 = fluorescence intensity of the assay measured at the start of the assay).

Experimental procedure to probe the effect of the structure of the thiol used to initiate the signal amplification reaction containing 4-11 (Experimental procedure corresponding to Figure 4-14)

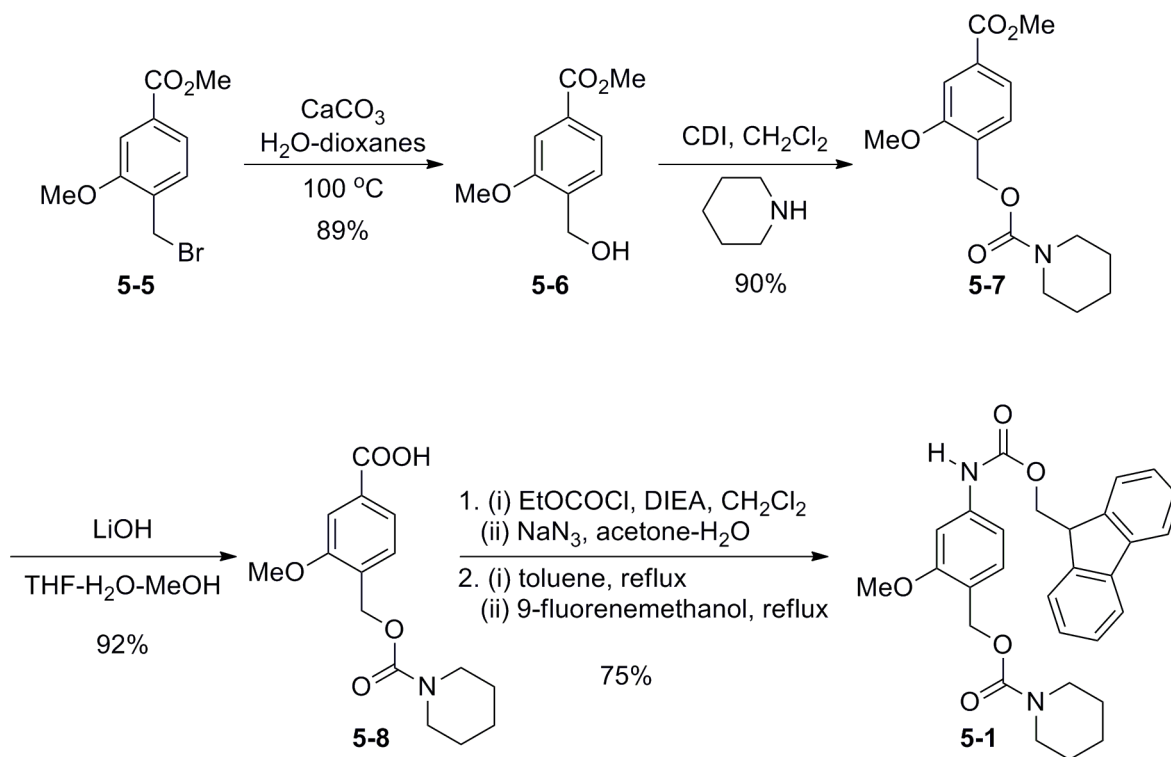
For water soluble thiols (L-cysteine, N-acetyl-L-cysteine, 2-mercaptoethanol, tiopronin, penicillamine): A thiol solution (200 μ L, 1.2 mM in 0.1 M HEPES buffer, pH 7.4, 1 mM EDTA) was added to a solution of the amplification reagent **4-11** (200 μ L, 4 mM in CH₃CN). The mixture was agitated using a vortex mixer for 2 s. For water insoluble thiols (thiophenol, 4-methoxythiophenol, 4-nitrothiophenol, 3-mercaptohexanol, 2-methyl-2-propanethiol): A thiol solution (100 μ L, 2.4 mM in CH₃CN) was added to a mixture of the amplification reagent **4-11** (100 μ L, 8 mM in CH₃CN) and 0.1 M HEPES buffer (200 μ L, pH 7.4, 1 mM EDTA). The resulting mixture was agitated using a vortex mixer for 2 s. At regular intervals, an aliquot (20 μ L) of the assay mixture was diluted with 1:1 CH₃CN-0.1 M HEPES buffer, pH 7.4, 1 mM EDTA (2 mL). The fluorescence emission intensity of the resulting mixture was obtained ($\lambda_{\text{ex}} = 325$ nm, $\lambda_{\text{em}} = 430$ nm). The fluorescent intensity was recorded as % of maximum fluorescence intensity obtained for the assay. The fluorescence intensity data were fitted with regression curves using regression function of SigmaPlot. For ease of analysis, the general equation of the regression curves were $y = a \times (1 - e^{-bt}) + c \times (1 - e^{-dt})$ (for the thiols L-cysteine, N-acetyl-L-cysteine, 2-mercaptoethanol, tiopronin, thiophenol, 4-methoxythiophenol, 4-nitrothiophenol, 3-

mercaptohexanol.), and $y = a \times (1 - e^{-bt})^c$ (for 2-methyl-2-propanethiol, and penicillamine); where y = “% of maximum signal”, t = time, and a – d were parameters calculated by SigmaPlot. The time for the signal to reach 50% of maximum ($= T_{50}$) was determined using the regression curves (i.e., $y = 50\%$ when $t = T_{50}$).

6.5 Chapter 5: Experimental procedures and characterizations⁸

Synthetic procedure

Synthesis of amplification reagent 5-1



2-Methoxy-4-(hydroxymethyl)-3-methoxybenzoate (5-6).

A suspension of methyl-(4-bromomethyl)-3-methoxybenzoate **5-5** (5.5 g, 21 mmol, 1 equiv) and CaCO_3 (110 mg, 0.42 mmol, 4.4 equiv) in 1:1 1,6-dioxane- H_2O (200 mL) was stirred at 100°C for 2 h. The reaction mixture was cooled to 20°C and neutralized to a pH 7 using 1 M HCl and the resulting mixture was extracted with CH_2Cl_2 (4×50 mL). The combined CH_2Cl_2 layers were

washed with brine (100 ml) and dried over anhydrous MgSO_4 . The MgSO_4 was filtered and the filtrate was concentrated under reduced pressure. The residue was purified by flash column chromatography (elution with 30% EtOAc/hexanes) to obtain 2-Methoxy-4-(hydroxymethyl)-3-methoxybenzoate **5-6** (3.7 g, 19 mmol, 89%) as a white solid. $^1\text{H-NMR}$ (400 MHz, CDCl_3): δ 7.58 (1H, d, $J = 7.6$), 7.38 (1H, s), 7.34 (1H, d, $J = 7.6$), 4.67 (2H, s), 3.89 (3H, s), 3.83 (3H, s), 3.4 (1H, s); $^{13}\text{C-NMR}$ (100 MHz, CDCl_3): δ 52.4, 55.2, 60.4, 110.4, 122.0, 127.3, 130.0, 134.6, 156.5, 167.0. The NMR data matches with literature values.⁹

2-Methoxy-4-(methoxycarbonyl)benzyl piperidine-1-carboxylate (**5-7**).

2-Methoxy-4-(hydroxymethyl)-3-methoxybenzoate **5-6** (3.7 g, 19 mmol, 1 equiv) was dissolved in dry CH_2Cl_2 (100 mL) and the solution was cooled to 0 °C. Carbonyldiimidazole (3.75 g, 23.1 mmol, 1.2 equiv) was added slowly to the stirring solution, and, after 5 min at 0 °C, the reaction mixture was warmed to room temperature. The reaction mixture was stirred at room temperature for 45 min, after which piperidine (2.3 mL, 23 mmol, 1.2 equiv) was added. The solution was stirred at room temperature for 3 h, and then was diluted with CH_2Cl_2 (100 mL). The resulting solution was washed with aqueous hydrochloric acid (0.01 M, 100 mL). The aqueous layer was separated and was successively extracted using CH_2Cl_2 (2×100 mL). The combined organic layers were washed with water (1×100 mL), brine (2×100 mL), and dried over anhydrous Na_2SO_4 . The Na_2SO_4 was removed by filtration and the resulting solution was concentrated under reduced pressure. The resulting white solid was purified using column chromatography (elution with 30% EtOAc/hexanes) to obtain 2-methoxy-4-(methoxycarbonyl)benzyl piperidine-1-carboxylate **5-7** (5.19 g, 16.9 mmol, 90%). IR (cm^{-1}) 2936, 2854, 1695; $^1\text{H-NMR}$ (400 MHz, CDCl_3): δ 7.64 (1H, d, $J = 7.8$), 7.52 (1H, s), 7.36 (1H, d, $J = 7.8$), 5.21 (2H, s), 3.91 (3H, s), 3.89 (3H, s), 3.48–3.46 (4H, m), 1.60–1.54 (6H, m); $^{13}\text{C-NMR}$ (100 MHz, CDCl_3): δ 24.4, 25.7, 44.9, 52.2, 55.6, 61.9, 110.9, 121.9, 127.7, 130.6, 131.0, 155.2, 156.7, 166.9; MS (TOF MS ES+, m/z): 330.3 (11, $\text{M} + \text{Na}^+$), 179.0 (100, $\text{M} - \text{C}_6\text{H}_{11}\text{O}_2\text{N}$); HRMS (TOF MS ES+, m/z) Calculated for $\text{C}_{16}\text{H}_{22}\text{NO}_5$ ($\text{M} + \text{H}^+$): 308.1498; Found: 308.1494.

3-Methoxy-4-[[piperidin-1-ylcarbonyl]oxy]methyl}benzoic acid (5-8).

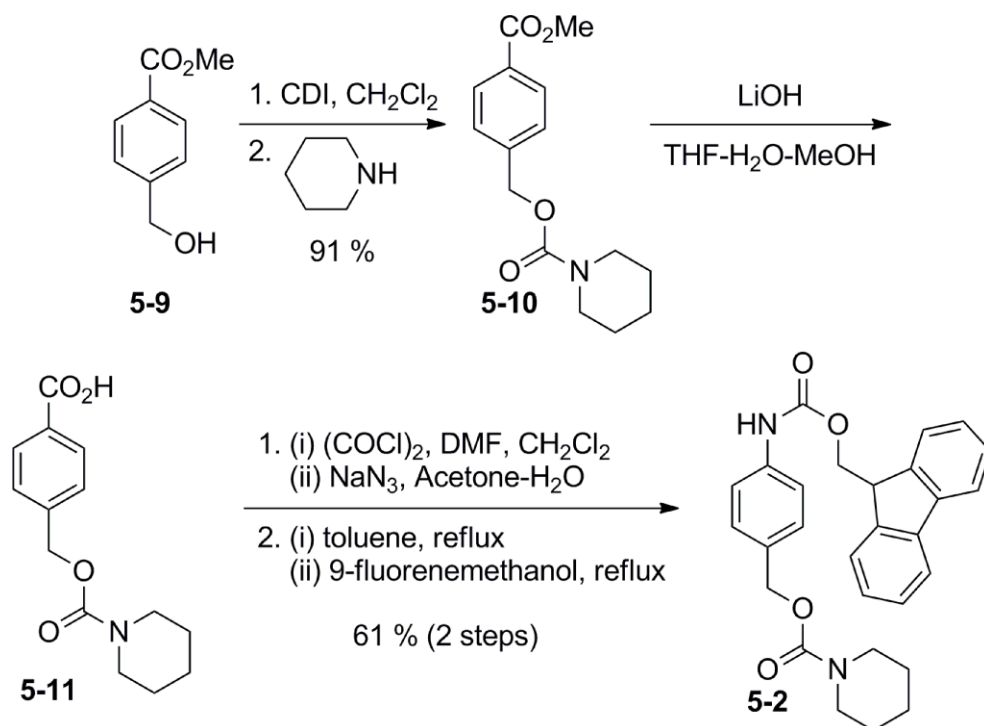
2-Methoxy-4-(methoxycarbonyl)benzyl piperidine-1-carboxylate **5-7** (4.42 g, 14.4 mmol, 1 equiv) was dissolved in 68 mL of THF and 27 mL of methanol. Lithium hydroxide monohydrate (0.84 g, 20 mmol, 1.4 equiv) dissolved in 27 mL of water was added to the THF–MeOH solution. The resulting solution was stirred for 10 h at room temperature. The solution was acidified by slow addition of aqueous hydrochloric acid (1 M, 25 mL), and was extracted using EtOAc (5 × 100 mL). The combined organic layers were washed with brine (1 × 100 mL) and dried over anhydrous Na₂SO₄. The Na₂SO₄ was removed by filtration and the resulting solution was concentrated under reduced pressure to obtain 3-methoxy-4-[[piperidin-1-ylcarbonyl]oxy]methyl}benzoic acid **5-8** (3.88 g, 13.2 mmol, 92%). IR (cm⁻¹) 2937, 2859, 2822, 2668, 1684; ¹H-NMR (400 MHz, CDCl₃): δ 12.24 (1H, br s), 7.73 (1H, d, *J* = 7.8), 7.58 (1H, s), 7.41 (1H, d, *J* = 7.8), 5.25 (2H, s), 3.90 (3H, s), 3.51–3.49 (4H, m), 1.59–1.57 (6H, m); ¹³C-NMR (100 MHz, CDCl₃): δ 24.3, 25.7, 45.0, 55.5, 62.1, 111.2, 122.6, 127.7, 130.0, 131.6, 155.4, 156.7, 171.1; MS (TOF MS ES⁻, *m/z*): 292.2 (100, *M* – H⁺); HRMS (TOF MS ES⁻, *m/z*) Calculated for C₁₅H₁₈NO₅ (*M* – H⁺): 292.1185; Found: 292.1201.

4-(((9H-fluoren-9-yl)methoxy)carbonylamino)-2-methoxybenzyl piperidine-1-carboxylate (5-1).

3-Methoxy-4-[[piperidin-1-ylcarbonyl]oxy]methyl}benzoic acid **5-8** (3.6 g, 12 mmol, 1 equiv) dissolved in 100 mL of dry CH₂Cl₂ was cooled to 0 °C with stirring. DIEA (4.8 mL, 27 mmol, 2.2 equiv) was added to this cooled solution, followed by drop-wise addition of ethyl chloroformate (2.6 mL, 27 mmol, 2.2 equiv). The reaction mixture was stirred at 0 °C for 1 h, after which the solution was warmed to room temperature and concentrated under reduced pressure. The residue was dissolved in acetone (50 mL), and the resulting solution was cooled to 0 °C. A solution of sodium azide (4.0 g, 62 mmol, 5.0 equiv) in cold water (50 mL) (~10 °C) was added drop-wise to the acetone solution. The resulting suspension was stirred vigorously at 0 °C for 1 h. The solution was diluted with EtOAc (100 mL) and the aqueous layer was separated. The aqueous layer was extracted using EtOAc (3 × 100 mL), and the organic layers were combined. These organic extracts were washed with brine (1 × 50 mL) and dried over anhydrous Na₂SO₄. The Na₂SO₄ was removed by filtration, and the resulting solution was concentrated under

reduced pressure to provide a yellow gelatinous residue. The residue was dissolved in dry toluene (50 mL) and the resulting solution was heated to 100 °C for 1 h. The hot solution was cooled to room temperature, after which 9-fluorenemethanol (870 mg, 14.9 mmol, 1.2 equiv) was added. The solution was heated to reflux (112 °C) for 10 h, after which the solution was cooled to room temperature and the solvent was removed under reduced pressure with gentle heating (40 °C). The residue was purified by column chromatography (gradient elution with 20–30% EtOAc/hexanes) to obtain 4-(((9H-fluoren-9-yl)methoxy)carbonylamino)-2-methoxybenzyl piperidine-1-carboxylate **5-1** (4.7 g, 9.7 mmol, 78%). IR (cm⁻¹) 2856, 2838, 1725, 1673, 1615; ¹HNMR (400 MHz, CDCl₃): δ 7.76 (2H, d, *J* = 7.4), 7.60 (2H, d, *J* = 7.4), 7.39 (2H, t, *J* = 7.4), 7.30 (2H, t, *J* = 7.4), 7.24 (1H, s), 7.21 (1H, d, *J* = 8.0), 7.07 (1H, s), 6.77 (1H, d, *J* = 8.0), 5.12 (1H, s), 4.50 (2H, d, *J* = 6.8), 4.25 (1H, t, *J* = 6.8), 3.78 (3H, s), 3.42 (4H, m), 1.55 (2H, m), 1.50 (4H, m); ¹³C-NMR (100 MHz, CDCl₃): δ 24.5, 25.8, 44.9, 47.2, 55.5, 62.2, 66.9, 101.7, 110.2, 120.1, 120.4, 125.1, 127.2, 127.9, 129.9, 139.1, 141.4, 143.8, 153.5, 155.7, 158.1; MS (TOF MS ES⁺, *m/z*): 509.1 (2, *M* + Na⁺), 358.1 (100, *M* – C₆H₁₁O₂N); HRMS (TOF MS ES⁺, *m/z*) Calculated for C₂₉H₃₄N₃O₅ (*M* + NH₄⁺): 504.2498; Found: 504.2509.

Synthesis of amplification reagent 5-2 (performed by Kyle Schmid)



4-(methoxycarbonyl)benzyl piperidine-1-carboxylate (**5-10**).

Methyl 4-(hydroxymethyl)benzoate **5-9** (0.66 g, 4 mmol, 1 equiv) was dissolved in dry CH₂Cl₂ (20 mL) and the solution was cooled to 0 °C. Carbonyldiimidazole (0.78 g, 4.8 mmol, 1.2 equiv) was added slowly to the stirring solution, and, after 5 min at 0 °C, the reaction mixture was warmed to room temperature. The reaction mixture was stirred at room temperature for 45 min, after which piperidine (0.47 mL, 4.8 mmol, 1.2 equiv) was added. The solution was stirred at room temperature for 12 h, and then was diluted with CH₂Cl₂ (20 mL). The resulting solution was washed with aqueous hydrochloric acid (0.01 M, 20 mL). The aqueous layer was separated and was successively extracted using CH₂Cl₂ (2 × 20 mL). The combined organic layers were washed with water (1 × 20 mL), brine (2 × 20 mL), and dried over anhydrous sodium sulfate. The sodium sulfate was removed by filtration and the resulting solution was concentrated under reduced pressure. The resulting white solid was purified using column chromatography (elution with 30% EtOAc/hexanes) to obtain 4-(methoxycarbonyl)benzyl piperidine-1-carboxylate **5-10** (1.0 g, 3.6 mmol, 91%). IR (cm⁻¹) 2940, 2856, 1723, 1701; ¹H-NMR (300 MHz, CDCl₃): δ 8.00 (2H, d, *J* = 8.2), 7.37 (2H, d, *J* = 8.2), 5.14 (2H, s), 3.87 (3H, s), 3.44–3.40 (4H, m), 1.56–1.50 (6H, m); ¹³C-NMR (100 MHz, CDCl₃): δ 24.2, 25.6, 44.8, 52.0, 66.0, 127.2, 129.5, 129.7, 142.2, 154.9, 166.7; MS (TOF MS ES+, *m/z*): 278.1 (15, *M* + H⁺), 149.0 (100, *M* – C₆H₁₁O₂N); HRMS (TOF MS ES+, *m/z*) Calculated for C₁₅H₂₀NO₄ (*M* + H⁺): 278.1392; Found: 278.1391.

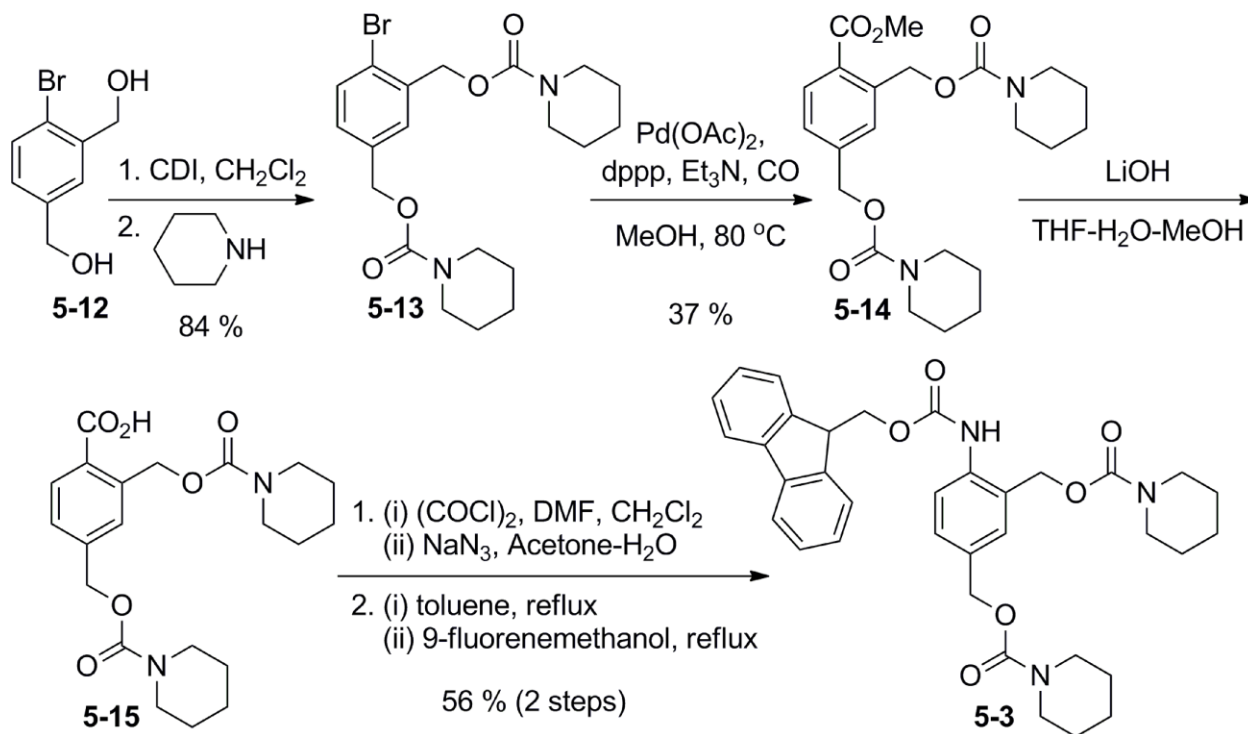
4-[(piperidin-1-ylcarbonyl)oxy]methyl}benzoic acid (**5-11**).

4-(methoxycarbonyl)benzyl piperidine-1-carboxylate **5-10** (0.95 g, 3.4 mmol, 1 equiv) was dissolved in 18 mL of THF and 6 mL of methanol. Lithium hydroxide monohydrate (0.20 g, 4.8 mmol, 1.4 equiv) dissolved in 6 mL of water was added to the THF–MeOH solution. The resulting solution was stirred for 10 h at room temperature. The solution was acidified to a pH of 2 by slow addition of aqueous hydrochloric acid (1 M), and was extracted using EtOAc (5 × 25 mL). The combined organic layers were washed with brine (1 × 50 mL) and dried over anhydrous sodium sulfate. The sodium sulfate was removed by filtration and the resulting solution was concentrated under reduced pressure to obtain 4-[(piperidin-1-ylcarbonyl)oxy]methyl}benzoic acid **5-11**, which was used without further purification.

4-(((9H-fluoren-9-yl)methoxy)carbonylamino)benzyl piperidine-1-carboxylate (**5-2**)

4-[[[(piperidin-1-ylcarbonyl)oxy]methyl]benzoic acid **5-11** (0.97 g, 3.7 mmol, 1 equiv) dissolved in 25 mL of dry CH₂Cl₂ and 1 mL of DMF was cooled to 0 °C with stirring. Oxalyl chloride (0.39 mL, 4.4 mmol, 1.2 equiv) was added to this cooled solution and the reaction mixture was stirred at 0 °C for 1 h, after which the solution was warmed to room temperature and concentrated under reduced pressure. The residue was dissolved in acetone (15 mL), and the resulting solution was cooled to 0 °C. A solution of sodium azide (0.72 g, 11.1 mmol, 3 equiv) in cold water (15 mL) (~10 °C) was added drop-wise to the acetone solution. The resulting suspension was stirred vigorously at 0 °C for 1 h. The solution was diluted with EtOAc (50 mL) and the aqueous layer was separated. The aqueous layer was extracted using EtOAc (3 × 30 mL), and the organic layers were combined. These organic extracts were washed with brine (1 × 50 mL) and dried over anhydrous sodium sulfate. The sodium sulfate was removed by filtration, and the resulting solution was concentrated under reduced pressure to provide a yellow gelatinous residue. The residue was dissolved in dry toluene (15 mL) and the resulting solution was heated to 100 °C for 1 h. The hot solution was cooled to room temperature, after which 9-fluorenemethanol (870 mg, 4.4 mmol, 1.3 equiv) was added. The solution was heated to reflux (112 °C) for 10 h, after which the solution was cooled to room temperature and the solvent was removed under reduced pressure. The residue was purified by column chromatography (gradient elution with 20–30% EtOAc/hexanes, then pure THF as eluent) to obtain 4-(((9H-fluoren-9-yl)methoxy)carbonylamino)benzyl piperidine-1-carboxylate **5-2** (1.03 g, 92.2 mmol, 61%). IR (cm⁻¹) 3292, 2937, 2855, 1732, 1676; ¹H-NMR (360 MHz, CDCl₃): 7.77 (2H, d, J = 7.5), 7.61 (2H, d, J = 7.5), 7.42–7.27 (8H, m), 6.72 (1H, s), 5.04 (1H, s), 4.54 (2H, d, J = 6.6), 4.27 (1H, t, J = 6.6), 3.42 (4H, m), 1.55 (6H, m); ¹³C-NMR (100 MHz, CDCl₃): δ 24.3, 25.7, 44.8, 47.1, 66.5, 66.8, 118.6, 120.0, 124.9, 127.1, 127.8, 128.9, 137.4, 141.3, 143.7, 155.3; MS (TOF MS ES+, m/z): 474.2 (40, M + NH₄⁺), 328.1 (100, M – C₆H₁₁O₂N); HRMS (TOF MS ES+, m/z) Calculated for C₂₈H₃₂N₃O₅ (M + NH₄⁺): 474.2393; Found: 474.2386.

Synthesis of amplification reagent 5-3



(4-bromo-1,3-phenylene)bis(methylene) dipiperidine-1-carboxylate (5-13).

(4-bromo-1,3-phenylene)dimethanol¹⁰ **5-12** (1.66 g, 7.7 mmol, 1 equiv) was dissolved in dry THF (40 mL) and the solution was cooled to 0 °C. Carbonyldiimidazole (3.24 g, 20 mmol, 2.6 equiv) was added slowly to the stirring solution, and, after 15 min at 0 °C, the reaction mixture was warmed to room temperature. The reaction mixture was stirred at room temperature for 3 hours, after which piperidine (4.56 mL, 46 mmol, 6.0 equiv) was added. The solution was stirred at room temperature for 14 h, and then was diluted with EtOAc (40 mL). The resulting solution was successively washed with aqueous NH₄Cl (40 mL), aqueous hydrochloric acid (0.1 M, 2 × 20 mL) and brine. The combined organic layer was dried over anhydrous Na₂SO₄. The Na₂SO₄ was removed by filtration and the resulting solution was concentrated under reduced pressure. The resulting white solid was purified using column chromatography (gradient elution with 20 – 60% EtOAc/hexanes) to obtain (4-bromo-1,3-phenylene)bis(methylene) dipiperidine-1-carboxylate **5-13** (2.85 g, 6.5 mmol, 84 %). IR (cm⁻¹) 2936, 2855, 1699; ¹H-NMR (400 MHz, CDCl₃): δ 7.53 (1H, d, *J* = 8.1), 7.38 (1H, s), 7.17 (1H, d, *J* = 8.1), 5.19 (2H, s), 5.08 (2H, s),

3.47–3.42 (8H, m), 1.59–1.54 (12H, m); ^{13}C -NMR (100 MHz, CDCl_3): δ 24.2, 24.2, 25.5, 44.7, 44.8, 65.9, 66.1, 122.2, 128.5, 132.6, 136.3, 136.5, 154.7, 154.8; MS (TOF MS ES+, m/z): 439.1 (100, $\text{M} + \text{H}^+$); HRMS (TOF MS ES+, m/z) Calculated for $\text{C}_{20}\text{H}_{28}\text{N}_2\text{O}_4\text{Br}$ ($\text{M} + \text{H}^+$): 439.1232; Found: 439.1232.

(4-(methoxycarbonyl)-1,3-phenylene)bis(methylene) dipiperidine-1-carboxylate (5-14).

An oven-dried 100-mL flask equipped with a stir bar was charged with (4-bromo-1,3-phenylene)bis(methylene)dipiperidine-1-carboxylate **5-13** (0.94 g, 2.1 mmol, 1equiv), $\text{Pd}(\text{OAc})_2$ (38 mg, 0.17 mmol, 0.08 equiv), dppp (141 mg, 0.34 mmol, 0.16 equiv), triethylamine (0.45 mL, 3.2 mmol, 1.5 equiv), and methanol (4.5 mL). The resulting brown solution was stirred at room temperature and CO gas was bubbled through it for 10 minutes. The reaction mixture was then stirred at 80 °C under an atmosphere of CO for 72 hours. The reaction mixture was cooled to room temperature and diluted with CH_2Cl_2 . The reaction mixture was filtered through a bed of celite and the filtrate was concentrated under reduced pressure. The residue obtained was purified using column chromatography (gradient elution with 20 – 40% EtOAc/hexanes) to obtain (4-(methoxycarbonyl)-1,3-phenylene)bis(methylene) dipiperidine-1-carboxylate **5-14** (325 mg, 0.78 mmol, 37 %). IR (cm^{-1}) 2937, 2855, 1700, 1684; ^1H -NMR (400 MHz, CDCl_3): δ 7.95 (1H, d, $J = 8$), 7.38 (1H, s), 7.34 (1H, d, $J = 8$), 5.52 (2H, s), 5.17 (2H, s), 3.89 (3H, s), 3.46 (8H, m), 1.59–1.55 (12H, m); ^{13}C -NMR (100 MHz, CDCl_3): δ 24.4, 24.5, 25.7, 30.2, 45.0, 52.3, 65.3, 66.3, 105.7, 126.3, 126.7, 128.1, 131.2, 139.4, 141.6, 155.2, 167.3; MS (TOF MS ES+, m/z): 419.2 (90, $\text{M} + \text{H}^+$), 290.1 (100, $\text{M} - \text{C}_6\text{H}_{11}\text{O}_2\text{N}$); HRMS (TOF MS ES+, m/z) Calculated for $\text{C}_{22}\text{H}_{31}\text{N}_2\text{O}_6$ ($\text{M} + \text{H}^+$): 419.2182; Found: 419.2178.

2,4-bis((piperidine-1-carboxyloxy)methyl)benzoic acid (5-15)

(4-(methoxycarbonyl)-1,3-phenylene)bis(methylene) dipiperidine-1-carboxylate **5-14** (60 mg, 0.14 mmol, 1 equiv) was dissolved in 0.5 mL of THF and 0.5 mL of methanol. Lithium hydroxide monohydrate (6.5 mg, 0.15 mmol, 1.1 equiv) dissolved in 0.2 mL of water was added to the THF–MeOH solution. The resulting solution was stirred for 12 h at room temperature. An additional amount of lithium hydroxide monohydrate (6.6 mg, 0.16 mmol, 1.1 equiv) dissolved in 0.4 mL of water was added to the reaction mixture and the reaction mixture was stirred at room temperature for another 10 hours. The solution was then acidified to a pH of 2 by slow

addition of aqueous hydrochloric acid (0.3 mL, 1 M), and was extracted using EtOAc (5 × 5 mL). The combined organic layers were washed with brine (2 × 5 mL) and dried over anhydrous sodium sulfate. The sodium sulfate was removed by filtration and the resulting solution was concentrated under reduced pressure to obtain 2,4-bis((piperidine-1-carboxyloxy)methyl)benzoic acid **5-15**, which was used without further purification.

(4-(((9H-fluoren-9-yl)methoxy)carbonylamino)-1,3-phenylene)bis(methylene) dipiperidine-1-carboxylate (5-3).

2,4-bis((piperidine-1-carboxyloxy)methyl)benzoic acid **5-15** (56 mg, 0.14 mmol, 1 equiv), dissolved in 1 mL of dry CH₂Cl₂ and 10 µL DMF, was cooled to 0 °C with stirring. Oxalyl chloride (36 µL, 0.43 mmol, 3.0 equiv) was added to this cooled solution and the reaction mixture was stirred at 0 °C for 1 h, after which the solution was warmed to room temperature and concentrated under reduced pressure. The residue was dissolved in acetone (0.5 mL), and the resulting solution was cooled to 0 °C. A solution of sodium azide (46 mg, 0.72 mmol, 5 equiv) in cold water (0.5 mL) (~10 °C) was added drop-wise to the acetone solution. The resulting suspension was stirred vigorously at 0 °C for 1 h. The solution was diluted with EtOAc (8 mL) and the aqueous layer was separated. The aqueous layer was extracted using EtOAc (3 × 5 mL), and the organic layers were combined. These organic extracts were washed with brine (2 × 5 mL) and dried over anhydrous Na₂SO₄. The Na₂SO₄ was removed by filtration, and the resulting solution was concentrated under reduced pressure to provide a yellow gelatinous residue. The residue was dissolved in dry toluene (1 mL) and the resulting solution was heated to 100 °C for 1 h. The hot solution was cooled to room temperature, after which 9-fluorenemethanol (28 mg, 0.14 mmol, 1 equiv) was added. The solution was heated to reflux (112 °C) for 5 h, after which the solution was cooled to room temperature and the solvent was removed under reduced pressure. The residue was purified by column chromatography (gradient elution with 20–30% EtOAc/hexanes) to obtain (4-(((9H-fluoren-9-yl)methoxy)carbonylamino)-1,3-phenylene)bis(methylene) dipiperidine-1-carboxylate **5-3** (47 mg, 0.08 mmol, 56 %). IR (cm⁻¹) 3256, 2937, 2855, 1734, 1697, 1672, 1605; ¹H-NMR (360 MHz, CDCl₃): 7.77 (2H, d, *J* = 7.5), 7.61 (2H, d, *J* = 7.5), 7.42–7.27 (8H, m), 6.72 (1H, s), 5.04 (1H, s), 4.54 (2H, d, *J* = 6.6), 4.27 (1H, t, *J* = 6.6), 3.42 (4H, m), 1.55 (6H, m); ¹³C-NMR (100 MHz, CDCl₃): δ 24.3, 25.7, 44.8, 47.1, 66.5, 66.8, 118.6, 120.0, 124.9, 127.1, 127.8, 128.9, 137.4, 141.3, 143.7, 155.3; MS (TOF

MS ES⁺, m/z): 615.3 (100, M + Na⁺); HRMS (TOF MS ES⁺, m/z) Calculated for C₃₅H₄₃N₄O₆ (M + NH₄⁺): 615.3183; Found: 615.3179.

4-(Allyloxycarbonylamino)-2-methoxybenzyl piperidine-1-carboxylate (5-4).

3-Methoxy-4-[[[(piperidin-1-ylcarbonyl)oxy]methyl]benzoic acid **5-8** (4.75 g, 16.2 mmol, 1 equiv) was dissolved in 150 mL of dry CH₂Cl₂ and cooled to 0 °C. DIEA (6.2 mL, 36 mmol, 2.2 equiv) was added to the solution followed by drop-wise addition of ethyl chloroformate (3.4 mL, 36 mmol, 2.2 equiv). The solution was stirred at 0 °C for 1 h, after which the reaction mixture was warmed to room temperature and all solvents were removed under reduced pressure. The resulting residue was dissolved in acetone (70 mL) and the solution was cooled to 0 °C. A solution of sodium azide (5.3 g, 81 mmol, 5 equiv) in cold water (70 mL) (~10 °C) was added drop-wise to the acetone solution. The resulting suspension was stirred vigorously at 0 °C for 2 h, after which the solution was diluted with EtOAc (200 mL) and the aqueous layer was separated. The aqueous layer was extracted using EtOAc (2 × 100 mL), and the combined organic extracts were washed with brine (2 × 100 mL) and dried over anhydrous Na₂SO₄. The Na₂SO₄ was removed by filtration, and the resulting solution was concentrated under reduced pressure to obtain a yellow gelatinous residue. The residue was dissolved in dry toluene (100 mL) and the resulting solution was heated to 110 °C for 1 h. The reaction mixture was cooled to room temperature, allyl alcohol (3.3 mL, 49 mmol, 3 equiv) was added, and the solution was heated to reflux (112 °C) for 12 h. The solution was cooled to room temperature and the solvent was removed under reduced pressure with gentle heating (40 °C). The residue was purified by column chromatography (gradient elution with 30–40% EtOAc/hexanes) to obtain 4-(allyloxycarbonylamino)-2-methoxybenzyl piperidine-1-carboxylate **5-4** (3.67 g, 10.5 mmol, 65%). IR (cm⁻¹) 3260, 3204, 3074, 2933, 2850, 1726, 1668, 1610; ¹H-NMR (400 MHz, CDCl₃): δ 7.43 (1H, s), 7.28 (1H, s), 7.21 (1H, d, J = 8.1), 6.82 (1H, d, J = 8.1), 5.94 (1H, m), 5.34 (1H, d, J = 17.2), 5.26 (1H, d, J = 15.7), 5.12 (2H, s), 4.65 (2H, d, J = 5.5), 3.79 (3H, s), 3.43 (4H, m), 1.57–1.55 (2H, m), 1.51 (4H, m); ¹³C-NMR (100 MHz, CDCl₃): δ 24.4, 25.7, 44.9, 55.4, 62.2, 65.7, 101.6, 110.1, 118.1, 120.0, 129.8, 132.5, 139.4, 153.4, 155.7, 158.0; MS (TOF MS ES⁺, m/z): 371.1 (4, M + Na⁺), 220.1 (100, M – C₆H₁₁O₂N); HRMS (TOF MS ES⁺, m/z) Calculated for C₁₈H₂₄N₂O₅Na (M + Na⁺): 371.1583; Found: 371.1576.

Experimental procedures to test the response of 5-1 to piperidine

Experimental procedure corresponding to Figure 5-4

A piperidine solution in water (7 μ L, 40 mM, 0.02 equiv) was added to a solution of **5-1** in DMSO (350 μ L, 40 mM) containing 61 mM anisole as the internal standard. At regular intervals, an aliquot (10 μ L) of the reaction mixture was diluted with acetonitrile (500 μ L) and the resulting solution was injected into an analytical reversed-phase HPLC coupled to a mass spectrometer. The LC-MS data were obtained on an Agilent Technologies 1200 series analytical reversed-phase HPLC coupled to an Agilent Technologies 6120 quadrupole mass spectrometer.

Experimental procedures to test the response of amplification reagent 5-1, 5-2, or 5-3 to piperidine

Experimental procedure corresponding to Figure 5-5 and 5-8

A piperidine solution in water (2 μ L, 2 M–2 mM, 1–0.001 equivalents relative to amplification reagent **5-1**, **5-2** or **5-3**) was added to a solution of the amplification reagent (**5-1**, **5-2** or **5-3**) in 9:1 DMSO–THF (100 μ L, 40 mM). At regular intervals, an aliquot (1 μ L) of the reaction mixture was diluted with THF (600 μ L) and the absorbance of the sample was measured at 305 nm. The absorbance values were normalized using the formula $A_{\text{normal}} = (A - A_0)/(A_{\text{max}} - A_0)$ where A_{normal} = normalized absorbance, A = absorbance at time t , A_0 = absorbance for a negative control, A_{max} = maximum absorbance obtained for a particular assay.

Experimental procedure corresponding to Figure 5-6

A stock dye solution (A) was prepared by dissolving bromocresol green (2 mg, 2.86 μ mol) and aqueous sodium hydroxide (2 μ L, 1 M) in isopropanol and by adjusting the volume of the solution to 100 mL using isopropanol. A piperidine solution in water (4 μ L, 20 mM) was added to a solution of **5-1** in DMSO (200 μ L, 40 mM). At regular intervals, an aliquot (1 μ L) of the reaction mixture was added to a 1 mL aliquot of solution A and the absorbance at 625 nm was measured after an incubation time of 20 minutes. The progress of the reaction also was monitored using the method described for Figure 5-5. Briefly, an aliquot (1 μ L) of the reaction mixture was diluted with THF (600 μ L) and the absorbance was measured at 305 nm.

Experimental procedure for control experiments to demonstrate that aniline is not sufficiently basic to deprotonate bromocresol green.

A stock dye solution (A) was prepared by dissolving bromocresol green (2 mg, 2.86 μmol) and aqueous sodium hydroxide (2 μL , 1 M) in isopropanol and by adjusting the volume of the solution to 100 mL using isopropanol. A solution of each of the amine in 50:1 DMSO- H_2O (1 μL , 40 mM) was added to a 1-mL aliquot of solution A and the absorbance at 625 nm was measured.

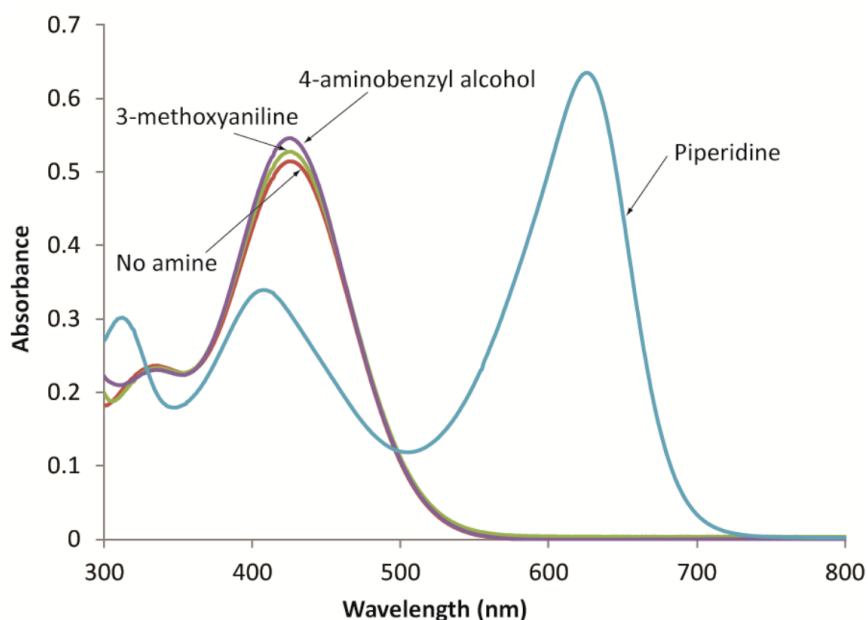


Figure 6-1. UV-Vis spectra of bromocresol green (1 mL, 28.6 μM , isopropanol) after addition of a solution of selected amines (1 μL , 50:1 DMSO- H_2O).⁸

Experimental procedure for the assay to detect palladium using reagents 5-1 and 5-4

A stock solution (Solution A) was prepared containing detection reagent **5-4** in THF (0.2 M) and phenylsilane (438 mM). Tri-*n*-butylphosphine (10 μL) was added to a solution of $\text{Pd}(\text{OAc})_2$ (1 mL, 0–32 ppm of Pd(II) in THF) and the resulting solution was mixed using a vortex mixer. After 5 minutes, an aliquot (100 μL) of this palladium solution was added to Solution A (100 μL) and the reaction mixture was agitated using a vortex mixture for 2 s. The solution was left undisturbed for 1 h. The reaction mixture was then diluted with water (40 μL). An aliquot (50

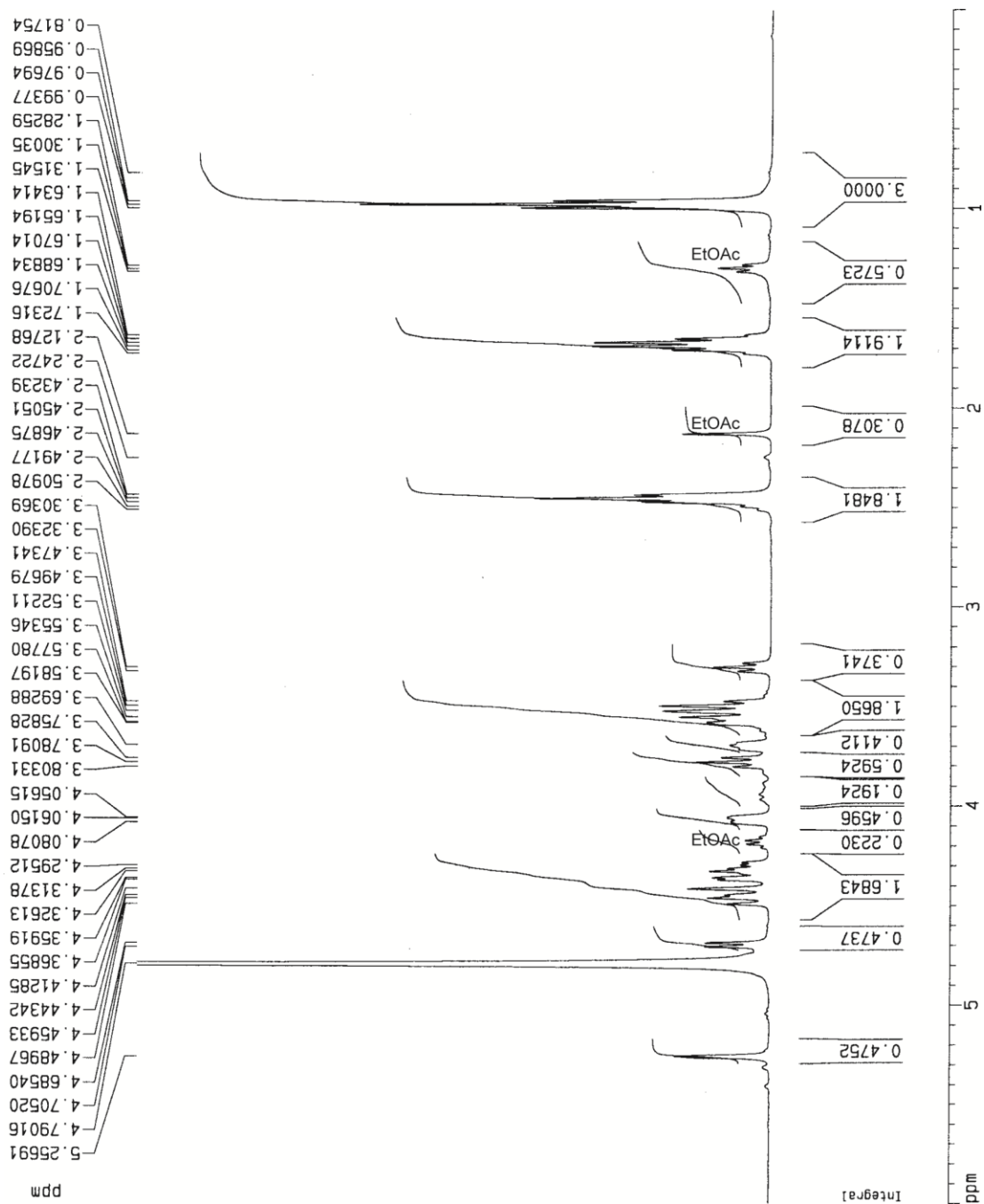
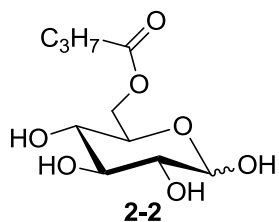
μL) of this solution was combined with a solution of amplification reagent **5-1** in DMSO (56.8 μM, 360 μL). The amplification reaction was allowed to proceed for 16 h. An aliquot (1 μL) of the reaction mixture was diluted with THF (600 μL) and the absorbance of the solution was measured at 305 nm using THF as the blank sample. The absorbance data obtained were normalized using the formula $A_{\text{normal}} = (A - A_0)/(A_{\text{max}} - A_0)$ where A_{normal} = normalized absorbance, A = absorbance measurements obtained for a reaction, A_0 = absorbance values for a negative control containing no added Pd(II), and A_{max} = maximum absorbance obtained.

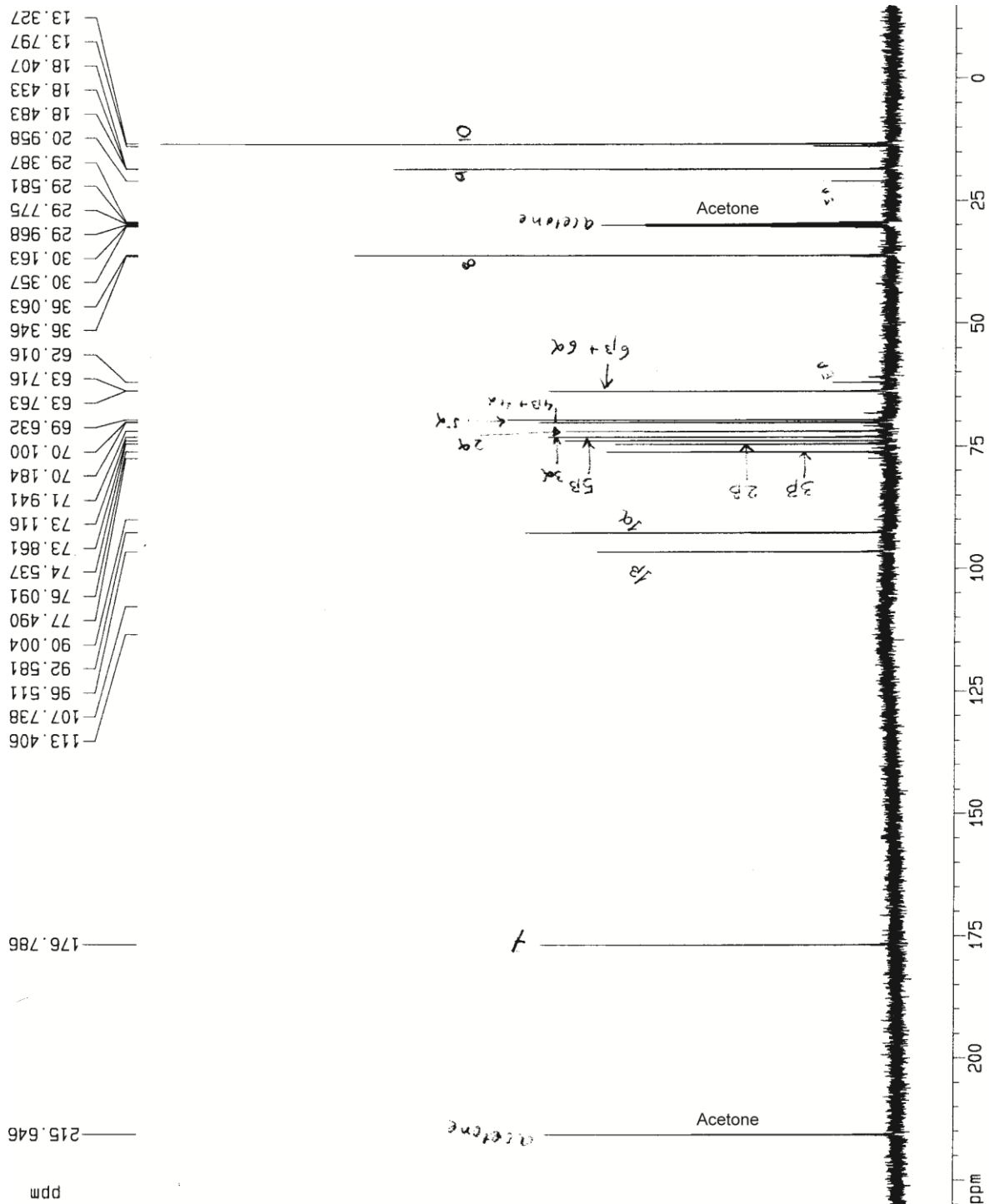
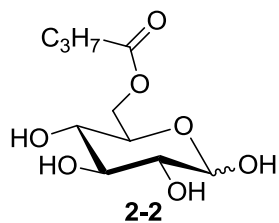
6.6 References

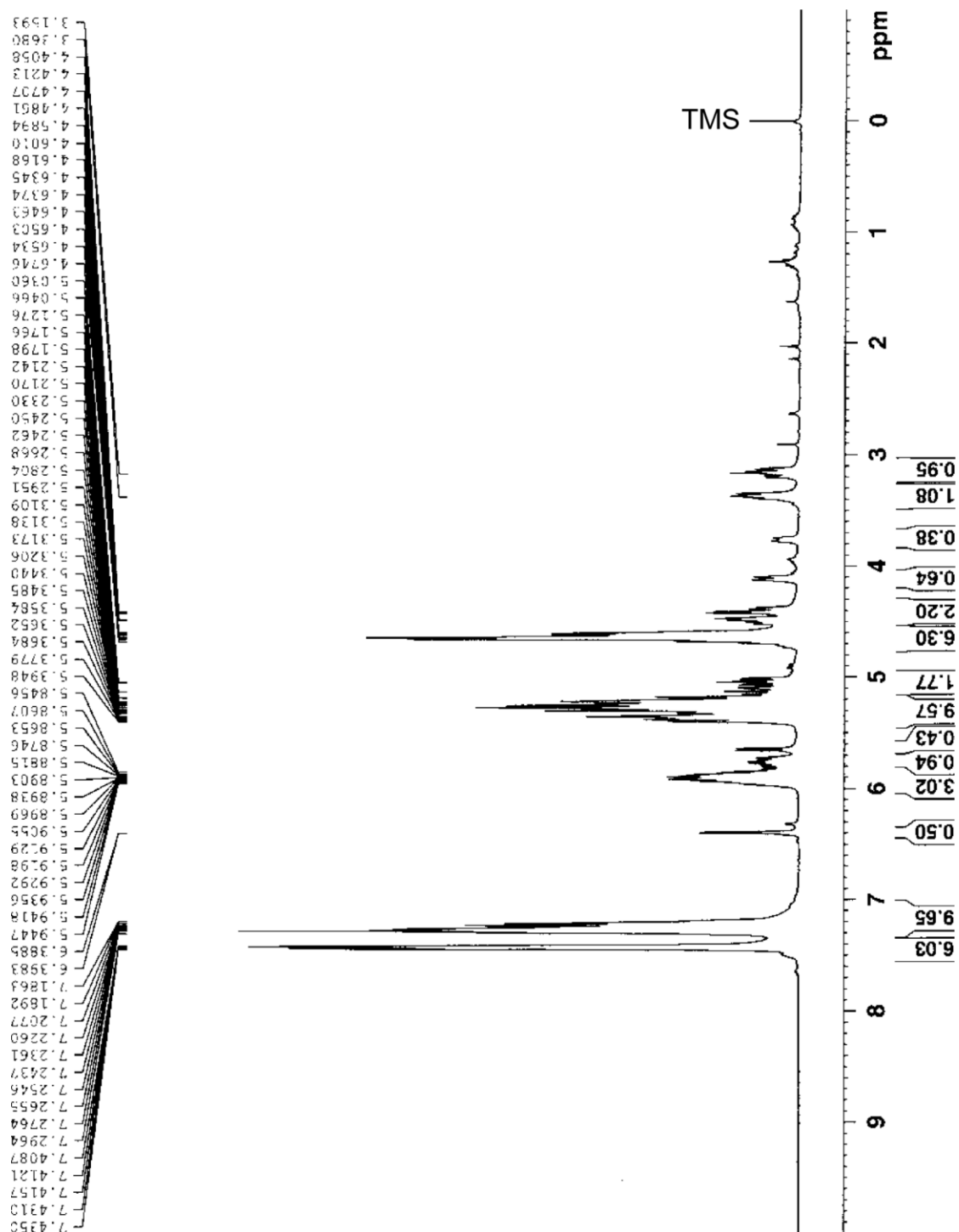
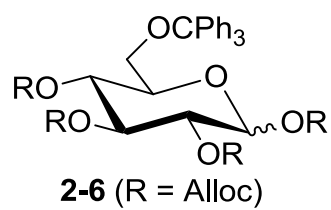
1. Pangborn, A. B.; Giardello, M. A.; Grubbs, R. H.; Rosen, R. K.; Timmers, F. J. *Organometallics* **1996**, *15*, 1518–1520.
2. Still, W. C.; Kahn, M., Mitra, A. *J. Org. Chem.* **1978**, *43*, 2923– 2925.
3. Mohapatra, H.; Phillips, S. T. Reagents and Assay Strategies for Quantifying Active Enzyme Analytes Using a Personal Glucose Meter. *Chem. Commun.* **2013**, *49*, 6134–6136.
4. Riva, S.; Chopineau, J.; Kieboom, A. P. G.; Klibanov, A. M. Protease-Catalyzed Regioselective Esterification of Sugars and Related Compounds in Anhydrous Dimethylformamide. *J. Am. Chem. Soc.* **1988**, *110*, 584–589.
5. Nuñez, S. A.; Yeung, K.; Fox, N. S.; Phillips, S. T. A Structurally Simple Self-Immolative Reagent That Provides Three Distinct, Simultaneous Responses per Detection Event. *J. Org. Chem.* **2011**, *76*, 10099–10113.
6. Mohapatra, H.; Phillips, S. T. Using Smell to Triage Samples in Point-of-Care Assays. *Angew. Chem. Int. Ed.* **2012**, *51*, 11145–11148.

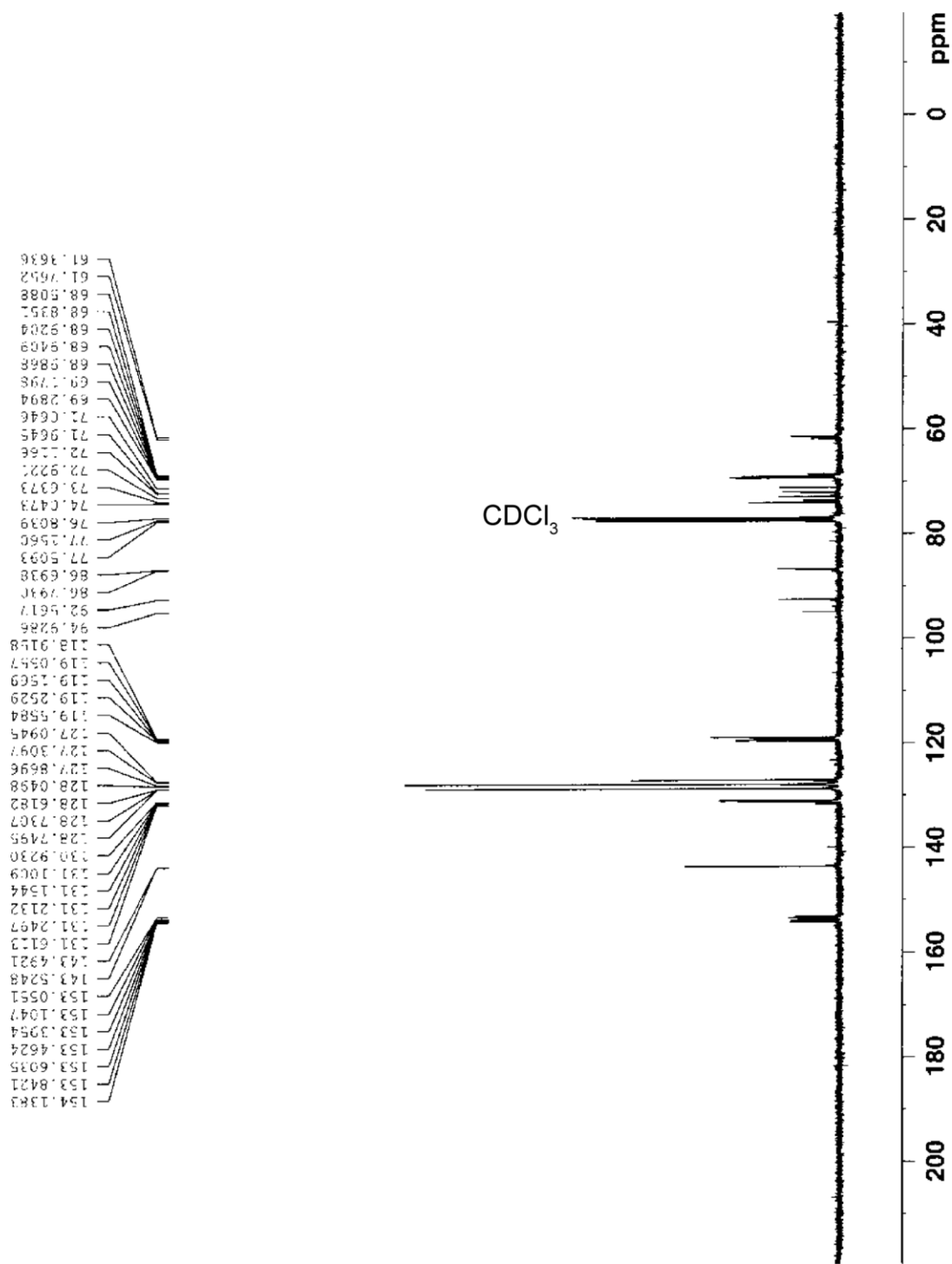
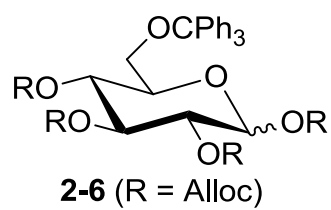
7. Martin, P. Access to the three subunits of the antitumor antibiotic CC-1065 by hetero-Cope rearrangement of vinyl N-phenylhydroxamates. *Helv. Chim. Acta.* **1989**, 72, 1554–1582.
8. Mohapatra, H.; Schmid, K. M.; Phillips, S. T. Design of Small Molecule Reagents That Enable Signal Amplification via an Autocatalytic, Base-Mediated Cascade Elimination Reaction. *Chem. Commun.* **2012**, 48, 3018–3020.
9. Cao, Y.; Yang, J. Development of a Folate Receptor (FR)-Targeted Indenoisoquinoline Using a pH-Sensitive N-Ethoxybenzylimidazole (NEBI) Bifunctional Cross-Linker. *Bioconjugate Chem.* **2014**, 25, 873–878.
10. Suzuki, D.; Urabe, H.; Sato, F. Metalative Reppe Reaction. Organized Assembly of Acetylene Molecules on Titanium Template Leading to a New Style of Acetylene Cyclotrimerization. *J. Am. Chem. Soc.* **2001**, 123, 7925–7926.

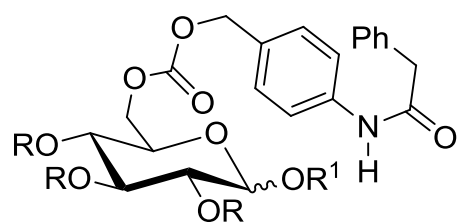
APPENDIX A: NMR SPECTRA



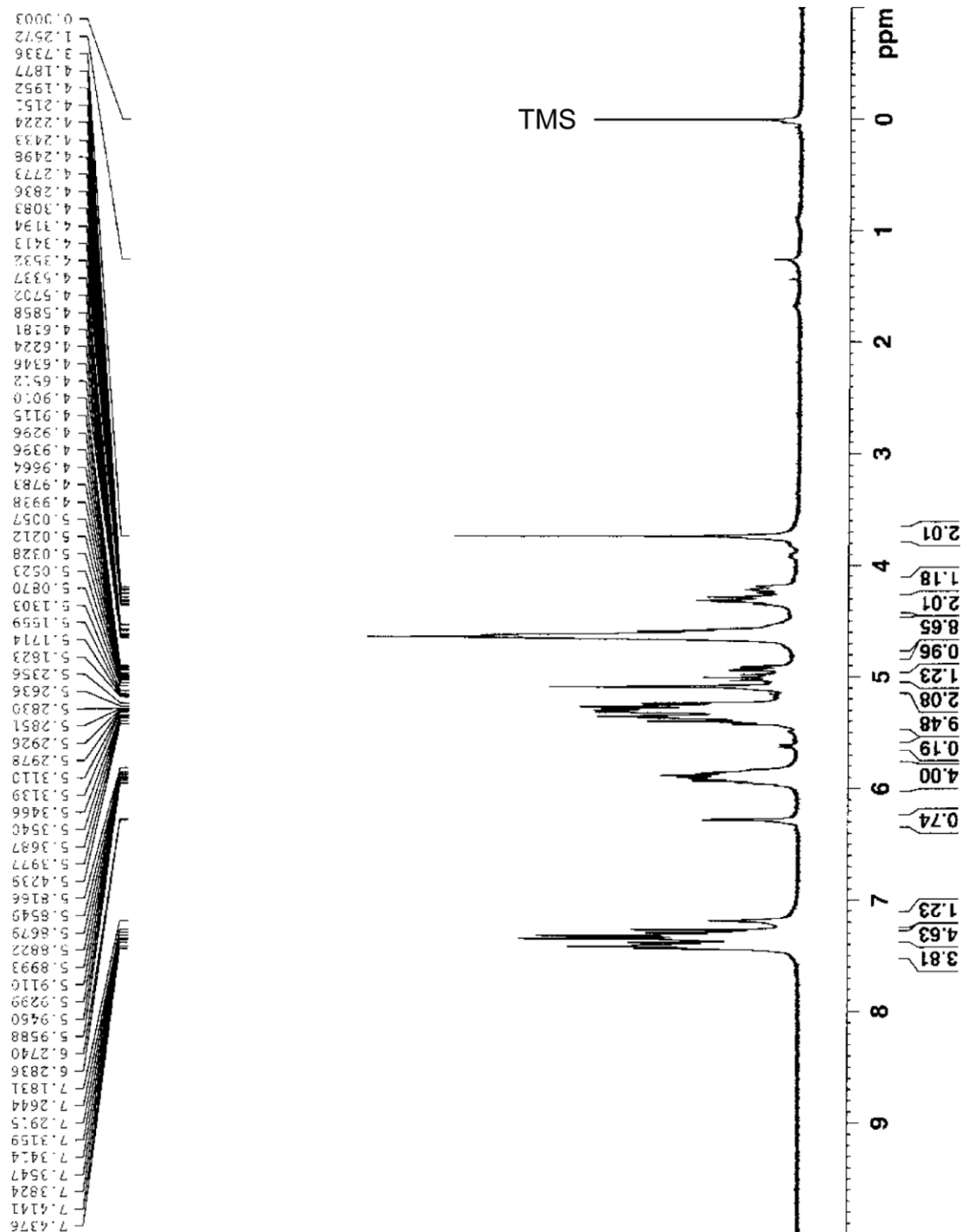


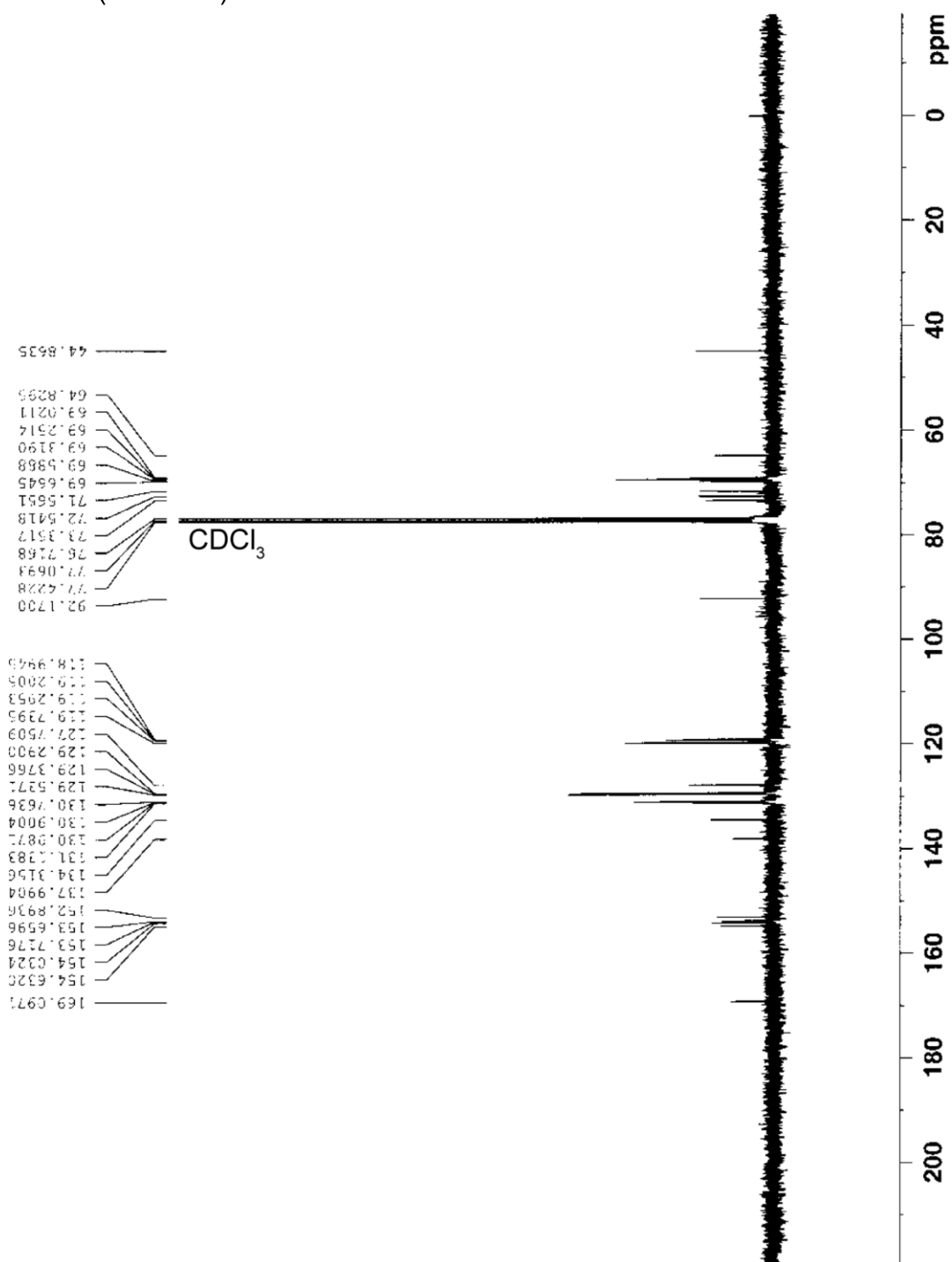
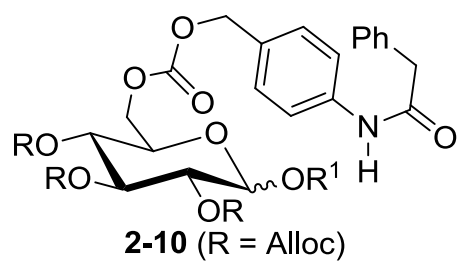


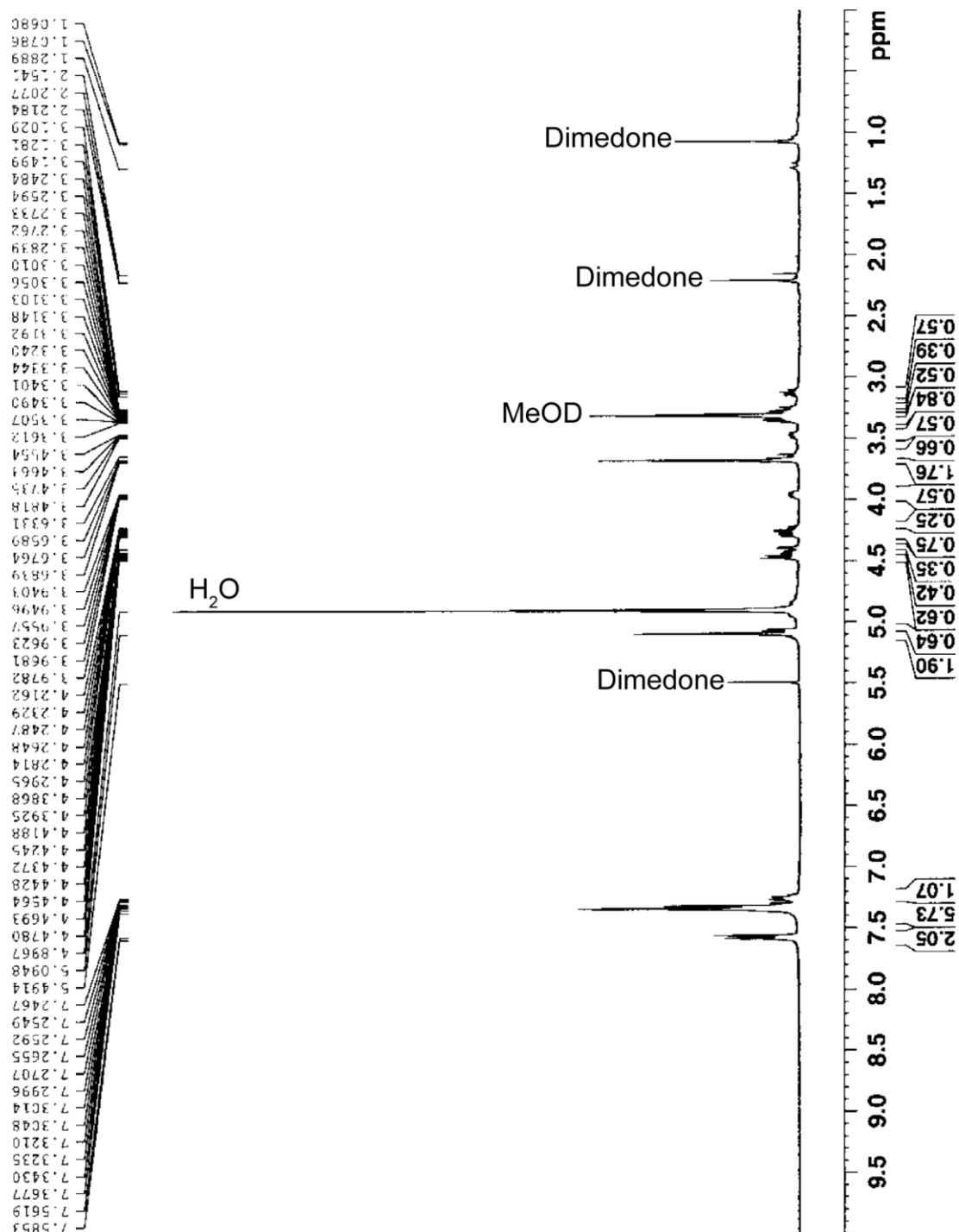
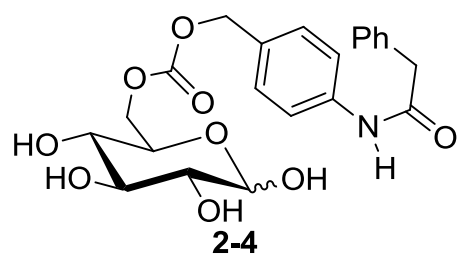


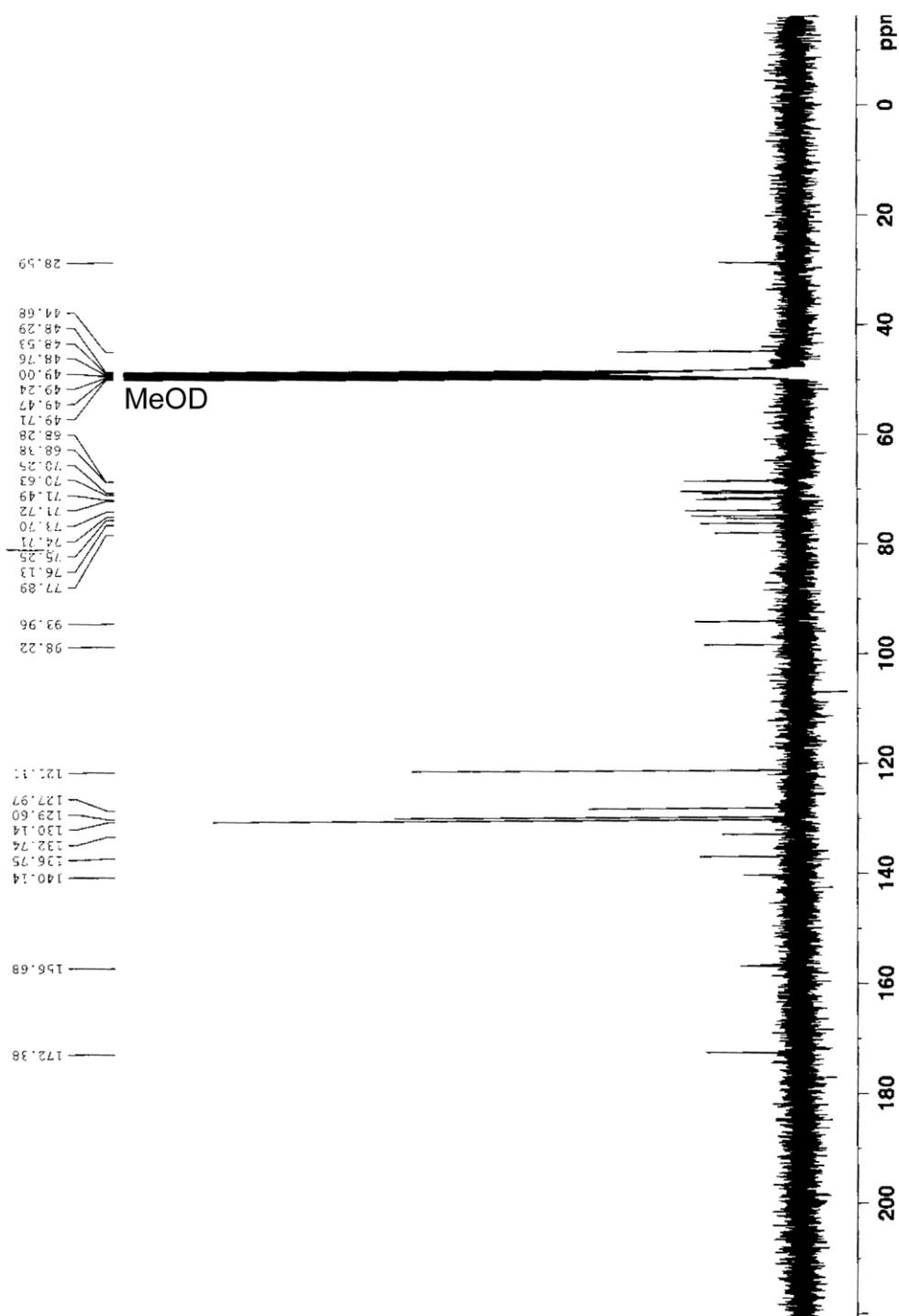
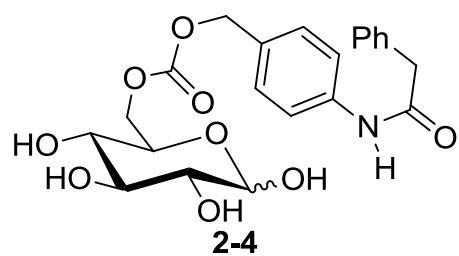


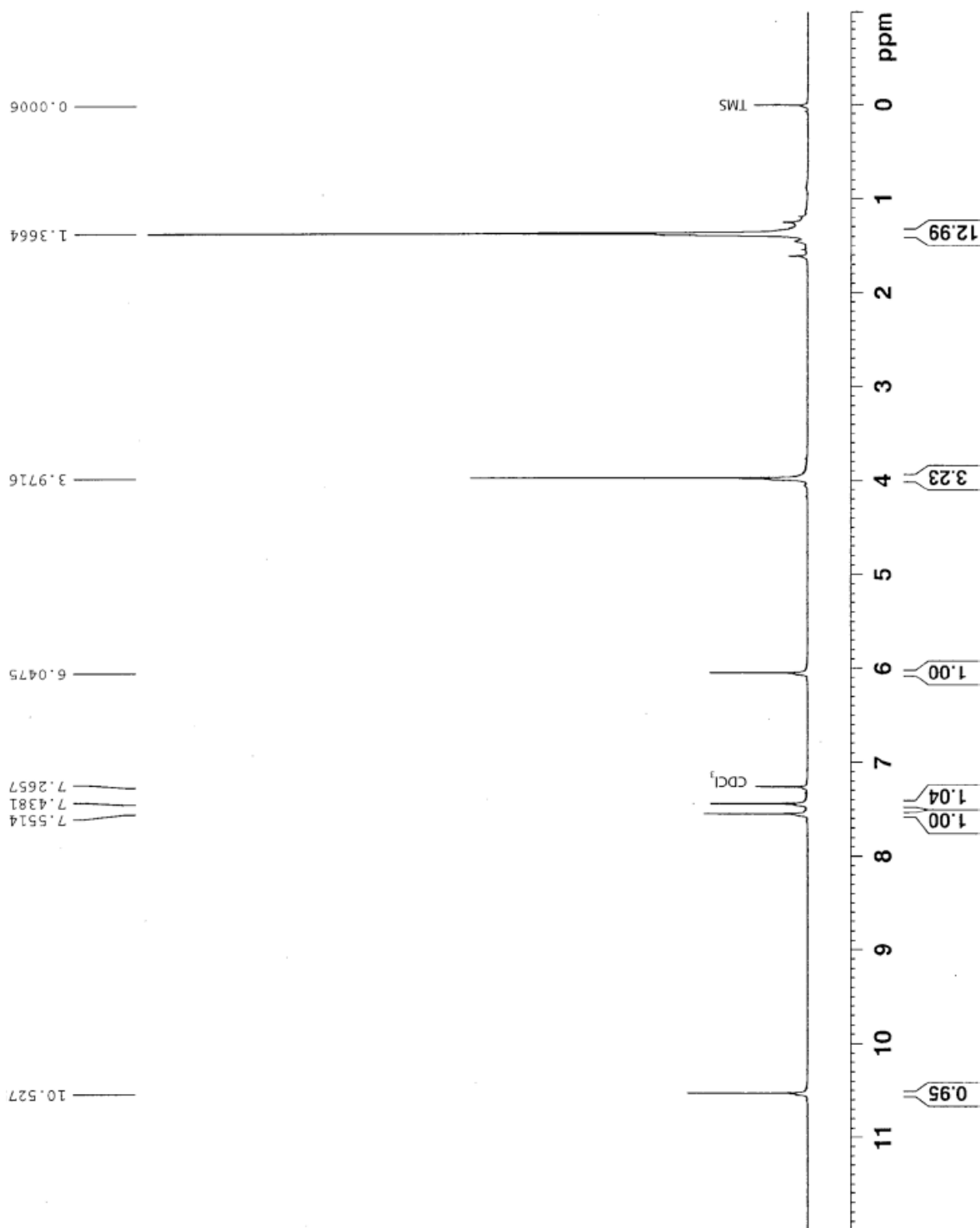
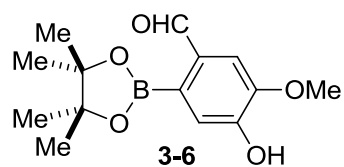
2-10 (R = Alloc)

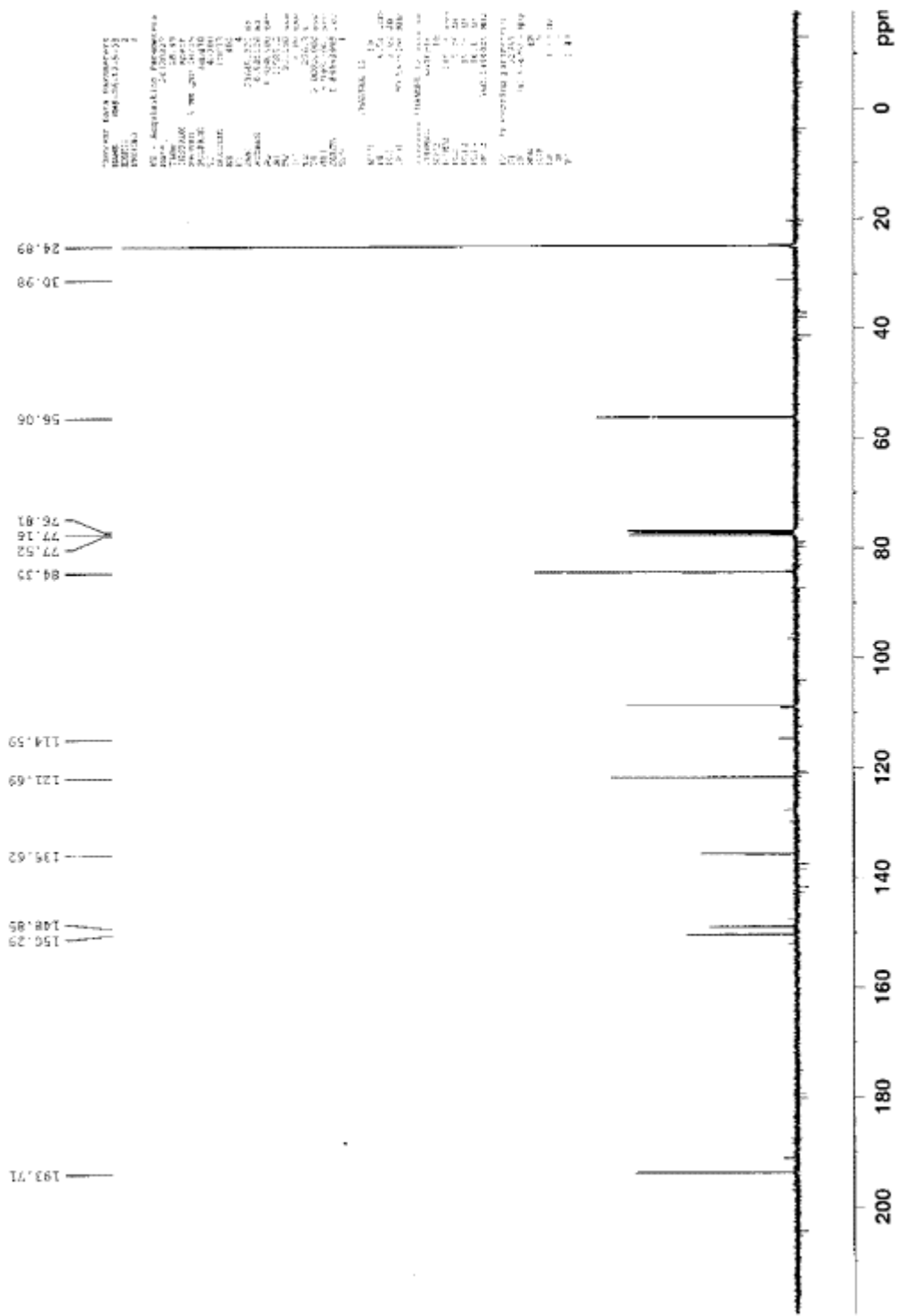
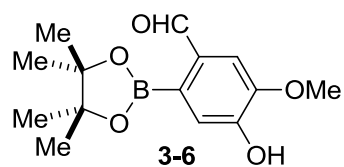


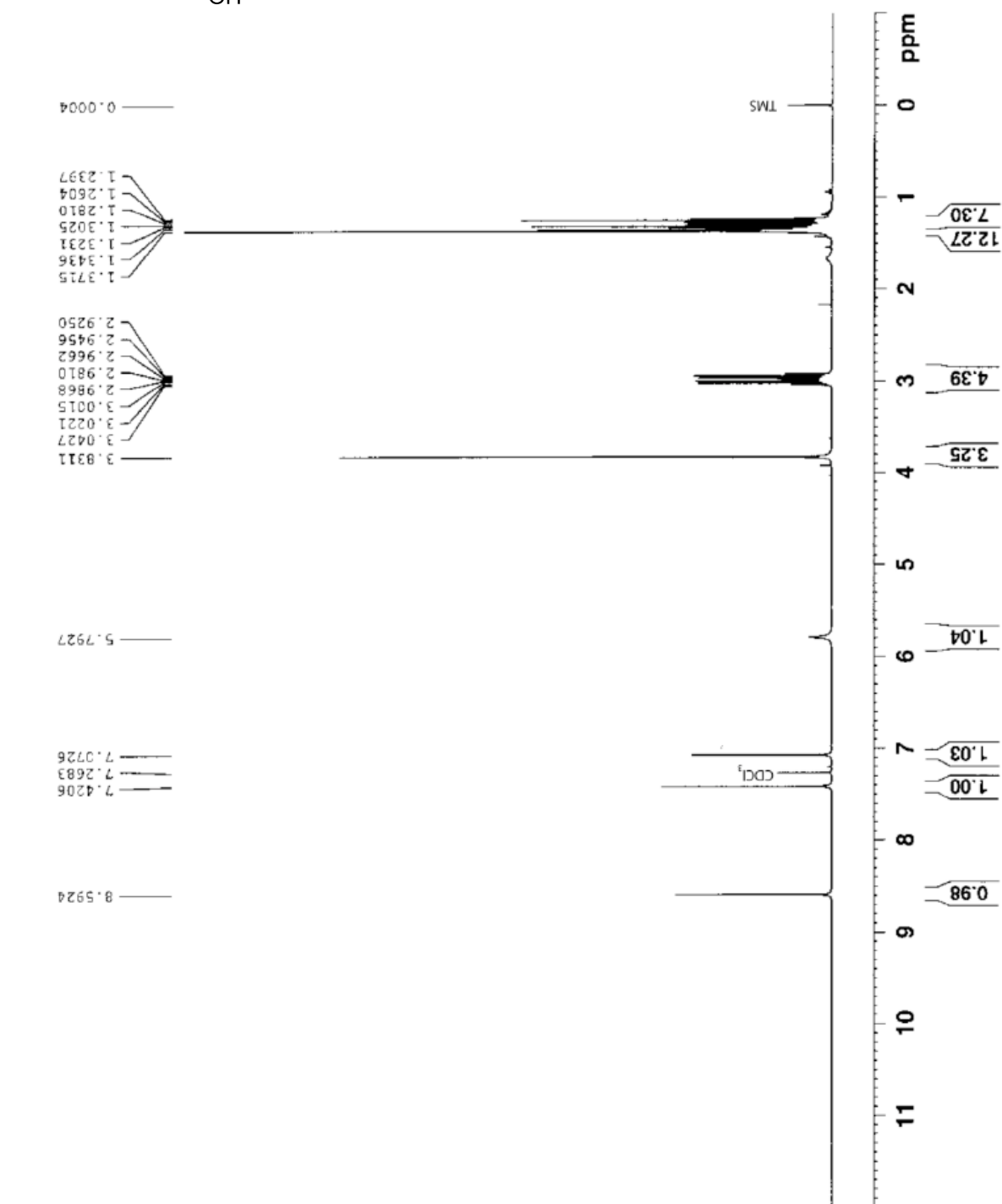
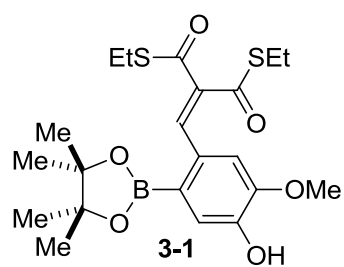


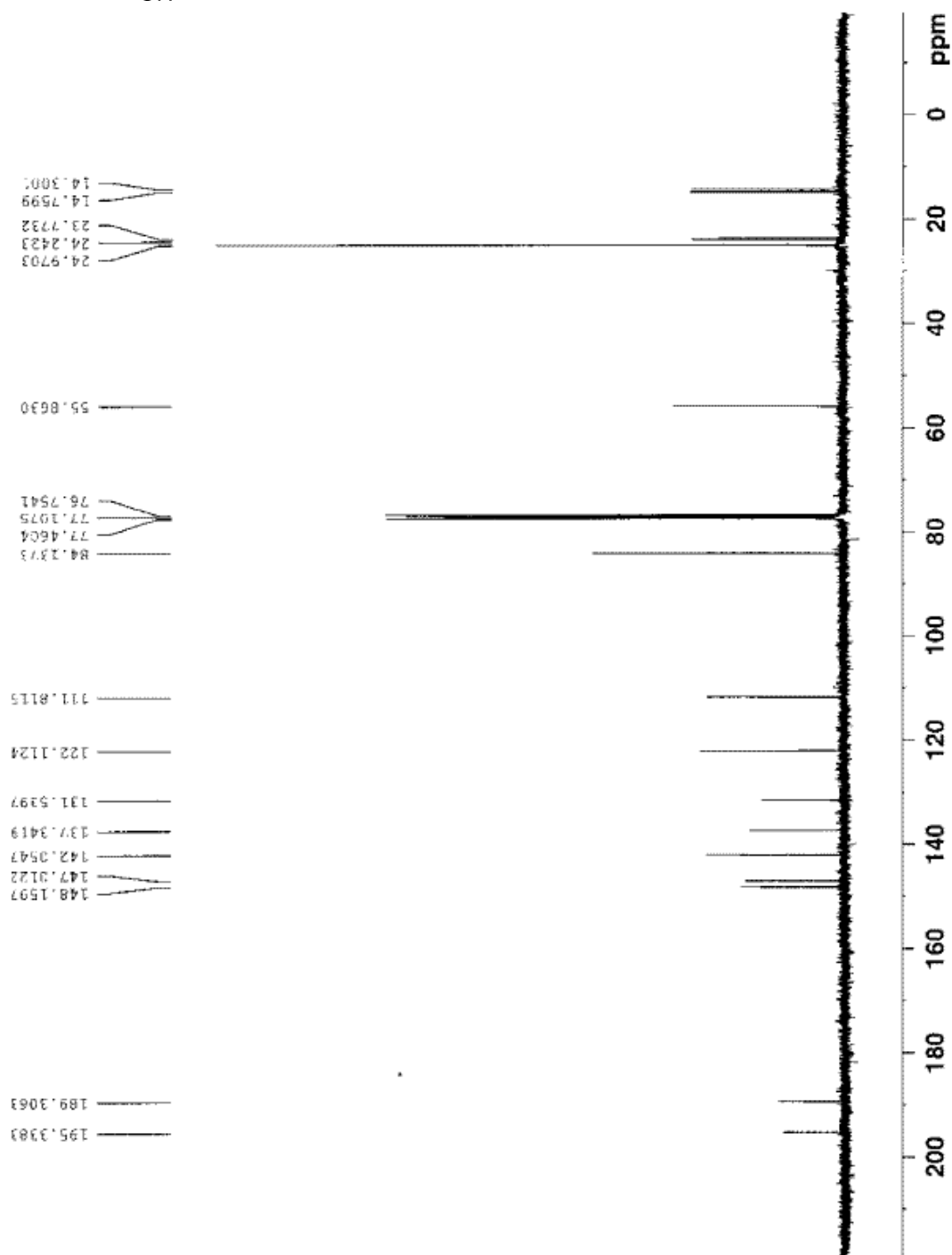
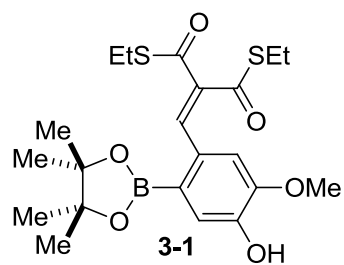


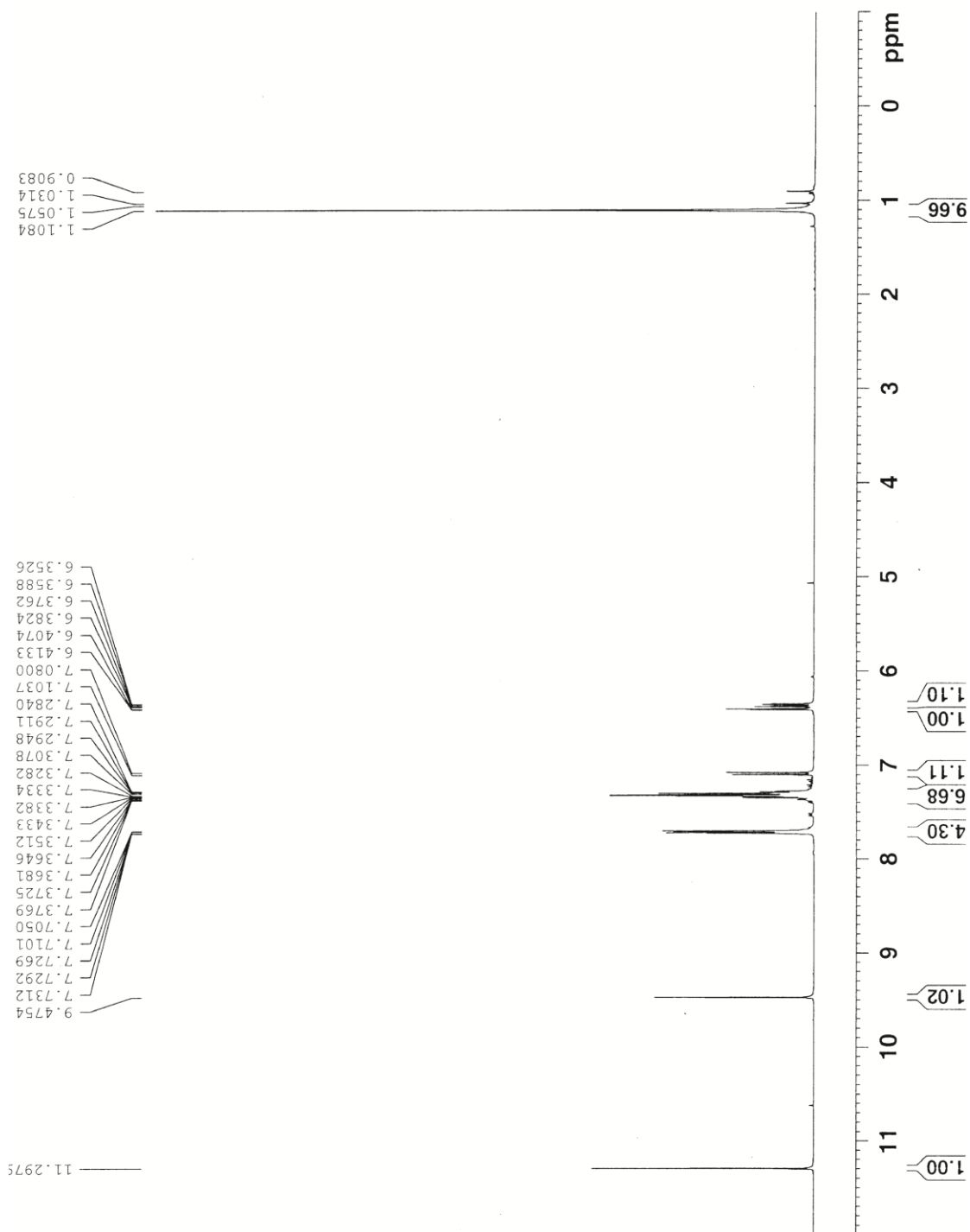
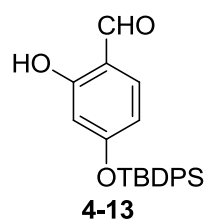


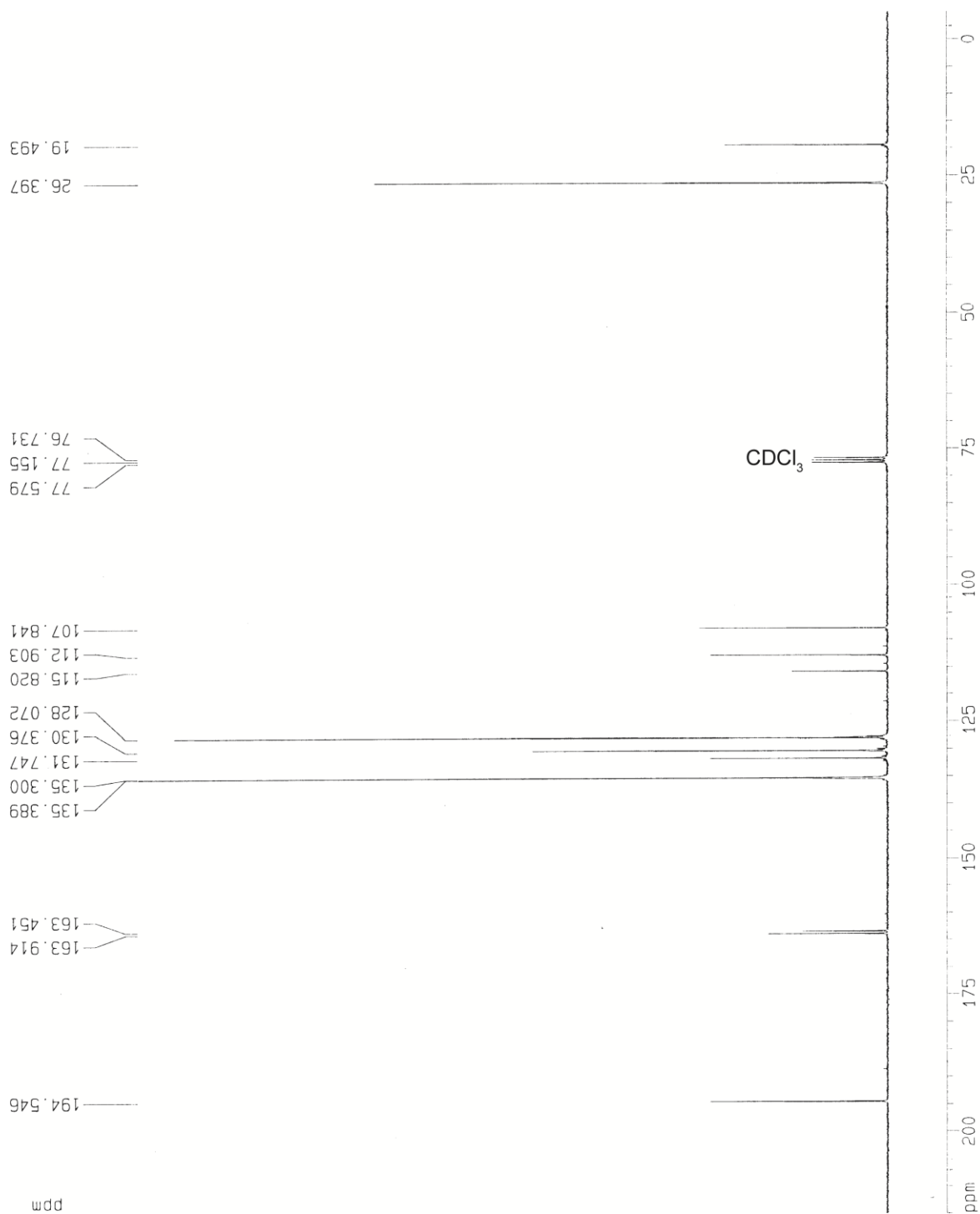
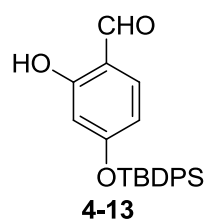


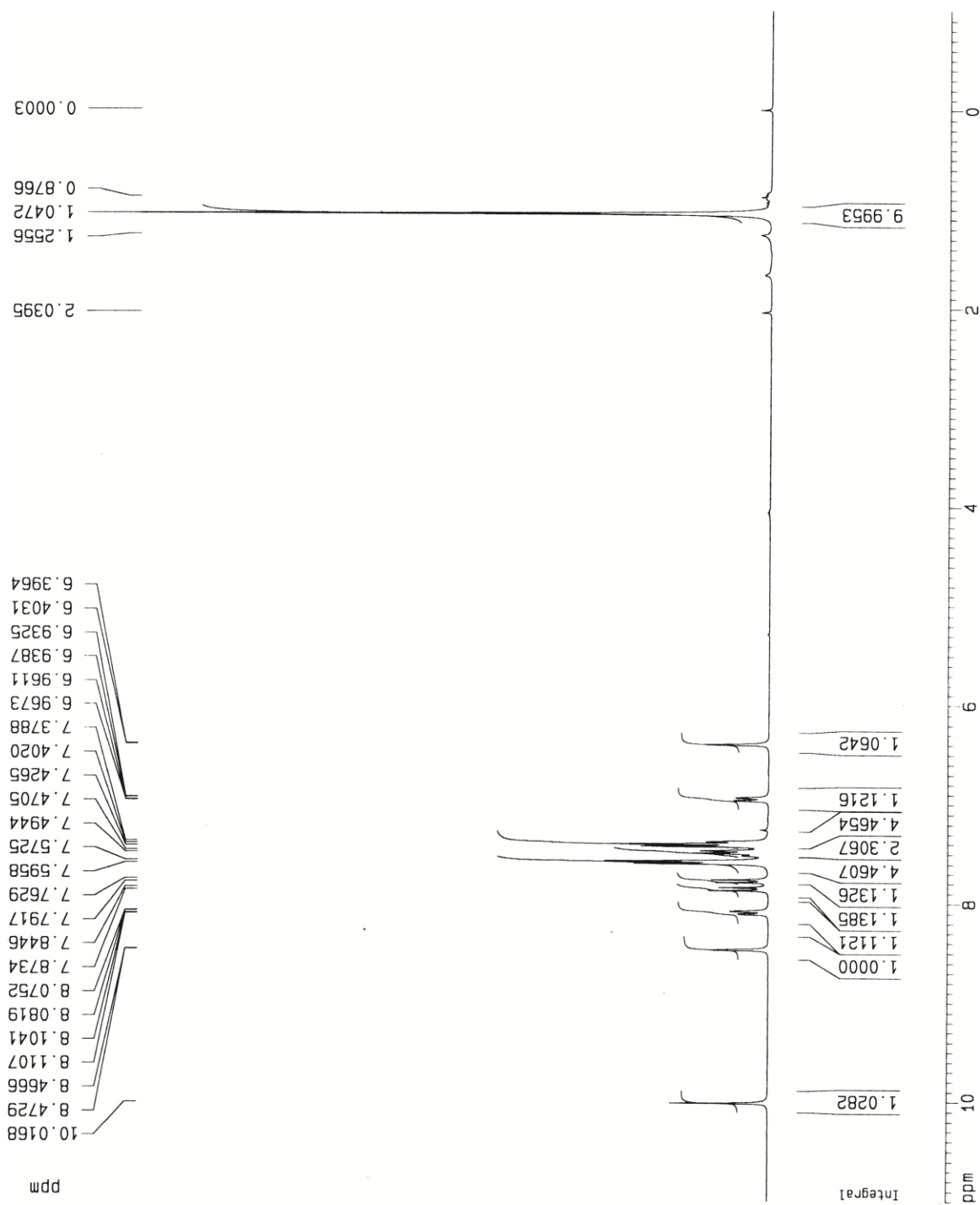
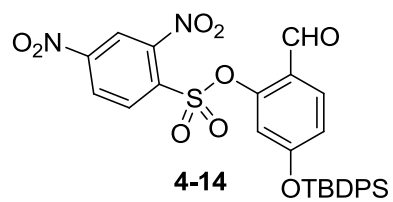


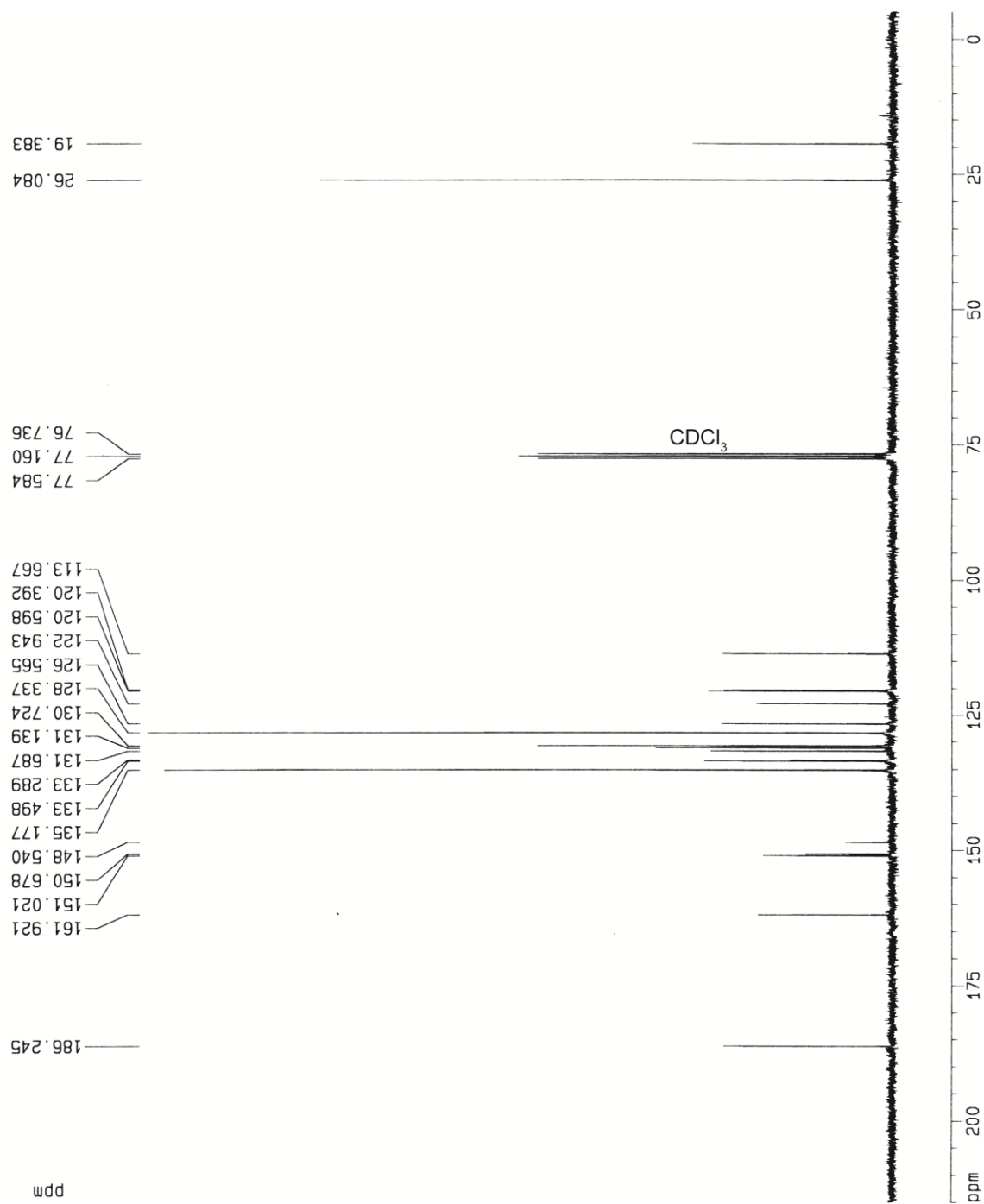
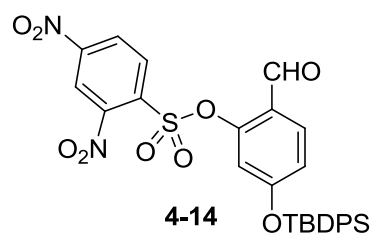


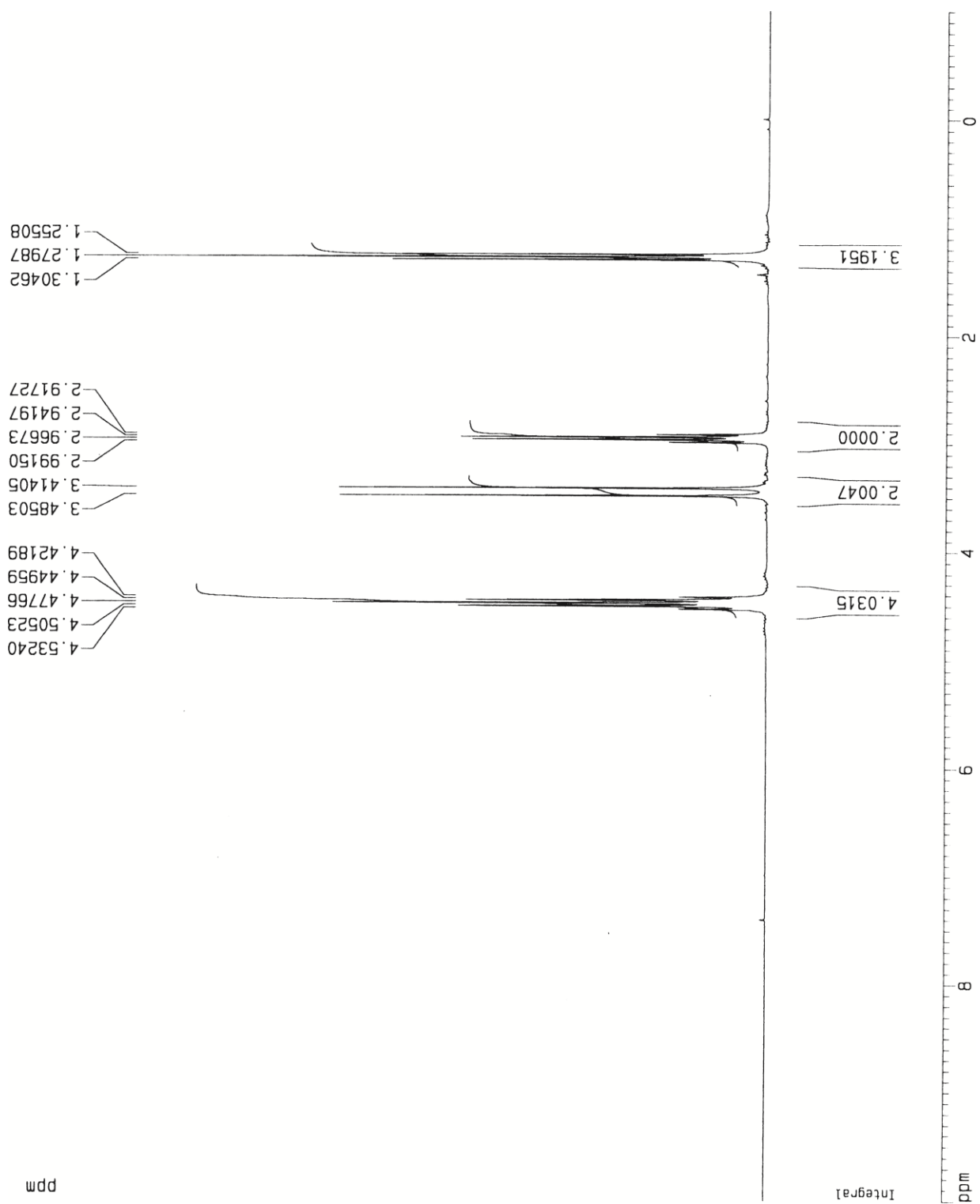
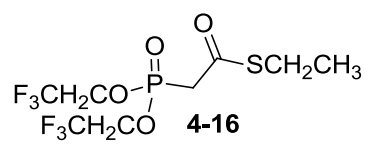


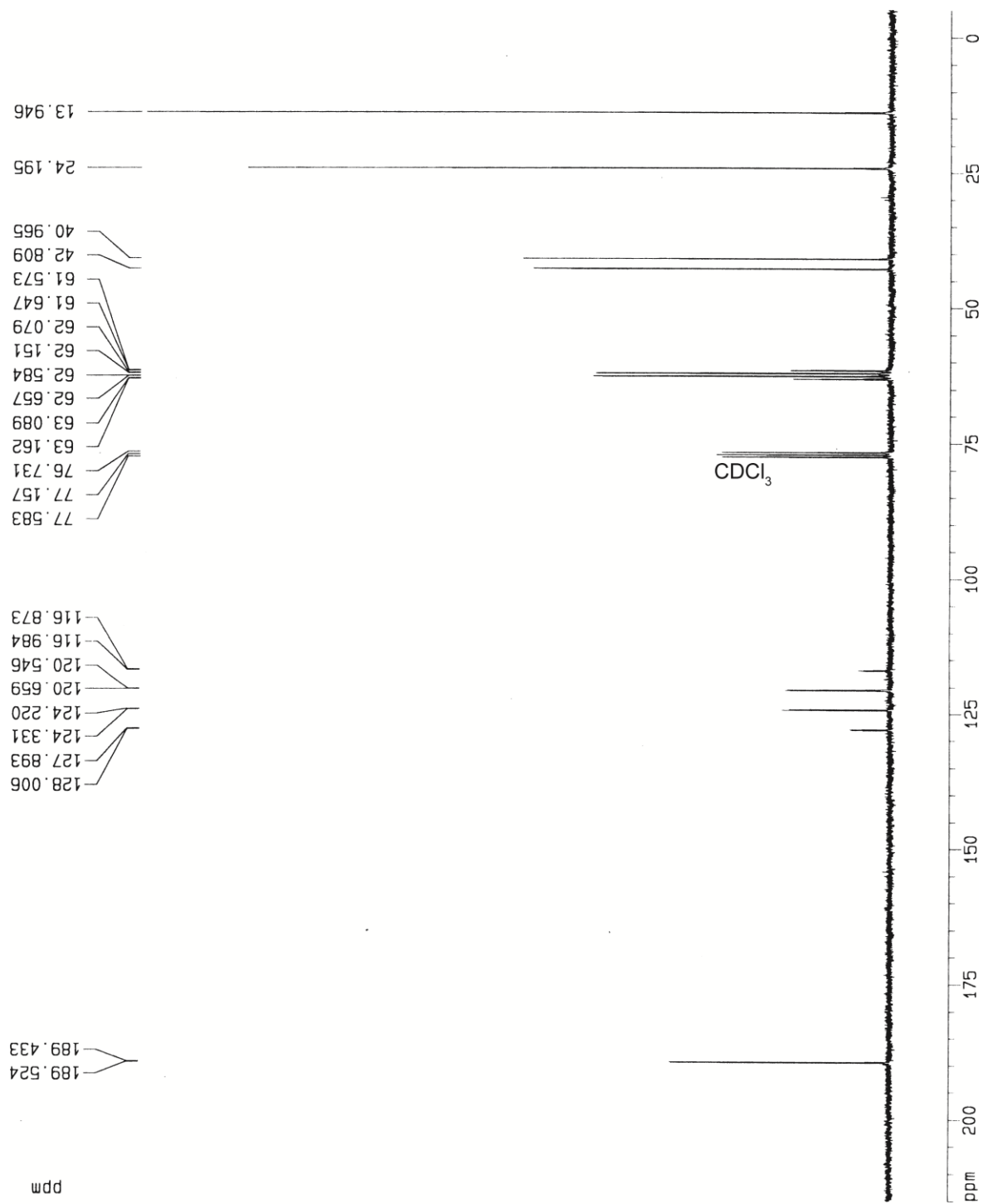
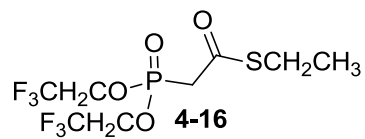


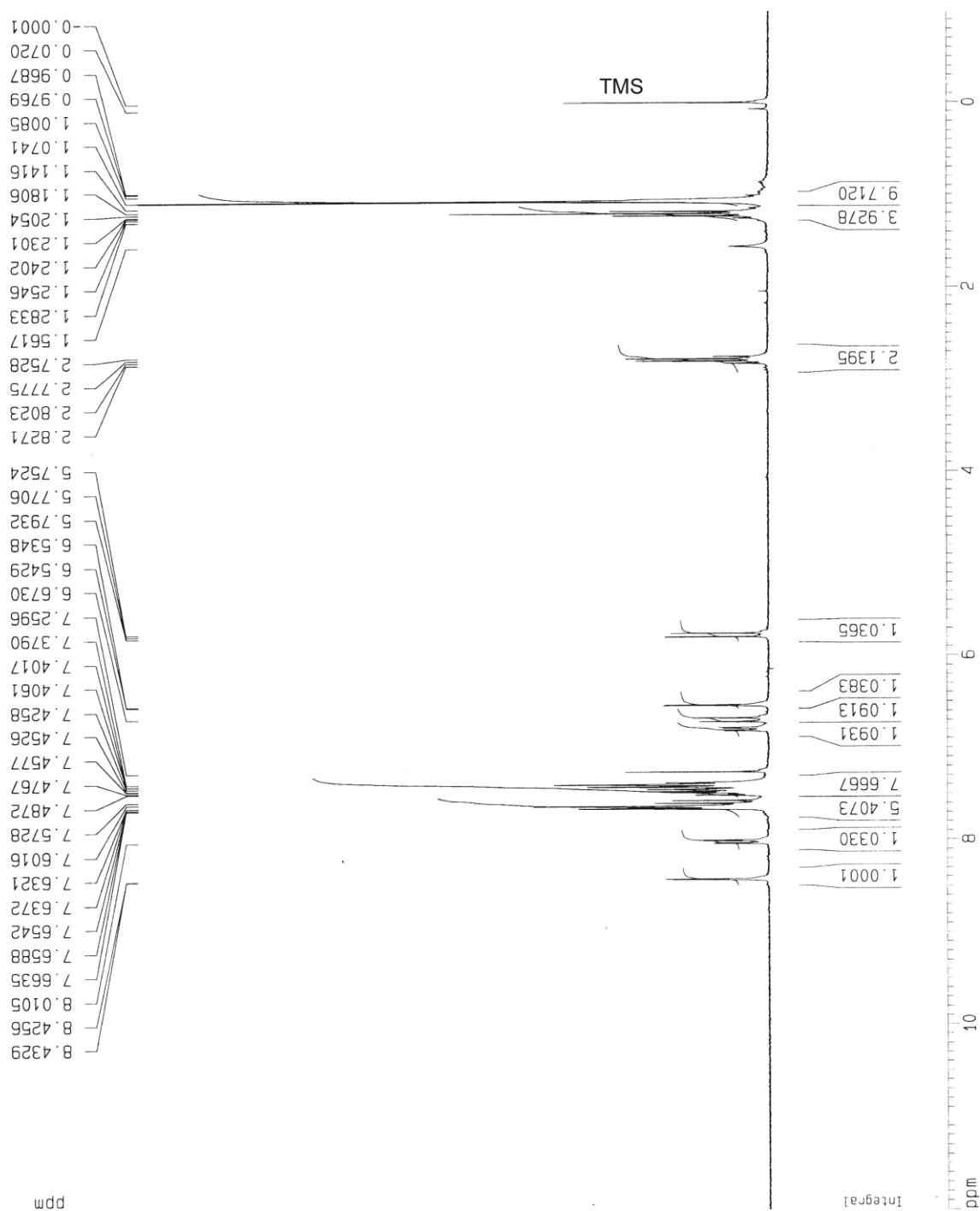
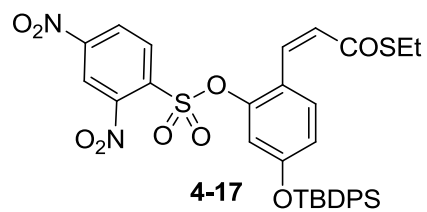


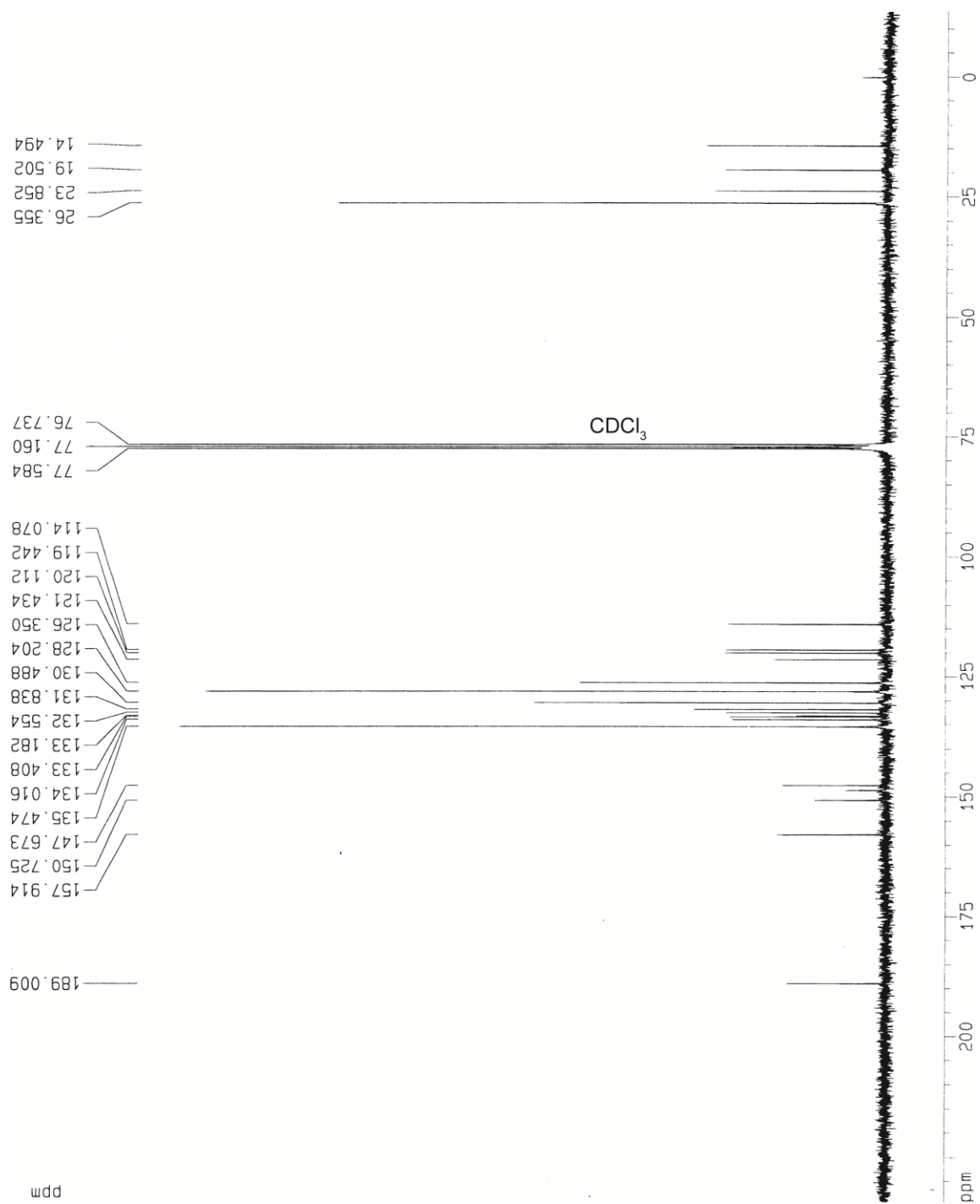
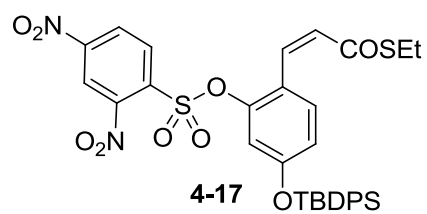


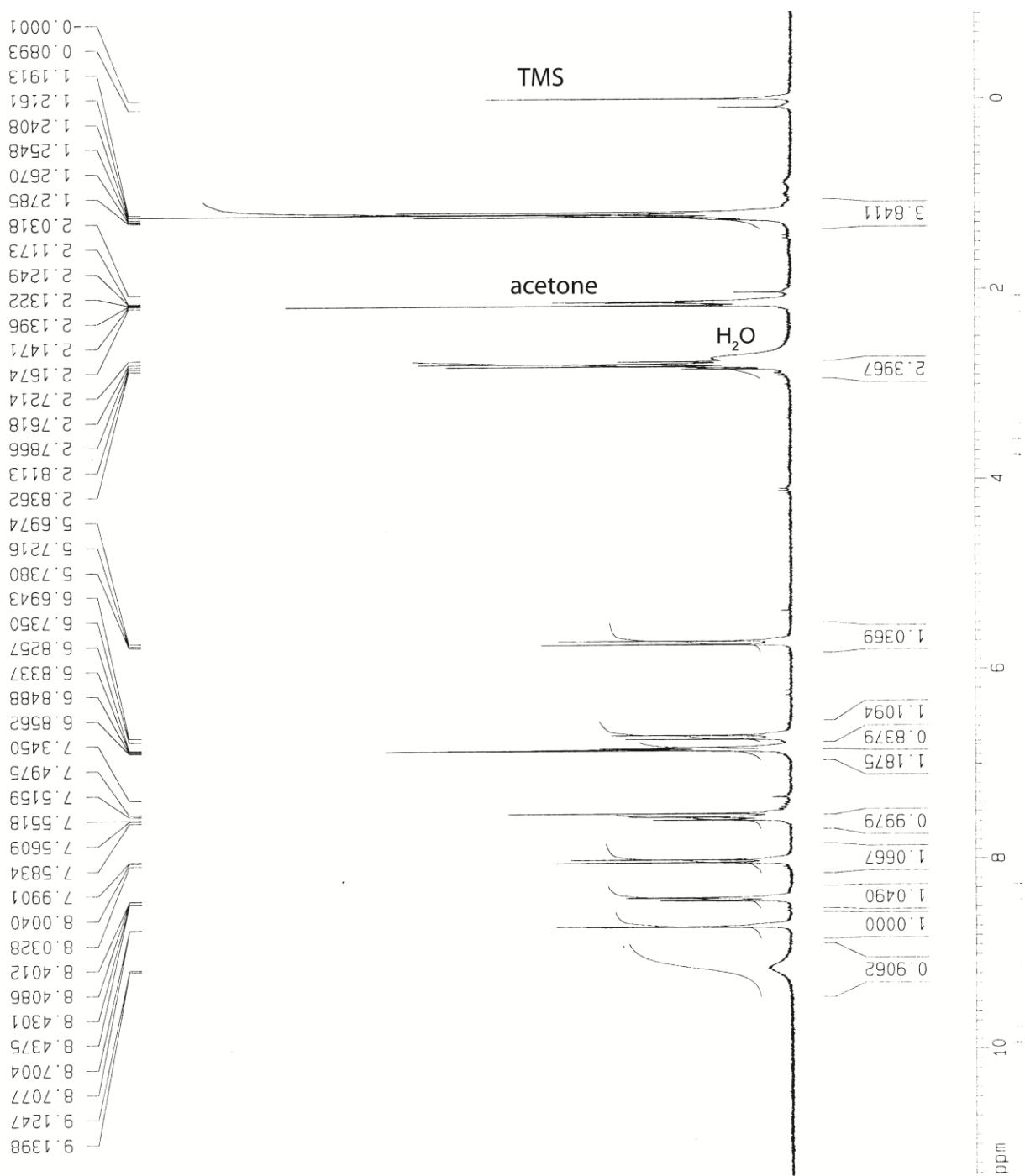
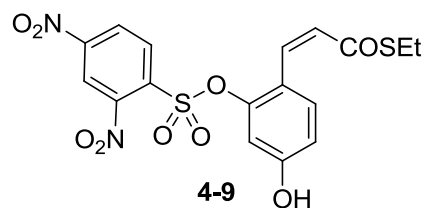


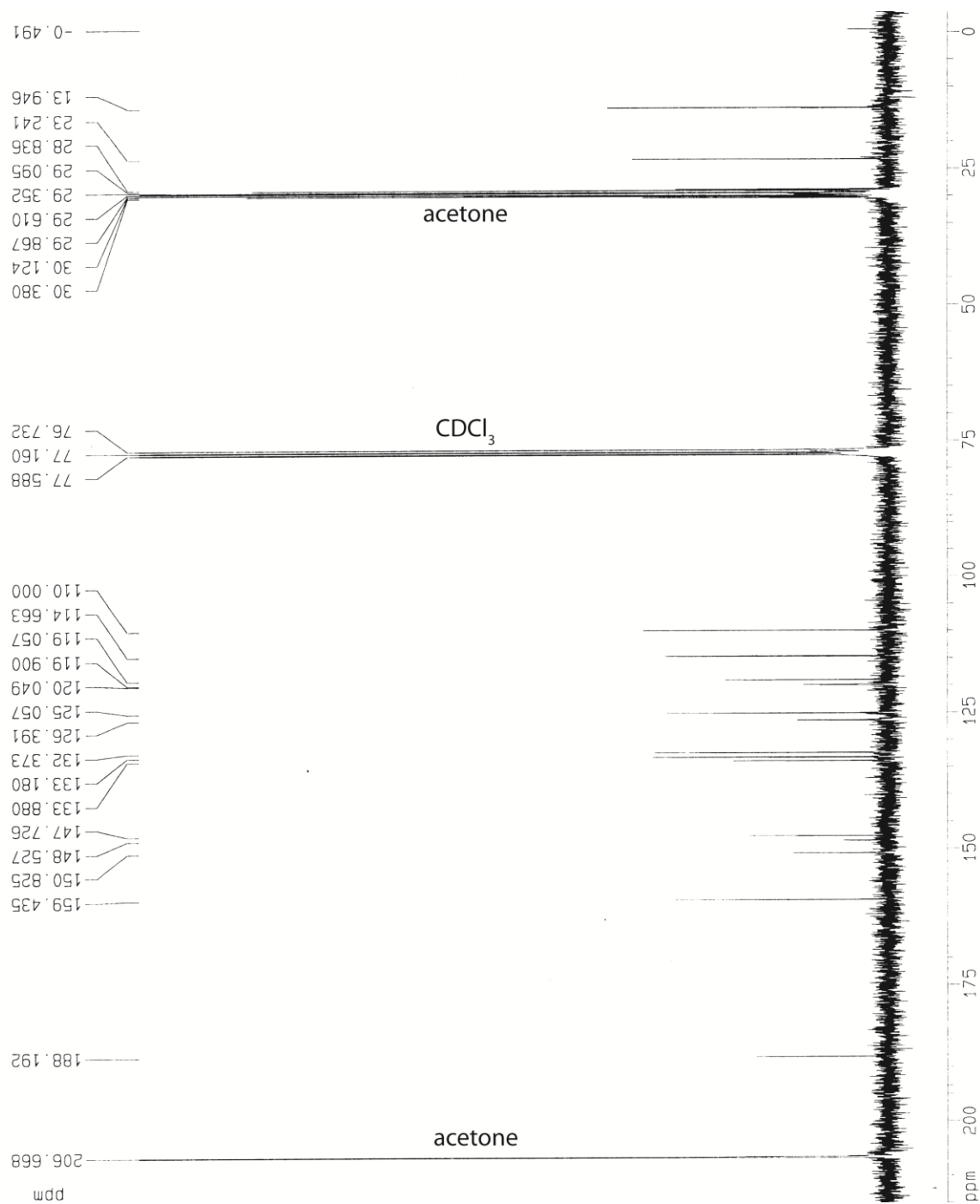
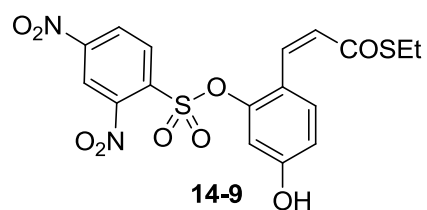


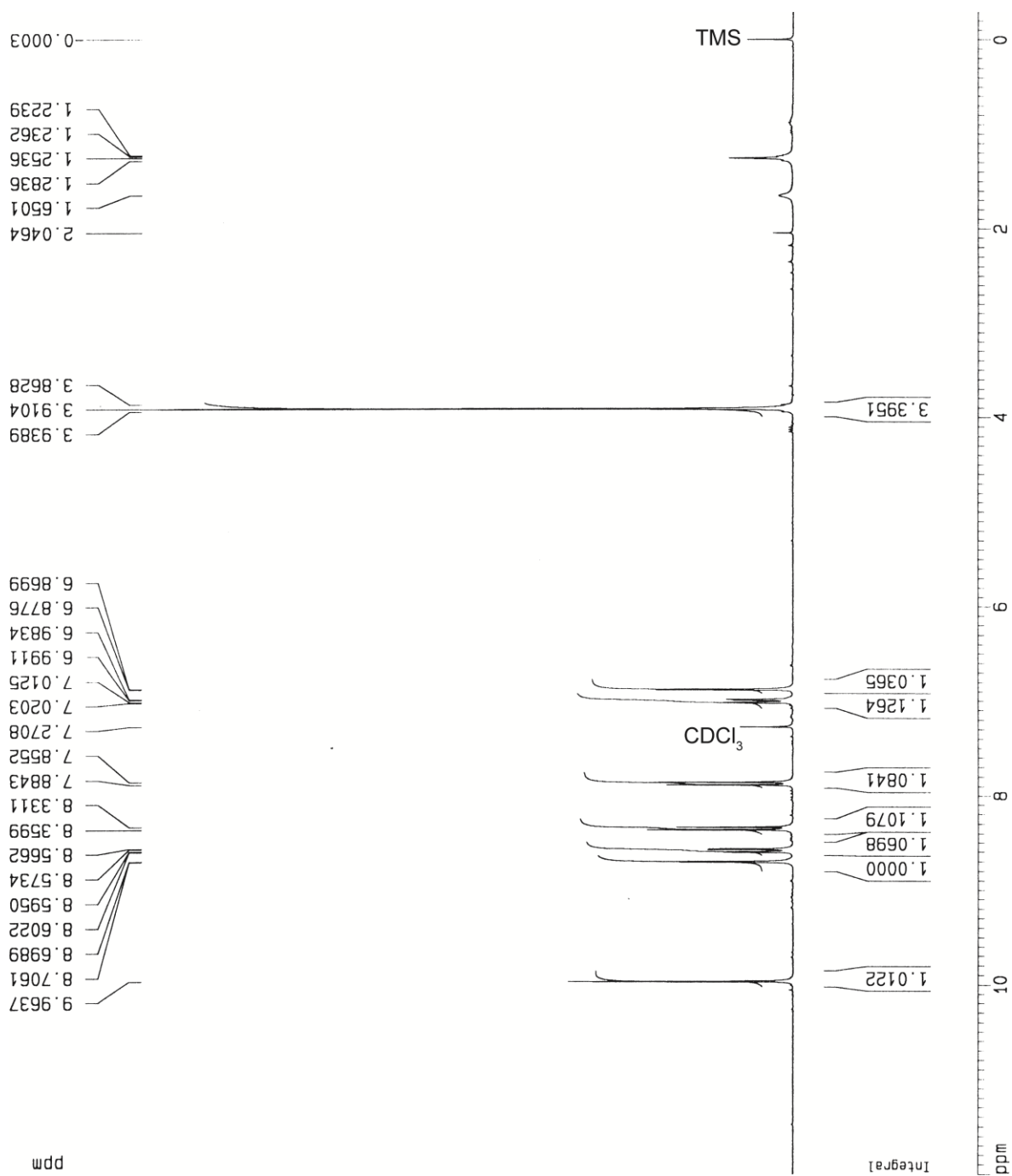
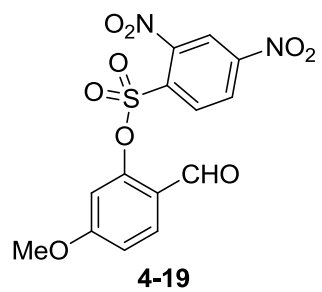


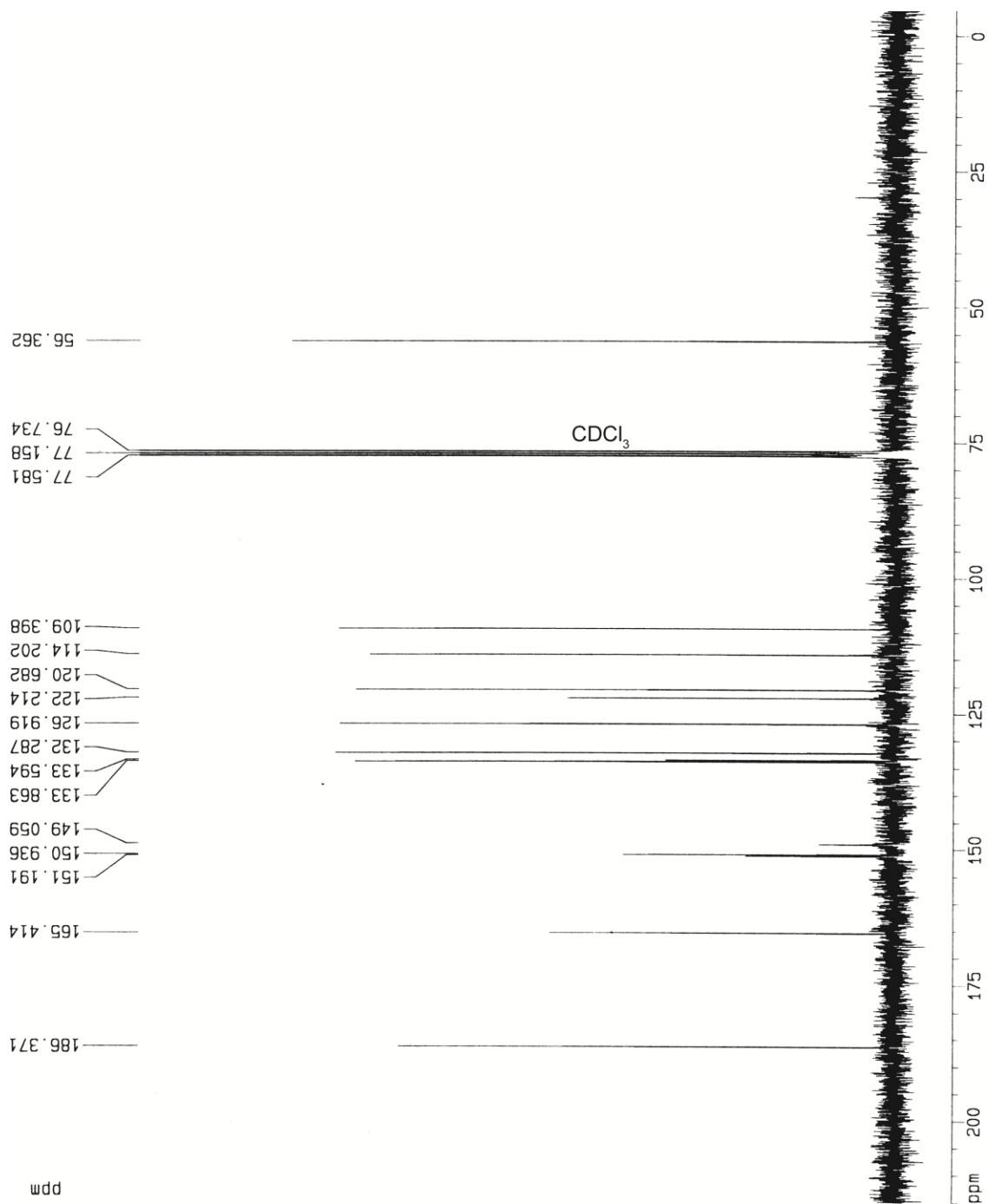
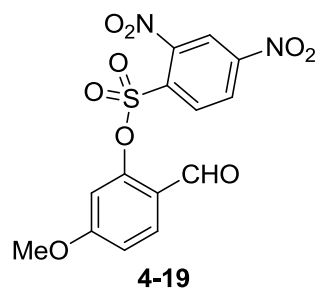


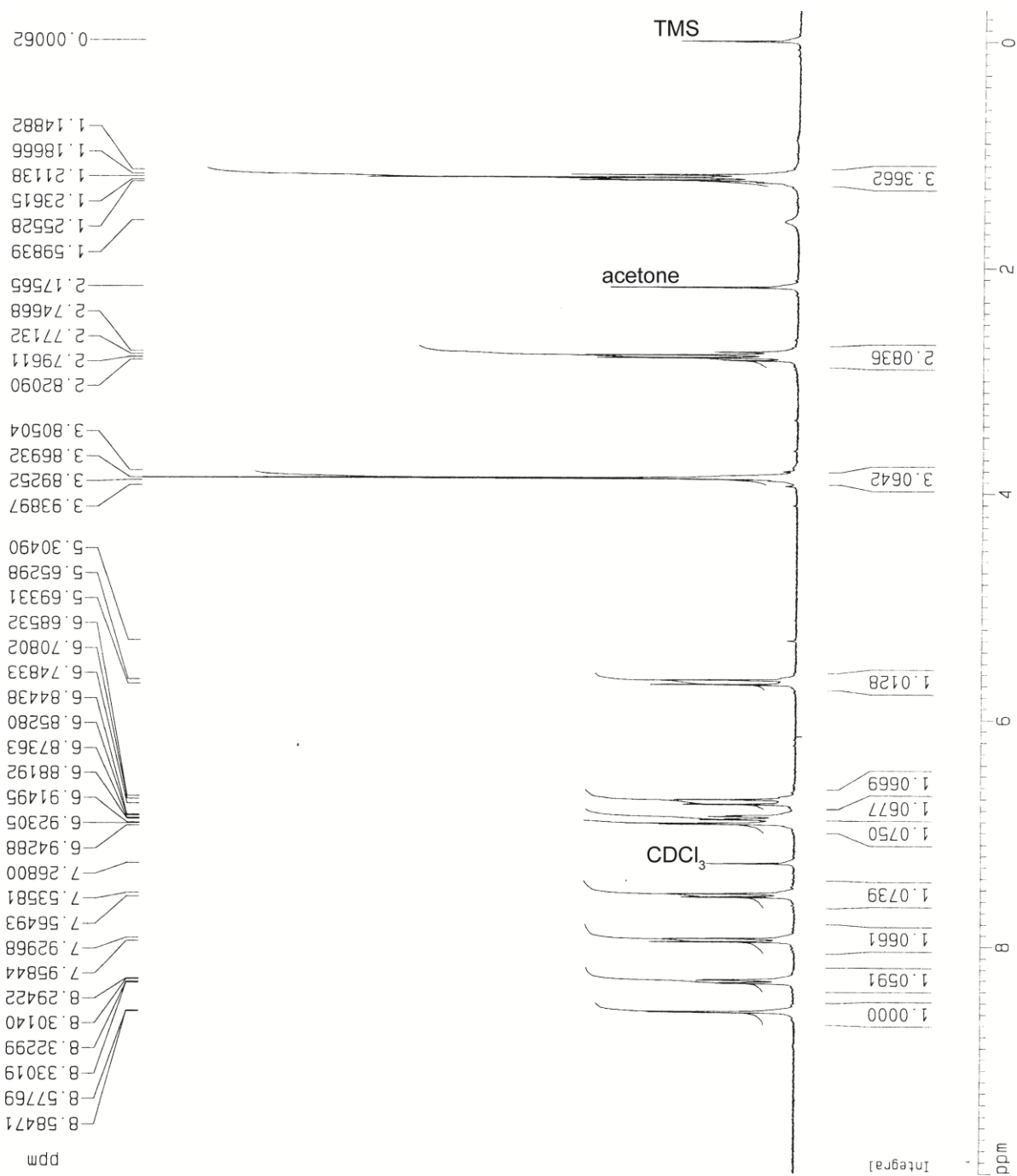
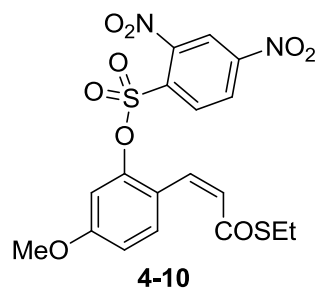


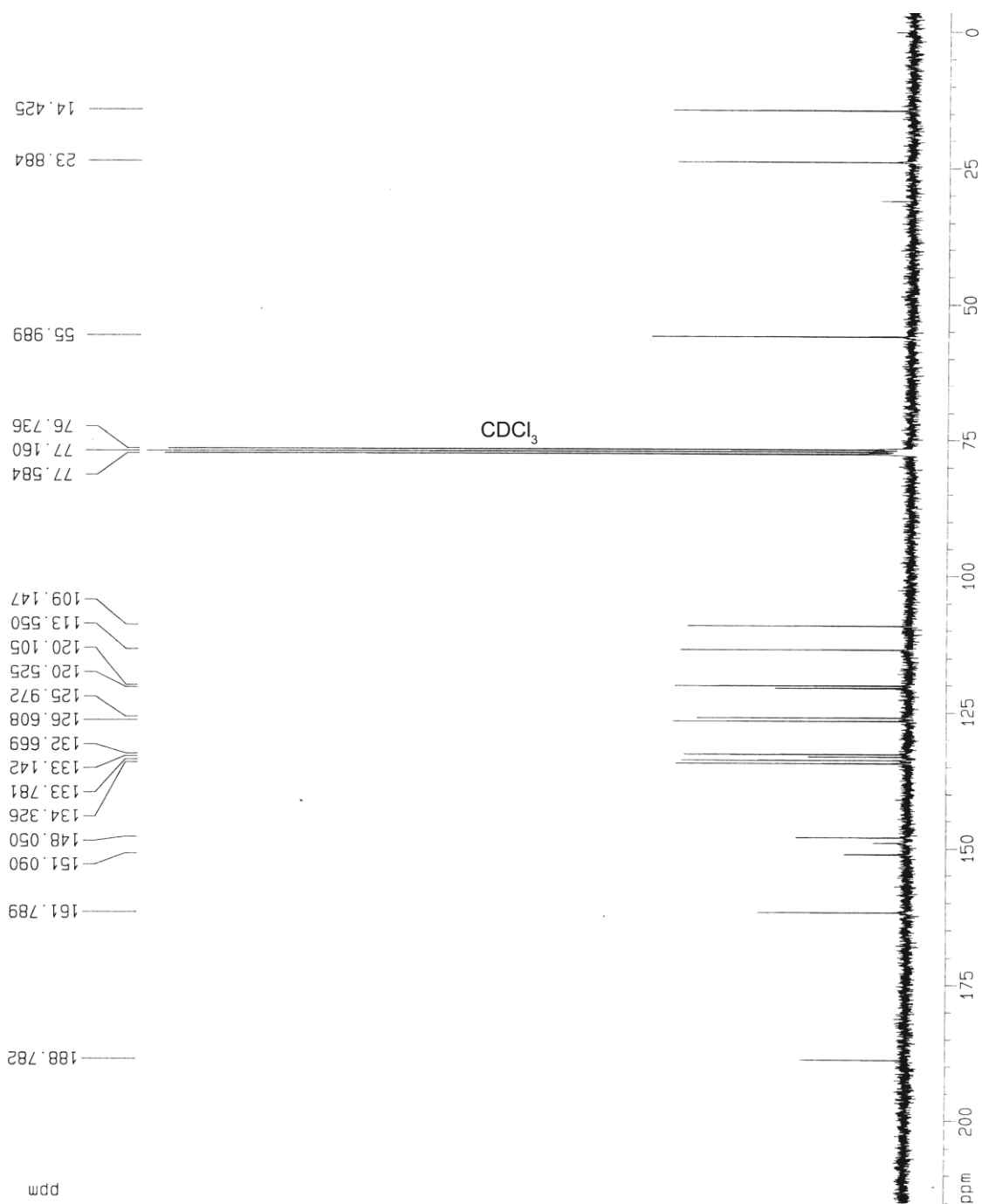
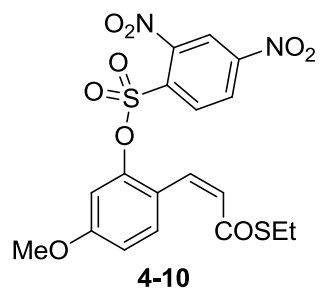


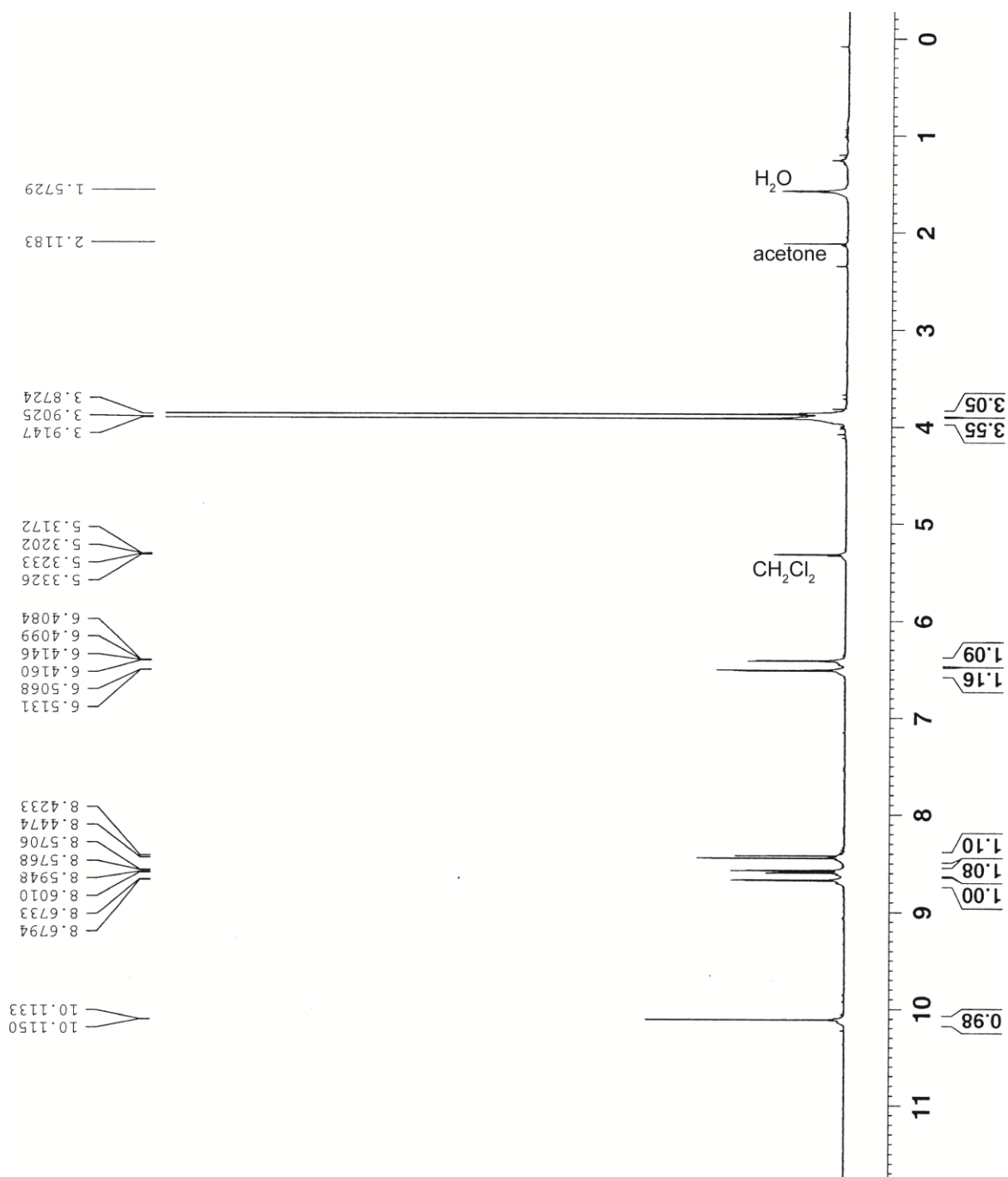
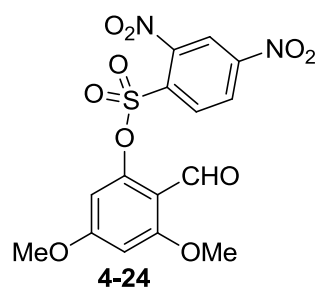


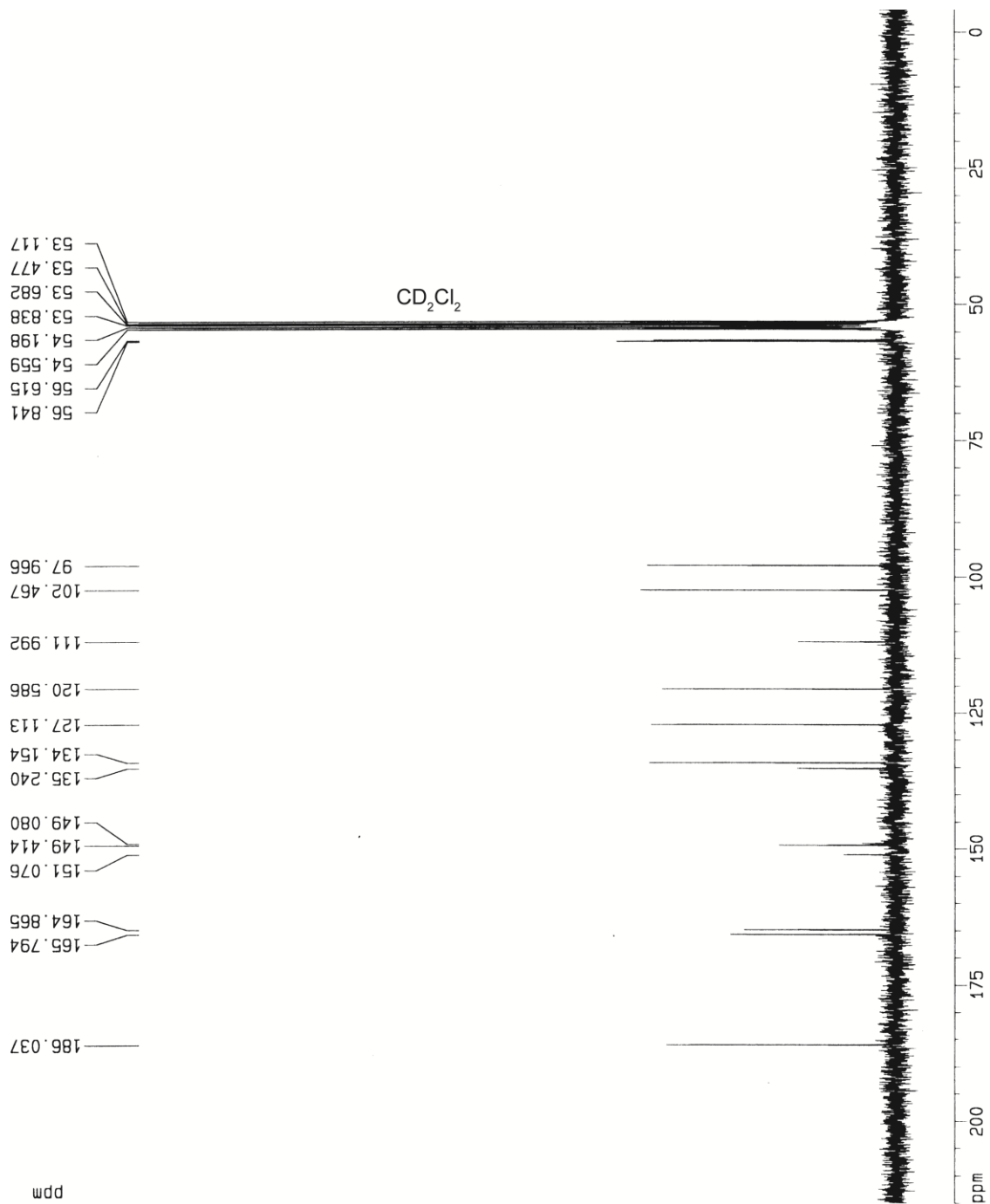
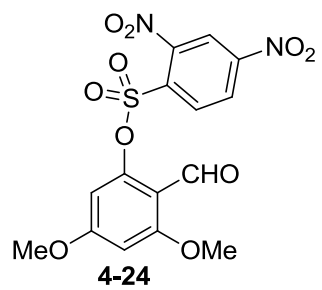


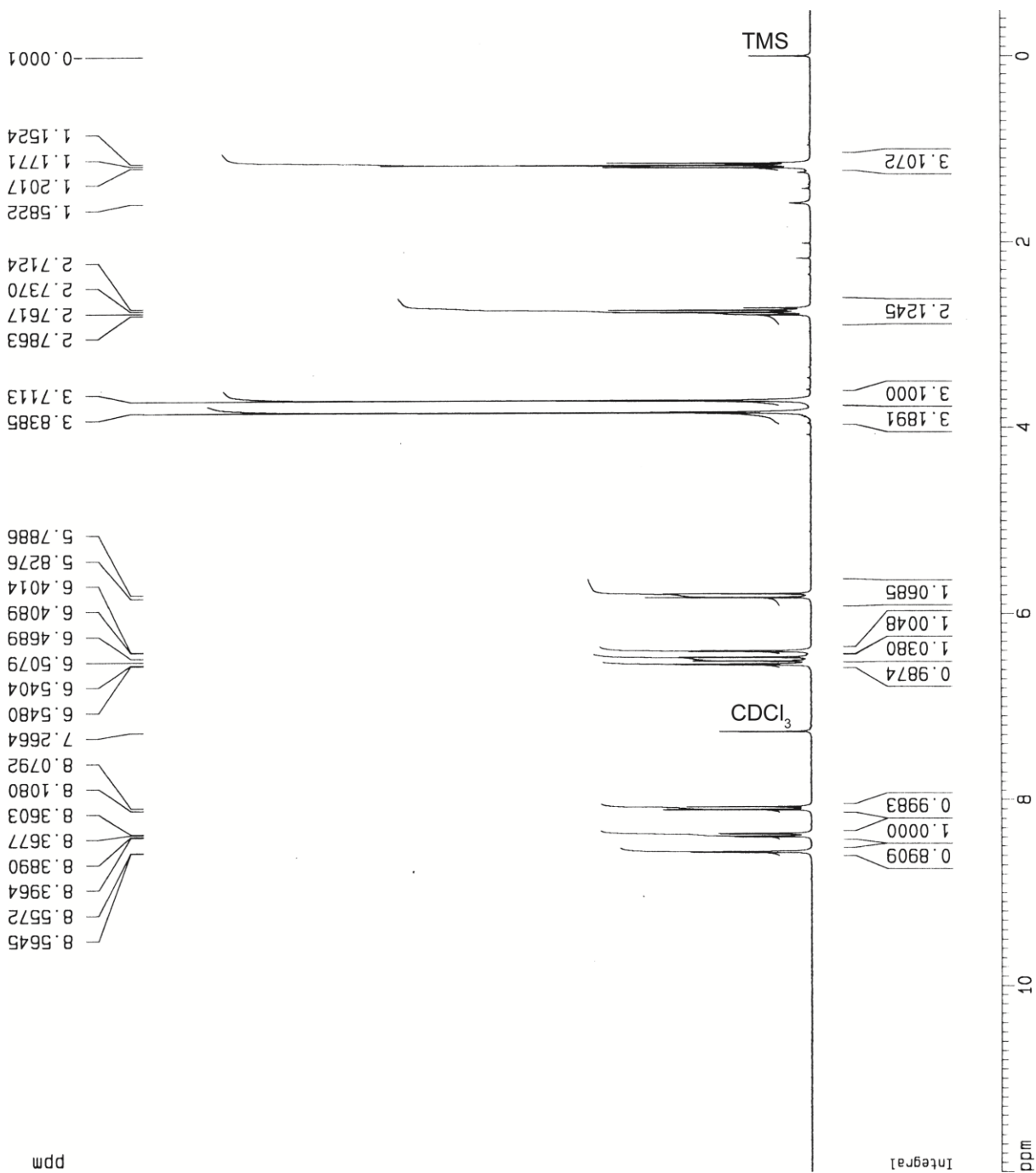
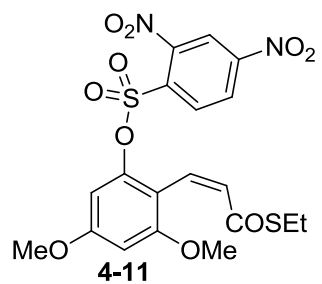


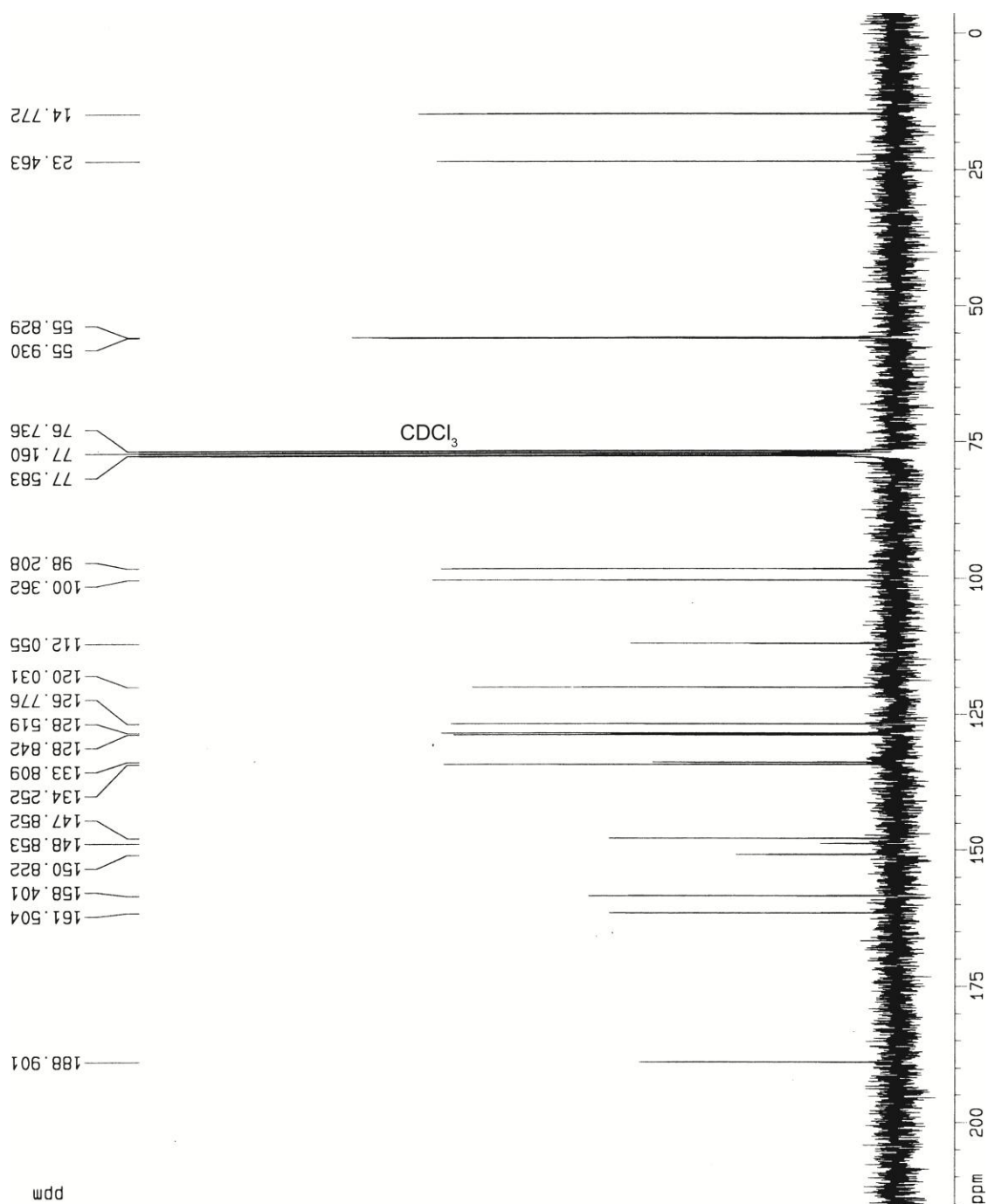
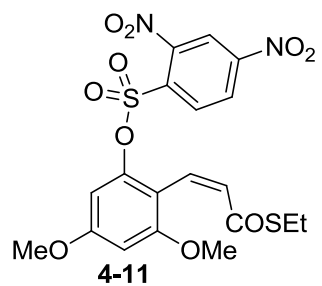


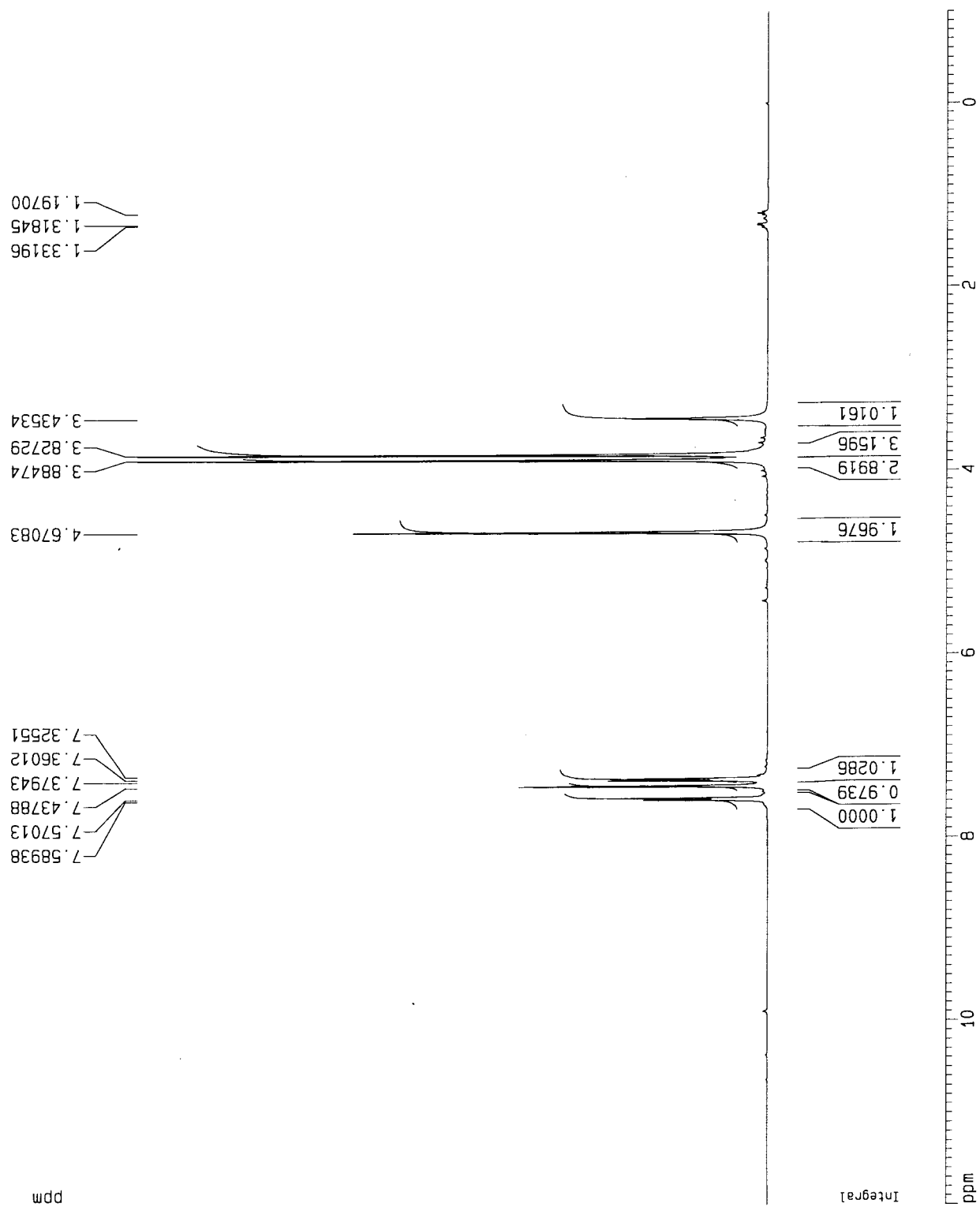
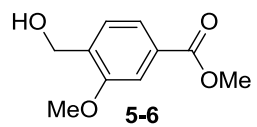


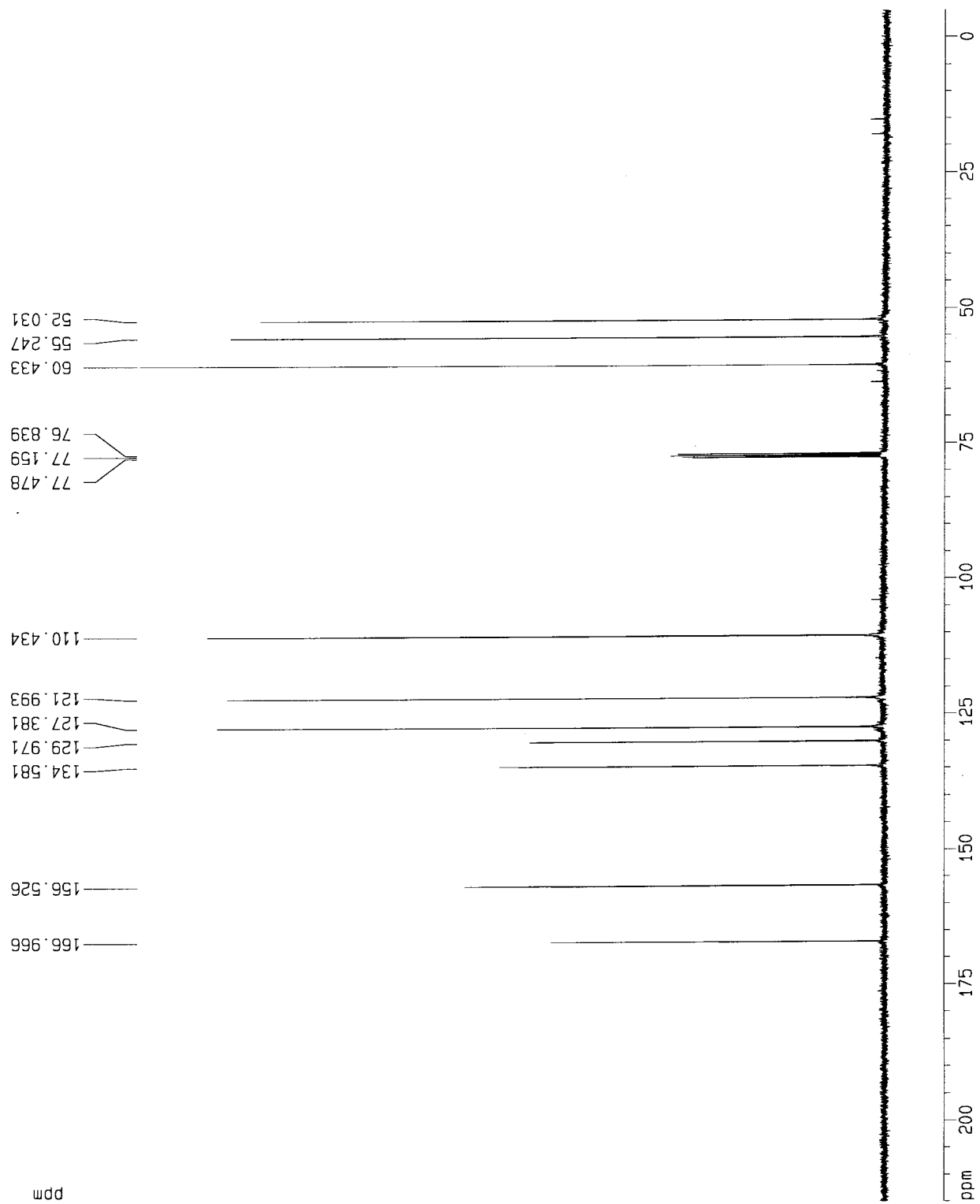
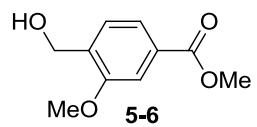


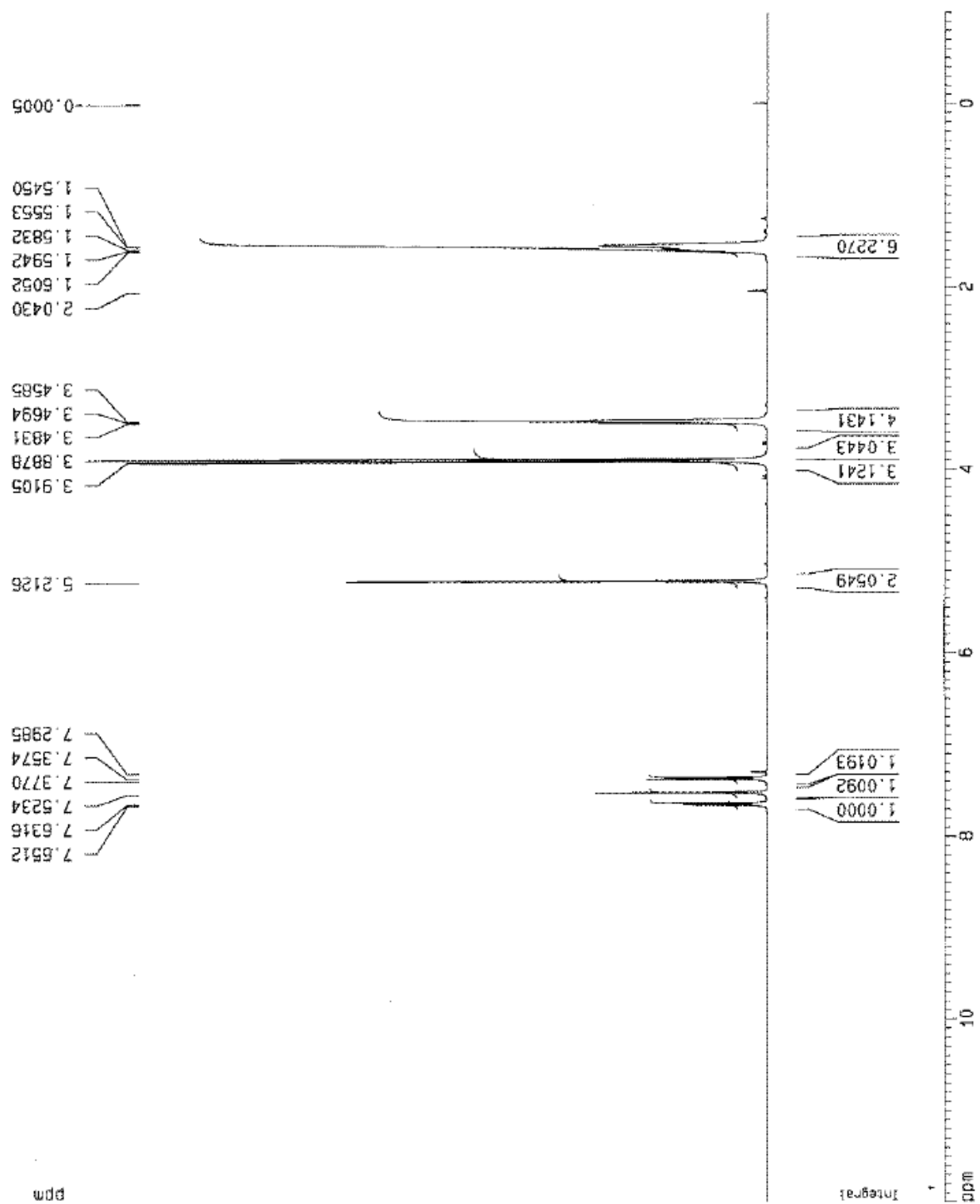
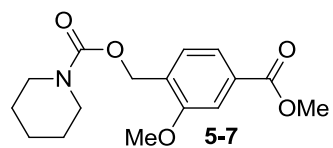


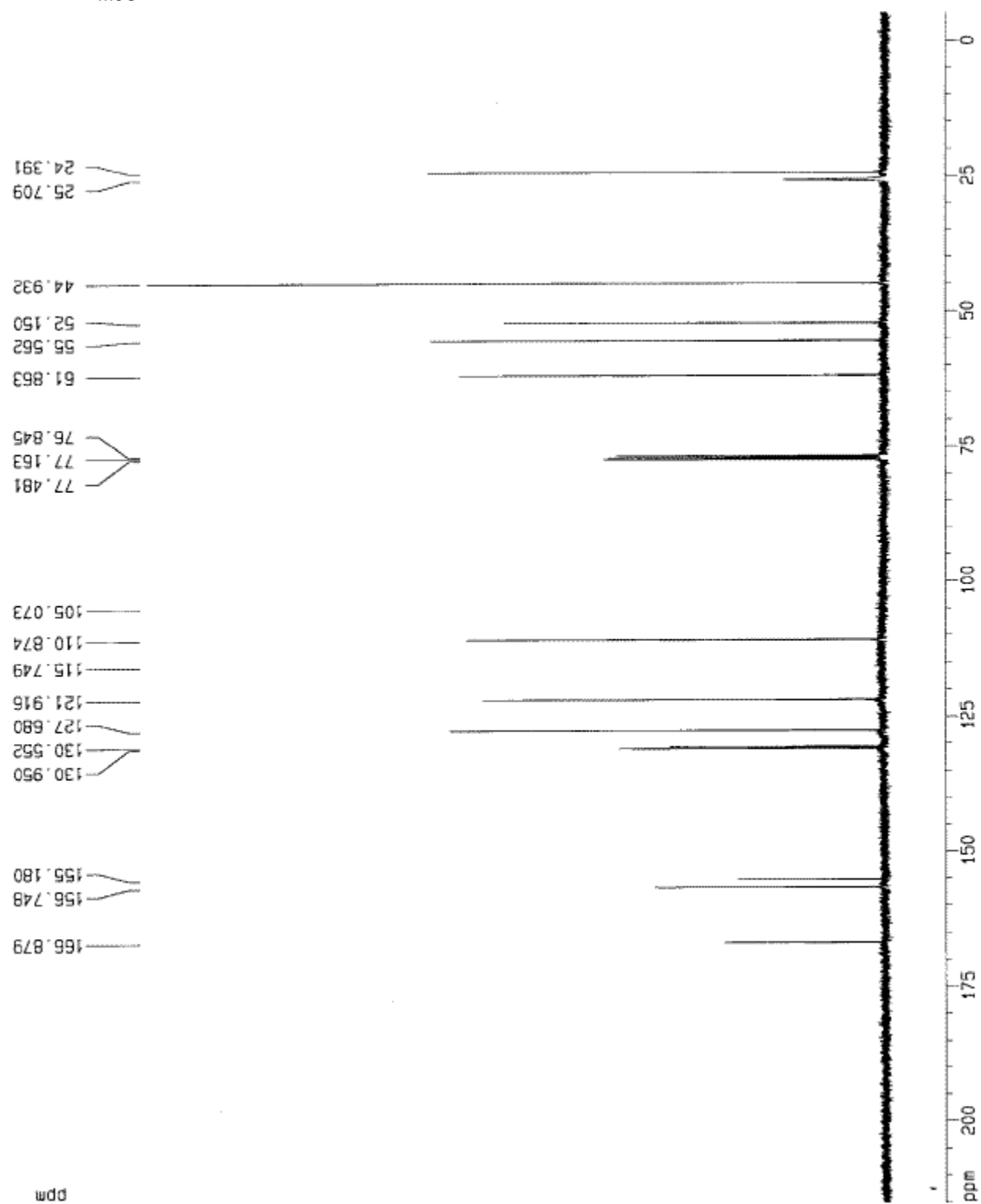
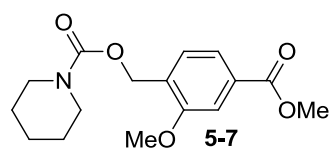


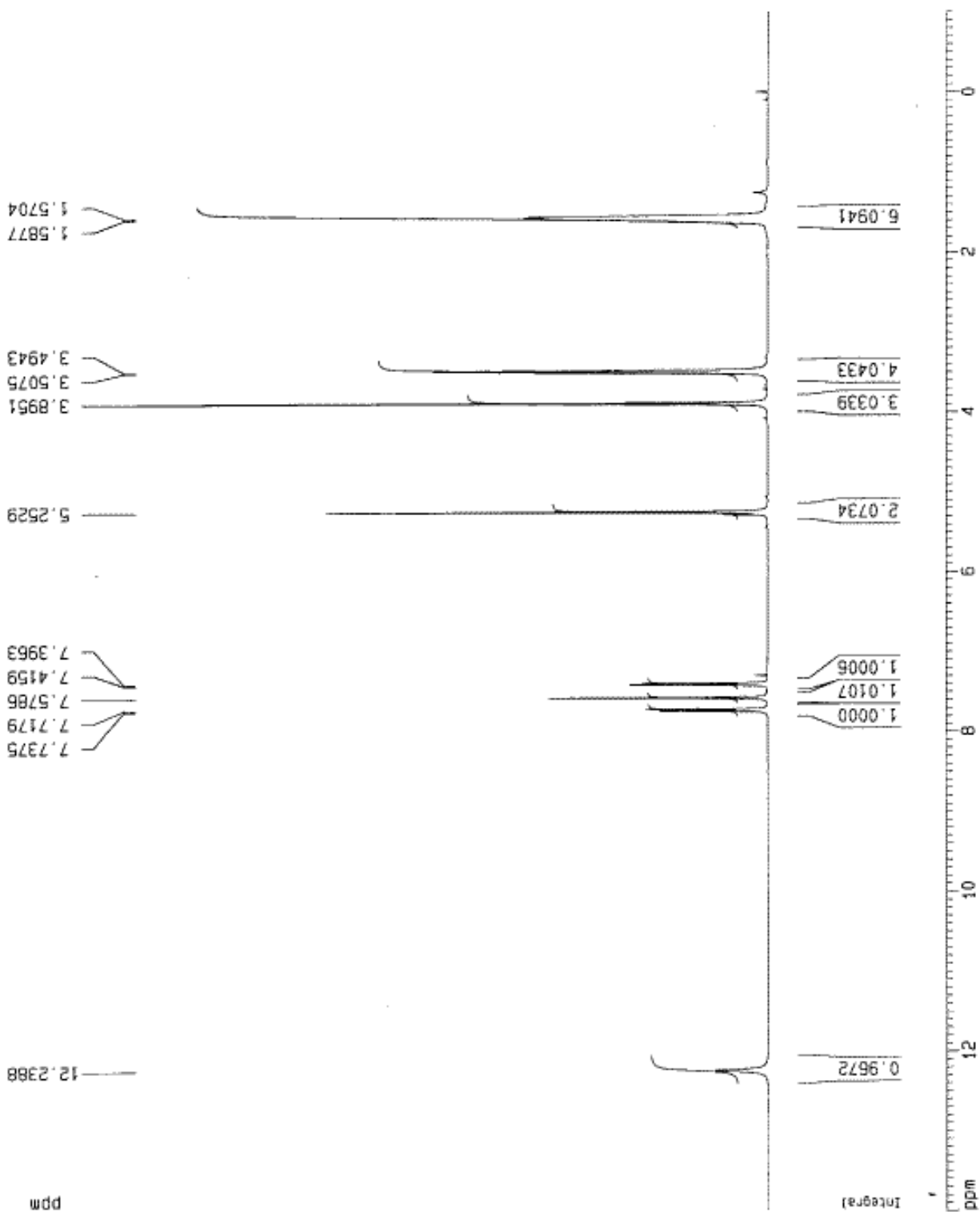
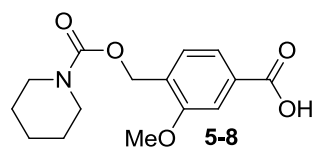


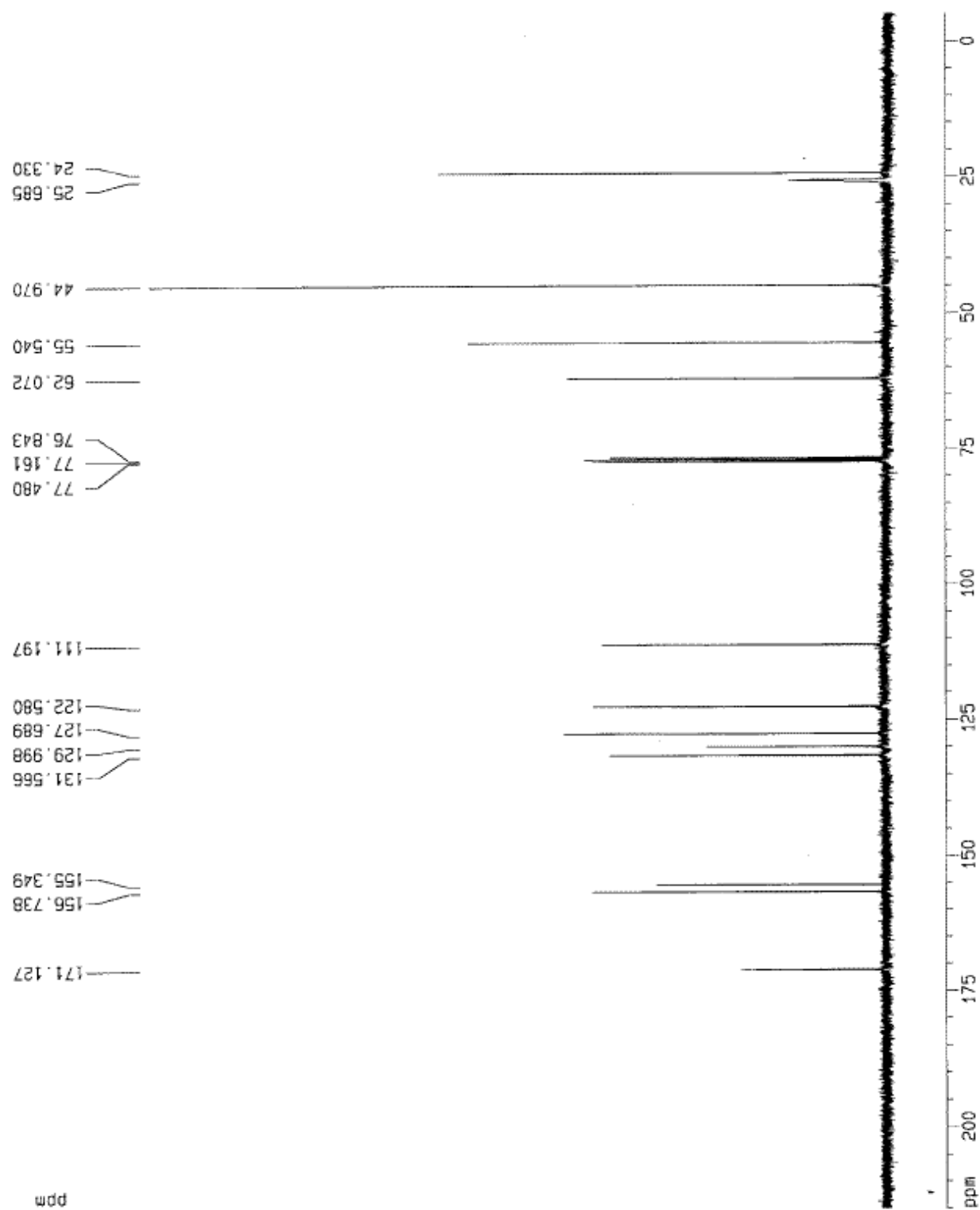
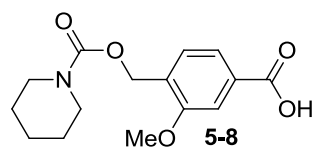


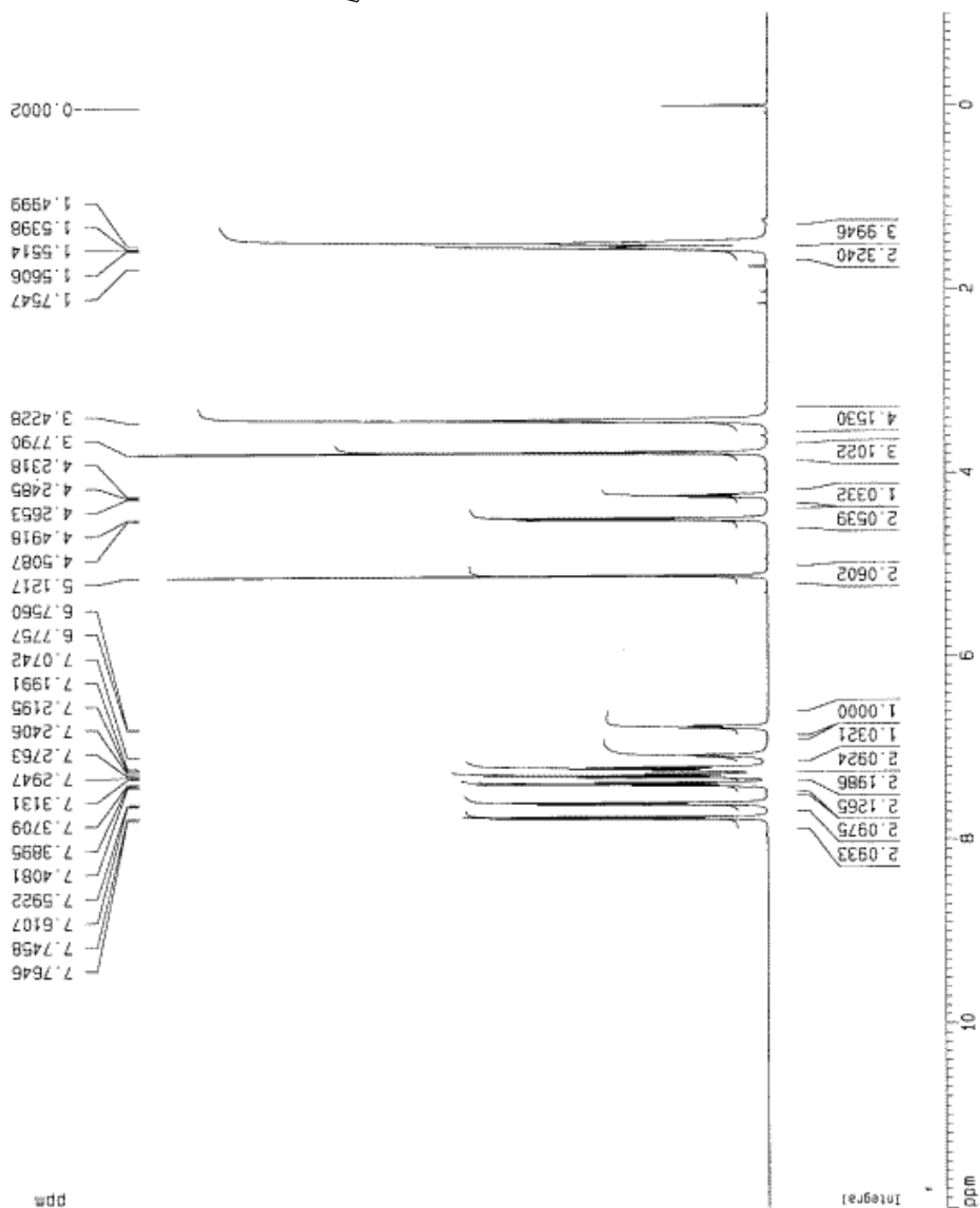
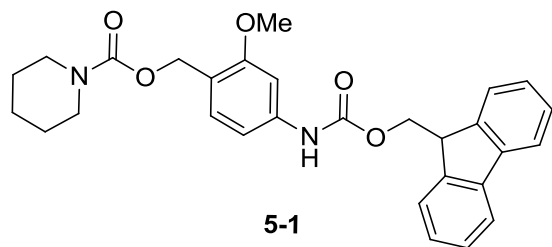


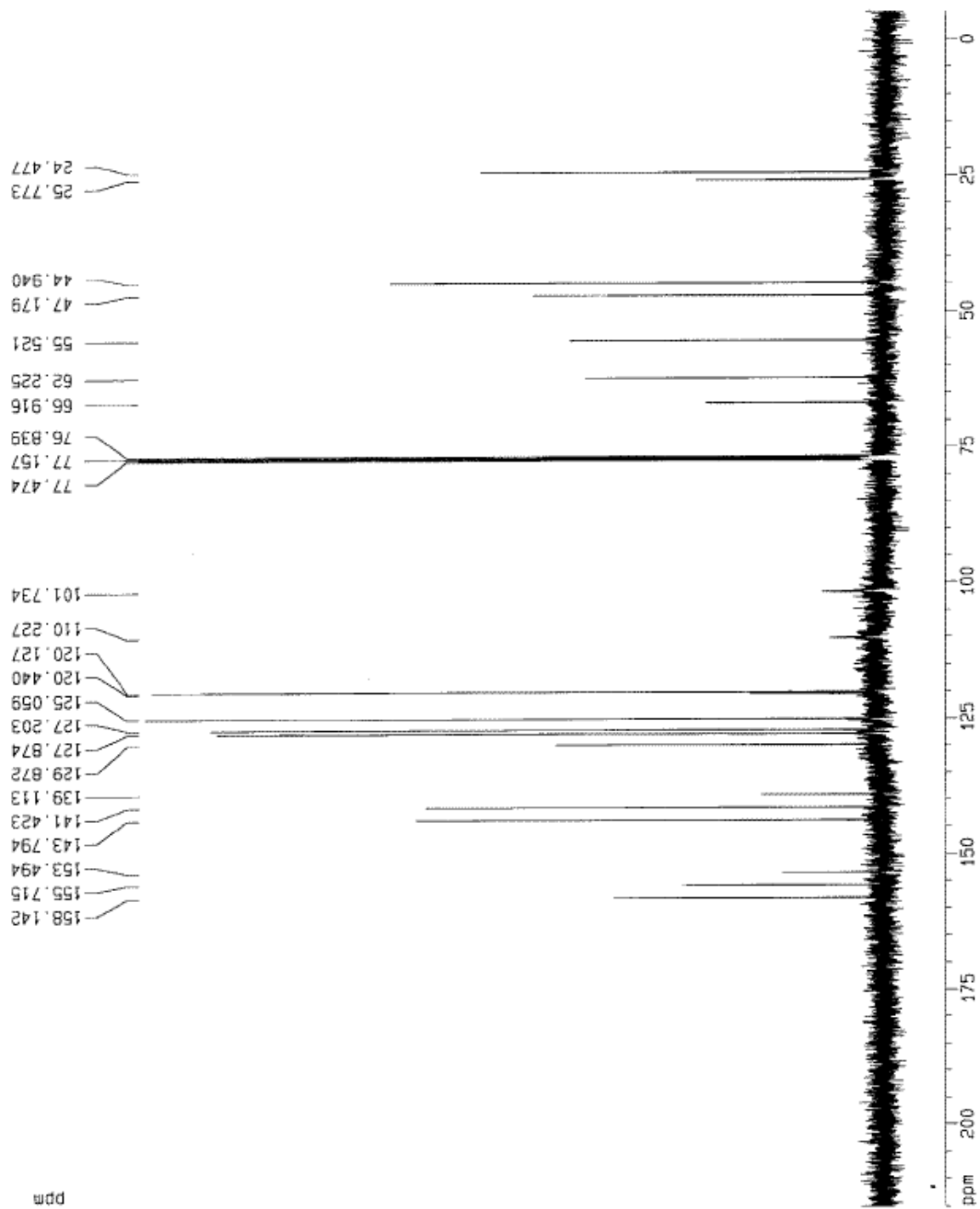
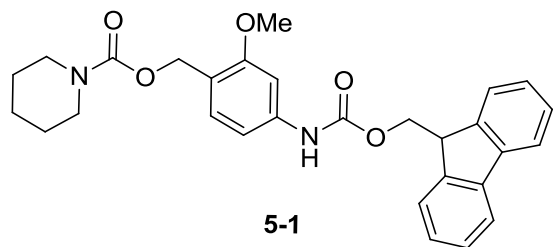


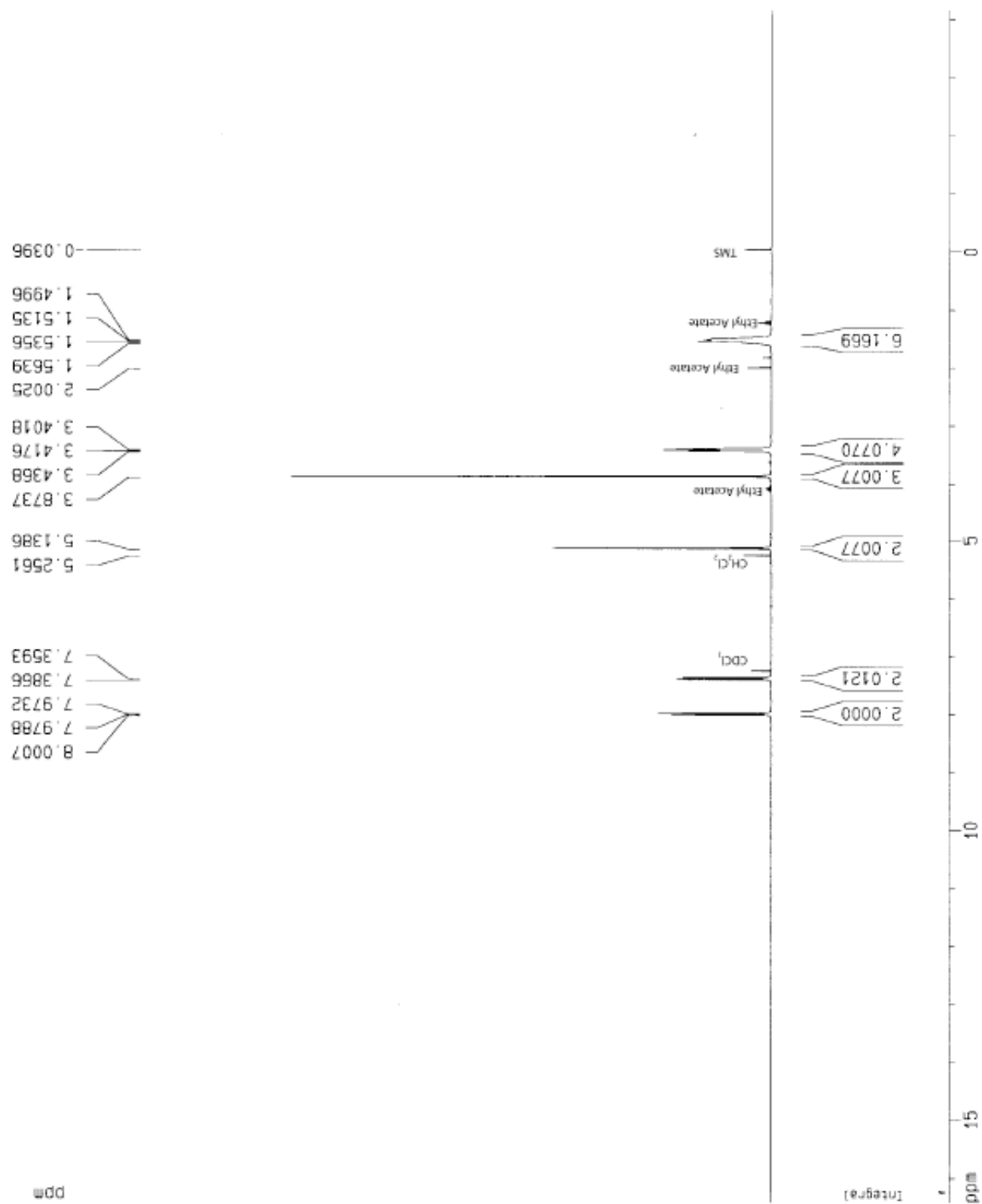
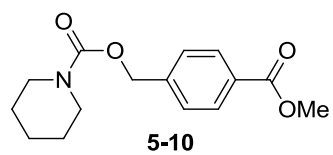


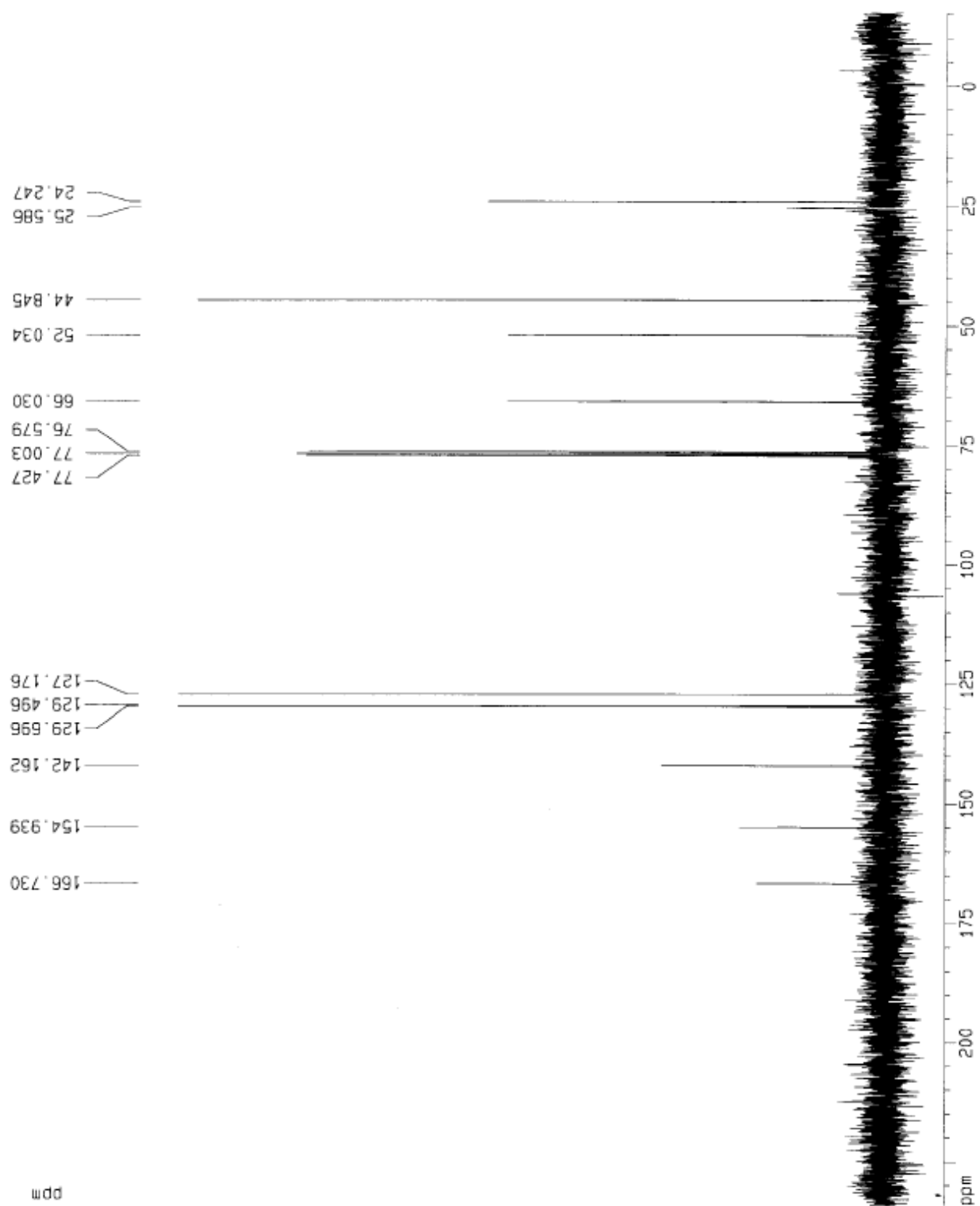
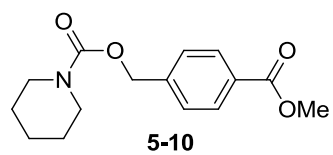


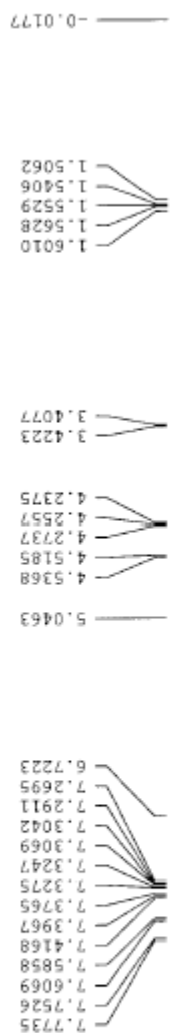
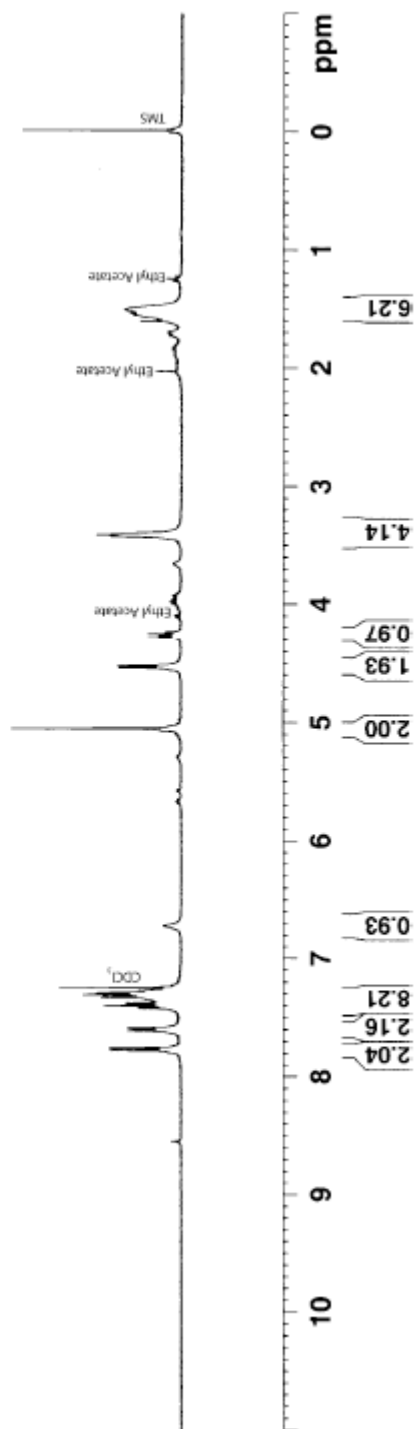
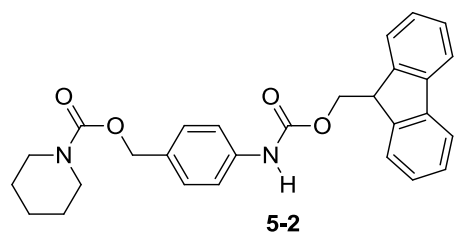


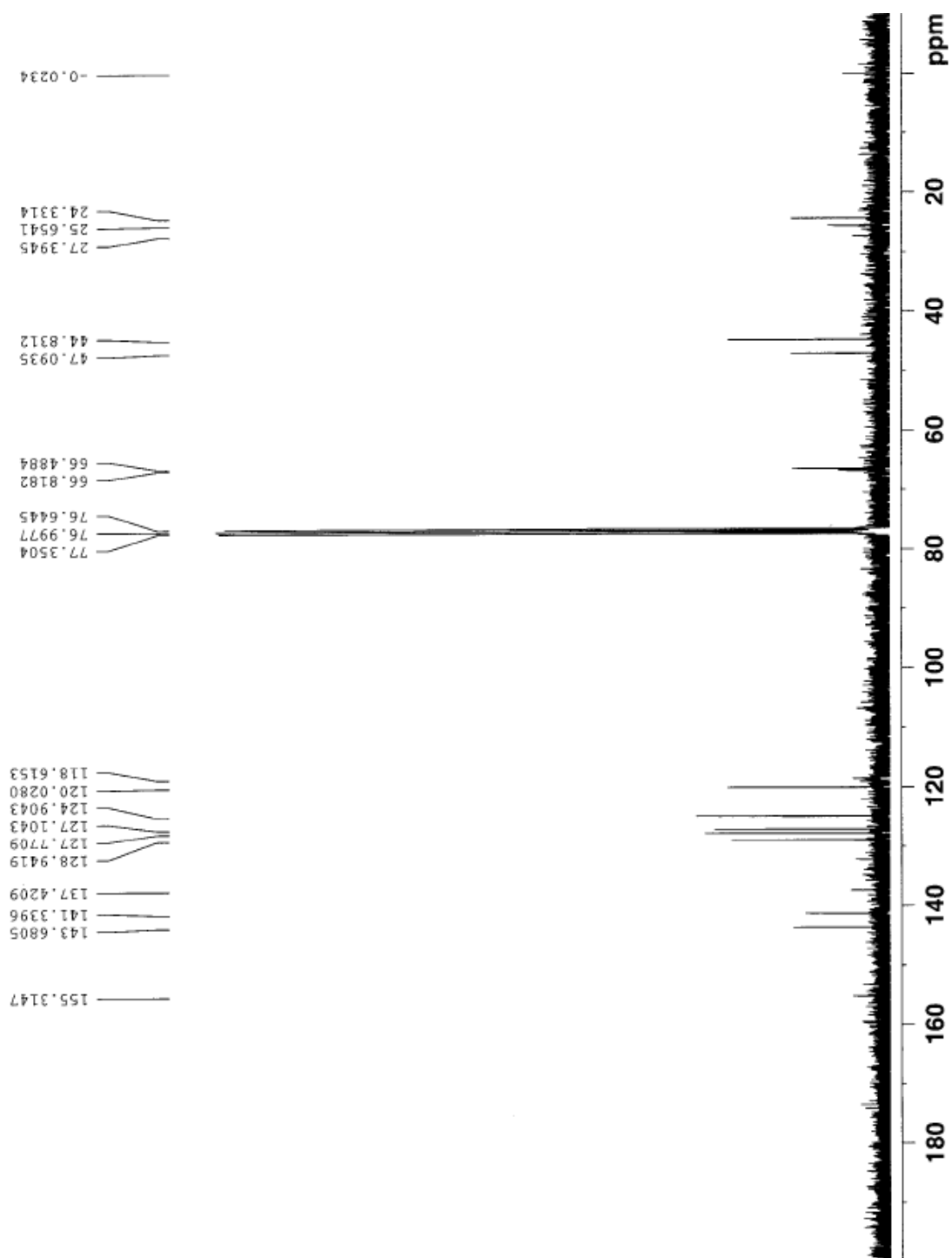
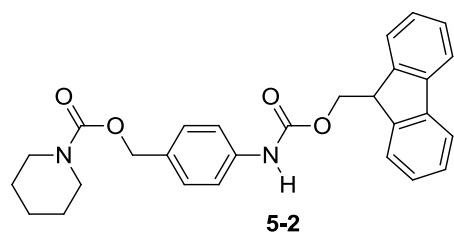


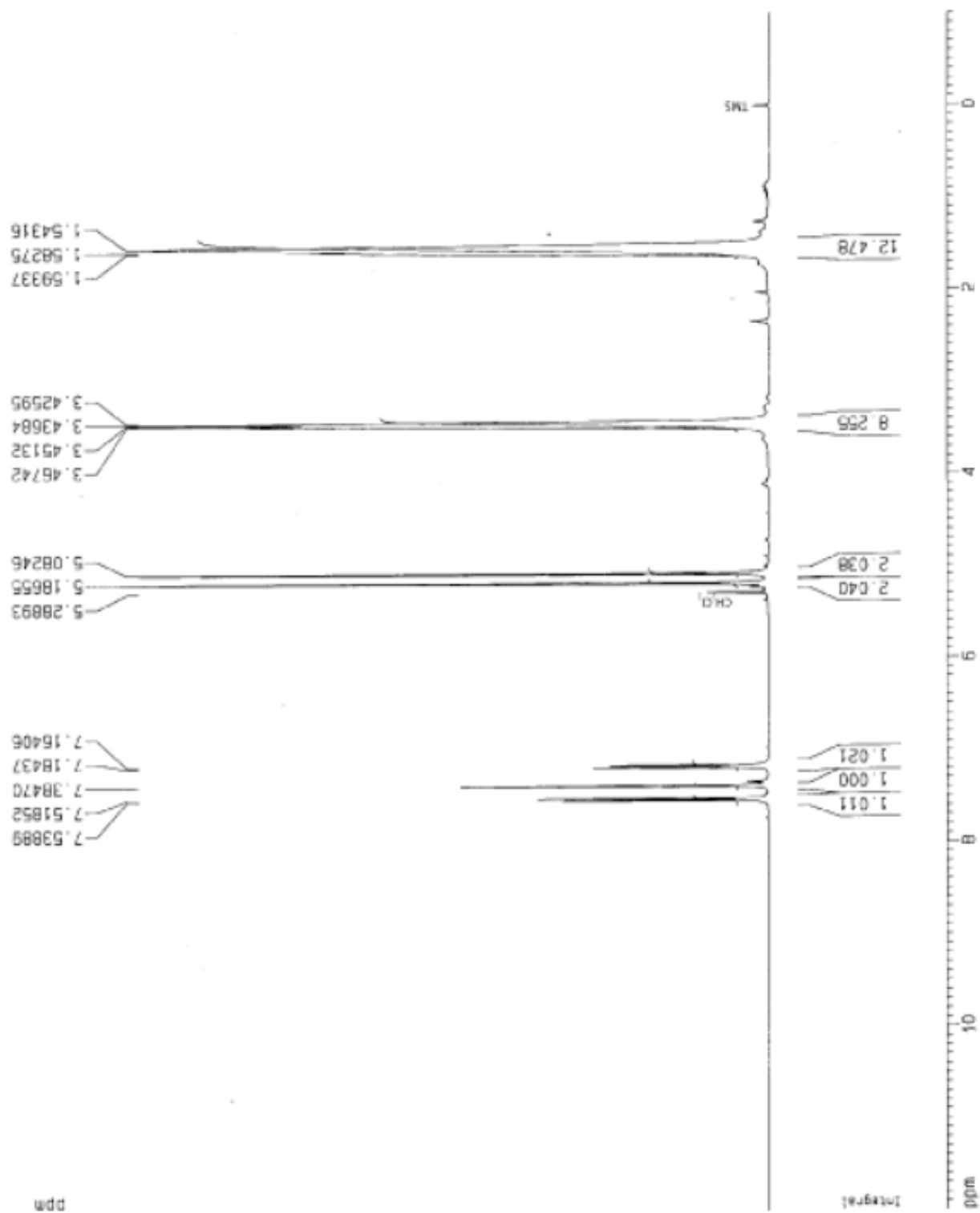
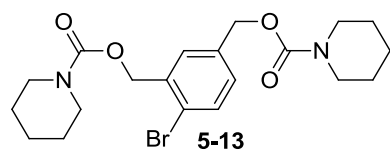


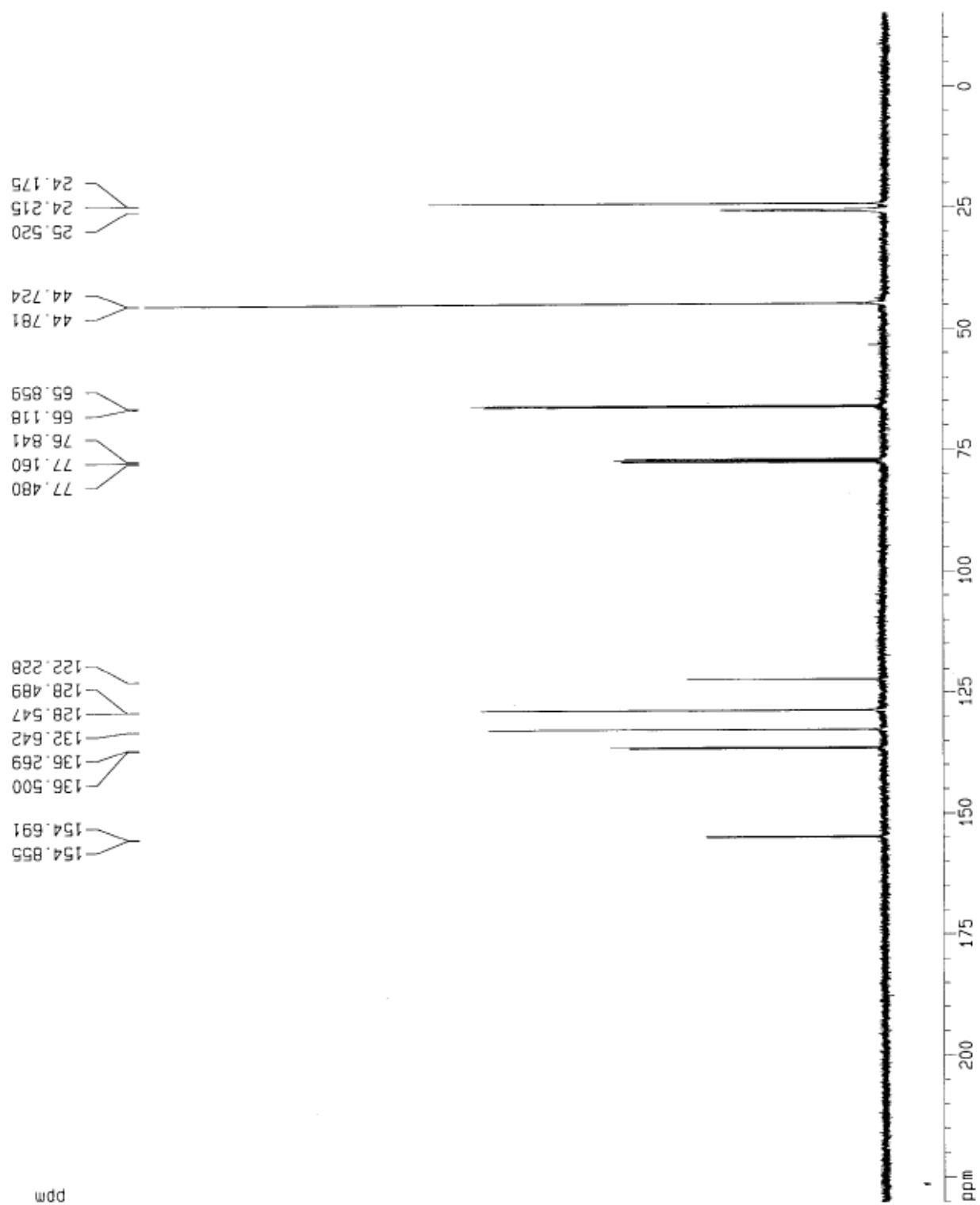
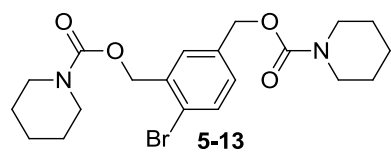


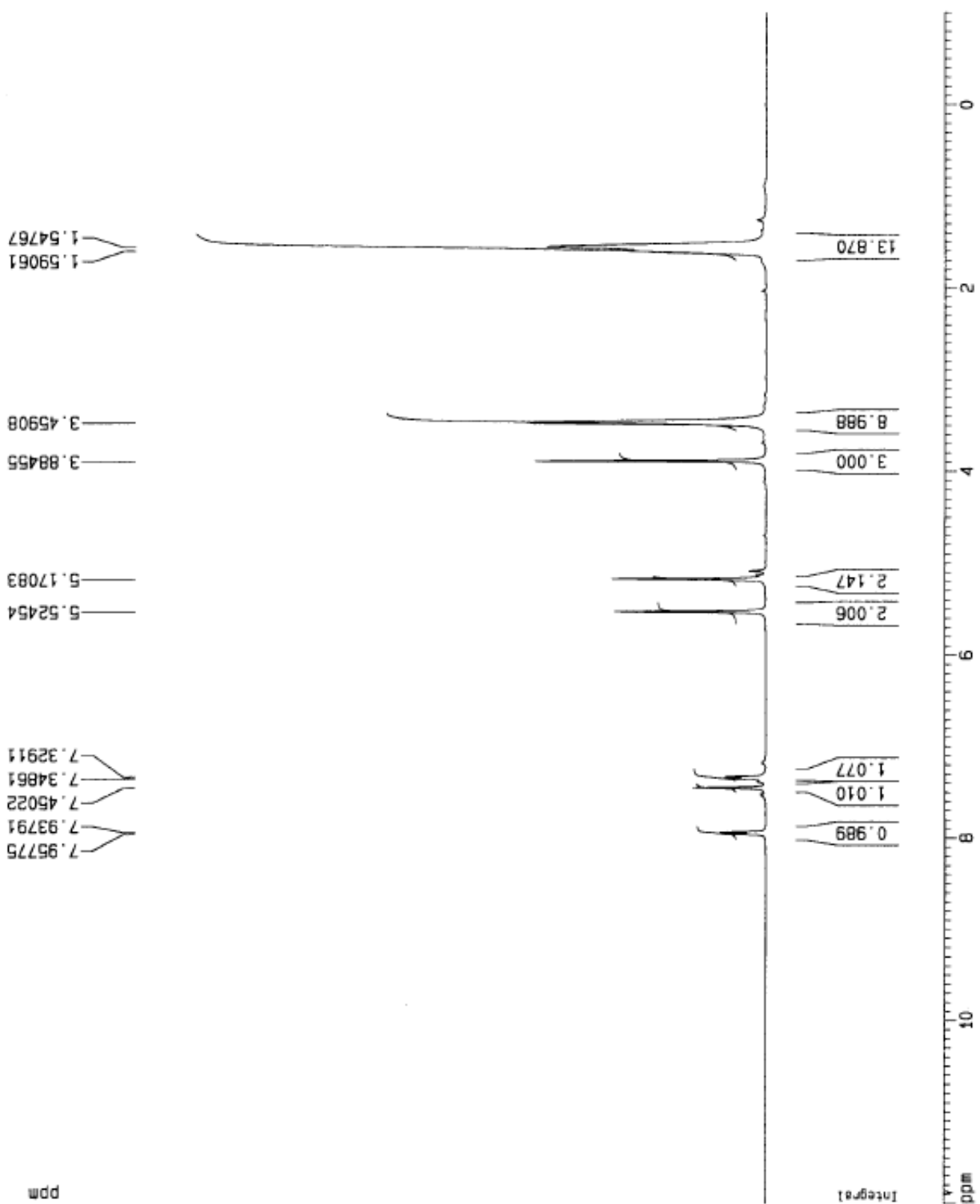
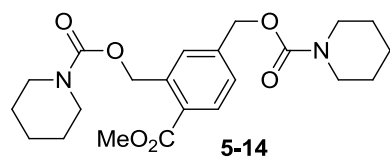


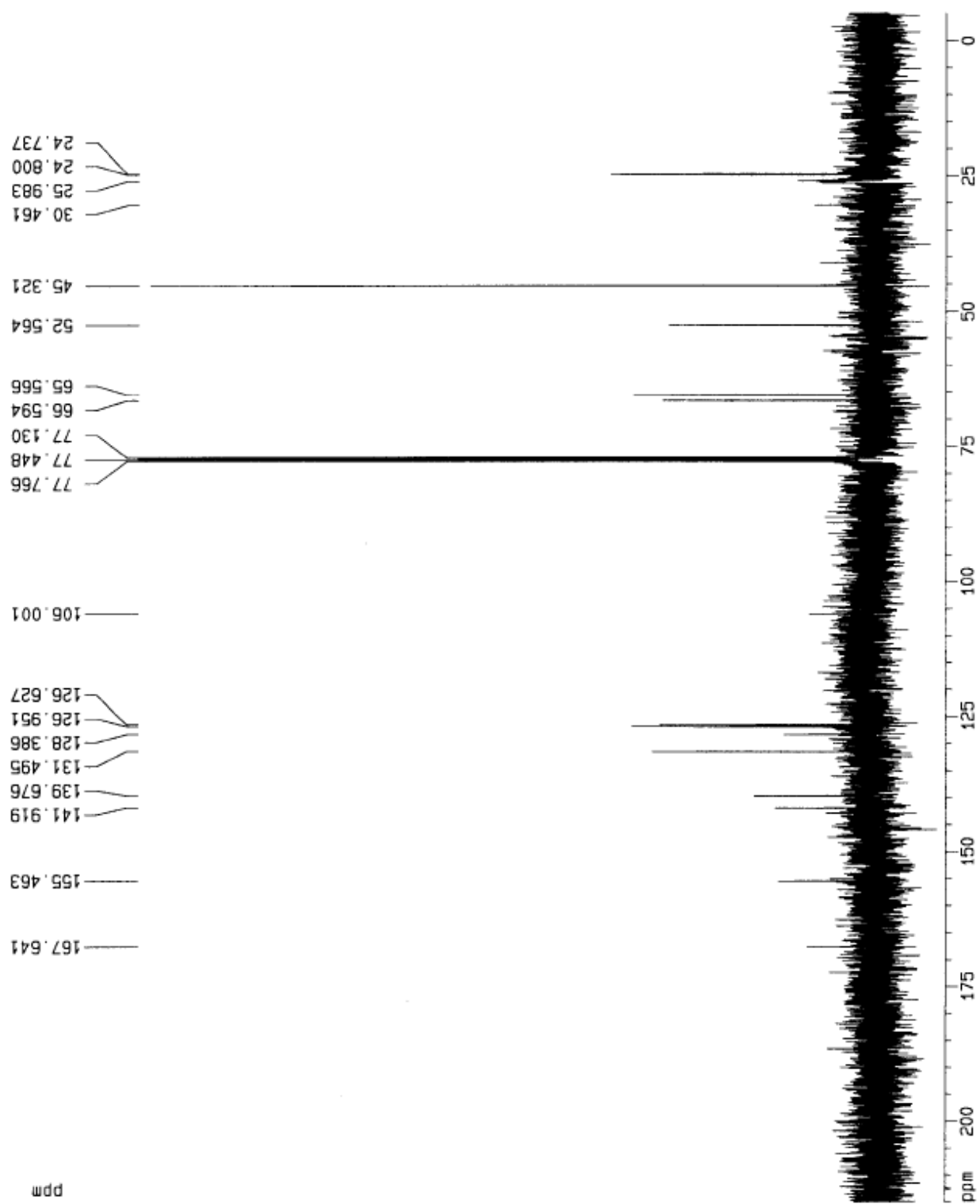
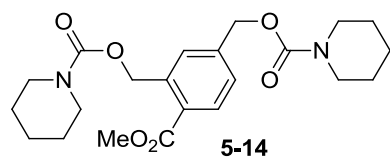


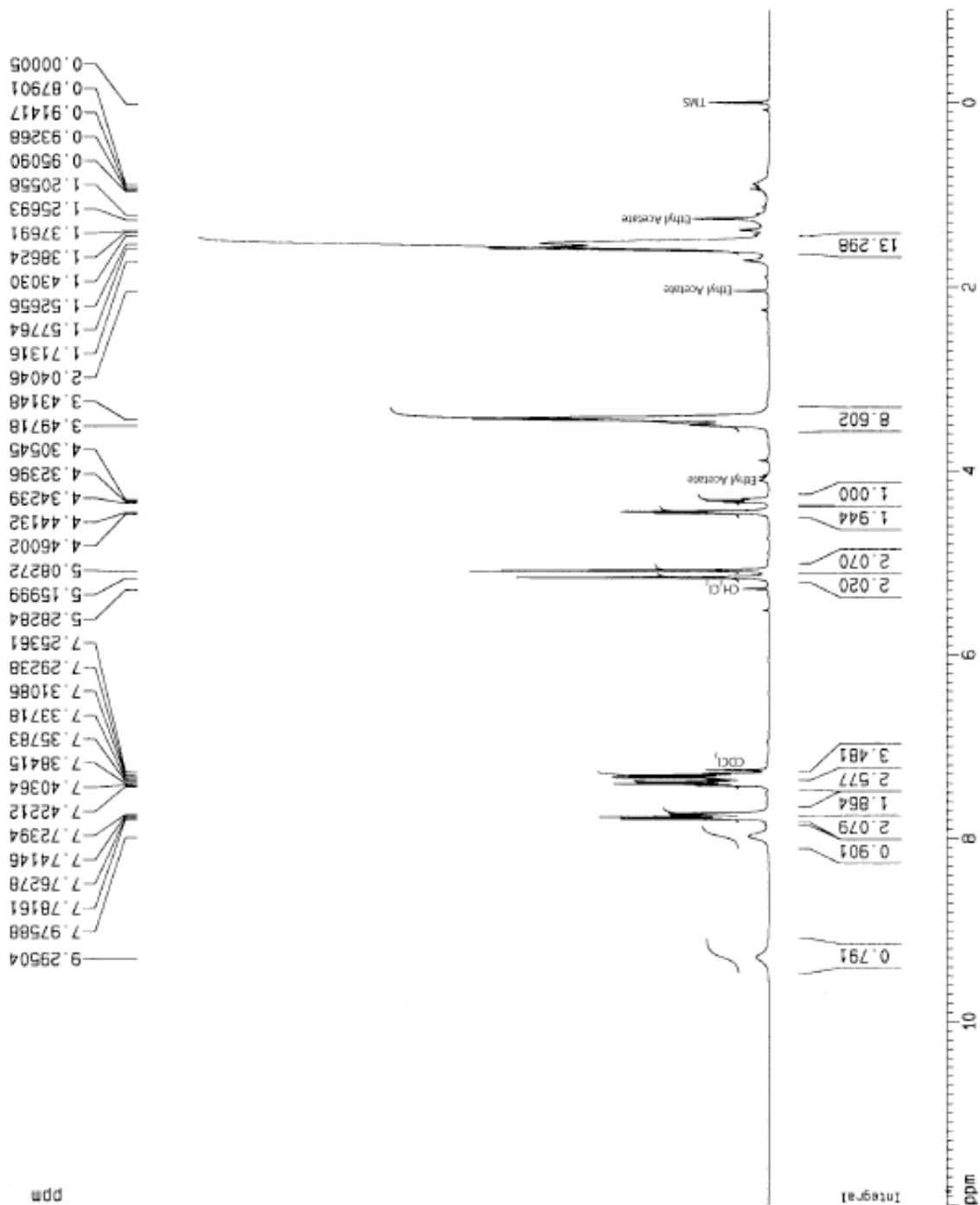
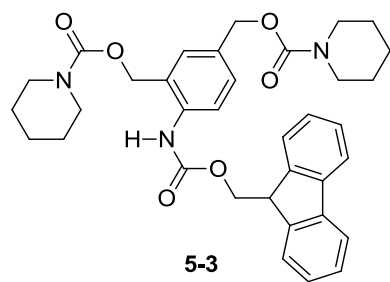


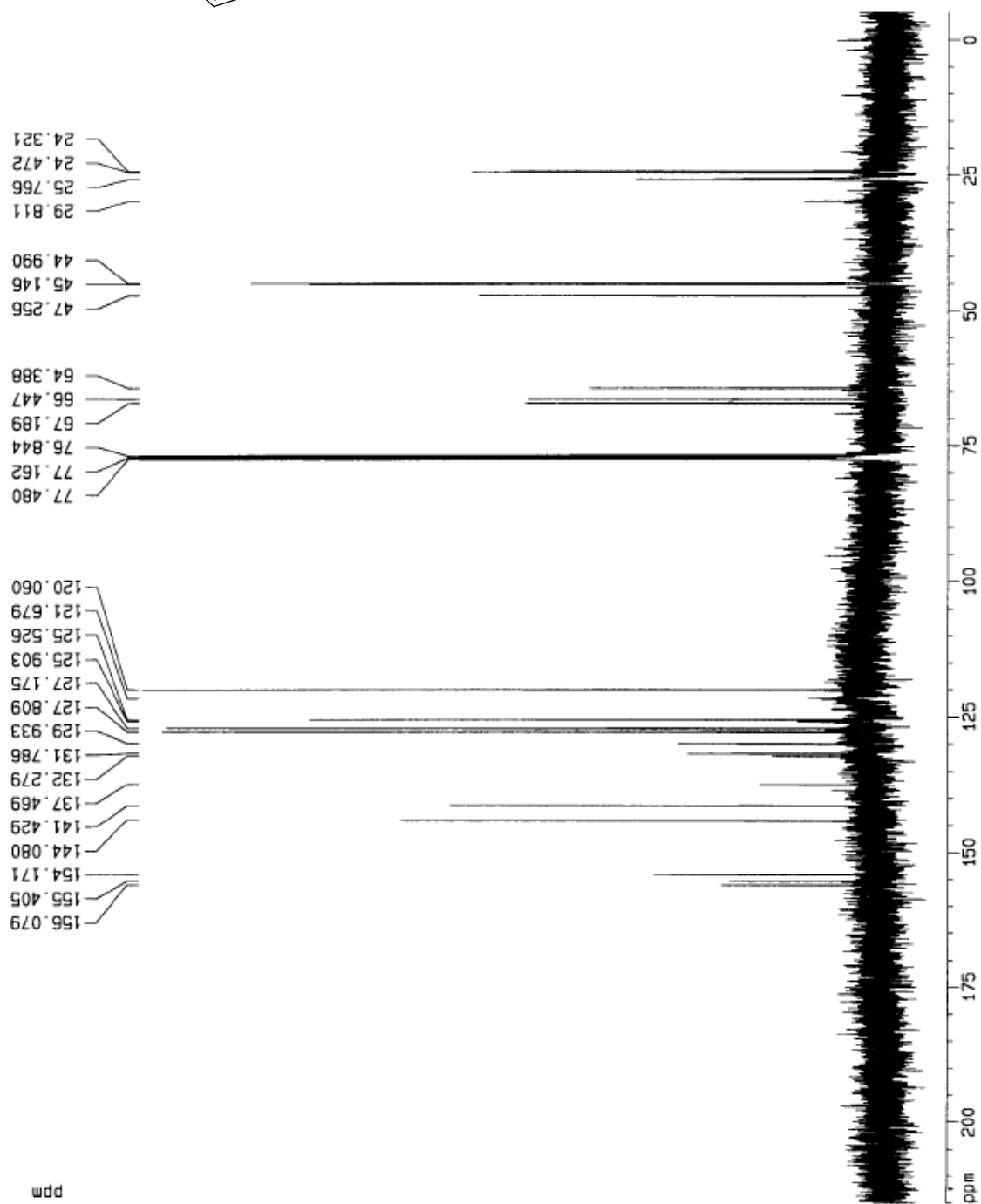
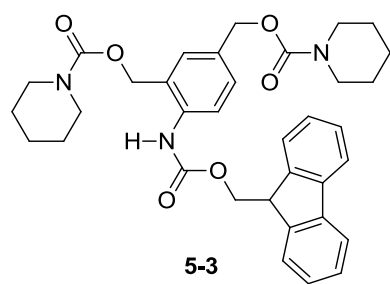


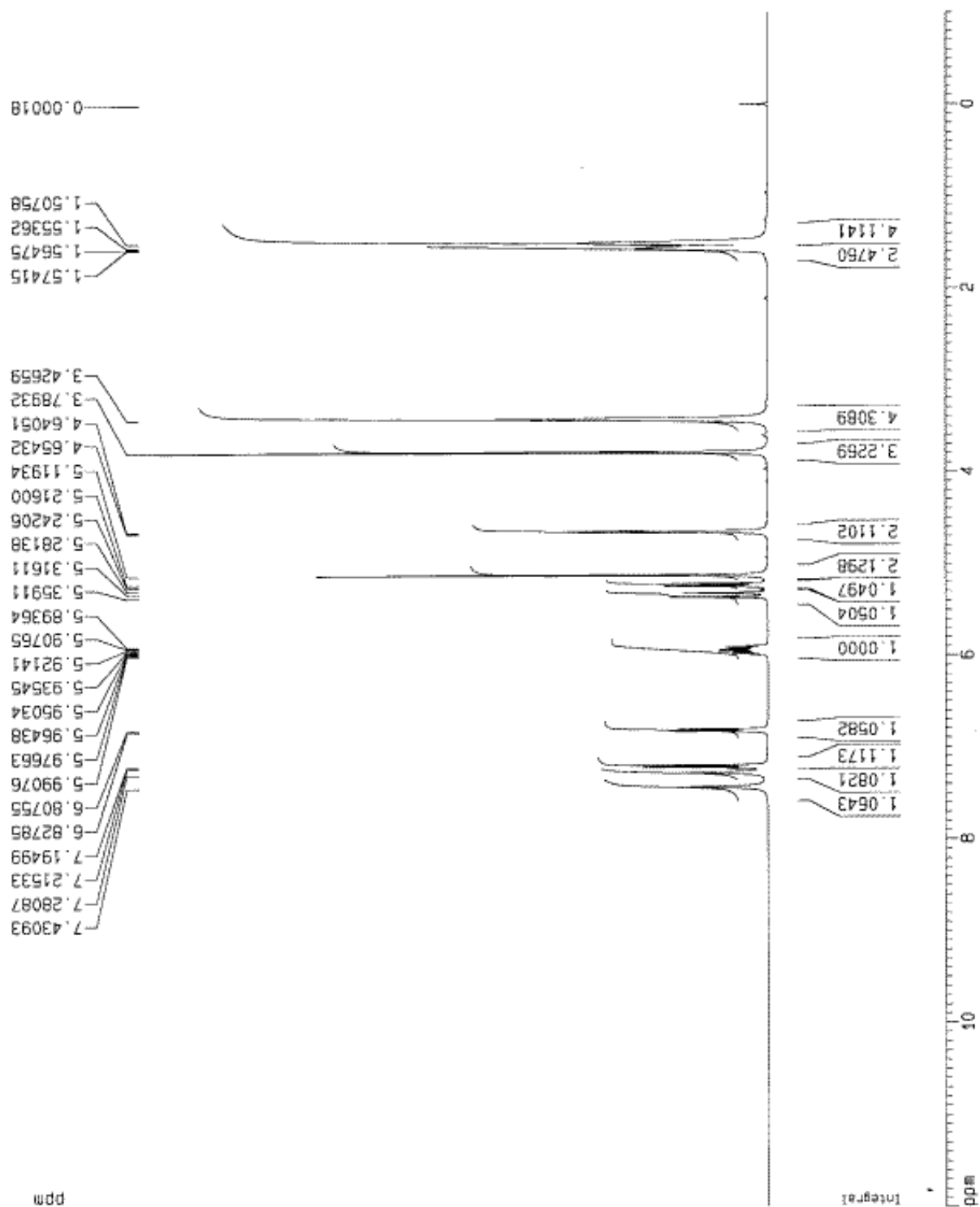
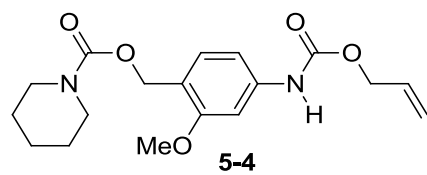


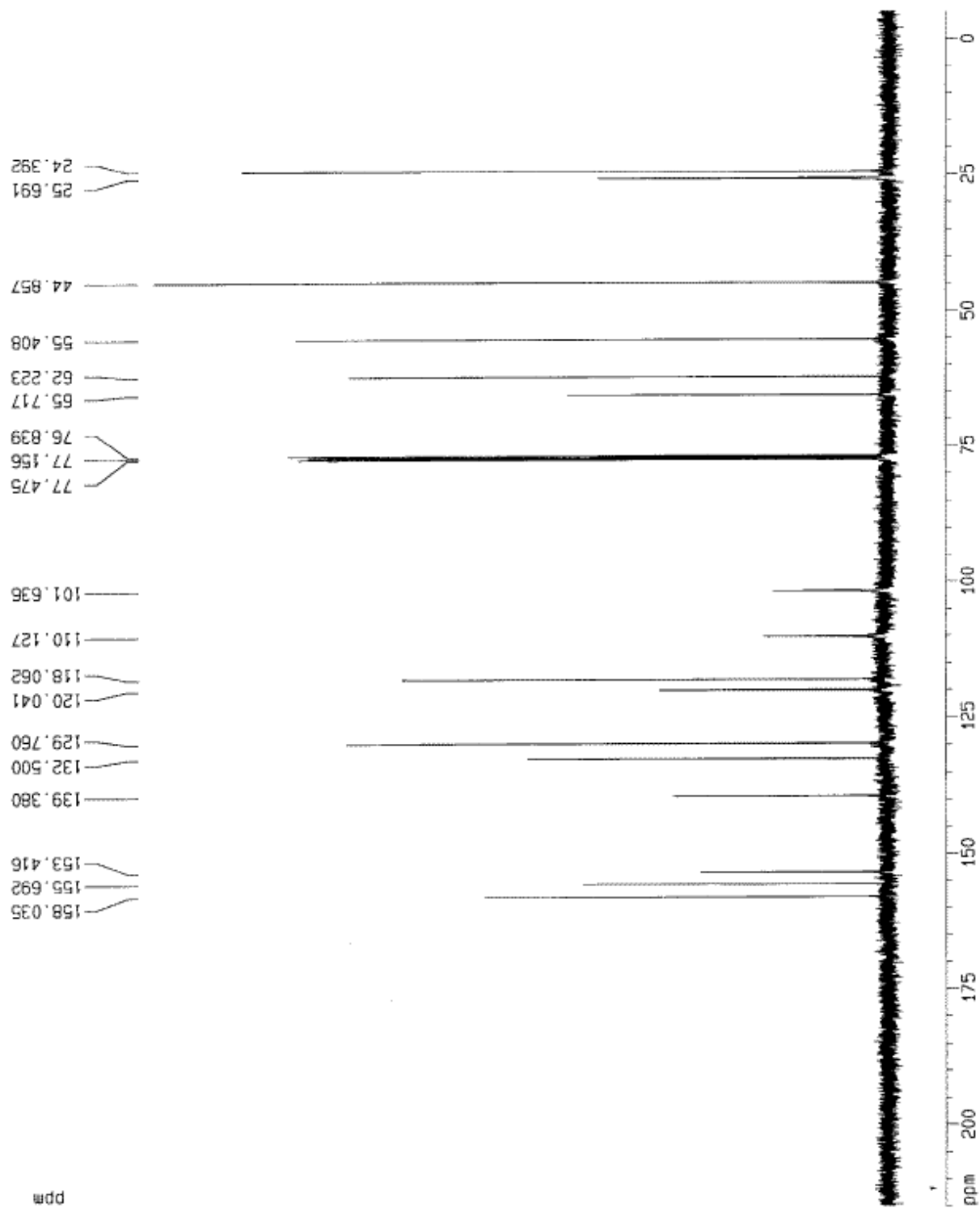
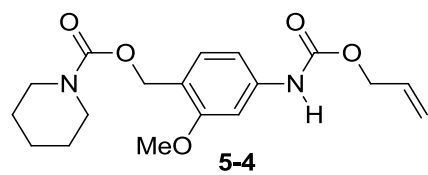












APPENDIX B: DATA TABLES

Chapter 2 data tables

Final glucose concentration in the assay mixture corresponding to Figure 2-3.

[β -galactosidase] / U mL ⁻¹	Meter Reading / mg dL ⁻¹		
	Trial 1	Trial 2	Trial 3
10.6	38	44	44
15.9	119	110	110
21.1	145	160	164
26.4	212	220	218
31.7	269	269	259
37.0	322	300	298

Final glucose concentration in the assay mixture corresponding to Figure 2-4.

[esterase] / U mL ⁻¹	Meter Reading / mg dL ⁻¹		
	Trial 1	Trial 2	Trial 3
2	195	194	190
4	199	199	191
12	218	212	211
20	237	243	250
40	277	276	264
80	383	392	370
120	481	491	497
160	559	569	544

Final glucose concentration in the assay mixture corresponding to Figure 2-5.

[alkaline phosphatase] / U L ⁻¹	Meter Reading / mg dL ⁻¹		
	Trial 1	Trial 2	Trial 3
40	62	56	57
60	105	102	110
100	172	182	164
200	310	327	314
300	416	425	416
400	481	487	473
500	528	552	514
600	578	575	575

Final glucose concentration in the assay mixture corresponding to Figure 2-6.

[PGA] / U mL ⁻¹	Meter Reading / mg dL ⁻¹		
	Trial 1	Trial 2	Trial 3
1	200	194	159
0.75	166	187	158
0.5	138	154	143
0.25	76	63	93
0.1	42	47	55
0.05	23	40	25

Final glucose concentration in the assay mixture corresponding to Figure 2-7.

[β-galactosidase] / U mL ⁻¹	Meter Reading / mg dL ⁻¹		
	Trial 1	Trial 2	Trial 3
0	99	96	96
1	96	98	95
5	107	101	100
10	107	112	113
15	124	121	117
20	125	123	126
30	143	152	141
50	178	181	164
100	259	260	269
160	390	374	361
200	420	419	428
260	502	504	503
300	534	548	512
340	593	551	598

Final glucose concentration in the assay mixture corresponding to Figure 2-8.

[alkaline phosphatase] / U L ⁻¹	Meter Reading / mg dL ⁻¹		
	Trial 1	Trial 2	Trial 3
0	92	87	99
2	109	110	104
4	118	115	117
6	125	130	126
8	144	141	137
10	157	175	165
20	217	229	218
30	281	271	268
40	320	328	310
60	418	407	399
80	456	462	455
100	511	505	499
120	535	534	561
140	559	573	551
160	564	585	574

Final glucose concentration in the assay mixture corresponding to Figure 2-9.

[PGA] / U mL ⁻¹	Meter Reading / mg dL ⁻¹		
	Trial 1	Trial 2	Trial 3
0.00	116	119	117
0.02	137	135	133
0.03	154	130	155
0.04	154	150	156
0.05	154	149	162
0.06	160	162	161
0.08	175	176	181
0.08	184	178	180
0.10	182	194	195
0.12	187	189	197
0.30	219	198	245
0.60	251	245	215
1.01	251	272	265

Final glucose concentration in the assay mixture corresponding to Figure 2-10

[ALP] [*] / U L ⁻¹	Meter Reading / mg dL ⁻¹		
	Trial 1	Trial 2	Trial 3
0	144	137	140
2	154	149	146
4	159	156	163
6	168	173	166
8	176	176	183
10	187	195	192
20	231	256	248
30	274	258	264
40	277	311	312
60	336	334	355
80	418	423	411
100	450	454	455
120	466	471	468
140	502	509	511
160	539	512	517

* [ALP] refers to the concentration of ALP in spiked serum sample.

Final glucose concentration in the assay mixture corresponding to Table 2-1

Serum Sample*	Meter Reading / mg dL ⁻¹					
	Negative Control			Test Sample		
	Trial 1	Trial 2	Trial 3	Trial 1	Trial 2	Trial 3
1	140	141	144	242	230	253
2	350	354	350	437	436	445
3	263	269	279	348	354	351

* Serum 1 refers to commercial horse blood serum. Serum samples 2 and 3 were prepared by adding 0.72 and 0.36 mg D-glucose to 600 μ L of commercial horse blood serum respectively.

Final glucose concentration in the assay mixture corresponding to Table 2-2

Time of assay	[PGA] / U mL ⁻¹	Meter Reading / mg dL ⁻¹			*Calculated [PGA] / U mL ⁻¹
		Trial 1	Trial 2	Trial 3	
Day 0	0.06	169	176	167	0.07 \pm 0.01
Day 7	0.06	155	154	151	0.05 \pm 0.00

* Calculated using the equation of the calibration curve in Figure 2-9 (inset) ($y = 121 + 709x$)

Chapter 3 data tables

Fluorescence emission intensity of the assay mixture corresponding to Figure 3-6.

[H ₂ O ₂] / μ M	Fluorescence emission intensity at 510 nm (I - I ₀)		
	Trial 1	Trial 2	Trial 3
0	0.00	0.00	0.00
1	1.97	1.81	2.18
2	3.92	3.90	4.02
3	5.71	6.03	6.47
4	7.44	7.71	7.95
6	12.08	12.33	12.83
8	16.92	15.66	16.11
10	18.94	18.47	18.64
20	42.52	48.49	39.87
30	62.61	61.67	61.22
40	77.14	81.51	77.58
50	109.02	100.09	99.33
60	124.12	115.49	112.13
70	143.32	134.19	132.23
80	151.42	148.39	142.93
90	164.92	157.99	151.33
100	174.92	171.19	172.63

Fluorescence emission intensity of the assay mixture corresponding to Figure 3-8a.

[β -Galactosidase] / nM	Fluorescence intensity at 510 nm (I - I ₀)		
	Trial 1	Trial 2	Trial 3
0	0	0	0
25	0.88	1.741	1.603
50	1.97	3.2663	3.579
75	4.87	6.811	4.909
100	7.44	9.391	6.671
200	16.06	12.261	14.061
300	18.68	22.081	21.361
400	23.88	29.061	25.931
500	29.76	34.151	31.811

Fluorescence emission intensity of the assay mixture corresponding to Figure 3-8b.

[ALP] / U·L ⁻¹	Fluorescence emission intensity at 510 nm (I – I ₀)		
	Trial 1	Trial 2	Trial 3
0	0.0000	0.0000	0.0000
10	0.4290	0.3330	0.3610
25	0.7760	0.7400	0.6520
50	1.1740	1.1790	1.0590
75	1.6220	1.5950	1.4250
100	2.4170	2.0290	2.0830
250	4.6400	4.3120	4.3220
500	7.8790	7.5010	7.6030
750	11.189	10.131	10.733
1000	13.879	14.301	14.023

Data obtained for the smell-based assay for the detection of β -D-galactosidase (16 out of 20 samples were identified correctly by smell alone)

Test no.	[β -galactosidase] / nM	Response
1	200	yes
2	200	no
3	200	yes
4	200	yes
5	200	yes
6	200	yes
7	200	yes
8	200	yes
9	200	yes
10	200	yes
11	0	no
12	0	no
13	0	yes
14	0	no
15	0	yes
16	0	no
17	0	no
18	0	no
19	0	no
20	0	yes

Data obtained for the smell-based assay for the detection of ALP (14 out of 20 samples were identified correctly by smell alone)

Test no.	[ALP] / U L ⁻¹	Response
1	100	yes
2	100	yes
3	100	yes
4	100	no
5	100	no
6	100	yes
7	100	no
8	100	yes
9	100	yes
10	100	yes
11	0	no
12	0	no
13	0	yes
14	0	no
15	0	no
16	0	yes
17	0	no
18	0	yes
19	0	no
20	0	no

Chapter 4 data tables

Fluorescence emission intensities corresponding to Figure 4-11

Fluorescence data for the assay containing 2 mM of **4-11** and 2 mM of ethanethiol in 1:1 CH₃CN-0.1 M HEPES buffer, pH 7.4, 1 mM EDTA.

Time(h)	Normalized fluorescence intensity		
	Trial 1	Trial 2	Trial 3
0.1	4.3	3.9	4.5
0.3	12.4	11.9	13.2
0.4	20.5	19.0	20.2
0.6	27.3	26.4	26.5
0.8	34.8	33.5	33.6
1.0	39.8	39.5	39.9
1.3	47.1	46.3	49.2
1.7	55.8	52.0	55.7
2.0	61.0	58.7	59.1
2.5	65.5	62.4	66.0
3.0	70.5	71.8	72.7
4.0	81.8	82.1	80.8
5.5	88.2	89.1	93.2
7.0	98.9	96.5	96.5
9.9	100.0	98.9	100.0
17.0	97.5	100.0	97.3

Fluorescence data for the assay containing 2 mM of **4-11** and 0.6 mM of ethanethiol in 1:1 CH₃CN-0.1 M HEPES buffer, pH 7.4, 1 mM EDTA.

Time(h)	Normalized fluorescence intensity		
	Trial 1	Trial 2	Trial 3
0.2	2.4	2.3	2.4
0.5	7.9	8.1	8.2
1.0	15.1	13.6	14.1
1.5	22.0	22.1	21.1
2.0	27.7	26.6	26.6
2.5	33.5	34.4	31.9
3.0	36.6	39.1	38.9
4.0	45.9	45.2	48.3
6.1	62.9	63.2	60.5
8.0	75.9	75.6	72.9
10.0	81.8	81.4	81.2
12.0	90.4	91.4	87.2
14.0	91.7	95.0	90.4

17.0	96.6	96.5	90.3
20.0	97.1	100.0	100.0
23.0	100.0	97.5	98.2

Fluorescence data for the assay containing 2 mM of **4-11** and 0.2 mM of ethanethiol in 1:1 CH₃CN-0.1 M HEPES buffer, pH 7.4, 1 mM EDTA.

Time(h)	Normalized fluorescence intensity		
	Trial 1	Trial 2	Trial 3
0.2	1.0	1.0	0.8
1.0	5.2	5.7	5.0
2.0	10.7	11.5	9.8
3.0	16.7	17.7	15.4
6.1	35.9	33.3	31.9
8.0	46.9	43.9	42.3
10.0	61.6	56.3	54.0
12.0	69.9	61.6	61.2
14.0	71.6	67.5	67.9
17.0	84.0	83.1	77.2
20.0	88.2	88.9	81.5
23.0	97.9	92.3	92.7
26.0	100.0	96.0	94.0
28.9	98.8	98.6	96.9
32.0	99.5	100.0	100.0

Fluorescence data for the assay containing 2 mM of **4-11** and 0.1 mM of ethanethiol in 1:1 CH₃CN-0.1 M HEPES buffer, pH 7.4, 1 mM EDTA.

Time(h)	Normalized fluorescence intensity		
	Trial 1	Trial 2	Trial 3
0.2	0.6	0.6	0.6
1.0	2.9	2.6	2.8
2.0	5.4	5.2	5.6
3.0	9.4	8.8	8.1
6.1	19.4	20.2	18.8
8.0	26.7	25.5	26.6
10.0	35.6	36.7	32.3
12.0	44.1	45.7	41.0
14.0	56.0	50.1	49.9
17.0	66.6	64.0	63.8
20.0	76.6	79.3	73.1
23.0	90.6	86.4	82.6
26.0	93.3	89.0	90.7

28.9	99.3	95.5	100.0
32.0	100.0	100.0	98.3

Fluorescence data for the assay containing 2 mM of **4-11** and 0.02 mM of ethanethiol in 1:1 CH₃CN-0.1 M HEPES buffer, pH 7.4, 1 mM EDTA.

Time(h)	Normalized fluorescence intensity		
	Trial 1	Trial 2	Trial 3
0.1	0.2	0.3	0.3
3.0	1.3	1.2	1.2
6.0	2.4	2.5	2.5
12.0	6.1	6.3	6.5
24.0	23.2	24.5	25.3
35.0	57.4	61.0	59.7
48.0	91.9	98.1	94.0
60.0	100.0	98.6	100.0
73.0	99.2	100.0	100.0

Fluorescence data for the assay containing 2 mM of **4-11** and 0 mM of ethanethiol in 1:1 CH₃CN-0.1 M HEPES buffer, pH 7.4, 1 mM EDTA.

Time(h)	Normalized fluorescence intensity		
	Trial 1	Trial 2	Trial 3
0.12	0.20	0.22	0.18
6	0.41	0.37	0.31
10	0.43	0.34	0.44
24	0.83	0.86	0.85
33	1.45	1.38	1.20
47	2.65	2.51	1.81
56.7	4.45	4.00	2.77
71	10.00	9.16	4.24

Fluorescence emission intensities corresponding to Figure 4-12

Fluorescence data for the assay containing 2 mM of **4-11**, 0 mM of **4-22**, and 0.02 mM of ethanethiol in 1:1 CH₃CN-0.1 M HEPES buffer, pH 7.4, 1 mM EDTA.

Time (h)	Normalized fluorescence intensity		
	Trial 1	Trial 2	Trial 3
3.1	0.0	0.0	0.0
8.2	1.7	1.8	1.9
22.7	12.0	14.8	15.8
32.3	29.7	32.6	35.4
47.6	68.2	70.7	75.0
71.0	95.4	100.0	100.0
80.4	100.0	98.8	96.9

Fluorescence data for the assay containing 2 mM of **4-11**, 1 mM of **4-22**, and 0.02 mM of ethanethiol in 1:1 CH₃CN-0.1 M HEPES buffer, pH 7.4, 1 mM EDTA.

Time (h)	Normalized fluorescence intensity		
	Trial 1	Trial 2	Trial 3
3.1	0.0	0.0	0.0
8.2	0.6	8.2	2.7
22.7	2.2	13.0	6.5
32.3	23.2	25.3	26.7
47.6	52.0	51.0	56.1
71.0	100.0	102.0	95.0
80.4	90.4	100.0	100.0

Fluorescence emission intensities corresponding to Figure 4-13

Fluorescence data for the assay containing 2 mM of **4-11**, 0 mM of **4-25**, and 0.02 mM of ethanethiol in 1:1 CH₃CN-0.1 M HEPES buffer, pH 7.4, 1 mM EDTA.

Time (h)	Normalized fluorescence intensity		
	Trial 1	Trial 2	Trial 3
0.1	0.2	0.3	0.2
6.0	1.8	2.2	1.9
10.0	3.5	3.4	3.5
24.0	14.0	15.9	14.7
33.0	29.3	30.3	30.7
47.0	61.1	64.2	62.7
56.7	80.9	85.0	83.2
71.0	78.2	89.5	89.8
80.9	100.0	98.7	100.0
96.3	94.7	100.0	92.8

Fluorescence data for the assay containing 2 mM of **4-11**, 1 mM of **4-25**, and 0.02 mM of ethanethiol in 1:1 CH₃CN-0.1 M HEPES buffer, pH 7.4, 1 mM EDTA.

Normalized fluorescence intensity		
Trial 1	Trial 2	Trial 3
0.2	0.2	0.2
1.9	1.7	1.8
3.3	3.1	2.9
15.3	13.4	13.0
32.9	28.3	30.4
67.2	58.9	61.6
83.0	74.4	77.8
95.2	90.2	87.6
94.8	82.1	99.3
100.0	100.0	100.0

Fluorescence emission intensities corresponding to Figure 4-14

Fluorescence data for the assay containing 2 mM of **4-11** and 0.6 mM of N-acetyl-L-cysteine in 1:1 CH₃CN-0.1 M HEPES buffer, pH 7.4, 1 mM EDTA.

Normalized fluorescence intensity			
Time (h)	Trial 1	Trial 2	Trial 3
0.33	11.6	11.3	11.6
1.0	29.1	29.0	28.8
2.1	46.5	49.1	47.9
4.0	68.7	71.3	73.2
7.0	89.1	86.8	82.9
10	93.7	96.6	92.9
12	95.0	96.6	92.4
15	95.2	100	99.7
19	100	98.9	100

Fluorescence data for the assay containing 2 mM of **4-11** and 0.6 mM of 2-mercaptoethanol in 1:1 CH₃CN-0.1 M HEPES buffer, pH 7.4, 1 mM EDTA.

Normalized fluorescence intensity			
Time (h)	Trial 1	Trial 2	Trial 3
0.15	2.01	2.17	2.20
1.0	11.3	11.6	11.9
2.0	18.3	19.1	18.1
3.5	27.4	29.8	27.4
5.0	37.1	39.5	35.6
8.0	59.5	61.0	57.1
11	73.2	75.0	78.7
14	89.2	88.5	91.4
17	93.9	90.7	91.9
21	97.4	98.8	96.3
26	100	100	100

Fluorescence data for the assay containing 2 mM of **4-11** and 0.6 mM of thiophenol in 1:1 CH₃CN-0.1 M HEPES buffer, pH 7.4, 1 mM EDTA

Normalized fluorescence intensity			
Time (h)	Trial 1	Trial 2	Trial 3
0.15	9.35	9.74	9.72
0.5	11.7	13.1	13.1
1.0	15.2	16.4	16.5
2.0	23.2	22.5	23.4
3.5	33.4	34.5	34.5
5.0	42.6	43.5	42.9
8.0	63.4	62.9	64.1
11	75.8	79.1	81.6
14	86.3	91.3	90.2
17	93.7	93.1	101
21	95.1	97.0	95.3
26	100	100	100

Fluorescence data for the assay containing 2 mM of **4-11** and 0.6 mM of 4-methoxythiophenol in 1:1 CH₃CN-0.1 M HEPES buffer, pH 7.4, 1 mM EDTA

Normalized fluorescence intensity			
Time (h)	Trial 1	Trial 2	Trial 3
0.33	43.7	46.1	42.9
1.0	50.1	52.5	48.9
2.1	59.9	64.5	61.9
4.0	72.8	76.7	72.8
7.0	90.7	90.2	89.3
10	93.8	97.9	96.1
12	96.5	99.5	97.9
15	100	99.1	96.8
19	99.2	100	100

Fluorescence data for the assay containing 2 mM of **4-11** and 0.6 mM of 4-nitrothiophenol in 1:1 CH₃CN-0.1 M HEPES buffer, pH 7.4, 1 mM EDTA

Time (h)	% of maximum signal		
	Trial 1	Trial 2	Trial 3
0.33	46.7	41.0	40.5
1.0	52.8	48.6	49.3
2.1	62.0	59.2	59.3
4.0	77.5	73.0	74.6
7.0	87.8	86.6	90.2
10	94.6	91.2	96.3
12	98.6	93.8	98.7
15	99.5	95.3	101
19	100	100	100

Fluorescence data for the assay containing 2 mM of **4-11** and 0.6 mM of 3-mercaptohexanol in 1:1 CH₃CN-0.1 M HEPES buffer, pH 7.4, 1 mM EDTA

Time (h)	% of maximum signal		
	Trial 1	Trial 2	Trial 3
1.5	7.91	8.65	9.05
3.0	23.6	24.3	23.5
5.0	46.0	46.8	44.1
8.0	67.4	66.8	65.8
10	72.4	78.0	76.0
13	83.4	85.8	84.8
16	90.1	92.5	93.4
21	92.4	96.6	95.4
26	100	96.5	97.6
30	94.2	100	100
34	92.0	98.3	99.5

Fluorescence data for the assay containing 2 mM of **4-11** and 0.6 mM of tiopronin in 1:1 CH₃CN-0.1 M HEPES buffer, pH 7.4, 1 mM EDTA

Time (h)	% of maximum signal		
	Trial 1	Trial 2	Trial 3
0.10	18.4	17.0	14.3
1.0	52.7	49.3	51.7
3.0	76.5	72.1	72.8
5.0	85.6	85.1	81.5
7.0	92.7	91.3	95.5
9.0	100	100	98.1
11	99.1	98.7	97.4
13	100	97.0	100

Fluorescence data for the assay containing 2 mM of **4-11** and 0.6 mM of 2-methyl-2-propanethiol in 1:1 CH₃CN-0.1 M HEPES buffer, pH 7.4, 1 mM EDTA

Time (h)	% of maximum signal		
	Trial 1	Trial 2	Trial 3
1.5	0.126	0.159	0.170
3.0	0.371	0.374	0.422
8.0	1.89	2.28	2.23
13	5.78	5.98	6.61
21	18.4	21.1	24.0
30	48.2	57.1	58.7
34	63.7	65.5	67.8
38	71.1	79.1	81.2
49	92.5	92.4	91.7
59	94.7	100	100
74	100	97.7	99.7

Fluorescence data for the assay containing 2 mM of **4-11** and 0.6 mM of penicillamine in 1:1 CH₃CN-0.1 M HEPES buffer, pH 7.4, 1 mM EDTA

Time (h)	% of maximum signal		
	Trial 1	Trial 2	Trial 3
0.1	0.068	0.114	0.158
3.0	0.826	1.227	0.813
9.0	5.45	4.31	5.86
13	12.8	8.47	16.1
23	47.6	33.8	51.9
34	82.9	74.7	92.6
48	95.8	91.7	99.7
59	93.2	97.7	96.9
71	100	100	100

T₅₀ values obtained from regression curves of above fluorescence intensity data.

Thiol	T ₅₀ (h)		
	Trial 1	Trial 2	Trial 3
L-cysteine	0.44	0.37	0.39
N-acetyl-L-cysteine	2.21	2.12	2.11
2-mercaptoethanol	6.29	6.06	6.22
Thiophenol	5.56	5.29	5.20
4-methoxythiophenol	1.06	0.81	1.08
4-nitrothiophenol	0.79	1.11	1.13
3-mercaptohexanol	5.86	5.58	5.74
Tiopronin	0.81	0.97	0.88
2-methyl-2-propanethiol	29.9	27.8	27.4
Penicillamine	22.9	26.5	21.3

Chapter 5 data tables

Normalized absorbance data corresponding to Figure 5-5

Normalized absorbance data for 1.0 equivalent of added piperidine.

Time (h)	Absorbance at 305 nm
0.00	0.0000
0.03	0.4231
0.06	0.7560
0.07	0.7884
0.09	0.8585
0.13	0.8669
0.16	0.9100
0.23	0.9485
0.20	0.9330
0.25	0.9342
0.32	1.0000
0.38	0.9621
0.45	0.9137

Normalized absorbance data for 0.01 equivalents of added piperidine.

Time (h)	Absorbance at 305 nm		
	Trial 1	Trial 2	Trial 3
0.01	0.0000	0.0000	0.0000
0.50	0.0697	0.0736	0.0692
1.0	0.1326	0.1375	0.1532
2.0	0.2718	0.2898	0.2943
3.0	0.4292	0.3933	0.4586
4.0	0.6109	0.5748	0.5946
5.0	0.7620	0.8160	0.8542
6.0	0.9500	0.8885	0.9313
7.0	0.9787	0.8940	0.9857
8.0	1.0000	1.0000	0.9447
9.0	0.9962	0.9393	1.0000

Normalized absorbance data for 0.1 equivalents of added piperidine.

Time (h)	Absorbance at 305 nm		
	Trial 1	Trial 2	Trial 3
0.01	0.0000	0.0000	0.0000
0.33	0.4124	0.4138	0.3765
0.66	0.5957	0.5597	0.6082
1.0	0.7283	0.7672	0.7462
1.3	0.8456	0.8379	0.8292
1.7	0.8506	0.9030	0.9091
2.0	0.9449	0.9815	0.9919
2.3	0.8981	0.9995	0.9496
2.7	0.9038	0.9639	0.9502
3.2	1.0000	1.0000	1.0000

Normalized absorbance data for 0.001 equivalents of added piperidine.

Absorbance at 305 nm			
Time (h)	Trial 1	Trial 2	Trial 3
0.01	0.0000	0.0000	0.0000
2.0	0.0074	0.0611	0.0338
4.0	0.0345	0.0494	0.0354
6.0	0.0686	0.0868	0.0692
8.0	0.1611	0.2180	0.1787
10	0.3675	0.4009	0.4102
12	0.6855	0.7183	0.7531
13	0.8102	0.8305	0.8390
14	0.9590	0.9545	0.9243
15	0.9666	0.9560	0.9540
16	0.9738	0.9307	1.0000
18	1.0000	1.0000	0.9957

Normalized absorbance data for 0.0 equivalents of added piperidine.

Absorbance at 305 nm			
Time (h)	Trial 1	Trial 2	Trial 3
0.01	0.0000	0.0000	0.0000
1.0	0.0131	0.0227	0.0264
3.0	0.0583	0.0375	0.1233
5.0	0.1022	0.0419	0.0638
7.0	-0.0020	0.1070	0.0082
9.0	0.0565	0.0916	0.1311
11	0.1268	0.1463	0.1362
13	0.0410	0.2878	0.1330
15.2	0.0430	0.1678	0.0389
17.3	0.1184	0.1789	0.0999
19	0.1797	0.1850	0.1800

Normalized absorbance data corresponding to Figure 5-6

Time(h)	Normalized absorbance at 305 nm	Normalized absorbance at 625 nm
	$(A - A_0)/(A_{\max} - A_0)$	$(A - A_0)/(A_{\max} - A_0)$
0	0.000	0.000
1	0.019	0.001
2	0.052	0.001
3	0.095	0.001
4	0.177	0.086
5	0.314	0.312
6	0.528	0.525
7	0.672	0.715
8	0.859	0.856
9	0.954	0.922
10	0.996	0.939
11	1.000	1.000

Normalized absorbance data corresponding to Figure 5-8

Normalized absorbance data for 0.01 equivalents of added piperidine to **5-1**.

Time (h)	Absorbance at 305 nm		
	Trial 1	Trial 2	Trial 3
0.01	0.0000	0.0000	0.0000
0.50	0.0697	0.0736	0.0692
1.0	0.1326	0.1375	0.1532
2.0	0.2718	0.2898	0.2943
3.0	0.4292	0.3933	0.4586
4.0	0.6109	0.5748	0.5946
5.0	0.7620	0.8160	0.8542
6.0	0.9500	0.8885	0.9313
7.0	0.9787	0.8940	0.9857
8.0	1.0000	1.0000	0.9447
9.0	0.9962	0.9393	1.0000

Normalized absorbance data for 0.0 equivalents of added piperidine to **5-1**.

Time (h)	Absorbance at 305 nm		
	Trial 1	Trial 2	Trial 3
0.01	0.0000	0.0000	0.0000
1.0	0.0131	0.0227	0.0264
3.0	0.0583	0.0375	0.1233
5.0	0.1022	0.0419	0.0638
7.0	-0.0020	0.1070	0.0082
9.0	0.0565	0.0916	0.1311
11	0.1268	0.1463	0.1362
13	0.0410	0.2878	0.1330
15.2	0.0430	0.1678	0.0389
17.3	0.1184	0.1789	0.0999
19	0.1797	0.1850	0.1800

Normalized absorbance data for 0.01 equivalents of added piperidine to **5-2**.

Absorbance at 305 nm			
Time (h)	Trial 1	Trial 2	Trial 3
0	0.0000	0.0000	0.0000
2	0.1531	0.1416	0.1418
4	0.3373	0.3939	0.3088
6	0.4748	0.4808	0.4719
8	0.5936	0.6146	0.5199
10	0.7017	0.6769	0.6533
12	0.7685	0.8124	0.7342
14	0.9166	0.8915	0.8607
16	1.0000	0.9403	0.9810
18	0.9818	1.0000	1.0000

Normalized absorbance data for 0.0 equivalents of added piperidine to **5-2**.

Absorbance at 305 nm			
Time (h)	Trial 1	Trial 2	Trial 3
0	0.0915	0.0948	0.1048
1	0.1017	0.0952	0.1014
2	0.1003	0.1008	0.1011
3	0.0995	0.0932	0.0279
4	0.0954	0.1006	0.1073
5	0.1027	0.1009	0.1061
7	0.1032	0.105	0.106
9	0.1073	0.104	0.1197
12	0.1023	0.1068	0.1023
16	0.1051	0.1048	0.1069
20	0.1036	0.1054	0.1098

Normalized absorbance data for 0.01 equivalents of added piperidine to **5-3**.

Absorbance at 305 nm			
Time (h)	Trial 1	Trial 2	Trial 3
0	0.0000	0.0000	0.0000
2	0.2999	0.3589	0.3398
4	0.4785	0.4318	0.4612
6	0.5455	0.6327	0.6080
8	0.7336	0.7995	0.7861
10	0.7476	0.7471	0.8874
12	0.7974	0.8342	0.9514
14	0.9726	0.9112	0.9722
16	0.9913	0.9325	0.9943
17	1.0000	1.0000	1.0000

Normalized absorbance data for 0.0 equivalents of added piperidine to **5-3**.

Absorbance at 305 nm			
Time (h)	Trial 1	Trial 2	Trial 3
0	0	0	0
1	0.1223	0.0021	0.0088
2	0.1172	-0.0275	-0.0052
3	0.0915	0.0126	0.0075
4	0.1234	0.0042	0.0134
5	0.0995	-0.0123	0.0165
7	0.1338	0.0382	0.0317
9	0.1575	0.0432	0.0446
12	0.1409	0.0199	0.0431
16	0.1278	0.0442	0.0346
20	0.1437	0.0139	0.0403

Normalized absorbance data corresponding to Figure 5-9

[Pd(II)] in ppm	Normalized absorbance at 305 nm (A - A ₀)/(A _{max} - A ₀)		
	Trial 1	Trial 2	Trial 3
0	0.0000	0.0000	0.0000
4	0.0110	0.0086	-0.0017
8	0.0202	0.0134	0.0004
10	0.0133	0.0103	0.0359
12	0.0735	0.0533	0.0190
14	0.1367	0.1269	0.2404
16	0.2905	0.2849	0.4375
20	0.7122	0.7112	0.8737
24	0.8936	0.8923	0.9797
28	0.9156	1.0062	0.9979
32	1.0000	1.0000	1.0000

APPENDIX C: PERMISSIONS TO REUSE COPYRIGHTED MATERIALS

RSC | Advancing the
Chemical Sciences

Royal Society of Chemistry
Thomas Graham House
Science Park
Milton Road
Cambridge
CB4 0WF

Tel: +44 (0)1223 420 066
Fax: +44 (0)1223 423 623
Email: contracts-copyright@rsc.org

www.rsc.org

Acknowledgements to be used by RSC authors

Authors of RSC books and journal articles can reproduce material (for example a figure) from the RSC publication in a non-RSC publication, including theses, without formally requesting permission providing that the correct acknowledgement is given to the RSC publication. This permission extends to reproduction of large portions of text or the whole article or book chapter when being reproduced in a thesis.

The acknowledgement to be used depends on the RSC publication in which the material was published and the form of the acknowledgements is as follows:

- For material being reproduced from an article in *New Journal of Chemistry* the acknowledgement should be in the form:
 - [Original citation] - Reproduced by permission of The Royal Society of Chemistry (RSC) on behalf of the Centre National de la Recherche Scientifique (CNRS) and the RSC
- For material being reproduced from an article *Photochemical & Photobiological Sciences* the acknowledgement should be in the form:
 - [Original citation] - Reproduced by permission of The Royal Society of Chemistry (RSC) on behalf of the European Society for Photobiology, the European Photochemistry Association, and RSC
- For material being reproduced from an article in *Physical Chemistry Chemical Physics* the acknowledgement should be in the form:
 - [Original citation] - Reproduced by permission of the PCCP Owner Societies
- For material reproduced from books and any other journal the acknowledgement should be in the form:
 - [Original citation] - Reproduced by permission of The Royal Society of Chemistry

The acknowledgement should also include a hyperlink to the article on the RSC website.

The form of the acknowledgement is also specified in the RSC agreement/licence signed by the corresponding author.

Except in cases of republication in a thesis, this express permission does not cover the reproduction of large portions of text from the RSC publication or reproduction of the whole article or book chapter.

A publisher of a non-RSC publication can use this document as proof that permission is granted to use the material in the non-RSC publication.

**JOHN WILEY AND SONS LICENSE
TERMS AND CONDITIONS**

Aug 26, 2014



This is a License Agreement between hemakesh mohapatra ("You") and John Wiley and Sons ("John Wiley and Sons") provided by Copyright Clearance Center ("CCC"). The license consists of your order details, the terms and conditions provided by John Wiley and Sons, and the payment terms and conditions.

All payments must be made in full to CCC. For payment instructions, please see information listed at the bottom of this form.

License Number	3431510612689
License date	Jul 17, 2014
Licensed content publisher	John Wiley and Sons
Licensed content publication	Angewandte Chemie International Edition
Licensed content title	Using Smell To Triage Samples in Point-of-Care Assays
Licensed copyright line	Copyright © 2012 WILEY-VCH Verlag GmbH & Co. KGaA, Weinheim
Licensed content author	Hemakesh Mohapatra, Scott T. Phillips
Licensed content date	Oct 4, 2012
Start page	11145
End page	11148
Type of use	Dissertation/Thesis
Requestor type	Author of this Wiley article
Format	Print and electronic
Portion	Full article
Will you be translating?	No
Title of your thesis / dissertation	Design of reagents for trace-level chemical detection and signal amplification
Expected completion date	Dec 2014
Expected size (number of pages)	250
Total	0.00 USD
Terms and Conditions	

TERMS AND CONDITIONS

This copyrighted material is owned by or exclusively licensed to John Wiley & Sons, Inc. or one of its group companies (each a "Wiley Company") or handled on behalf of a society with which a

Wiley Company has exclusive publishing rights in relation to a particular work (collectively "WILEY"). By clicking accept in connection with completing this licensing transaction, you agree that the following terms and conditions apply to this transaction (along with the billing and payment terms and conditions established by the Copyright Clearance Center Inc., ("CCC's Billing and Payment terms and conditions"), at the time that you opened your Rightslink account (these are available at any time at <http://myaccount.copyright.com>).

Terms and Conditions

- The materials you have requested permission to reproduce or reuse (the "Wiley Materials") are protected by copyright.
- You are hereby granted a personal, non-exclusive, non-sub licensable (on a stand-alone basis), non-transferable, worldwide, limited license to reproduce the Wiley Materials for the purpose specified in the licensing process. This license is for a one-time use only and limited to any maximum distribution number specified in the license. The first instance of republication or reuse granted by this licence must be completed within two years of the date of the grant of this licence (although copies prepared before the end date may be distributed thereafter). The Wiley Materials shall not be used in any other manner or for any other purpose, beyond what is granted in the license. Permission is granted subject to an appropriate acknowledgement given to the author, title of the material/book/journal and the publisher. You shall also duplicate the copyright notice that appears in the Wiley publication in your use of the Wiley Material. Permission is also granted on the understanding that nowhere in the text is a previously published source acknowledged for all or part of this Wiley Material. Any third party content is expressly excluded from this permission.
- With respect to the Wiley Materials, all rights are reserved. Except as expressly granted by the terms of the license, no part of the Wiley Materials may be copied, modified, adapted (except for minor reformatting required by the new Publication), translated, reproduced, transferred or distributed, in any form or by any means, and no derivative works may be made based on the Wiley Materials without the prior permission of the respective copyright owner. You may not alter, remove or suppress in any manner any copyright, trademark or other notices displayed by the Wiley Materials. You may not license, rent, sell, loan, lease, pledge, offer as security, transfer or assign the Wiley Materials on a stand-alone basis, or any of the rights granted to you hereunder to any other person.
- The Wiley Materials and all of the intellectual property rights therein shall at all times remain the exclusive property of John Wiley & Sons Inc, the Wiley Companies, or their respective licensors, and your interest therein is only that of having possession of and the right to reproduce the Wiley Materials pursuant to Section 2 herein during the continuance of this Agreement. You agree that you own no right, title or interest in or to the Wiley Materials or any of the intellectual property rights therein. You shall have no rights hereunder other than the license as provided for above in Section 2. No right, license or interest to any trademark, trade name, service mark or other branding ("Marks") of WILEY or its licensors is granted hereunder, and you agree that you shall not assert any such right, license or interest with

respect thereto.

- NEITHER WILEY NOR ITS LICENSORS MAKES ANY WARRANTY OR REPRESENTATION OF ANY KIND TO YOU OR ANY THIRD PARTY, EXPRESS, IMPLIED OR STATUTORY, WITH RESPECT TO THE MATERIALS OR THE ACCURACY OF ANY INFORMATION CONTAINED IN THE MATERIALS, INCLUDING, WITHOUT LIMITATION, ANY IMPLIED WARRANTY OF MERCHANTABILITY, ACCURACY, SATISFACTORY QUALITY, FITNESS FOR A PARTICULAR PURPOSE, USABILITY, INTEGRATION OR NON-INFRINGEMENT AND ALL SUCH WARRANTIES ARE HEREBY EXCLUDED BY WILEY AND ITS LICENSORS AND WAIVED BY YOU
- WILEY shall have the right to terminate this Agreement immediately upon breach of this Agreement by you.
- You shall indemnify, defend and hold harmless WILEY, its Licensors and their respective directors, officers, agents and employees, from and against any actual or threatened claims, demands, causes of action or proceedings arising from any breach of this Agreement by you.
- IN NO EVENT SHALL WILEY OR ITS LICENSORS BE LIABLE TO YOU OR ANY OTHER PARTY OR ANY OTHER PERSON OR ENTITY FOR ANY SPECIAL, CONSEQUENTIAL, INCIDENTAL, INDIRECT, EXEMPLARY OR PUNITIVE DAMAGES, HOWEVER CAUSED, ARISING OUT OF OR IN CONNECTION WITH THE DOWNLOADING, PROVISIONING, VIEWING OR USE OF THE MATERIALS REGARDLESS OF THE FORM OF ACTION, WHETHER FOR BREACH OF CONTRACT, BREACH OF WARRANTY, TORT, NEGLIGENCE, INFRINGEMENT OR OTHERWISE (INCLUDING, WITHOUT LIMITATION, DAMAGES BASED ON LOSS OF PROFITS, DATA, FILES, USE, BUSINESS OPPORTUNITY OR CLAIMS OF THIRD PARTIES), AND WHETHER OR NOT THE PARTY HAS BEEN ADVISED OF THE POSSIBILITY OF SUCH DAMAGES. THIS LIMITATION SHALL APPLY NOTWITHSTANDING ANY FAILURE OF ESSENTIAL PURPOSE OF ANY LIMITED REMEDY PROVIDED HEREIN.
- Should any provision of this Agreement be held by a court of competent jurisdiction to be illegal, invalid, or unenforceable, that provision shall be deemed amended to achieve as nearly as possible the same economic effect as the original provision, and the legality, validity and enforceability of the remaining provisions of this Agreement shall not be affected or impaired thereby.
- The failure of either party to enforce any term or condition of this Agreement shall not constitute a waiver of either party's right to enforce each and every term and condition of this Agreement. No breach under this agreement shall be deemed waived or excused by either party unless such waiver or consent is in writing signed by the party granting such waiver or consent. The waiver by or consent of a party to a breach of any provision of this Agreement shall not operate or be construed as a waiver of or consent to any other or subsequent

breach by such other party.

- This Agreement may not be assigned (including by operation of law or otherwise) by you without WILEY's prior written consent.
- Any fee required for this permission shall be non-refundable after thirty (30) days from receipt by the CCC.
- These terms and conditions together with CCC's Billing and Payment terms and conditions (which are incorporated herein) form the entire agreement between you and WILEY concerning this licensing transaction and (in the absence of fraud) supersedes all prior agreements and representations of the parties, oral or written. This Agreement may not be amended except in writing signed by both parties. This Agreement shall be binding upon and inure to the benefit of the parties' successors, legal representatives, and authorized assigns.
- In the event of any conflict between your obligations established by these terms and conditions and those established by CCC's Billing and Payment terms and conditions, these terms and conditions shall prevail.
- WILEY expressly reserves all rights not specifically granted in the combination of (i) the license details provided by you and accepted in the course of this licensing transaction, (ii) these terms and conditions and (iii) CCC's Billing and Payment terms and conditions.
- This Agreement will be void if the Type of Use, Format, Circulation, or Requestor Type was misrepresented during the licensing process.
- This Agreement shall be governed by and construed in accordance with the laws of the State of New York, USA, without regards to such state's conflict of law rules. Any legal action, suit or proceeding arising out of or relating to these Terms and Conditions or the breach thereof shall be instituted in a court of competent jurisdiction in New York County in the State of New York in the United States of America and each party hereby consents and submits to the personal jurisdiction of such court, waives any objection to venue in such court and consents to service of process by registered or certified mail, return receipt requested, at the last known address of such party.

WILEY OPEN ACCESS TERMS AND CONDITIONS

Wiley Publishes Open Access Articles in fully Open Access Journals and in Subscription journals offering Online Open. Although most of the fully Open Access journals publish open access articles under the terms of the Creative Commons Attribution (CC BY) License only, the subscription journals and a few of the Open Access Journals offer a choice of Creative Commons Licenses:: Creative Commons Attribution (CC-BY) license Creative Commons Attribution Non-Commercial (CC-BY-NC) license and Creative Commons Attribution Non-Commercial-NoDerivs (CC-BY-NC-ND) License. The license type is clearly identified on the article.

Copyright in any research article in a journal published as Open Access under a Creative Commons License is retained by the author(s). Authors grant Wiley a license to publish the article and identify itself as the original publisher. Authors also grant any third party the right to use the article freely as long as its integrity is maintained and its original authors, citation details and publisher are identified as follows: [Title of Article/Author/Journal Title and Volume/Issue. Copyright (c) [year] [copyright owner as specified in the Journal]. Links to the final article on Wiley's website are encouraged where applicable.

The Creative Commons Attribution License

The Creative Commons Attribution License (CC-BY) allows users to copy, distribute and transmit an article, adapt the article and make commercial use of the article. The CC-BY license permits commercial and non-commercial re-use of an open access article, as long as the author is properly attributed.

The Creative Commons Attribution License does not affect the moral rights of authors, including without limitation the right not to have their work subjected to derogatory treatment. It also does not affect any other rights held by authors or third parties in the article, including without limitation the rights of privacy and publicity. Use of the article must not assert or imply, whether implicitly or explicitly, any connection with, endorsement or sponsorship of such use by the author, publisher or any other party associated with the article.

For any reuse or distribution, users must include the copyright notice and make clear to others that the article is made available under a Creative Commons Attribution license, linking to the relevant Creative Commons web page.

To the fullest extent permitted by applicable law, the article is made available as is and without representation or warranties of any kind whether express, implied, statutory or otherwise and including, without limitation, warranties of title, merchantability, fitness for a particular purpose, non-infringement, absence of defects, accuracy, or the presence or absence of errors.

Creative Commons Attribution Non-Commercial License

The Creative Commons Attribution Non-Commercial (CC-BY-NC) License permits use, distribution and reproduction in any medium, provided the original work is properly cited and is not used for commercial purposes.(see below)

Creative Commons Attribution-Non-Commercial-NoDerivs License

The Creative Commons Attribution Non-Commercial-NoDerivs License (CC-BY-NC-ND) permits use, distribution and reproduction in any medium, provided the original work is properly cited, is not used for commercial purposes and no modifications or adaptations are made. (see below)

Use by non-commercial users

For non-commercial and non-promotional purposes, individual users may access, download, copy,

display and redistribute to colleagues Wiley Open Access articles, as well as adapt, translate, text- and data-mine the content subject to the following conditions:

- The authors' moral rights are not compromised. These rights include the right of "paternity" (also known as "attribution" - the right for the author to be identified as such) and "integrity" (the right for the author not to have the work altered in such a way that the author's reputation or integrity may be impugned).
- Where content in the article is identified as belonging to a third party, it is the obligation of the user to ensure that any reuse complies with the copyright policies of the owner of that content.
- If article content is copied, downloaded or otherwise reused for non-commercial research and education purposes, a link to the appropriate bibliographic citation (authors, journal, article title, volume, issue, page numbers, DOI and the link to the definitive published version on **Wiley Online Library**) should be maintained. Copyright notices and disclaimers must not be deleted.
- Any translations, for which a prior translation agreement with Wiley has not been agreed, must prominently display the statement: "This is an unofficial translation of an article that appeared in a Wiley publication. The publisher has not endorsed this translation."

Use by commercial "for-profit" organisations

Use of Wiley Open Access articles for commercial, promotional, or marketing purposes requires further explicit permission from Wiley and will be subject to a fee. Commercial purposes include:

- Copying or downloading of articles, or linking to such articles for further redistribution, sale or licensing;
- Copying, downloading or posting by a site or service that incorporates advertising with such content;
- The inclusion or incorporation of article content in other works or services (other than normal quotations with an appropriate citation) that is then available for sale or licensing, for a fee (for example, a compilation produced for marketing purposes, inclusion in a sales pack)
- Use of article content (other than normal quotations with appropriate citation) by for-profit organisations for promotional purposes
- Linking to article content in e-mails redistributed for promotional, marketing or educational purposes;
- Use for the purposes of monetary reward by means of sale, resale, licence, loan, transfer or other form of commercial exploitation such as marketing products

- Print reprints of Wiley Open Access articles can be purchased from:
corporate-sales@wiley.com

Further details can be found on Wiley Online Library
<http://olabout.wiley.com/WileyCDA/Section/id-410895.html>

Other Terms and Conditions:

v1.9

You will be invoiced within 48 hours of this transaction date. You may pay your invoice by credit card upon receipt of the invoice for this transaction. Please follow instructions provided at that time.

To pay for this transaction now; please remit a copy of this document along with your payment. Payment should be in the form of a check or money order referencing your account number and this invoice number RLNK501354517.

Make payments to "COPYRIGHT CLEARANCE CENTER" and send to:

Copyright Clearance Center

Dept 001

P.O. Box 843006

Boston, MA 02284-3006

Please disregard electronic and mailed copies if you remit payment in advance.

Questions? customercare@copyright.com or +1-855-239-3415 (toll free in the US) or +1-978-646-2777.

Gratis licenses (referencing \$0 in the Total field) are free. Please retain this printable license for your reference. No payment is required.
